Simulation results for further extrapolation of Use Case 3

V1.0

Deliverable D9.5

23/12/2019

This project has received funding from the European Union's Horizon 2020 research and innovation programme under grant agreement n°731289

ID & Title :	D9.5– Simulation results for further extrapolation of Use case 3		
Version :	V 1.0	Number of pages:	196

Short Description

Based on the experience and feedback gathered through Use case 3, Deliverable 9.5 presents in a first part how local flexibility could develop in the future, through value creation and adequacy between demand and offer.
In a second part, it details prospective grid simulations performed with current PV generation and electrical vehicle scenarios for 2035 on the MV network where use case 3 was implemented, in order to assess where, why and how many constraints could occur in this specific scenario in the future.

Revision history

Version	Date	Modifications' nature	Author
0.1	09.09.2019	Document initialized	Wagner, Casacci
0.2	25.11.2019	All chapters provided	Mulenet, Wagner, Bruschi, Casacci, Lehec, Guichard
0.3	13.12.2019	Final version after peer review	Mulenet, Wagner, Bruschi, Casacci, Lehec, Guichard, Gross
1.0	23.12.2019	Final version	Casacci, Lehec, Guichard, Wagner

Accessibility

☒Public	☐ Consortium + EC	☐ Restricted to a specific group + EC	☐ Confidential + EC

Owner/Main responsible

Name(s)	Function	Company	Visa
Vanessa CASACCI	Nice Smart Valley Project Manager	EDF	

Author(s)/contributor(s): company name(s)

ENGIE, Enedis, EDF, GRDF

Reviewer(s): company name(s)

Company	Name(s)
AVACON	Gross

Approver(s): company name(s)

Company	Name(s)
Enedis	Dumbs

Work Package ID	WP 9	Task ID	T9.9

Disclaimer: This report reflects only the author's view and the Agency is not responsible for any use that may be made of the information it contains.

EXECUTIVE SUMMARY

Use case 3 of the French demo Nice Smart Valley aimed at designing and testing a competition-based local flexibility mechanism to manage distribution grid constraints. This document presents the results of the various analyses and simulations carried out by EDF, ENGIE, GRDF and Enedis regarding the future flexibility development on a local scale. It aims at enriching the state of the art on that matter.

The first chapter deals with value creation from flexibility and describes the current flexibility needs nationwide and potentially in distribution grids, their definition, their characteristics, their usage, and their activation modalities. It describes how the future use of flexibility for DSO services could be combined with flexibility mechanisms at the national level as well as with energy efficiency services for the customer. This combination of different services, which requires the ability for the aggregators to share a given flexibility source among various uses, and stack the different values, seems crucial to make profitable business models and thus local flexibility a reality. An insight is also given in how sector coupling based on smart gas solutions will participate in this value creation.

The second chapter addresses the conditions to be fulfilled for the aggregators to be able to develop attractive offers for the customer. Solutions are presented to overcome the lack of interest of customers regarding the complexity of the concept of flexibility, to access and gather data and to build free competitive mechanisms.

Finally, the third chapter is independent from the previous ones and presents in detail a set of simulations that were performed on the MV network, on 2 primary substations of the French demo's Use case 3 experiments, to evaluate how and where distribution grid constraints could appear in the future. Simulations were run at a time horizon of the year 2035, taking into account future energy efficiency measures while extrapolating to a higher penetration of PV generation and electric vehicle charging stations. This simulation approach aimed at evaluating the characteristics of the flexibility that could be used in the future. The results are directly bound to the full set of assumptions of the considered development scenario and cannot be extrapolated to other areas. For instance (see 4.3 for an exhaustive list of assumptions), it was considered that:

- The power output of all producers was supposed to be synchronous (i.e peak PV production at the same time)
- The network was kept unchanged between 2017 and 2035, i.e., it was assumed that there were no grid reinforcements in the future (whereas in reality investment programs such as protection against extreme climate conditions or old cables renewal naturally increase the capacity of the grid).
- LV connected generation and EV charging points were taken into account, whereas secondary substations and the LV network were not simulated.

The results show that:

- Constraints appear only in N-1 configuration of the MV network (reconfiguration following an outage or a temporary withdrawal of an asset)
- The constraints are mainly caused by power generation. Some load constraints that are already there today remain until 2035 despite energy efficiency hypotheses. Electric vehicle charging does not create constraints under our hypothesis on charging profiles.
- The results are highly dependent on how the PV and EV connection points are spread over the network.

TABLE OF CONTENT

LIST OF TABLES

LIST OF FIGURES

1. INTRODUCTION

1.1. Scope of the document

Deliverable 9.5 describes and summarizes the simulations and extrapolations made on Use case 3 to draw how it could be extrapolated in the future.

1.2. Notations, abbreviations and acronyms

The table below provides an overview of the notations, abbreviations and acronyms used in the document.

ACRONYM	Definition
ACR	Regional Control Agency (in its French acronym)
DER	Distributed Energy Resources
DSO	Distribution System Operator
DSR	Demand side response
GFU	Grid Forming Unit
GSU	Grid Supporting Unit
LV	Low Voltage
MV	Medium Voltage
CHP	Combined Heat & power
SOC	State of Charge
TSO	Transmission System Operator

2. VALUE CREATION THANKS TO LOCAL FLEXIBILITY

2.1. Current flexibility needs nationwide and in the distribution grid

Demand flexibility has for long been used to respond to the needs of national supply/demand balance and congestions in the public transmission system.

Today, flexibility reserves account for about 3 GW in France, and consist of:

- Adjustable industrial sites (steel industry, chemical industry, etc.), regulated 24hr/7d,
- Commercial or industrial production sites equipped with emergency diesel generators (e.g. EDJ tariffs in particular),
- Residential customers with TEMPO subscription contracts, accounting for around 600 MW flexibility, where customers shift and/or cut back their energy consumption by using back-up oil- or wood-burning systems on so-called “strained days”.

These demand cutbacks, primarily in large-size sites, are characterized by low capacity costs and high activation costs.

The value of cutbacks is essentially linked to capacity, i.e. it enables grid looping in strained situations; in France, this relates to wintertime consumption peaks linked to the high heat-sensitivity of our electrical system. It provides what is called “insurance value”, and this value is remunerated via the recently established capacity mechanism.

Faster load shedding mechanisms are also used for system balancing: system services and fast reserves are complementary to help balance the frequency in the event of an occasional supply/demand imbalance (incorrect prediction, unplanned event in a power generation facility, etc.).

The Smart Grid economic study headed by RTE has shown that the flexibility level for the national electrical system (supply/demand balance and transmission grid congestion) is currently sufficient with 3 GW for the current mix; but with the sharp development of renewables and reduced nuclear power output by 2035, the system would need increased flexibility resources (due primarily to wind intermittence in wintertime), possibly up to a few dozen GW and covered by various mechanisms (industrial load shedding, residential cutbacks, additional batteries and PSP stations).

Accordingly, the French PPE multi-annual energy master plan includes a target to develop demand cutbacks to 6.5 GW by 2028, along with the launch of an RFQ intended to support the industry and develop cutback capacities. At this time, the price capped at €30/kW/year fails to allow any significant development of new cutback capabilities.

On the distribution network today, over 40,000 sites contribute to national flexibility, accounting for a total potential power in excess of 1 GW. But there is no system to leverage the value of local flexibility to respond to constraints in the distribution grid since the need is extremely low.

2.1.1. Characteristics of the available flexibilities

At the level of the distribution network, there are different types of flexibilities:

- Consumption flexibility
  - Flexible use: Electrical use whose use can be temporarily postponed without impacting the customer: thermal use of electricity (heating, air conditioning, domestic hot water) or industrial process using electricity with inertia (industrial furnace, industrial refrigeration, ventilation) or upstream or downstream storage (grinding, pumping). Flexibility here comes from implicit storage and can be modelled in this way.
  - Interruptible use: Electrical use whose use can be interrupted with an impact on the customer: industrial process without the possibility of upstream or downstream storage or involving human resources. Example of a production line.
  - Hybrid use: Electrical use whose use can be substituted by a use having the same utility from another energy such as gas: example of hybrid rooftops or hybrid boilers
- Production flexibility
  - Back-up engines: These generators have been installed for electrical emergency purposes. They can be used occasionally as long as it does not put at risk the stock of fuel required for the emergency function.
  - Intermittent renewable production: these productions can be interrupted when they are in operation
  - Cogeneration: simultaneous production of electricity and heat from gas. Electricity production can be started without the need for heat or interrupted occasionally.
- Flexibility of electrical storage: The decision to install local storage is linked to a local need, whether it is to optimize self-consumption, service to the distribution network or electrical back-up. The reason why electricity storage is installed forces its use for other peripheral reasons.

2.1.2. Flexibility as a part of energy efficiency

There are three types of energy efficiency action:

1. **Type 1 / Consuming less**: sustainable reduction of the customer's energy needs in volume
2. **Type 2 / Consuming better by structurally shifting consumption** during optimal hours according to a static economic signal. This results in a reduction in the cost of supplying the consumer with iso-utility for him. Examples: recharging the domestic hot water tank or reducing the cost of heating by anticipating the heating of the building. In the latter case, the volume of energy consumed may increase but the cost of energy supply to deliver the comfort function will be lower.
3. **Type 3 / Consumption better by punctually shifting consumption** during periods according to a dynamic economic signal or direct control[1] of consumption by a third

[1] In this case, despite direct control, there is still an underlying economic signal to modulate consumption. Example of the fixed premium for the frequency adjustment of the transmission system.

party. The consumption profile is here desoptimized compared to static optimization. This distortion must therefore create more value than that which is destroyed as a result of desoptimization.

Flexibility is the ability to modulate its consumption or its production according to an external signal. So type 2 and 3 actions are flexibilities.

2.1.3. Modalities of activation and mobilization of available flexibility: current use of flexibility

2.1.3.1. Static or dynamic activation

Static flexibility can be mobilized through a static and differentiated economic signal according to the hours/days/months of the year. For example, the price of electricity consumed in €/MWh and differentiated according to periods or the price of contracted capacity in €/MW. This flexibility can be mobilized by a structural adaptation of the behavior or by the use of devices to control uses according to the consumer's tariff signal.

Dynamic flexibility is activated according to the varying needs of the electrical system.

Today, static flexibilities are mobilized by the distribution system operator via the routing tariff signal. Its structure is defined nationally but its hourly settings are made according to local needs of the TSO. Static activations are recurrent. They are based on flexibilities whose activation cost is lower than the cost to the power system in the event of non-activation. Today, these flexibilities are coming from flexible uses, hybrid uses, intermittent interruptible production and storage.

Dynamic flexibilities are currently mainly used to provide a service to the transmission system operator (system services, erasure tender) and to obtain capacity certificates. Dynamic activations are triggered by a variable economic signal that can be very high in some cases. These activations are based on all types of flexibilities.

The modalities for activating flexibilities (dynamic or static) are not mutually exclusive. They are complementary.

2.1.4. Trade-off between static and dynamic flexibilities

The flexibilities tested as part of the French demonstrator Nice Smart Valley are dynamic. Nevertheless, it is necessary to consider that static flexibilities could at least partially meet the challenges of postponing investments in the distribution network.

As example, the development of a fleet of electric vehicles could create strong constraints if it was not considered that recharging should take place largely during periods of low constraint due to a tariff management of the recharge.

These static flexibilities have the disadvantage that they cannot be remunerated differently according to the value they create and cannot cover the variety of flexibility characteristics necessary to meet the needs of distribution system operators. Thus, they do not send a signal to the market to create maximum value for the electrical system. They will therefore

certainly have to be combined with dynamic flexibilities whose level of remuneration and activation characteristics can be adapted to the challenges on a given area.

2.1.5. Future needs for flexibility in the distribution grid

Flexibility in the distribution system presents two main benefits:

- Facilitate customer connections and feed-in of renewable energies in existing grids,
- Optimize the design and operation of the distribution grid.

The value for the Distribution System Operator is as follows:

- For planning: reduce occasionally the strain level on a piece of grid equipment (e.g. substation, power line) in order to defer or even avoid its reinforcement. The maximum flexibility value would then correspond to the value of the postponed or avoided investment costs, along with the proportion of non-distributed or non-injected power, as the case may be.
- For operation: restore power faster to some cut-off customers, or reduce the number of power cuts caused by works or incidents on the Public Distribution Grid. The value saved would then be equivalent (apart from any investment decision by Enedis) to the cost of the temporary solution (e.g. sending emergency gensets). Two situations are then possible:
    - If the flexibility can avoid sending out emergency facilities (e.g. gensets), its maximum value would be the full cost of the temporary solution plus the portion of non-distributed power.
    - If the flexibility can limit the operating time of gensets, its maximum value then becomes equivalent to the variable portion of gensets operating costs plus the portion of non-distributed power.

The needs for grid reinforcement may result from several causes:

- Offtake constraints linked to the connection of a new consumer to the grid,
- Feed-in constraints linked to the connection of renewables to a MV grid.

Note: Here, we disregard the issue of support to construction works since this is a limited situation with a lower value considering that they can frequently be planned by Enedis, as well as incidents that are difficult to predict and highly localised by nature.

A. Offtake issue

The economic benefit of demand cutbacks can reside in the ability to defer grid reinforcement works on the power infrastructure.

Such deferred investments will primarily depend on:

- The leeway in transit capacity at distribution substations (MV, MV/HV) and on various grid equipment units, e.g. power lines and cables. It should be noted that this margin may be higher or lower depending on the date of the latest reinforcement works carried out on the grid. The grid reinforcement value is therefore highly local.

- The demand growth expected at local level.
- Connections of new consumers.

The grid reinforcement cost in €/kW also depends on the grid typology: urban, suburban or rural.

The parameters are therefore primarily local and difficult to extend generally at national level.

It should be noted that forecasts on consumption and demand peaks at national level are on a downtrend (in energy) over the coming years[2].

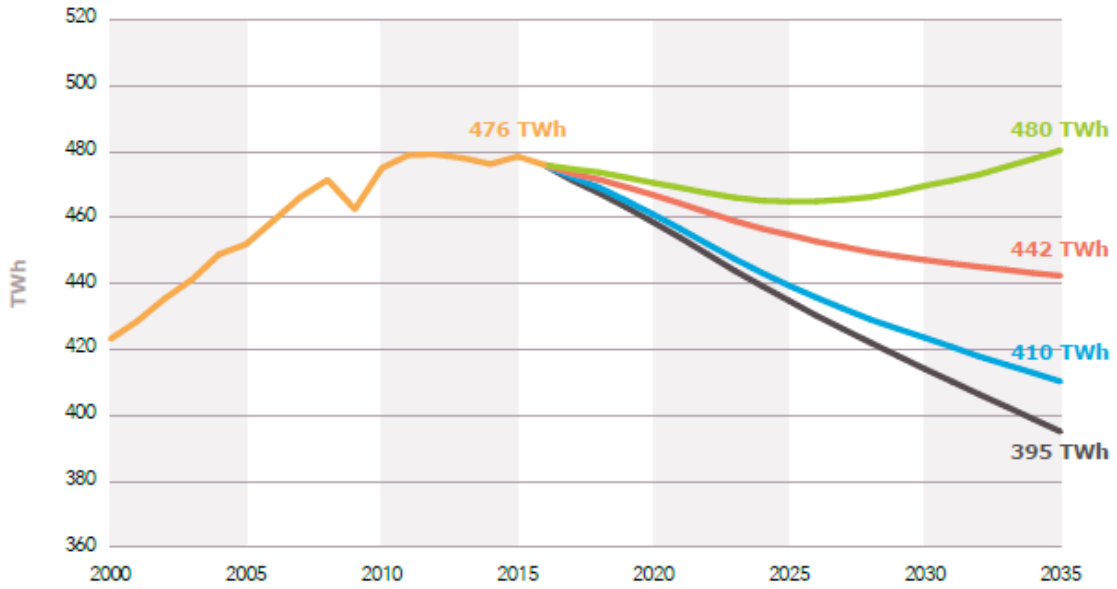

Figure 1 - Trajectories of annual domestic electricity consumption

BP RTE 2017 - Normal climate, continental France

Thanks to energy efficiency measures (heat pumps instead of Joule heating, insulation and thermodynamic water heaters instead of Joule water heaters), the electricity demand peaks should be sharply lowered or at the very least stay close to the current peak level in all cases analysed[3]. Massive electrification of uses, among which electric vehicles, alone would be likely to change the situation somewhat, particularly if EV recharging is not controlled.

[2] BP RTE 2017

[3] *Enjeux du développement de l'électromobilité pour le système électrique RTE*, AVERE May 2019

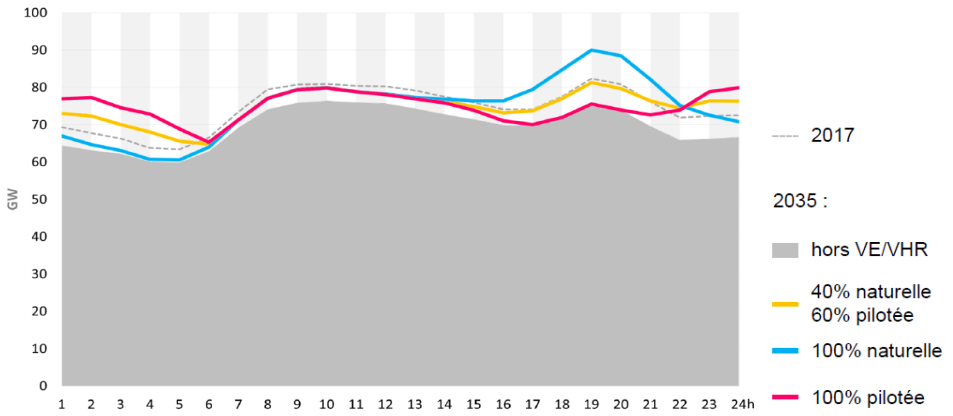

Figure 2 - Load curve comparison 2017 and 2035 depending on recharging mode of 15 million EVs - Avere RTE study2

On this point, the AVERE study revealed that with simple regulation such as "TIME OF USE" (incentive to schedule vehicle recharging at a time when the grid is the least constrained and electricity price is the lowest), the major portion of the peak value (shown in green in the graph below) can be captured.

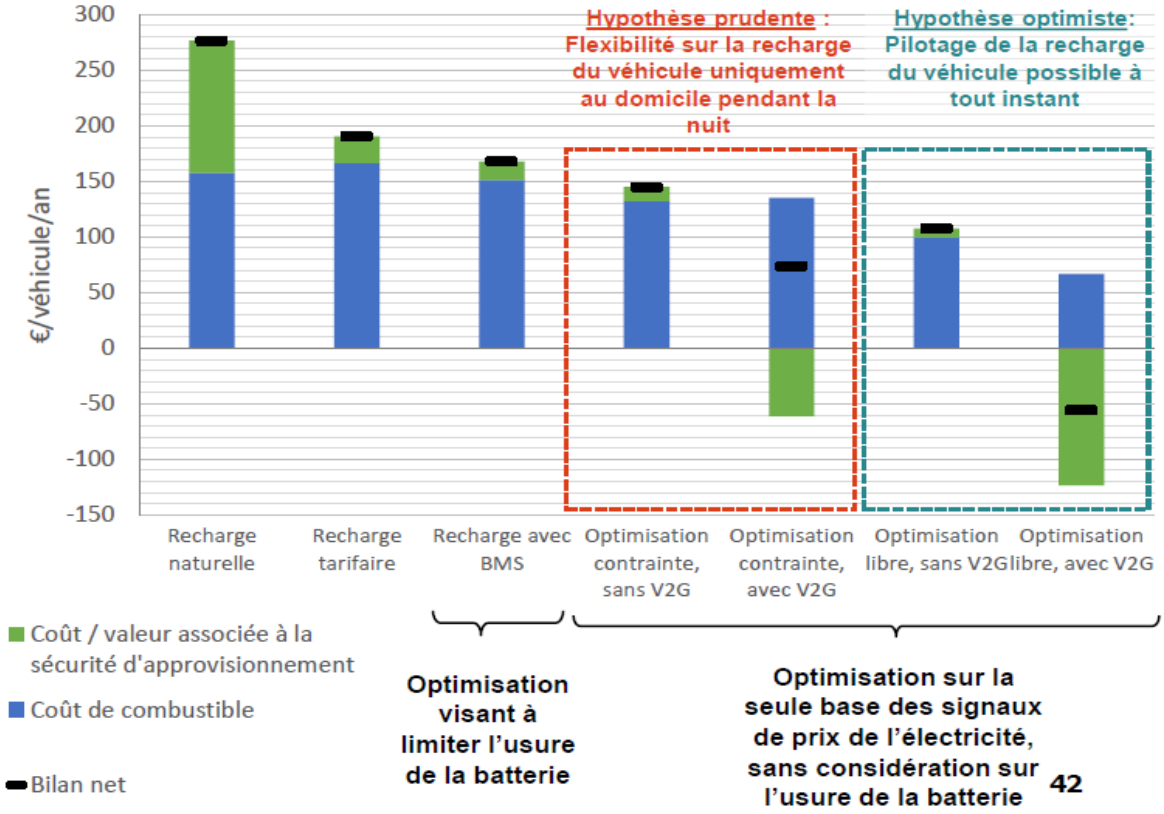

Figure 3 - Annual costs of electric vehicle recharge according to the recharge regulation strategy as related to supply & demand balance

Excl. TURPE tariff and taxes - Scenario Ampère 2035

The national environment is therefore not favourable to leveraging the economic value of solving congestions on distribution grids. The number of constrained situations arising from congestion issues will be extremely limited on the French territory due to the current design size of the grid and to the limited growth expected in peak demand. This statement might

be nuanced based on the variability of situations found at local scale that could generate pockets of value under some configurations.

However, for an approximate estimate of the economic value of the distribution grid investments deferred via flexibility resources, it is possible to refer to the recent Enedis[4] study defining the economic value of flexibility in distribution grids.

The economic capacity value is based primarily on the requirements of service continuity (customer power cuts) that Enedis must take into account for investing in grid reinforcement. The low occurrence of such situations (e.g. substation failure) leads Enedis to define a value for deferred investments between €0 and €24/kW/year. This wide range of magnitude results from the fact that the power cutback requests that enable the investment to be deferred are highly dependent on the situations encountered and on their infrequent occurrence.

The maximum value that Enedis would be prepared to pay to solve a situation of congestion would therefore be a maximum of €24/kW/year.

In case of activation – an extremely low occurrence (risk of customer power cuts) – the value delivered to the community for activations facilitating power restoration of cut-off customers, could vary from €0 to € 20k/MWh, depending on the service delivered locally (power restoration time and number of customers).

In extremely rare situations on a national scale, it will be necessary to demonstrate the reliability of power cutbacks versus grid reinforcement, taking into account the value of the service delivered to the community and to the system operator.

B. Feed-in issues

Projections into a future world with a sharp growth of decentralized renewable energies, indicate that the major constraints to be expected in LV and MV grids will involve the integration of solar PV and wind power, which raises issues of injection into the grids.

The recent Enedis study on the Nice Smart Valley[5] case and the CARROS site trial clearly shows a constrained situation in summer, and even from March to May, when the local MV output is high.

In the event of a sharp solar PV growth, the occurrence of such cases will be higher than cases of Offtake issues (cf. Figure 15).

In order to avoid grid reinforcement in response to a feed-in constraint, resolving a situation of power surge in the distribution grid may ultimately require two levers:

- Peak shaving of solar PV output,

[4] Economic valuation of advanced functions on Enedis distribution grids 2017. Contribution of public DSOs - http://www.enedis.fr/developper-les-smart-grids#onglet-valorisation-economique

[5] Simulation 2035 Nice Smart Valley - Enedis October 2019

- Absorption of the output via a dedicated storage system or consumption postponed to solar hours locally.

There again, these levers must be reliable whenever the strains occur, in order to substitute for a grid reinforcement option that would deliver strong guarantees.

It might be expected that the business model would require smart connection offers where producers who want to install their own power facilities and might generate power surges, would need to propose solutions to smooth out their output peaks (battery, peak shaving, absorption by one or several customers with "postponable" consumption, e.g. heat or cold storage).

2.1.6. Adaptation of flexibilities to the characteristics of needs

The ability of flexibility to meet the challenges of distribution system operators depends on the following points:

- **Sufficient availability in the areas concerned**: Flexibility is only valuable if the capacity available at local level is high enough to avoid the use of the usual alternative solutions of network operators. Thus, if we assume that the development of flexibility at national level remains constant, it appears that without a specific incentive to develop flexibility in a given area, capacity will in most cases be insufficient to meet the needs of the distribution system operator so that it won't be an alternative solution for the DSO.

- **Product characteristics of flexibility required to meet needs**: Flexibility characteristics are variable. Their ability to meet the needs of the distribution system operator depends on parameters such as:
  - Minimum and maximum activation times: flexible uses associated with inertial energy storage and electricity storage cannot be activated for a very long period. This is limited energy resource flexibility.
  - Frequency of calls: interruptible uses cannot often be activated because it penalizes consumers' economic activity.
  - Guaranteed or not: the availability of certain flexibilities is not guaranteed in the face of need. However, it should be considered that this unavailability may be correlated with a lack of need for flexibility. As example, constraints in the event of heating peaks may require an availability commitment in order to reduce consumption in the event of excessive peaks. A flexibility composed of electric heating cannot guarantee a fixed power because the controllable power depends on the outside temperature. However, this flexibility is really available on days of constraint. As such, the verification by the distribution system operator of the availability of contractually guaranteed flexibility should consider the correlation of the flexible power available with the need for flexibility.

- **Characteristic of the economic incentive or value created for the electricity system**: Some flexibilities require investments for mobilization as a service for the distribution system operator. To develop flexible capabilities, a market player must have enough visibility on its revenues. As such, variable incomes remunerating infrequent activations (e.g. incidents on the distribution network) will not make it possible to build a business plan encouraging specific recruitment in a given area. For

this reason, flexibility will probably be easier to develop to meet a reduction in the fixed expenses of the distribution system operator.

Conclusion

The flexibility needs on the French distribution grid by 2035 remain limited and should be examined in correlation with the growing electrification of uses and forms of post-meter storage (e.g. second-live batteries).

Moreover, if there is no significant need for flexibility to date, the development of renewable production and electrical usages should generate some in the future.

This market is nevertheless limited over this time frame. At the UFE Conference in October 2019, the Enedis Engineering & Grid Department noted that the economic value of the flexibility market by 2030 for the entire French system may reach around €1 M/year on the offtake side and around €10 M/year on the feed-in side.

2.2. The value of gas solutions for local flexibility

2.2.1. Gas solutions can technically bring flexibility to the local network

In order to provide useful flexibility to the local network, gas solutions must match the technical criteria of the distribution system operator. Those criteria are numerous :

- Reaction time: ability to answer within a limited amount of time;
- Activation duration: minimum and maximum duration during which the flexibility solutions must be activated. These parameters depend on the local constraints' characteristics ;
- Delay between two activations: minimum time during which a same flexibility solution won't be activated;
- Schedule: daily and seasonal time slots during which the flexibility solutions are available for activation;
- Frequency: number of activations during a day. This parameter should depend on the local constraints' characteristics.

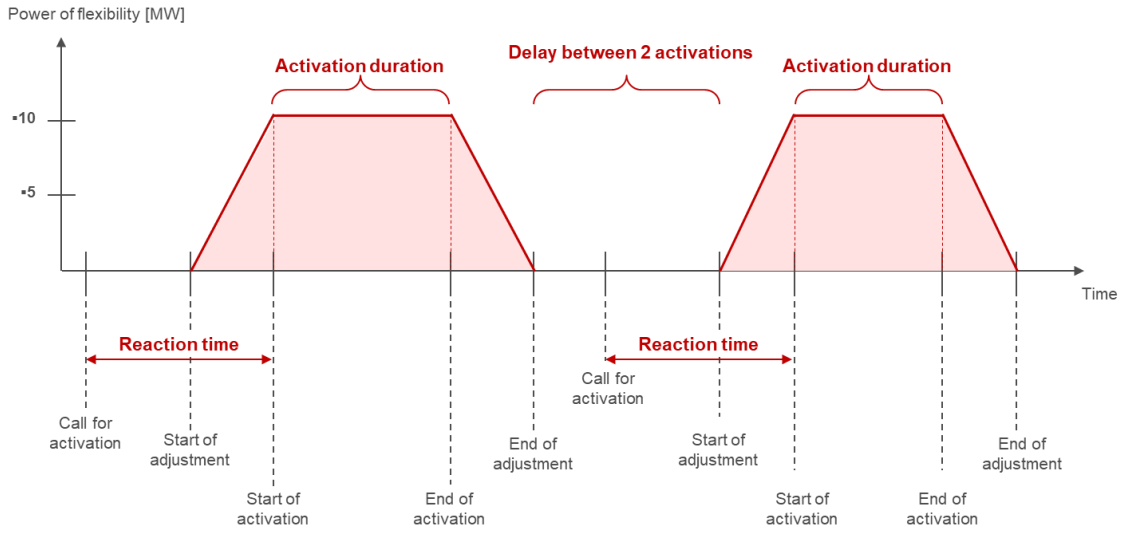

Figure 4 - schematic diagram of the characteristics of a flexibility

The ability to match those criteria is key for the value of local flexibility, as no substitute could be available locally in a case of a failure, contrary to what is possible at the national flexibility market level. Those criteria depend on the local constraints, and may vary between different locations.

All three tested gas solutions – Combined Heat & Power (CHP), hybrid boiler and hybrid rooftop are able to match those criteria, at least in one of the tested locations.

Table 1 - Comparison of local network flexibility requirements and gas solution capabilities

Product criteria	Product defined in InterFlex	Gas solutions		
		CHP	Hybrid boiler	Hybrid Rooftop
Reaction time	D-1 to intraday	✓ *< 5 min*		
Duration	30-min to 2 hours	✓ *no limit*	✓ *Winter: no limit Summer: 2 hours maximum*	✓ *Winter: no limit Summer: 2 hours maximum*
Schedule	Depending on the location	✓ *Winter: heating only during night (18h-6h) Summer: not use*	✓ *Winter: heating (7h-23h) Summer: cooling (7h-18h)*	✓ *Winter: heating (7h-15h) Summer: cooling (7-15h)*
Frequency	Up to 2 per day	✓ *no limit*		
Delay Between two activations	Superior to 2 hours	✓ *no limit*	✓ *Winter: no limit Summer: 2 hours minimum*	✓ *Winter: no limit Summer: 2 hours minimum*

To provide local flexibility, gas solutions have several technical advantages compared to other flexibility solutions. Indeed, these technologies are not limited by a storage or a time threshold to avoid the reduction of the comfort of the final consumer. Therefore, their advantages are:

- Very low reaction time, often less than 5 minutes, without any warning requirement;
- Long potential duration, thanks to the ability of the technology to substitute electricity consumption by gas consumption: the customer is not impacted – in production, or in comfort – by the flexibility;
- No limit on activation frequency;

InterFlex demonstrated that the three gas solutions tested are completely able to participate to a solution preventing local network constraints.

2.2.2. Value of local flexibility of gas solutions in the InterFlex configuration

Additionally to the ability to resolve local constraints, the value generated for the community thanks to the gas solution for the local constraints simulated by Enedis depend on three other parameters:

- The location of each gas solution;
- The time of occurrence of local constraint;
- The power provided by each of the gas solution.

Concerning the location and the time of occurence, Enedis has identified and characterized, within the InterFlex area, the local constraints for each local network (Lingostière, Carros, Guillaumes, Isola). The match between the need of local flexibility and the local capabilities of the installed gas solutions have been assessed time slot by time slot, location by location. Indeed, some areas requires flexibility either in summer or in winter, either at night or during the day, whereas all gas solutions are not able to provide flexibility at anytime – e.g. the CHP is not working in summer. This match is presented on **Erreur ! Source du renvoi introuvable.**, where gas solutions capability and local network requirement are mapped.

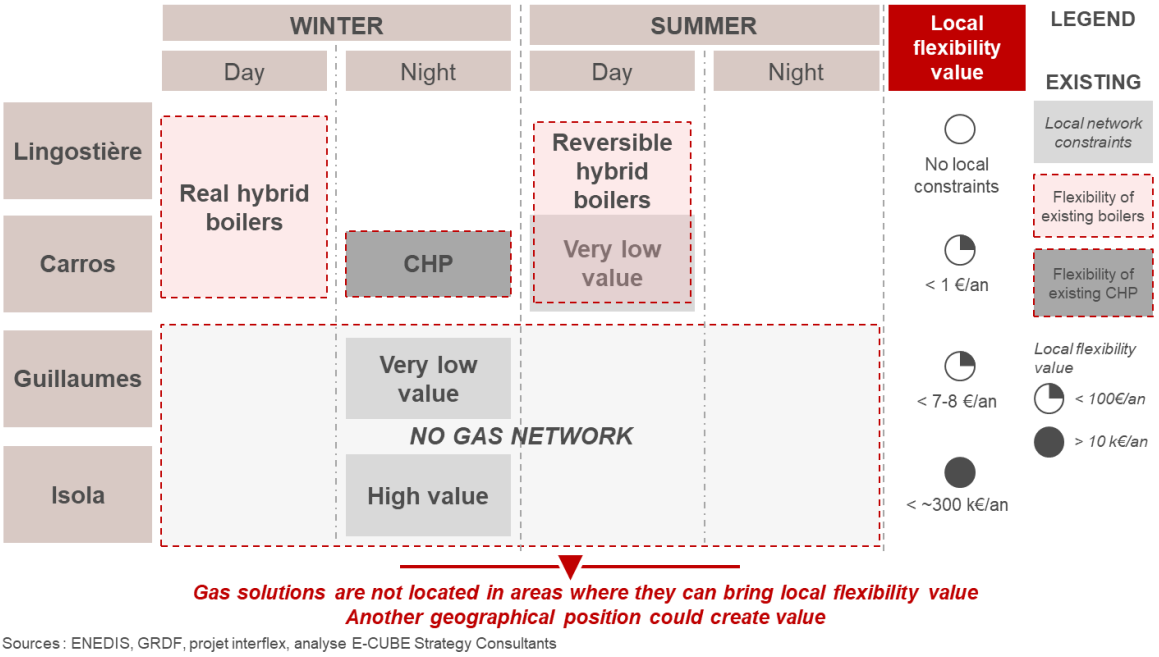

Figure 5 - table of cross-analysis of the capabilities of flexibility gas solutions with local network needs

The **Erreur ! Source du renvoi introuvable.** shows that:

- In areas where local flexibility value is very high – Guillaumes, Isola – there is no gas network, and therefore no gas solutions. This is due to the isolated and inaccessible nature of these areas, while the gas network has historically been built in relatively dense and easily accessible areas, where it is profitable for the community.
- In only one area, Carros, hybrid boilers may bring value to the local network in summer. In all other places, there is no local constraints, highlighting that the local electricity grid in these areas is not constrained, that the evolution of consumption and production are not in a position to put the local network in difficulty.

Therefore, the value of gas solutions for the local network in InterFlex is limited to the Carros location. Enedis has characterized this constraint at Carros with the following characteristics:

- maximum 0,45 MW,
- up to 9 times a year,
- that shall last less than 40 minutes,
- mainly in July, at mid-day.

Due to these characteristics, of the 12 gas equipments[6] installed for the InterFlex experimentations, only three could have provided flexibility to relieve the local constraints: the reversible hybrid boilers that are in Carros – the only ones able to provide flexibility in summer. This limit the potential flexibility theoretically offered to the local network to ~3 kW, which is less than 1% of the maximum constraint.

[6] 10 hybrid boiler, 1 CHP and 1 hybrid rooftop

Moreover, Enedis analysed the upper bound of the value of local flexibility in Carros and found a value of less than 1 €/year due to a very low probability of occurrence of the constraint[7].

In conclusion, if the InterFlex experimentation demonstrated the ability of gas solutions to provide local flexibility services, the current location of these gas solutions and the lack of constraints in the local electricity network reduce the theoretical value of local flexibility to almost zero. Consequently, we propose to extend the analysis by considering other location assumptions and constraints within a sensitivity analysis.

2.2.3. Sensitivity analysis: extrapolation of the value of local flexibility in theoretical situations outside InterFlex

The goal of this sensitivity analysis is to assess an upper bound of the value of local flexibility for gas solution, in a context more favorable than the local network of InterFlex. It is based on theoretical values from E-CUBE's report on local flexibility for CRE[8], which assessed the order of magnitude of the value of local flexibility at the scale of France. Therefore, it is not representative of one specific area.

The use case considers that the gas solutions fleet – the same that was tested at InterFlex - is assumed to be within a local network with N-1 constraints – not as many as in Isola or Guillaumes, not as few as in Carros.

The E-CUBE report analyzed the N-1 situations in France to identify those that could be resolved by flexibility solutions efficiently. The report found that an order of magnitude of 1300 constraints yearly could be managed by local flexibility, with an average value of ~4 €/kW/event.

It leads to a value of 20€/kW, which is consistent with, Enedis[9] evaluation of flexibility value (in between 0 an 24€/kW/year).

Under such assumptions, and if the complete fleet of gas solutions tested in InterFlex was in the same network, it could have expected to create ~750 €/year of value for the local network, split as follow:

- ~50 €/year for the hybrid boiler (2,57 kW expected over the year on average);
- ~500 €/year for the CHP (27 kW);
- ~200 €/year for the hybrid rooftop (~10 kW)

This value must not be considered as an expectancy of the local flexibility value from gas solution at the national scale, but as an upper bound value of local flexibility from gas solutions in places where there are N-1 constraints. It shows that gas solutions in constrained

[7] Which require a simultaneous event of network fault and of high consumption

[8] https://www.cre.fr/Documents/Publications/Etudes/etude-sur-les-mecanismes-de-valorisation-des-flexibilites-pour-la-gestion-et-le-dimensionnement-des-reseaux-publics-de-distribution-d-electricite

[9] Economic valuation of advanced functions on Enedis distribution grids 2017. Contribution of public DSOs - http://www.enedis.fr/developper-les-smart-grids#onglet-valorisation-economique

local networks could generate up to 20 €/kW/year under favorable assumptions in terms of locations, local constraints and value.

2.2.4. Conclusion on the abilities and values of smart gas solutions for the local constraints in Nice Smart Valley

The InterFlex's results on the value of local flexibility from gas solutions show that:

- Smart gas solutions are technically and economically capable of meeting the constraints of the electricity grid operator - examples: incidents of over-consumption, over-production (in the future), need for grid reinforcement.
- However, within the InterFlex network, the absence of value linked to the constraints of the electricity network in areas where gas is distributed implies that there is no local flexibility value for smart gas installations.

This is a limit to multi-energy flexibility: the areas where the electricity grid is most likely to be constrained - distance from the grid, difficult to access area, mountains, etc. - should not be areas where gas is often present.

On a more prospective view, the study conducted by E-CUBE for the CRE in 2017 suggests that situations where smart gas solutions have value could exist. The additional value for smart gas flexibilities could then be positive, reaching a maximum of 9 to 20 €/$kW_{flexibility}$/year.

However, given that these stresses should mainly be in areas where gas is not present, and that these values correspond to cases of significant stresses, they shall not be the norm. The areas where smart gas solutions could have local value are: mainly urban areas where (1) electricity consumption/production is dynamic (fast evolution, requiring the local electricity network to adapt itself, invest or find flexibility solutions), and (2) the ability to improve electricity networks locally at low cost (for technical and cost reasons - particularly land) is low.

3. PERSPECTIVE ON THE DEVELOPPMENT OF OFFERS

3.1. Conditions to develop tomorrow's offers

The development of tomorrow's offers involves

1. reduce the cost of access to flexibility,
2. to have the necessary elements for the construction of the offers, such as the characteristics of the necessary flexibilities and the geographical areas concerned,
3. to allow the valuation of flexibilities on several mechanisms,
4. to organize a mechanism to promote free competition,
5. to prepare this new contract today.

3.1.1. Need to reduce the costs of access to flexibility

Recruitment costs are currently too high in comparison with revenue for this market to develop, for the following reasons.

Lack of consumer interest in flexibility

Consumers want above all to reduce their energy bills while improving their comfort. They are not interested in a value proposition based on flexibility because the annual benefit is too low (5% gain on the electricity bill on average) compared to the complexity and perceived constraints of the offer.

To overcome this hurdle, it seems interesting to integrate the value of flexibility into a global energy efficiency approach aimed at meeting key consumer expectations. Flexibility then only serves to reduce the cost of service provided to the customer by using the control systems set up as part of the offer in order to enhance flexibility on different value pockets.

Lack of maturity of consumers

The vast majority of consumers are unaware of the new challenges facing the electricity system as part of the energy transition. The stakes around flexibility can be perceived as a regression in the quality of supply.

There is a need to further educate the consumer to become an actor in the energy system.

The value proposition is too complex for consumers

Consumers are not aware of the organization of the electricity system and the different roles involved in the supply (supplier, balance responsible, aggregator, distribution and transmission system operator). However, they are confronted with it because of regulatory constraints that confront consumers with this complexity via signature forms that have been designed for large industrial customers.

This complexity disrupts the contracting process and at the same time does not fulfil its informative role since the consumers who sign do not understand the form meaning.

It is necessary to simplify procedures by adapting them to residential customers and small and medium-sized companies.

Installation costs are too high compared to the value

Access to flexibility requires the implementation of a command and control chain that is costly in comparison to the gains. These costs could be reduced by developing communication standards that would make it possible to manage customer usage without installing specific equipment.

3.1.2. Have the necessary elements for the construction of the offers

To build offers market players need information about the characteristics of the flexibility that the network operator is looking for. Indeed, they need elements to determine the type of flexibility they need to buy. As these flexibility monetization offers are aimed at a mass

market or medium-sized customers, they must be standardized in order to be economically relevant.

3.1.3. Valuation of flexibilities on several mechanisms

The value of local flexibility alone is not sufficient to finance the development of a flexibility portfolio to date. It is necessary to be able to value a given flexibility on several pockets of complementary values when relevant.

3.1.4. Organization of a mechanism promoting free competition

Free and healthy competition is necessary to allow the distribution system operator to buy local flexibility at the best price. This must be considered in the organization of local mechanisms and in the publication of data on the functioning of the market.

1- Information required for recruitment:
   a. As the need for flexibility is very localized, aggregators need very specific information to determine relevant prospection areas.
   b. Need to get the consumption history of local consumers and producers who have agreed in order to finely assess their available flexibility and its value.
   c. In case of new local market: need to publish the reasons for the existence of this market so that the aggregators can assess the economic opportunity to recruit and offer the DSO flexibility on a given area.
   d. In the case of an existing market: need for a transparent publication of historical price data to encourage aggregators to develop flexibility in areas where it has the most value.

2- The aggregators need the merit order rules of the offers if ever the merit order would effectively depend on other parameters than its price alone. For example, its location relative to the transformer sub-station could have an impact on the value for the DSO. Therefore, in order to recruit the most valuable flexibility, the aggregator need to know the merit order rules involving other parameters than the price if any.

3- Additional elements required for free competition.
   a. Level playing field between technologies that provide flexibility (generation, consumption and storage);
   b. Possibility for new entrants to enter the local market after it started.

3.1.5. New markets

The implementation of these new local mechanisms will be complex and should take several years to lead to an operational target mechanism. Due to this complexity, it is necessary to build this mechanism step by step, while considering the feedback from the tested offers.

Hence, it is necessary to get prepared by developing local portfolios and the local use of flexibility, even in the absence of short-term needs, through some kind of public support mechanisms (such as the TSO flexibility capacity tender in France). Otherwise, when flexibility will be required, for lack of preparation, the only solution is likely to be to reinforce networks; which may cost more. So this short-term investment is needed to create more long-term value for the electrical system and the consumer.

3.2. Synthesis of missing ingredients to be tested elsewhere

- According to the studies carried out, excluding incidents periods and grid reconfiguration, the constraints appear mainly due to the development of local production in the face of stagnant or declining consumption.
- Constraint events on the distribution network are likely to occur for a few hours a year when production is too high in comparison with consumption. The project did not consider the management of production systems and the economic opportunity of such management as an alternative and in addition to the consumption flexibility.
- In addition, the project only considered dynamic flexibilities. However, it appears that part of the needs could be covered by a durable deformation (static flexibilities) of the load curves. These deformations could occasionally be supplemented by dynamic deformations activated according to punctual needs or constrains. Such a mix of static and dynamic flexibilities while providing the same service to the distribution network might increase customers' acceptance. This needs to be tested.
- Finally, the project tested an operational mechanism but did not study the modalities for the progressive deployment of these mechanisms in terms of the development of tools, processes and increasing complexity of the mechanism, which must be adapted to financial issues.

4. MV NETWORK SIMULATIONS IN 2035/2036 IN USE CASE 3 AREAS

4.1. Context and objective

The study below follows on from two previous simulation campaigns which made it possible to:

- estimate useful flexibility volumes which could resolve possible constraints on the electricity grid and then from this deduce flexibility products (cf. Appendix 1 to D9.1); and
- analyse the impact of the location of flexibility on useful volumes (cf Appendix C §1.1).

The objective of this new simulation campaign was to analyse how the constraints identified in the previous simulation campaigns could evolve by around 2035, taking into account scenarios of introduction of electric vehicles, renewable energies, and changing customer uses on the grid.

The new simulations were performed mostly in the same context as for the study performed in 2017 on the potential constraints that could appear on today's grid. In other words, only situations of HV power loss and/or loss of the HV/MV transformer are studied. The list of zones analysed in the framework of *Nice Smart Valley* is as follows:

Table 2 - Summary table of N-1 situations tested

Test zone	Component faults or works leading to the studied N-1 recovery situation
Isola2000	HV branch substation
Guillaumes	HV branch substation with a single transformer
Broc-Carros	HV/MV transformer (substation with a single transformer)

4.2. Assumptions and input data

A number of assumptions were defined in order to limit the range of possibilities by freezing certain parameters.
The assumptions detailed in this study are made within the framework of a smart grid demonstrator and do not reflect the current planning methods of Enedis. Moreover, the approaches used cannot be directly extended to all the grids managed by Enedis, because the situations studied within the framework of NSV are particular and are in no way representative of all of Enedis's grids.

4.3. The grid

For these simulations, we have chosen to start again **with a grid identical to that simulated during the first two simulation campaigns**. Note that in reality the grid evolves as connections and consolidation are performed, and that the results of the simulations may differ depending on the simulation dates. The reason why this choice was made is that it makes it possible to compare more effectively the results in 2015/2016 with the results obtained after 2035/2036 trajectory simulations. Moreover, it is not possible at present to know how the grid will have developed by 2035.
Depending on the zone, the amplitude of consumption and production levels may be such that the recovery situation could differ from one hour to the next. For these simulations, we have chosen to freeze the N-1 situation in the worst case at maximum production. Note that the flexibility volumes and the constraints are upper bounds and not minimum volumes.
This analysis avoids any probabilistic consideration related to the appearance of the N-1 configuration studied. Also, **the economic aspect is not studied**.

4.3.1. PACA 2035 scenario

To establish its projections in a context of massive integration of production based on renewable energies, electric vehicles and changing consumer uses on the 2035 horizon, Enedis used scenarios based on 500 determinants[10].

Four scenarios have been defined by Enedis for the Provence-Alpes-Côte d'Azur (PACA) region, with annual time intervals corresponding to four possible trajectories:

- Purple scenario: economic vitality (+1.7%/year GDP) and demographic vitality, development of RES and substantial electrification of transport.
- Grey scenario: economic growth (+1.3%/year GDP) and population growth, development of RES, energy efficiency and electric transport.
- Green scenario: economic growth (+1.3%/year GDP) and population growth, significant energy transition effort (RES, energy efficiency, electric transport).
- Blue scenario: low economic growth (+0.6%/year GDP) and low population growth, slow energy transition, and forced low energy consumption.

The following matrix diagram puts into perspective changes in the various criteria.

[10] Parameters of the model making it possible to establish the scenario on the local level.

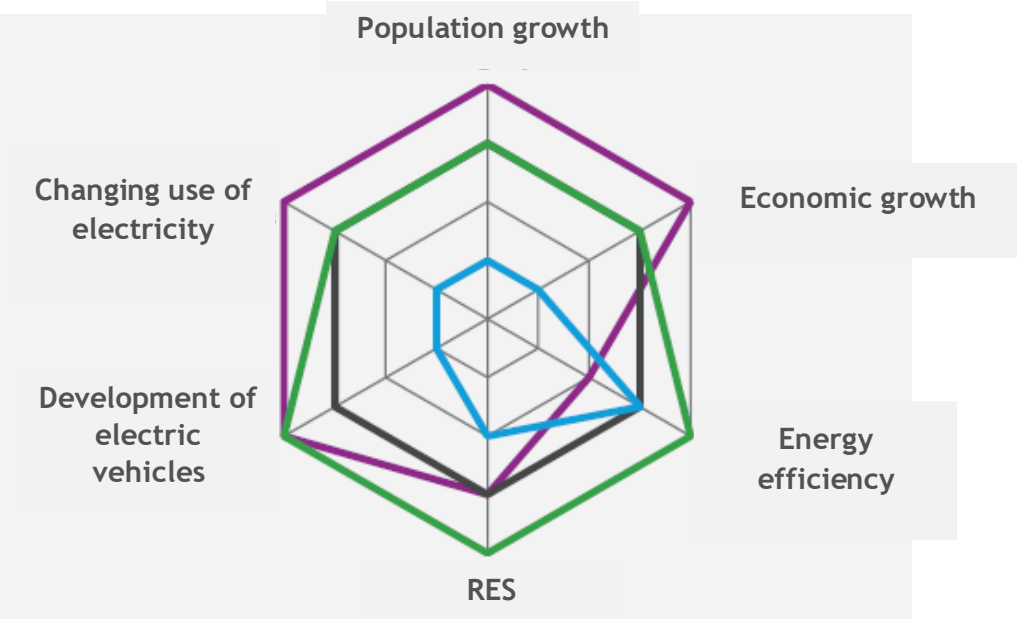

Figure 6 – Spider-web matrix showing the differences between the scenarios

A large part of the territories in the Nice Smart Valley project are located in the NCA metropolis. The consortium wanted to leave the choice of scenario up to the NCA metropolis. ***Since the metropolis selected the green scenario, it is therefore this scenario that Enedis took into account for its simulations.***

For these simulations, we took into account and processed the following data extracted from the green scenario:

- The number of electric vehicles of various types (residential, business, car sharing programmes, etc.) in districts having test grids.
- The quantity of photovoltaic installations connected to the MV and LV grids in the region, as an annual moving average, at all voltage levels.

These data were used in the preliminary processing described below (cf. § 4.4).

4.3.2. Consumption (excluding EVs)

The first step was to obtain a charge curve accounting for the estimate of the zone's state of charge in 2035. To do this, Enedis started again from the two years of net consumption charge curves[11] of the source substations studied for the constrained periods. As a reminder, the data are segmented into two periods: "Summer"[12] and "Winter & Inter-season"[13]. ***The***

[11] The net consumption corresponds to the active power passing through the source substation, to which is added the power injected by the producers connected to said substation. This power therefore corresponds to the total consumption of the substation (customers' consumption + losses).

[12] Considered here as the period between 1 June and 30 September.

[13] Considered here as the period between 1 October and 31 May.

underlying assumption is that the charge curves of adjacent source substations in a given geographic area are identical[14] (in form and level).

4.3.3. Electric vehicles

Location of charging points

The setting up of electric vehicle charging points in the test grids was carried out by an approach developed for Enedis's national impact studies on electric mobility.

Enedis has worked on models making it possible to distribute these charging points over the MV/LV substations studied in accordance with deployment of the green scenario.
For placing the electric vehicle charging points, the number, type and power of the charging points to be installed in each MV grid were defined by means of algorithms based on random sampling in predefined likelihood functions.

Enedis has developed prospective scenarios taking into account assumptions relating to the development of electric mobility. Processing of these scenarios makes it possible to have projections, on the district level, concerning the introduction of electric vehicles by around 2035. At the level of each district, these vehicles were divided into categories according to probabilities relating to housing areas.

4.3.4. Categories of electric vehicles taken into account

In this study, three types of electric vehicle charging points (CPs) are considered:

- Residential charging points (residential CP - 3.7 and 7.4 kVA).
- Corporate charging points (corporate CP - 3.7, 7.4 and 22 kVA).
- Charging points dedicated to shared mobility (car sharing CP - 3.7, 7.4 and 22 kVA).

Note that the public charging points were not modelled here, because there were major uncertainties concerning their use when working out this set of assumptions.

Enedis considered that each category of vehicle cannot be recharged on all types of charging points. For example, a residential vehicle will not be recharged on charging points dedicated to shared mobility. Hence, "fractions" of charging points of each type have been allocated per vehicle for each category. In rural areas, for example, a charging point at home will be assumed for each vehicle, but also a charging point at work for several vehicles. In this way, the numbers of charging points by type of district were obtained.

[14] This assumption was able, in particular, to simplify the automation of simulations.

4.3.5. Distribution of electric vehicles on the grid

The number of charging points defined previously now has to be distributed over the electricity grid. This was done by considering all the LV grids in the district and identifying for each grid the potential locations for charging points of each type. For example, for charging points of the corporate type, we located so-called "professional" customers that are considered able to receive a corporate type charging point. The distribution of the charging points of each type between grids is then performed in proportion to the number of potential locations associated with that type.

4.3.6. EV charge curve

Having available the list of MV/LV substations to which electric vehicle charging points will be connected, Enedis created curves representing one recharge per day for each of these MV/LV substations. They were defined by means of likelihood functions based notably on other smart grid projects in France. The charge curves are aggregated at the level of an MV/LV substation, which means that they may contain a large number electric vehicles in recharging, or none.

At first approach, it was decided that the daily EV charge curve for a given MV/LV substation would be repeated for all the other days simulated. At the electric vehicle charging level, each curve therefore corresponds to an illustration of a possible consumption curve for a given day. The possible variations regarding electric vehicle recharging are therefore not taken into account in modelling the charge at the level of the MV/LV substations.

We have seen how the electric vehicles case was dealt with, and we will now examine the case of production.

4.3.7. Production

The idea was to take the figures of the green scenario and distribute the additional RES production (by comparison with the existing situation) by process (hydropower and PV in this case) and by power on the Enedis grids. This distribution is done for MV and LV.

4.3.8. Hydropower production

Since the development of hydropower is now very limited, ***Enedis has not assumed any increase in hydropower production levels on its grids***. It would indeed have been very complex to project scenarios with the integration of new hydropower producers, not for reasons of potential location, but from the viewpoint of estimation of injection curves. Models for the prediction of hydropower production are very complex because they depend on numerous non-measured local parameters.

4.3.9. Wind power production

For the PACA region, wind power production was broken down by producer categories (3, 6, 9 and 12 MVA). Given that there is little wind power production planned on the regional level in the green scenario, the random samples obtained via the wind power distribution algorithms seldom place this on the source substations studied in NSV. That is why these simulations contain no new wind power producers in 2035.

4.3.10. Photovoltaic power production

Sampling via a Monte-Carlo algorithm was performed in order to distribute the PV volumes of the green scenario over the zones of the Nice Smart Valley project. Within the framework of Nice Smart Valley, it seemed interesting to carry out batteries of simulations with different PV placements[15] . This small number of PV placement samples therefore does not cover all the possibilities, but could highlight certain trends or effects.

For the PACA region, photovoltaic power production was broken down by producer categories: 3, 6, 9 and 12 MVA.

Regarding photovoltaic power production, it was considered that the existing producers remained in place and that the producers on direct feeders of power less than 12 MVA would increase their power by 10% ("repowering" for the producers not needing to redo their connection).

These sampling operations were performed in order to obtain a distribution of PV (in power and location). Two cases should be considered: production on a mixed feeder and production on a direct feeder[16]. Note that in both cases, and at this stage, the algorithm does not include a thorough topographic analysis, and production could be placed in potentially unsuitable areas.

For production on mixed feeder:

The placement algorithm randomly selects MV feeders according to probabilities specified below, and identifies, on each of them, a random MV/LV substation on which to connect the producer. For each MV feeder, the useful information for working out probabilities concerns the type of zone in which the MV/LV substations are located (including the Emerald Zones).

The Emerald Zones are not used here as quality-of-supply zones, but they can characterize the type of territory (very urban/urban/rural/very rural). The distinction in the "FACE" regime is characterized by only two categories allowing a breakdown of production into 8 classes. These classes made it possible to identify how production is currently distributed on the distribution grids. These same classes were then used again to distribute the production to be included on mixed feeders.

[15] Given the time allotted, only 3 different placements were analysed.

[16] Enedis considered that the power thresholds above which producers are connected by direct feeder remain identical to the case in 2019.

For production on direct feeder:

For production on direct feeder, a map of France was therefore considered (taking out the forests, cities, etc.). This gives potential zones in which to include RES production. Then, like in the case of mixed feeders, we use the probabilities of categorization of existing production per region to do sampling. An algorithm then made it possible to link the GPS coordinate of the production farm to the nearest source substation.

New producers were connected directly to the half-panels in HV/MV substations without taking into consideration a connection cable length.

For LV production:

For LV production, a study of the existing situation was performed to identify the types of MV/LV substations most suitable for the insertion of LV PV. It took into account:

- Rural/urban area.
- Grid density (number of LV customers/grid length).
- Substation power.

These elements made it possible to define probabilities of appearance of PV per MV/LV substation. Random sampling was then used to place photovoltaic production on the grid.

4.4. Pre-processing

A number of pre-processing operations were performed to be able to initiate simulations and obtain results.

4.4.1. Consumption (excluding EVs)

As said earlier, the first step was to obtain a charge curve accounting for the state of charge in 2035. The idea was therefore to identify the proportion of heating in the charge curve 2015/2016 in order to take into account the thermal improvement of buildings in 2035.

Change in the proportion of heating

At Enedis, the consumption of a source substation is modelled via three parameters: a constant similar to the average power of the source substation in question, a temperature spline, then a calendar spline. The idea behind this modelling is to estimate that the variability of consumption of a source substation relative to a mean depends exclusively on the temperature and the period in question.

The heat-sensitive fraction of the charge was accordingly isolated and modified in the conditions explained below.

Note that the heat-sensitive charge includes the heating fraction but potentially other heat-sensitive uses. ***We have assumed that heat-sensitive*** *(representating* the improvement in the buildings' thermal envelope) ***uses are reduced by 15%.***

To convert the charge curve for 2015/2016 into a charge curve in 2035/2036, Enedis retrieved temperature curves from 2015/2016 and then applied a consumption reduction factor of 15% explained above and chosen arbitrarily modelling the improvement in the buildings' thermal envelope.

Note: The same principle was applied to know the air conditioning fraction in the charge curve.

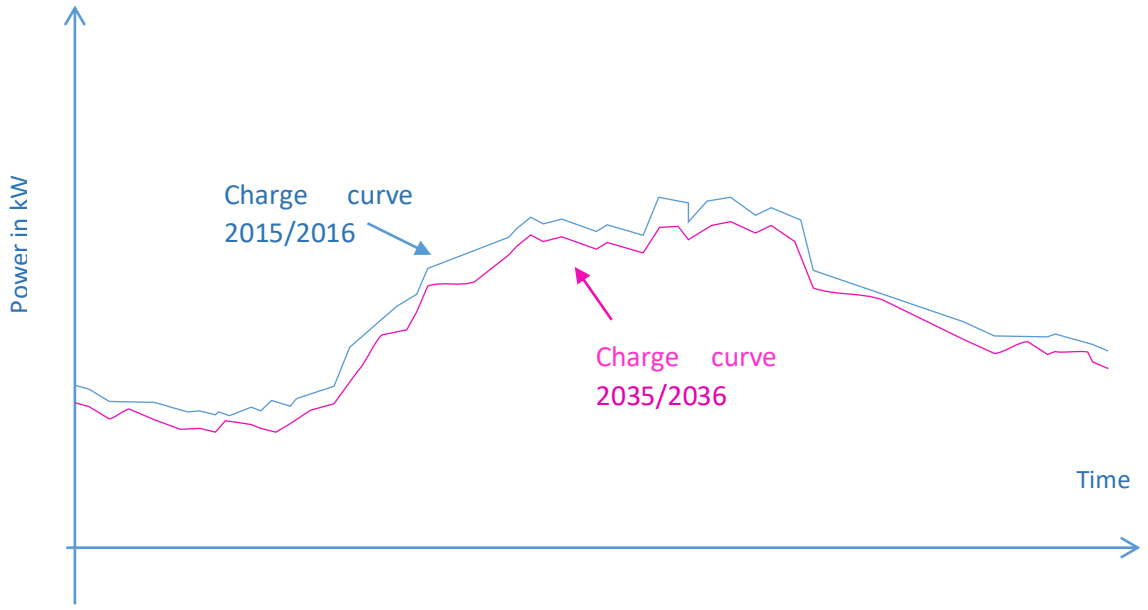

Figure 7 - Example of charge curves simulated in 2035 after allowing for the improvement in thermosensitivity

4.4.2. EV charge curve

As already mentioned, Enedis has worked on models making it possible to distribute these charging points over the MV grid studied. Enedis's Nice Smart Valley team was able to benefit from other work related to the impact of the electric vehicle on the grid. Algorithms were therefore used again to obtain charge curves for all types of charging points.

For each of the substations listed in Enedis's green scenario, random sampling was performed to calculate and define an overall curve for each MV/LV substation.

The Table 2 below presents a fictitious example illustrating the approach.

Table 3 - Breakdown of charges by CP and type of terminal for an imaginary MV/LV substation

	Residential CP			Corporate CP			Car sharing CP		
Power	3.7 kW	7.4 kW	22 kW	3.7 kW	7.4 kW	22 kW	3.7 kW	7.4 kW	22 kW
Quantity	2	1	0	6	1	0	1	3	1

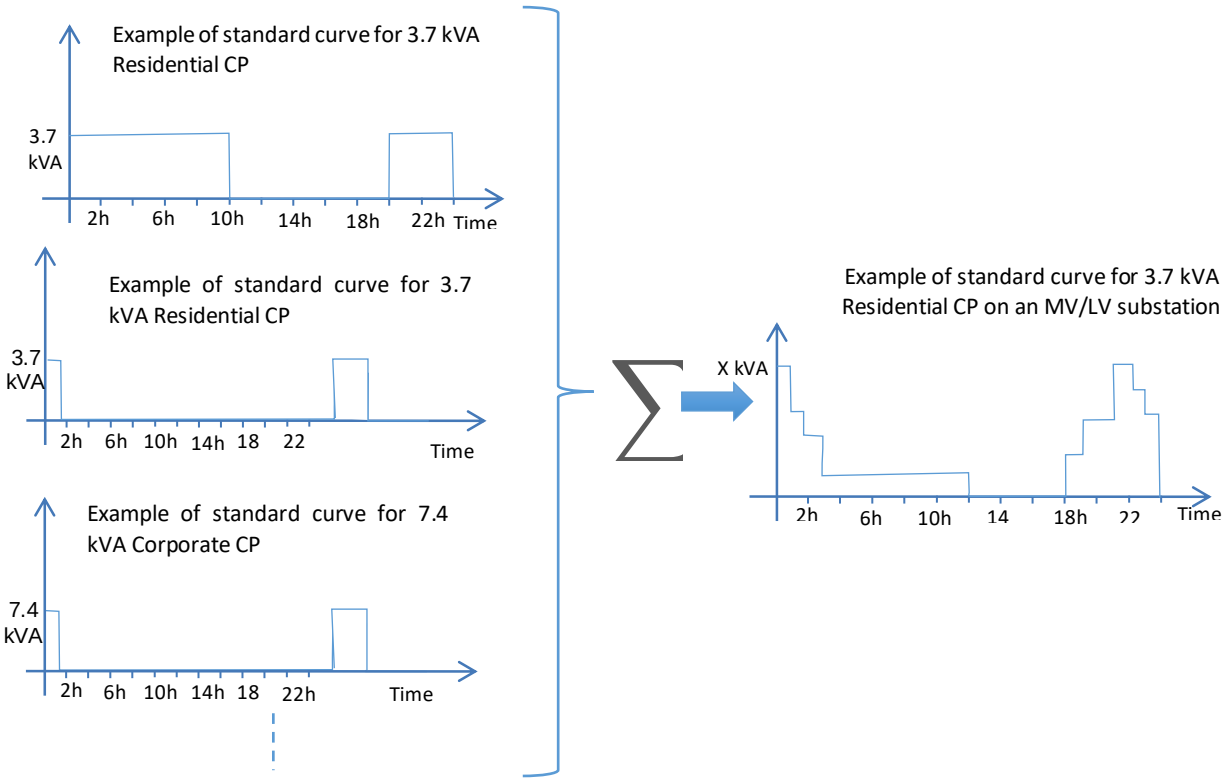

Figure 8 – Example of imaginary electric vehicle charge curves for an MV/LV substation

4.4.3. Photovoltaic power production curve

Enedis has insolation curves (solar radiation on the ground) coming from the ARPEGE 100 model of Météo France[17].

With a view to simplifying the procedure, Enedis assumed that photovoltaic panels (existing and new) received sunlight identically, without considering the orientation of the panels. This factor will probably have the effect of increasing the constraints obtained in the results for the following sections. Note that, for self-consumption purposes, it is not uncommon to have photovoltaic panels oriented so as to produce less energy over one day, but especially over periods where panels facing full south would produce less.

These normalized production curves[18] do not take into account the real-world environment of the producers (effect of shading, for example).

[17] Based on the ARPEGE 100 data flow, 27 variables (temperature, solar radiation, wind at various altitudes, convective energy, precipitation, etc.) are extracted on a grid configuration covering France in a spatio-temporal manner with very great precision (0.1° latitude/longitude, i.e. 11 x 7 km, hourly interval) and on a horizon of 4 days. This weather data flow allows the Enedis forecasting tool to have novel variables such as the risk of storms, precipitation or nebulosity, etc.

[18] We assumed that all the panels were facing full south and that solar radiation (as a %) multiplied by the PV producer's installed capacity (in kW) gave its production at a given time interval. Accordingly, the charge factor as a % is equivalent to the solar radiation as a %.

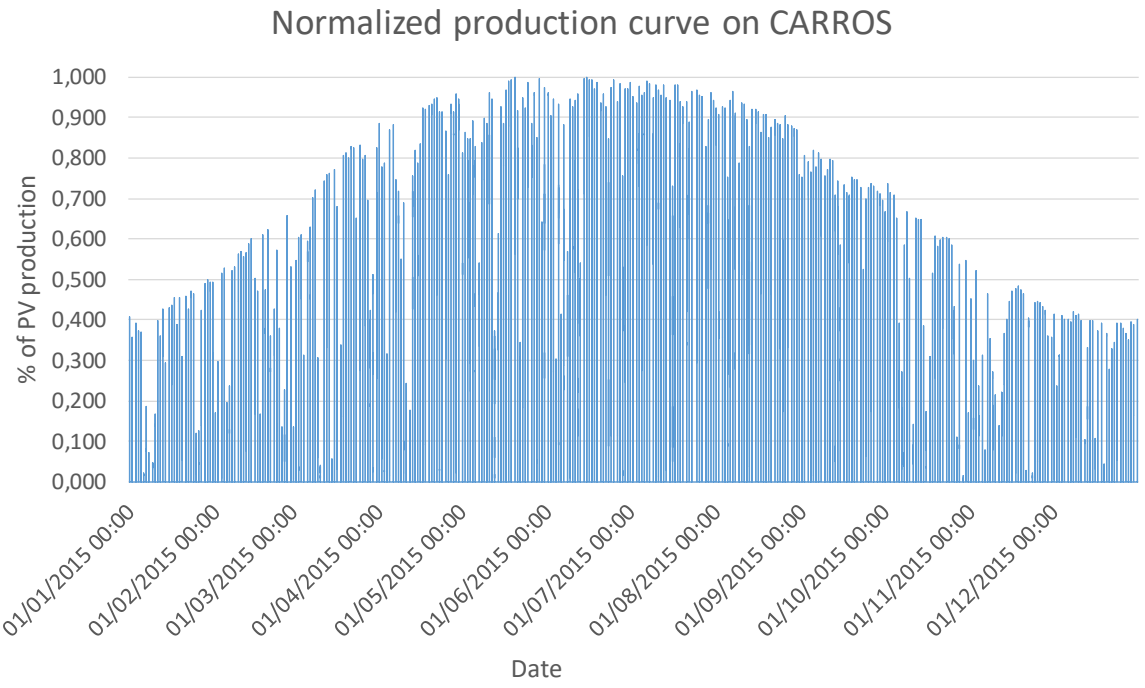

Figure 9 – Normalized PV production curve on the CARROS zone

We assumed that the existing producers would still be present on the 2035 horizon. They were assigned the same normalized injection curve as the new PV producers. A simple multiplication of the normalized curve by the producer's maximum capacity gives the producer's production curve.

4.4.4. Hydropower production curve

As was written previously, it is not common to predict the injection curve of a run-of-river hydropower producer, because it depends on numerous parameters which are hardly predictable, such as melting snow and precipitation (cf. § 4.3.8). It was therefore decided to use injection curves from 2015/2016 in the simulations for 2035/2036.

4.5. Results

The following section outlines the principle, the results and the analyses of the various simulations performed on the zones of the Nice Smart Valley project in the green scenario.

4.5.1. Definitions of constraints

During the various simulations several types of constraints were monitored:

- Current in grid equipment in draw-off and injection (lines/cables): Compliance with the IMAP values[19] for cables and lines.
- Current in the HV/MV transformer: Compliance with the capacitance thresholds of the transformer, which are 110% in N configuration and 125% in N-1 configuration.
- Current at the feeder terminal: Compliance with the 400 A threshold which is related to the capacitance of the feeder circuit breakers.
- Voltage rise: Compliance with the 2% threshold in voltage rise.
- Voltage drop: Compliance with the thresholds of 5% in normal configuration and 8% in backup configuration.

The useful flexibility volumes[20] for resolving constraints were calculated with the diffuse flexibility mode (cf. APPENDIX C -$ 1.1).

4.5.2. Principle of the simulations

The principle of the simulations was to simulate possible states of the grid. To do so, Enedis used the charge curves established earlier and simulated each state of the grid. In other words, for each grid, all the 10-minute points for two years were tested.

There were three major stages in these simulations:

- Establishment of the N or N-1 configuration which will be fixed for the whole battery of simulations.
- Initiation of loadflow calculations according to the charge scenarios.
- Verification of the presence or absence of constraints.

To verify the presence or absence of constraints, we have chosen to represent the results via 3-dimensional graphs by seasonality, to show the impact of each parameter on the constraints. Here are the graphs which will be presented in the following sections:

- Graph 1: Consumption (excluding EVs), PV, and EV consumption.
- Graph 2: Consumption (excluding EVs), PV, and hydropower production.

[19] IMAP: "Intensité Maximale Admissible Possible" (maximum possible acceptable current).

[20] Useful flexibility volume: Corresponds to the flexibility volume making it possible to resolve the electrical constraint.

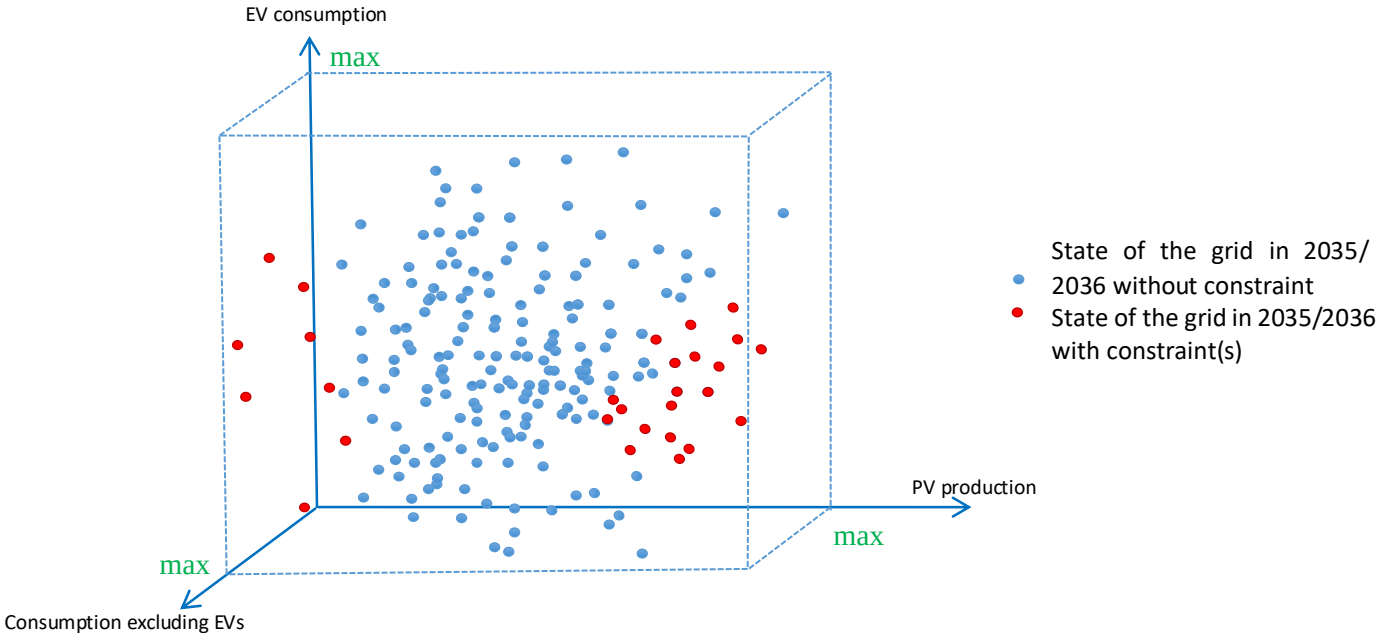

Figure 10 – Graphic example of results in 3D (consumption, PV production and EV consumption)

To simulate all these constrained states, the charge curves were used:

- Charge curve of estimated consumption excluding electric vehicles in 2035/2036.
- Charge curves of electric vehicles by MV/LV substation (cf. § 4.4.2).
- Curves of PV production per MV/LV substation (cf. § 4.4.3).

When the simulations were very time-consuming[21], Enedis used a simplified method to reduce all the points to be simulated.

The idea is to start with the extremes (Max. production & Min. consumption / Min. production & Max. consumption). If there is no constraint, then the intermediate scenarios are not calculated (because no constraint); otherwise, the space is reduced gradually until there are no more constraints.

- Here are the extreme cases taken into account:

Table 1 - Examples of extreme cases simulated

Extreme case	Consumption excluding EVs	EV consumption	Production (PV and hydropower)
1	Maximum	Maximum	Minimum
2	Minimum	Minimum	Maximum

[21] This depended notably on the quantity of calculations performed by the software. For example, in a dense zone with a lot of looping in the grid topology, the calculation time is longer than for a low-density zone.

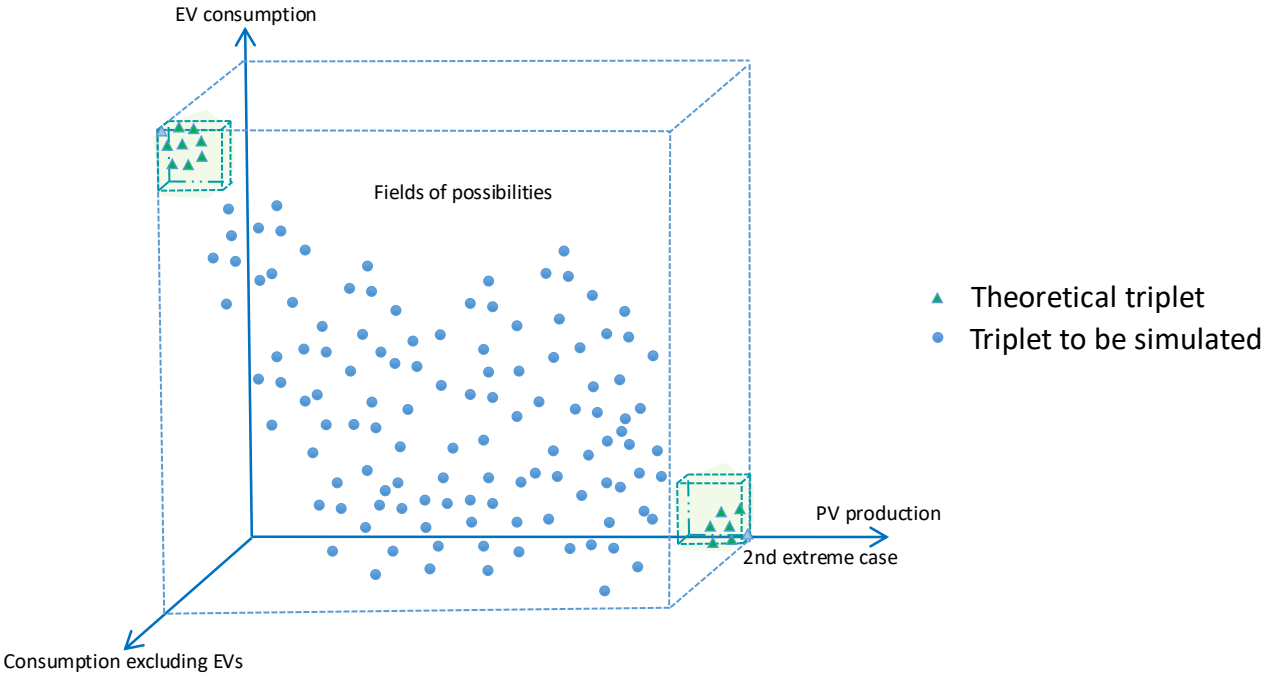

Figure 11 – Explanatory diagram of the point restriction method

The batteries of simulations are initiated based on the results of this analysis:

- If there is no constraint, there is no need to run the battery of simulations.
- If there are constraints, the part of the cube that could be constrained is simulated. The constraints are plotted in layers: first the voltage rise constraints, then the current constraints at the HV/MV transformer level, down to the feeder-terminal current constraints, which gives the impression of layers of colours.

Note that the points in current constraints at the HV/MV transformer level are also in voltage rise constraints and that the points in feeder-terminal current constraints are also in current constraints at the HV/MV transformer level and in voltage rise constraint.

4.5.3. Summary of results

Table 4**Erreur ! Source du renvoi introuvable.** and Table 5**Erreur ! Source du renvoi introuvable.** show the situations analysed with the related input data and summarize the results.

Legend:

- U ↗ : High-voltage constraint.
- U ↘ : Low-voltage constraint.
- I_{Line} : Related current constraint in at least one line/cable.
- $I_{Transfo}$: Related current constraint in at least one HV/MV transformer.

Table 4 - Recap of simulated situations and results obtained in a normal situation (N)

No.	Zone	Season	PV location (sampling)	EV location (sampling)	Constraints		% of constrained points
					Yes/No	Types	
1	Carros	Summer	1	1	NO	-	-
2			2		NO	-	-
3			3		NO	-	-
4		Winter & Inter-season	1		NO	-	-
5			2		NO	-	-
6			3		NO	-	-
7	ISOLA	Winter & Inter-season	1		NO	-	-
8			2		NO	-	-
9			3		NO	-	-
10		Summer	1		NO	-	-
11			2		NO	-	-
12			3		NO	-	-

Erreur ! Source du renvoi introuvable.

As a reminder, the N-1 situations looked at are:

- ISOLA2000: N-1 HV (HV branch substation);
- GUILLAUMES: N-1 HV (HV branch substation and substation with a single transformer);
- BROC CARROS: N-1 HV/MV transformer (substation with a single transformer).

Table 5 - Recap of situations simulated in degraded configuration

o.	Zone	Season	PV location (sampling)	EV location (sampling)	Constraints		% of constrained points
					Yes/No	Types	
13	Carros	Summer	1	1	No	-	-
14			2		No	-	
15			3		Yes	U ↗	3
16		Winter & Inter-season	1		No	-	-
17			2		No	-	-
18			3		Yes	U ↗	0.38
19	Isola	Winter & Inter-season	1		Yes	U ↗ U ↘ I_{Line} $!_{Transfo}$	5.57
20			2		Yes	U ↗ U ↘ I_{Line} $!_{Transfo}$	12.26
21			3		Yes	U ↗ U ↘ I_{Line} $!_{Transfo}$	5.64
22		Summer	1		Yes	U ↗ I_{Line} $!_{Transfo}$	25.73
23			2		Yes	U ↗ I_{Line} $!_{Transfo}$	35.49
24			3		Yes	U ↗ I_{Line} $!_{Transfo}$	25.83

Note that the results for the third zone, "Guillaumes", are not presented here because they were still being gathered at the time of writing this report.

In light of the results shown in the table, the following observations can be made:

- In Carros, only one of the three locations for the PV scenarios would lead to voltage rise constraints in N-1 configuration for certain times simulated. The other two locations showed no constraint. This could be explained by the fact that one of the PV location placements in Carros showed the installation of a higher level of PV, which results in a higher probability of occurrence of constraints.
- In Isola only the locations in N-1 configuration would result in constraints (all types of constraints), notably because there is very substantial production in the zone. Note that there remain some draw-off constraints at night, when there is no photovoltaic power production.

4.5.4. Results of simulations on the CARROS zone

In this section, only the simulations with constraints will be detailed.

4.5.4.1. Results of simulations corresponding to situation 15

As a reminder, simulation 15 corresponds to the following situation:

Table 6 - Recap of input data used

Simulation 15	
Scenario	Green
PV locations	3
EV locations	1
Situation	N-1
Seasonality	Summer

For information's sake, Figure 12 **Erreur ! Source du renvoi introuvable.**below shows the location of the big producers on the constrained feeder.

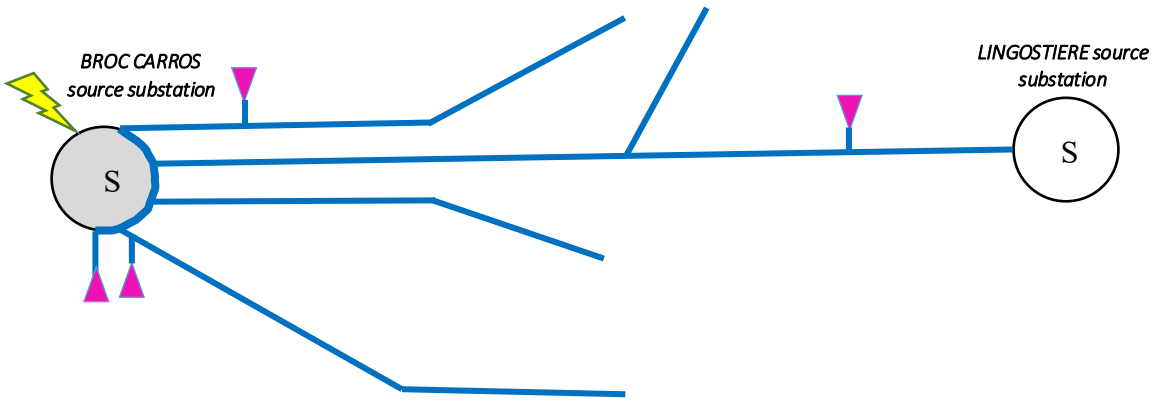

Figure 12 - Diagram of the constrained feeder with location of the big producers (>250 kVA)

Three of the four producers are located near the Broc Carros source substation. A single producer is connected to the Lingostière backup feeder which helps restore power for customers connected to the Broc Carros source substation.

3D graph with consumption (excluding EVs), PV production and EV consumption

The following graph (**Erreur ! Source du renvoi introuvable.**) shows the EV consumption and PV values and consumption (excluding EVs) for the case expressed in **Erreur ! Source du renvoi introuvable.**. It shows a single type of constraint in voltage rise. The constraints appear at ***consumption levels below 6 MW***, i.e. about 56% of the feeder's maximum charge, and when the ***injection of the photovoltaic panels exceeds 9.5, i.e. about 65% of their installed capacity***.

The simulated placement does not contain a sufficient charge ***to generate draw-off constraints***. We can see that the maximum EV consumption is relatively low relative to the PV level. These EVs added to the simulated charge of 2035/2036 ***result in no current constraint during consumption peaks as*** could be seen potentially in 2015/2016.

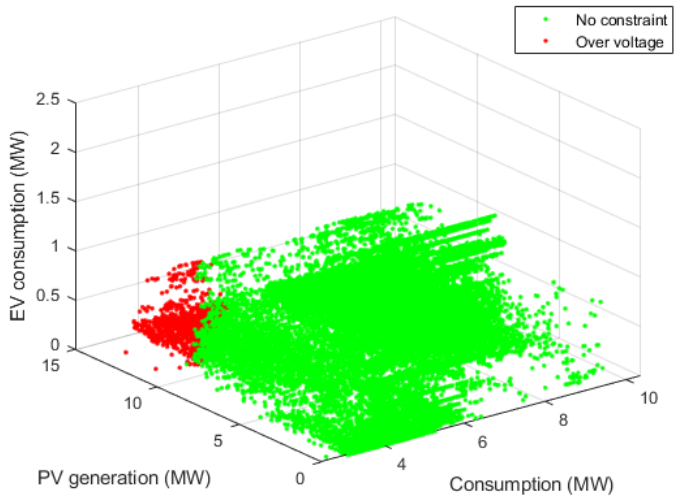

Figure 13 – 3D graph: Consumption (excluding EVs), PV Production and EV Consumption for the constrained backup feeder at Carros in summer, on the assumption of an N-1 configuration

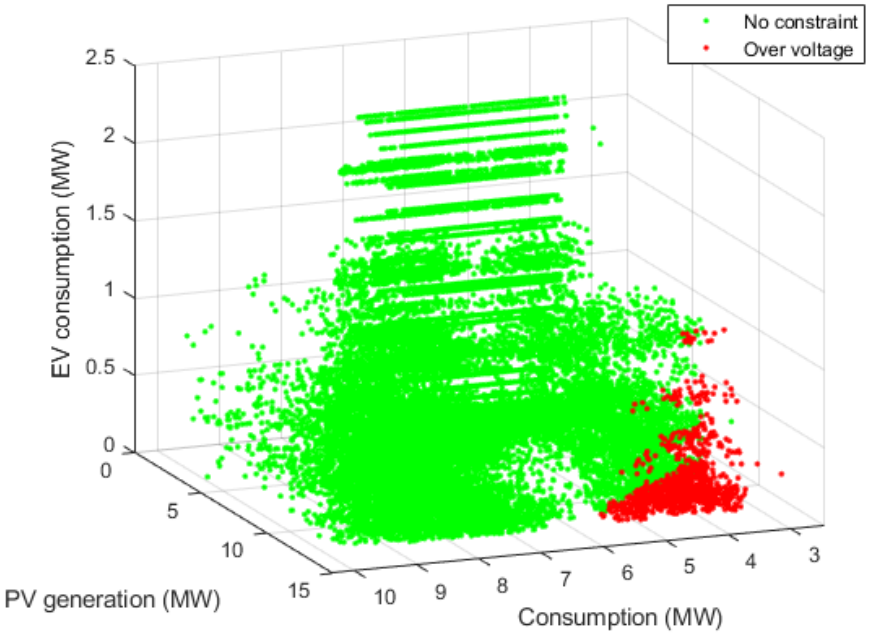

Figure 14 – Another view of the 3D graph: Consumption (excluding EVs), PV Production and EV Consumption for the constrained backup feeder at Carros in summer, on the assumption of an N-1 configuration

A second 3D graph was plotted in order to show the influence of hydropower production on the quantity of constrained points.

3D graph with consumption (excluding EVs), PV production and hydropower production

We can see that there are constraints ***only when consumption is relatively low*** (<60% of the maximum charge), which can be explained by the ***high level of photovoltaic production*** during these times. The constraints are exacerbated ***by the hydropower production***.

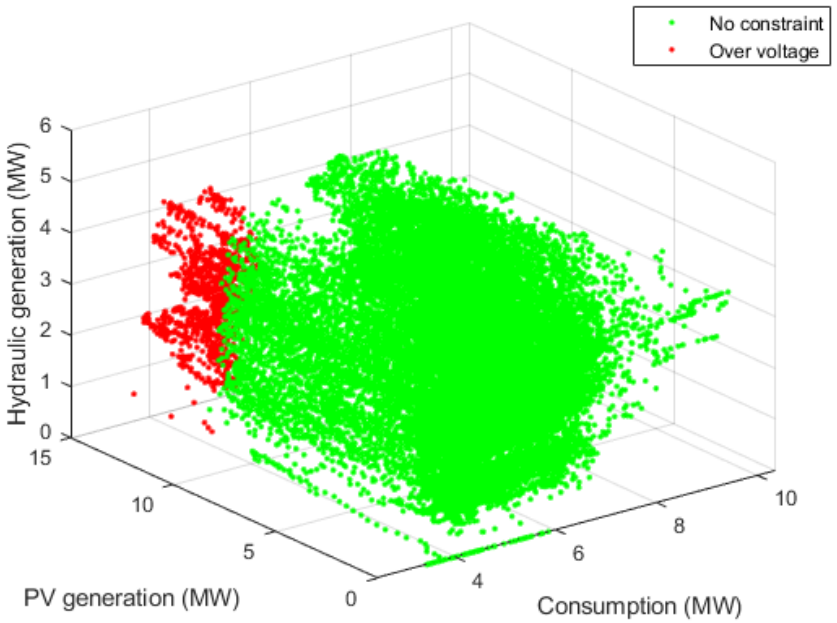

Figure 15 – 3D graph: Consumption (excluding EVs), PV Production and Hydropower Production for the constrained backup feeder at Carros in summer, on the assumption of an N-1 configuration

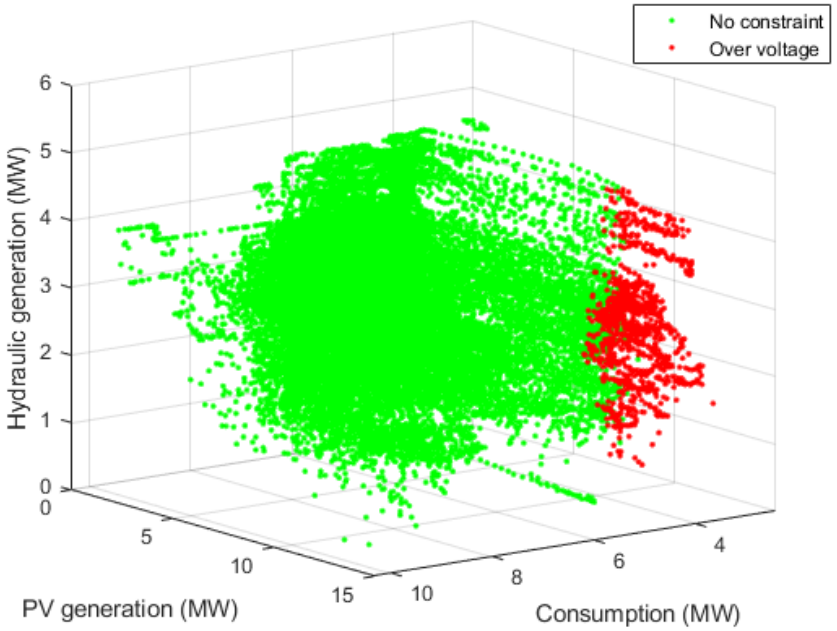

Figure 16 – Another view of the 3D graph: Consumption (excluding EVs), PV Production and Hydropower Production for the constrained backup feeder at Carros in summer, on the assumption of an N-1 configuration

Erreur ! Source du renvoi introuvable. Table 7 below shows the maximum flexibility volumes for the voltage rise constraint, **on the assumption of an HV N-1 configuration over**

the two summers of 2035/2036. The useful diffuse[22] flexibility volume making it possible to avoid constraints over the two years simulated is 2.63 MW for an increase in consumption or 3.26 MW for a decline in production. This difference can be explained by the location of production and consumption: in this case, the utility of flexibility in production is less than that for consumption (cf. APPENDIX C - § 1 Impact of the location of flexibility). This difference could also be explained by the fact that production is injected at fixed and negative tanφ. Accordingly, when the injected production is reduced, the consumption of reactive power is reduced. There are therefore two conflicting effects, one positive regarding a reduction of the constraint (decline in production) and the other negative (decline in consumption of reactive power). In the case of consumption flexibility, since tanφ is positive with consumption, both effects go in the same direction.

Table 7 – Useful flexibility volume resolving summer constraints

Type of flexibility	Volume of flexibility for voltage rise in MW	Flexibility proportion (Volume flexibility / maximum consumption or production of the useful area)%
Increase in consumption	2.6	25
Reduction in MV production	3.26	22

The results representing the existence of constraints have been presented, and we will now present more detailed duration and period results for the voltage rise constraint.

Time slots of constraint occurrence

Figure 17**Erreur ! Source du renvoi introuvable.** below presents useful flexibility activation durations according to activation times. The graph includes:

- A third dimension (coloured) which represents the maximum production perceived by photovoltaic power production during the constraint.
- A fourth dimension (size of the circles) representing the maximum consumption level obtained throughout the constraint.

[22] Diffuse flexibility: application of a single flexibility factor to all customers either in consumption (excluding EVs) or on PV production.

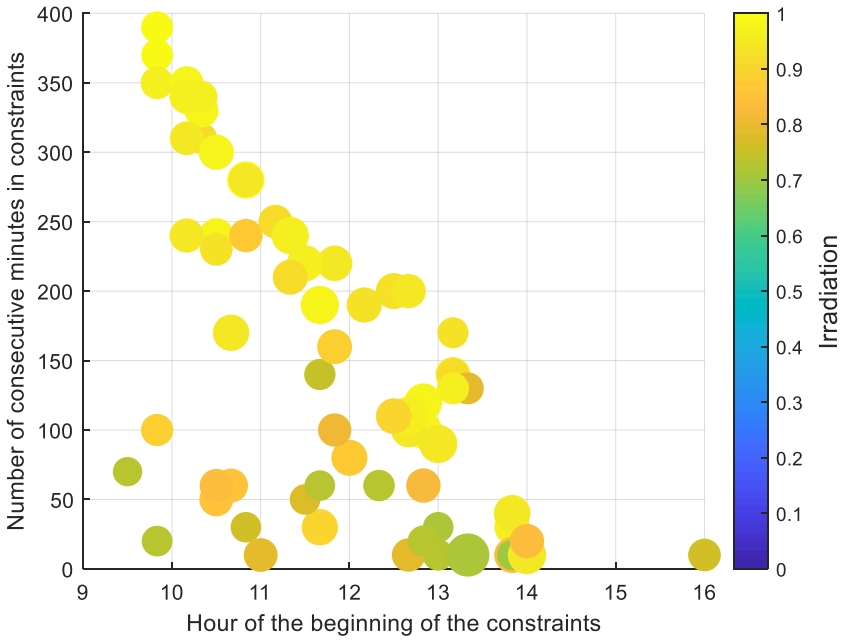

Figure 17 – Number of consecutive minutes potentially in current constraint in an equipment, over two summers, on the assumption of an HV N-1 configuration and according to the time of occurrence (size of the circles = maximum consumption level seen during the constraint).

After simulations, we can note that most of the potential constraints apparently occur between 11.00 am and 2.00 pm. It is worth noting that the longest potential constraints apparently occur between 9.00 am and 11.00 am. There is admittedly less PV production (even though it will only increase), but there is also less consumption. It can also be noted that there is not necessarily a precise correlation between the duration of the constraint and the PV production level. This is logical in that it is consumption and production which are to be taken into account in simulations of grid constraints.

Figure 18 **Erreur ! Source du renvoi introuvable.**below shows the same results, with this time, for the 4th dimension, the magnitude of the constraint (or the magnitude of the flexibility capable of resolving the constraint). The larger the circle, the closer one is to the maximum constraint obtained during this study[23].

[23] For example, if there is a voltage rise ranging between +2.8% and +2%, +2.8% is the largest circle.

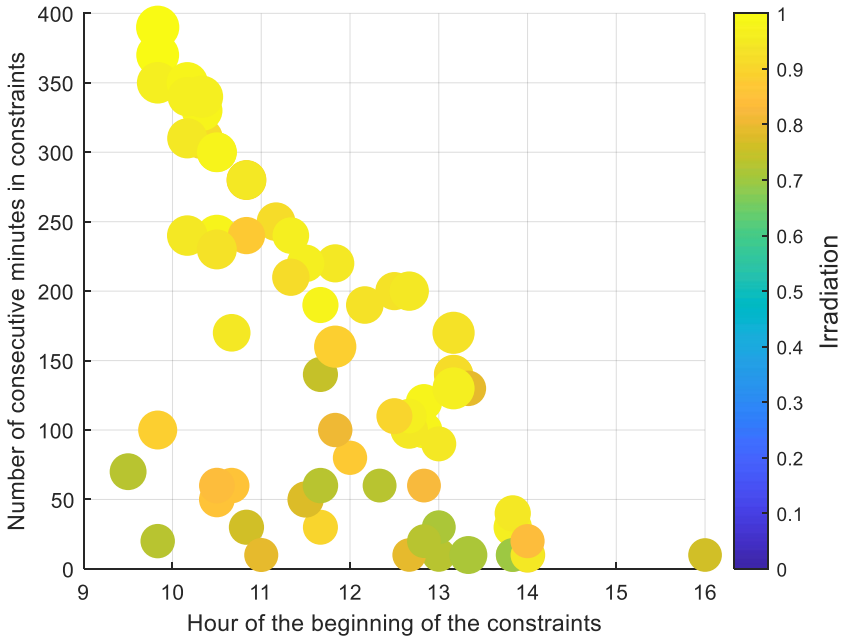

*Figure 18 – Number of consecutive minutes potentially in current constraint in an equipment, over two summers, on the assumption of an HV N-1 configuration and according to the time of occurrence (size of the circles = relative significance of the constraint)**Erreur ! Source du renvoi introuvable.** shows the distribution of grid constraints over the various months from June to September of the two summers in question. We can see that flexibility activations apparently occur over the four summer months.*

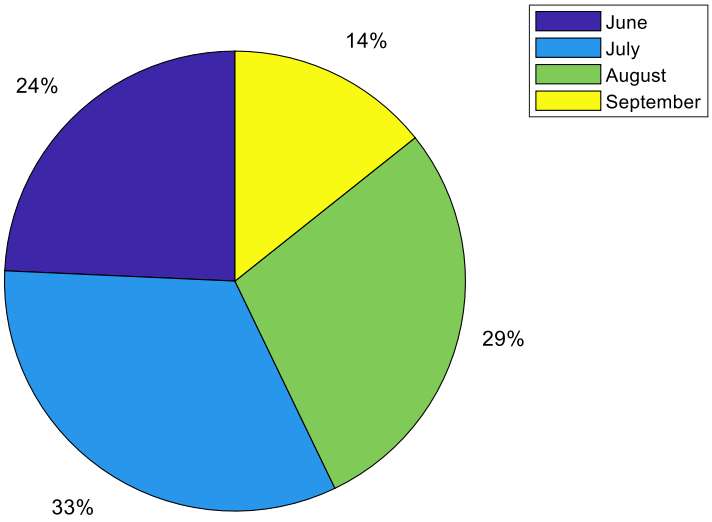

Figure 19 – Distribution of grid constraints over the various months of the seasonality in question on the assumption of an HV N-1 configuration

This substation supplies an industrial zone, so consumption in the zone remains fairly stable during the week and is far lower on the weekend.
Erreur ! Source du renvoi introuvable. Shows the distribution of grid constraints over the various days of the week for the two summers in question.

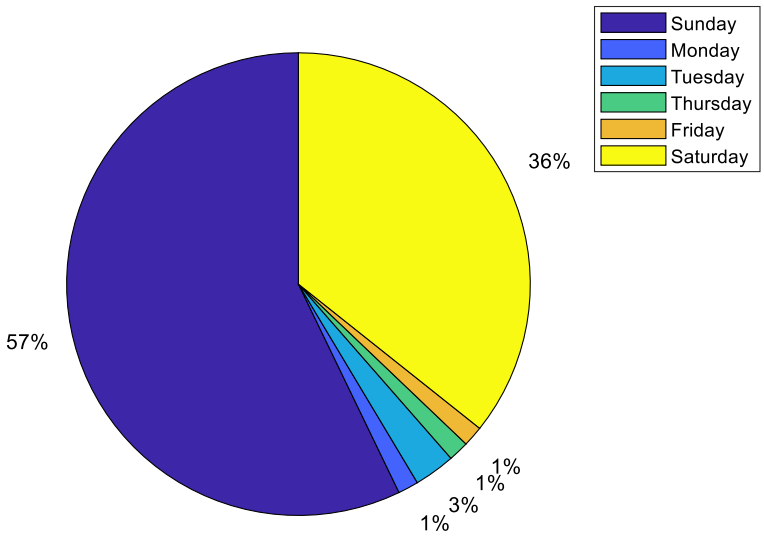

Figure 20 – Distribution of grid constraints over the various days of the week of the seasonality in question, on the assumption of an HV N-1 configuration

In 93% of cases, the two days of the week for which there are apparently potential flexibility needs are Sundays and Saturdays. One possible interpretation would be to say that these days are non-working days for a large proportion of people, and as the zone is a mainly an industrial zone, the decline in business activity would not be offset by household consumption. Thus, the increasing potential gap between production and consumption would become very substantial.

4.5.4.2. Results of simulations corresponding to situation 18

As a reminder, simulation 18 corresponds to the following situation:

Table 8 - Recap of situations simulated

Simulation 18	
Scenario	Green
PV locations	3
EV locations	1
Situation	N-1
Seasonality	Winter & Inter-season

The quantity and location of MV producers is the same as for the battery of simulations 15.

We have chosen to show the results in the same way as for the summer season.

3D graph with consumption (excluding EVs), PV production and EV consumption

The constraints appear at ***consumption levels below 5 MW***, i.e. about 45% of the feeder's maximum charge, and when ***the injection of the photovoltaic panels exceeds 11.6 MW, i.e. about 78% of their installed capacity***.

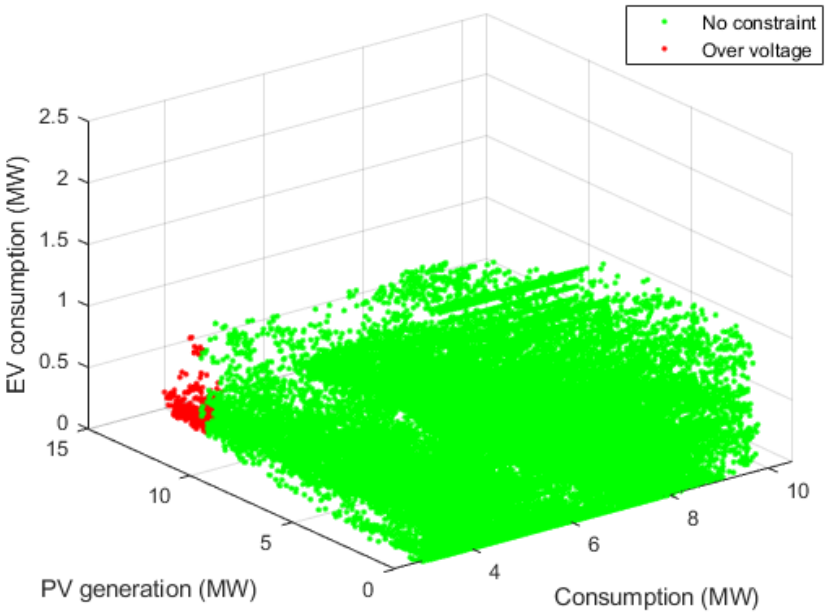

Figure 21 – 3D graph: Consumption (excluding EVs), PV Production and EV Consumption for the constrained backup feeder at Carros in winter & inter-season, on the assumption of an N-1 configuration

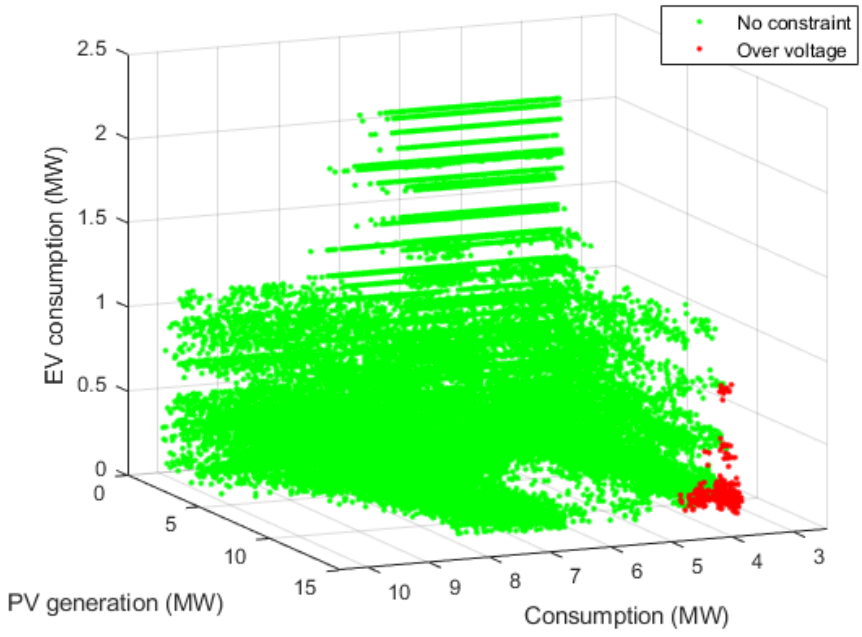

Figure 22 – Another view of the 3D graph: Consumption (excluding EVs), PV Production and EV Consumption for the constrained backup feeder at Carros in winter & inter-season, on the assumption of an N-1 configuration

In the same way as for the calculations in summer, we can see that ***the maximum level of EV consumption is relatively low relative to the PV production level***. These EVs added to the simulated charge of the winters and inter-seasons in 2035/2036 ***result in no current constraint during consumption peaks***.

A second 3D graph was plotted in order to show the influence of hydropower production at the time of the constraints.

3D graph with consumption (excluding EVs), PV production and hydropower production

We can see that there are constraints only when consumption is relatively low (<60% of the maximum charge), which can be explained by the high level of photovoltaic production during these times. The constraints are exacerbated ***by the hydropower production***.

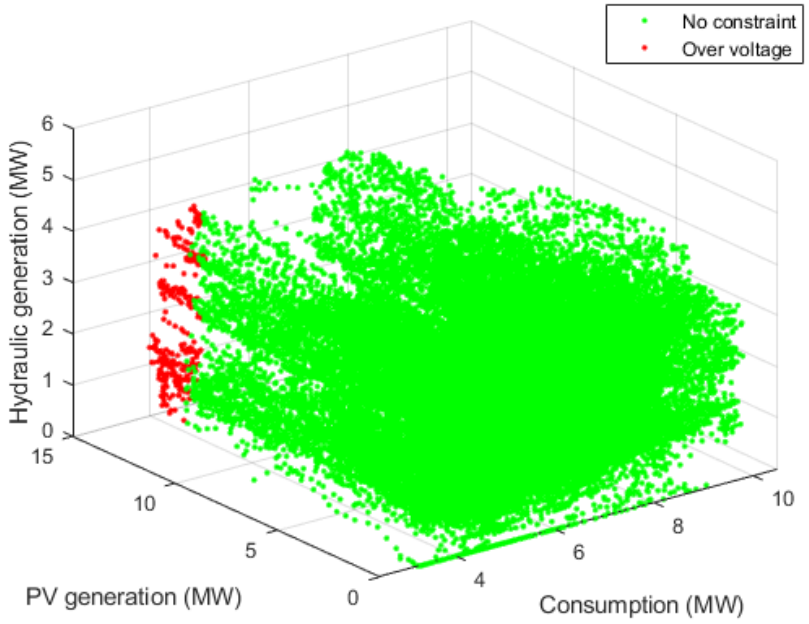

Figure 23 – 3D graph: Consumption (excluding EVs), PV Production and Hydropower Production for the constrained backup feeder at Carros in winter & inter-season, on the assumption of an N-1 configuration

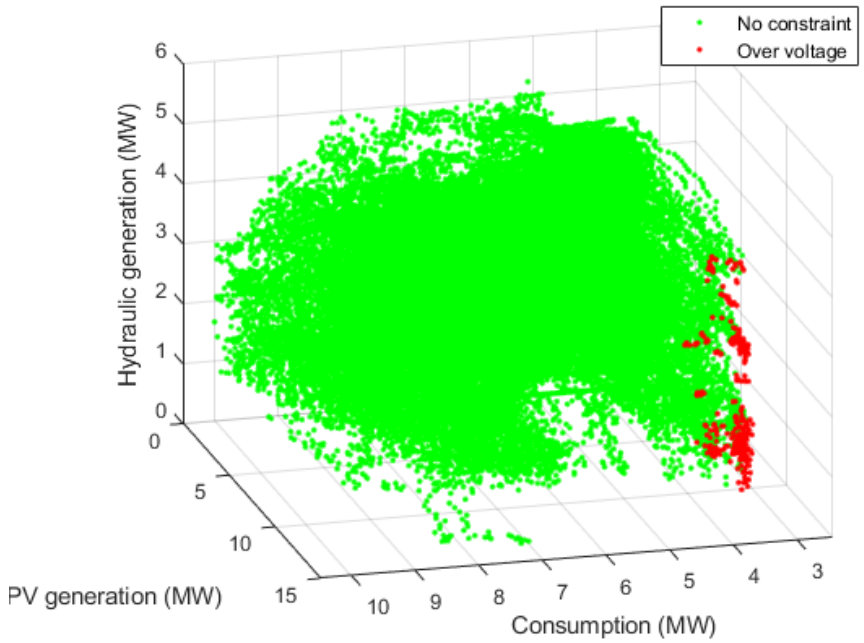

Figure 24 – Another view of the 3D graph: Consumption (excluding EVs), PV Production and Hydropower Production for the constrained backup feeder at Carros in winter & inter-season, on the assumption of an N-1 configuration

Erreur ! Source du renvoi introuvable. Table 9 shows the maximum flexibility volumes for the voltage rise constraint, **on the assumption of an HV N-1 configuration over the two full years of summer 2035/2036**. The useful flexibility volume making it possible to avoid constraints during these two years ranges between 1.25 MW for an increase in consumption and 1.65 MW for a decline in production. As before, the explanation for the difference lies in the impact of the location of flexibility. This difference could also be explained by the fact that production is injected at fixed and negative tanφ. Accordingly, when the injected production is reduced, the consumption of reactive power is reduced. There are therefore two conflicting effects, one positive regarding a reduction of the constraint (decline in production) and the other negative (decline in consumption of reactive power). In the case of consumption flexibility, since tanφ is positive with consumption, both effects go in the same direction.

Table 9 – Useful flexibility volume resolving winter & inter-season constraints

Type of flexibility	Volume of flexibility for voltage rise in MW	Flexibility proportion (Volume flexibility / maximum consumption or production of the useful area)%
Increase in consumption	1.25	12%
Reduction in MV production	1.65	11%

The overall results having been presented, we will now present more detailed duration and period results in the voltage rise constraint.

Time slots of constraint occurrence

Figure 25 **Erreur ! Source du renvoi introuvable.**below presents useful flexibility activation durations according to activation times. The graph includes:

- A third dimension (coloured) which represents the maximum insolation perceived by photovoltaic power production during the constraint.
- A fourth dimension (size of the circles) representing the maximum consumption level obtained throughout the constraint.

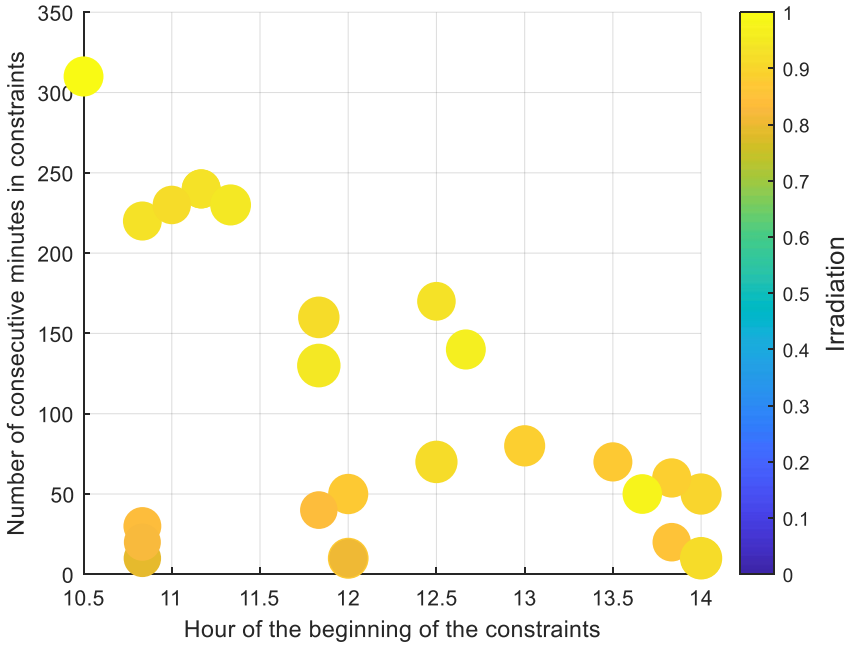

Figure 25 - Number of consecutive minutes potentially in current constraint in an equipment, over two winters and inter-seasons, on the assumption of an HV N -1 configuration and according to the time of occurrence (size of the circles = maximum consumption level seen during the constraint).

After simulations, we can note that all the potential constraints apparently occur between 10.30 am and 2.00 pm, with fairly high PV production levels and low consumption levels.

Erreur ! Source du renvoi introuvable. Figure 26 below shows the same results, with this time, for the 4th dimension, the magnitude of the constraint (or the magnitude of the flexibility capable of resolving the constraint). The larger the circle, the closer one is to the maximum constraint obtained during this study[24].

[24] For example, if there is a voltage rise ranging between +2.8% and +2%, +2.8% is the largest circle.

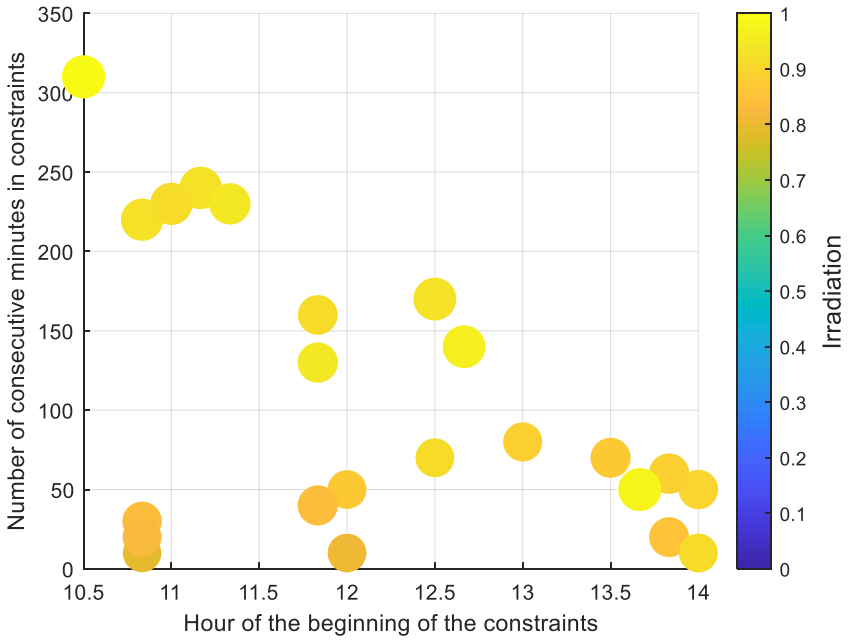

Figure 26 – Number of consecutive minutes potentially in current constraint in an equipment, over two winters and inter-seasons, on the assumption of an HV N-1 configuration and according to the time of occurrence (size of the circles = relative significance of the constraint).

Note that in the remainder of this deliverable, the graphs representing constrained months and days and their analyses have been placed in APPENDIX B: 2035 MV grid simulations: analysis of constraints spread per month and per day. However, the overall results will be presented in tables.

Table 10 - Detail of constrained periods

Distribution of constraints	Months impacted	Days of the week impacted
	March - April - May	Thursday - Saturday - Sunday

4.5.4.3. Conclusion

This study on the Carros zone shows that the potential constraints will be related to the massive arrival of RES on the grid. These will apparently occur first on non-working days given the typology of the industrial zone, and then, if more RES is introduced, during the week (not seen here).

4.5.5. Results of simulations on the ISOLA zone

All the batteries of simulations in N-1 configuration on the ISOLA zones yields to constraints. They are thus all described in detail in APENDIX A: Results of simulations on the ISOLA zone.

4.6. Conclusion

As a reminder, the results presented here do not take into account the probability of occurrence of a situation in degraded configuration.

The analysis of the results for two *Nice Smart Valley* zones enables us to highlight several points.

First, the results for Carros and Isola show that the grids could without difficulty cope with the introduction of electric vehicles in accordance with the scenarios modelled in this study. This is because the improvement in the building efficiency (enhanced thermal envelope of the buildings) modelled in this study tends to reduce the overall electric consumption excluding electric vehicles on the 2035 horizon. Electric vehicles, for their part, will represent an additional use which lead to a load increase. The performed simulations make it possible to assess the impact of these two antagonistic effects. The simulation results show that, generally, EVs' consumption will have a limited impact on the grids, especially given the overall decline in consumption. Note that this conclusion holds for the assumptions chosen for these simulations. These assumptions could change as behaviours and recharging technologies are refined.

Next, the results show that the introduction of renewable/variable production could generate constraints on the grid. As a reminder, Enedis chose to simulate the impact of the future connection of EVs and PV producers to the existing grid, i.e. without taking into account the reinforcements that would be made if the connections of these assets were to generate constraints. In the framework of these assumptions, we have been able to see that photovoltaic power production could generate constraints in a degraded situation. This is mainly due to the modelled high PV production level and the asynchronism between production and consumption.[25]

These results also show that the location of flexibility had an impact on the flexibility volume (cf. APPENDIX C - § 1 on the impact of the location of flexibility on the flexibility volume). Since the consumers are not distributed in the same way as the power producers, the impact of a given flexibility volume distributed homothetically does not have the same usefulness depending on the type of flexibility.

Finally, the results also show major possible high-voltage constraints in N-1 configuration. This shows the potential benefits of implementing in the power generation units local voltage regulation functions (such as Q(U)), thereby making it possible to limit the constraints in situations of heavy injection.

[25] Note that, in these simulations, the producers injected at fixed tan φ.

5. GENERAL CONCLUSION

The Use case 3 of the French Demo enabled to analyzed how flexibility could be used to manage distribution grid constraints in the future through a market approach.

The constraints to be managed through the use of flexibility will be temporary, not frequent, and mainly caused by local generation. The simulations performed in the area of the French demonstration cannot be extrapolated nationwide but show how long term grid planning will become highly dependent on a lot of parameters –and thus more and more complex - as local generation will increase.

Meanwhile, the project considers that further investigations on flexibility implementation should be performed in a pragmatic way, especially to see how simpler mechanisms could increase customer acceptance and awareness. It seems unwise to design mechanisms of a high complexity as flexibility use for the distribution grid will be progressively implemented - starting with low and localized volumes. Projects like Nice Smart Valley show that complexity is a major hurdle for customers.

APPENDIX A: Results of simulations on the ISOLA zone

1. Results of simulations corresponding to situation 19

As a reminder, simulation 19 corresponds to the following situation:

Table 11 - Recap of situations simulated

Simulation 19	
Scenario	Green
PV locations	1
EV locations	1
Situation	N-1
Seasonality	Winter & Inter-season

For information's sake, Figure 27 below shows the location of the big producers on the constrained feeder.

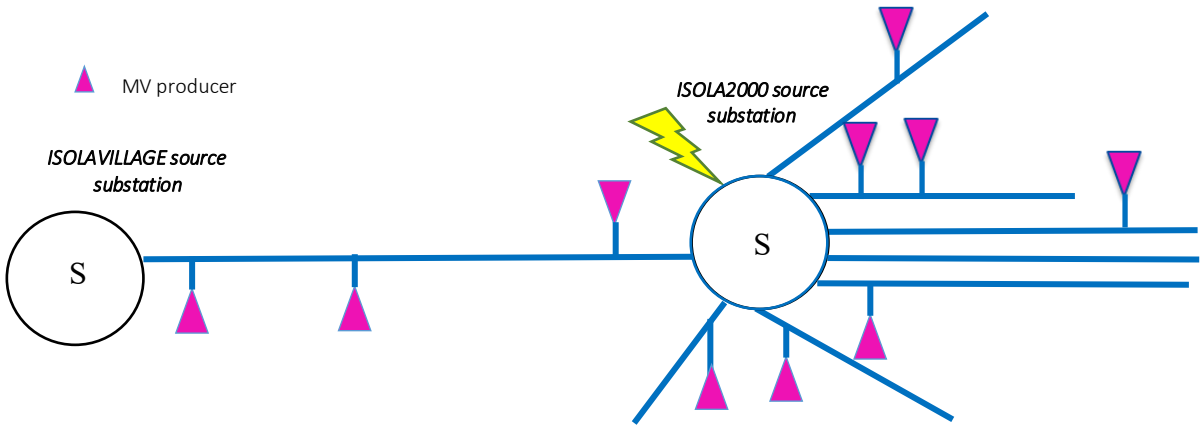

Figure 27 – Diagram of the constrained feeder with location of the big producers (>250 kVA)

The location of PV production resulted in a large number of producers to be connected to the Isola2000 source substation. We can see that there are 8 new producers, with at least 2 MW installed capacity added.

3D graph with consumption (excluding EVs), PV production and hydropower production

The graph below shows the states under constraint or not depending on the levels of hydropower production, PV production and consumption (excluding EVs):

- according to the locations simulated;
- for the constrained backup feeder and the constrained transformer;
- in a recovery configuration in an HV N-1 situation for winters and inter-seasons;
- in projected conditions in 2035/2036.

The graph shows five types of constraints:

- Overcurrent in grid equipment in draw-off and injection (lines/cables).
- Overcurrent in the HV/MV transformer.
- Overcurrent at the feeder terminal.
- Voltage rise
- Voltage drop.

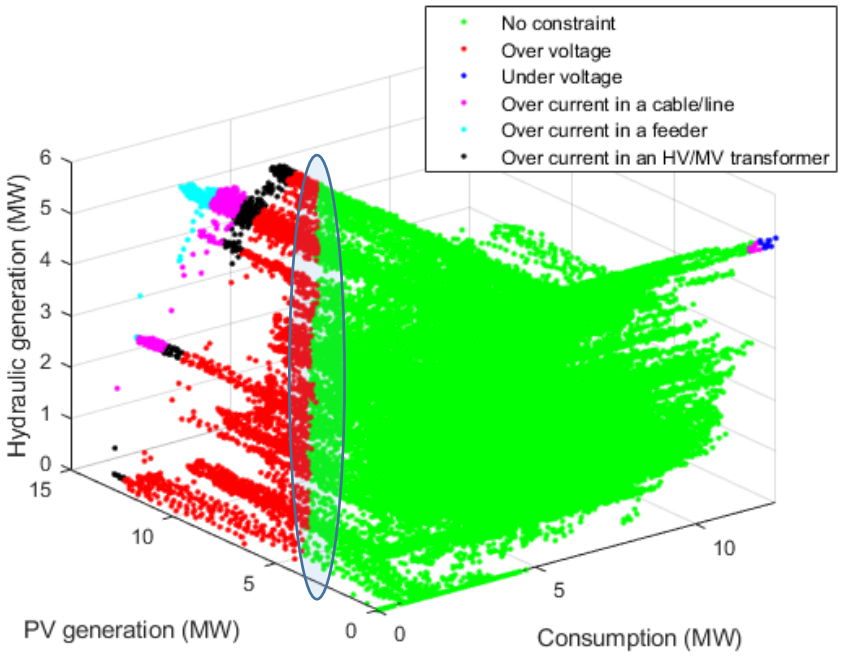

Figure 28 – 3D graph: Consumption (excluding EVs), PV Production and Hydropower Production for the constrained backup feeder at Isola in winter & inter-season, on the assumption of an N-1 configuration

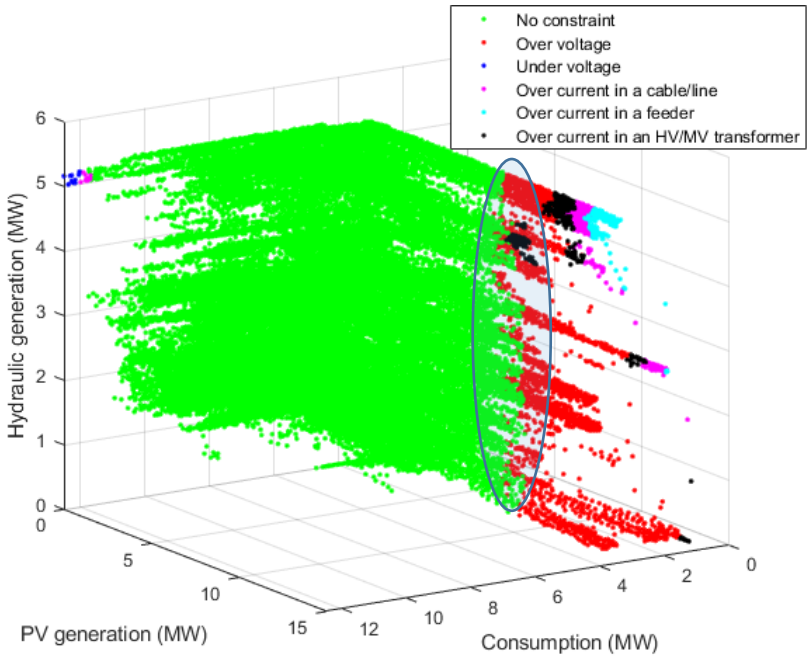

Figure 29 - Another view of the 3D graph under constraints: Consumption (excluding EVs), PV Production and Hydropower Production for the constrained backup feeder at Isola in winter & inter-season, on the assumption of an N-1 configuration

We can see clearly on this graph the separation between zones under current constraint and zones with no current constraints. On the other hand, it is not possible to distinguish very clearly between the voltage constraint zone and the zone with no constraint, the "encircled zone". This is notably due to the fact that other factors are involved, in particular the consumption level of the electric vehicles, which, although sometimes very low and not shown here, could result in a transition from an unconstrained state to a constrained state.

Regarding constraints related to the injection of production, these appear at ***consumption levels lower than or equal to 6 MW***, i.e. about 49% of the feeder's maximum charge, and when the ***injection of the photovoltaic panels exceeds 3.4 MW, i.e. about 22% of their installed capacity***.

Regarding constraints related to draw-off, these appear at ***high consumption levels exceeding 11.7 MW***, i.e. about 93% of the feeder's maximum charge, and when the ***injection of the photovoltaic panels is zero***.

Erreur ! Source du renvoi introuvable. Table 12 shows the flexibility volumes that can resolve the worst constraint of each type, **on the assumption of an HV N-1 configuration over the two summers of 2035/2036**. The maximum constraint for voltage rise does not occur at the same time as the other production-related constraints. The inversion of the consumption flexibility volume/production flexibility volume ratio is therefore potentially normal and it could be explained by several reasons. One of those reasons would be the distribution of hydropower which is not the same at these two times: in one case the two producers produce, while in the other case only one of the two. This difference could also be explained by the fact that production is injected at fixed and negative tanφ. Accordingly, when the injected production is reduced, the consumption of reactive power is reduced. There are therefore two conflicting effects, one positive regarding a reduction of the constraint (decline in production) and the other negative (decline in consumption of reactive

power). In the case of consumption flexibility, since tanφ is positive with consumption, both effects go in the same direction.

Table 12 – Useful flexibility volumes capable of resolving the various constraints and the ratio of useful flexibility to the consumption or PV production of the area

Type of flexibility	Type of constraint:					
	Current (injection)	Current at the feeder terminal (injection)	Current in the transformer (injection)	Voltage rise	Voltage drop	Current (draw-off)
Rise in consumption	2.95 MW 24%	1.7 MW 14%	4.5 MW 36%	6.26 MW 50%	-	-
Fall in consumption	-	-	-	-	-0.55 MW -4%	-0.8 MW -6%
Fall in MV production	2.75 MW 19%	1.6 MW 11%	3.9 MW 28%	7.63 MW 54%	-	-

Time slots of constraint occurrence

The overall results concerning the existence of constraints have been presented, and we will now present more detailed duration and period results for each type of constraint.

Current constraint in injection and draw-off**Erreur ! Source du renvoi introuvable.** below presents useful flexibility activation durations according to activation times. The graph includes:

- A third dimension (coloured) which represents the maximum insolation perceived by photovoltaic power production during the constraint.
- A fourth dimension (size of the circles) representing the maximum consumption level obtained throughout the constraint.

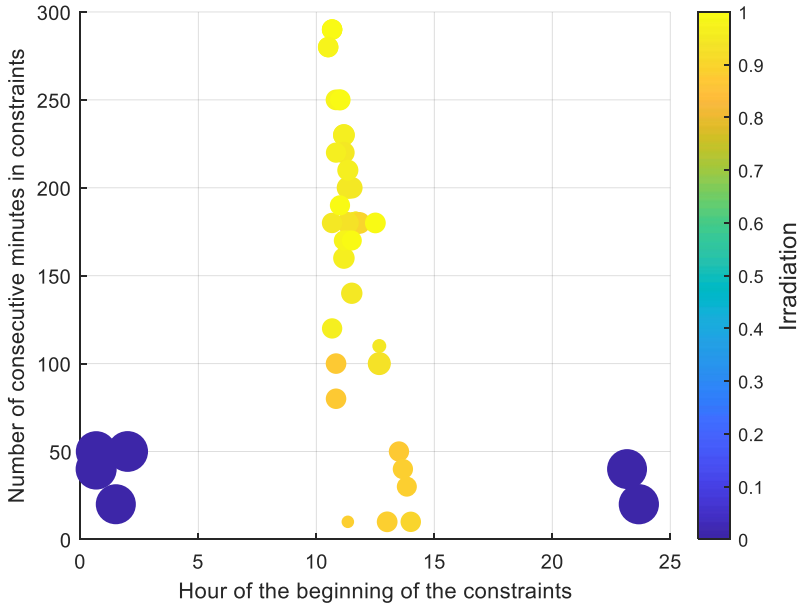

Figure 30 – Number of consecutive minutes potentially in current constraint in an equipment, over two winters and inter-seasons, on the assumption of an HV N-1 configuration and according to the time of occurrence (size of the circles = maximum consumption level seen during the constraint).

Note that the colour of the points corresponds to the max. Production level seen by the photovoltaic panels during the constrained period and not to the power produced at the time of appearance of the constraint.

After simulations, we can note that:

- For injection constraints, most of the potential constraints apparently occur between 10.00 am and 3.00 pm, with low consumption and a high level of photovoltaic power
- For draw-off constraints, most of the potential constraints apparently occur between 11.00 pm and 2 o'clock in the morning, with a very high consumption level and a photovoltaic power level of zero.
- It is worth noting that the longest potential constraints, for their part, apparently occur between 10.00 am and 1.00 pm.

Erreur ! Source du renvoi introuvable. Figure 31 below shows the same results, with this time, for the 4th dimension, the magnitude of the constraint (or the magnitude of the flexibility capable of resolving the constraint). The larger the circle, the closer one is to the maximum constraint obtained during this study[26]. With this second graph we note that for injection-related constraints, in most cases, the longer the duration of the constraint, the higher the useful flexibility level making it possible to avoid the constraint. For draw-off-related constraints, the volume is greatest when the constraint appears very early in the morning.

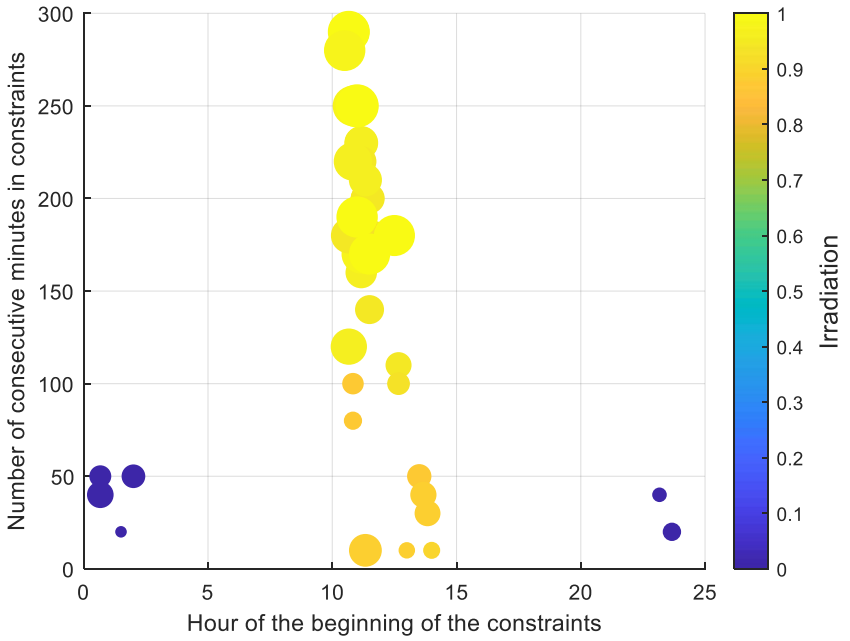

[26] For example, if there is a voltage rise ranging between +2.8% and +2%, +2.8% is the largest circle.

Figure 31 – Number of consecutive minutes potentially in current constraint in an equipment, over two winters and inter-seasons, on the assumption of an HV N-1 configuration and according to the time of occurrence (size of the circles = relative significance of the constraint).

The graphs representing constrained months and days and their analyses have been placed in appendices. The following table presents the concatenated results.

Table 13 - Detail of constrained periods

Distribution of constraints	Months impacted	Days of the week impacted
Distribution of draw-off constraints	November – December	Monday - Tuesday - Wednesday – Sunday
Distribution of injection constraints	April – May –	Every day of the week

Current constraint at the feeder terminal

Erreur ! Source du renvoi introuvable. Figure 32 below presents useful flexibility activation durations according to the constraint occurrence times. The graph includes:

- A third dimension (coloured) which represents the maximum insolation perceived by photovoltaic power production during the constraint.
- A fourth dimension (size of the circles) representing the maximum consumption level obtained throughout the constraint.

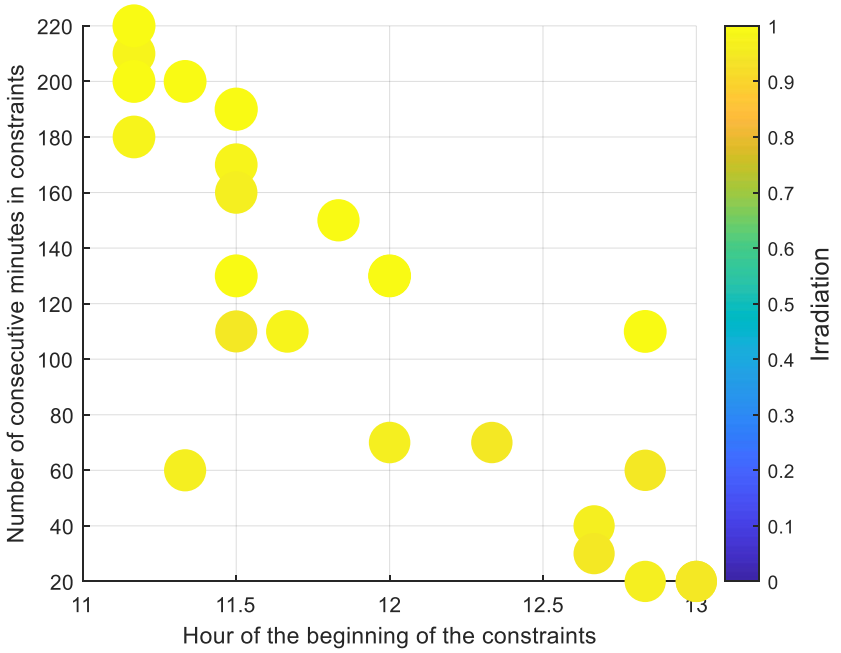

Figure 32 – Number of consecutive minutes potentially in current constraint at the feeder terminal, over two winters and inter-seasons, on the assumption of an HV N-1 configuration and according to the time of occurrence (size of the circles = maximum consumption level seen during the constraint).

After simulations, we can note that all the potential constraints apparently occur between 11.00 am and 1.00 pm, when consumption is low and PV production increases. It is worth noting that the longest potential constraints apparently occur before midday. This is due to

the fact that the PV production profile rises to a maximum when the sun is at its zenith, and then comes back down.

Erreur ! Source du renvoi introuvable. Figure 33 below shows the same results, with this time, for the 4th dimension, the magnitude of the constraint (or the magnitude of the flexibility capable of resolving the constraint). The larger the circle, the closer one is to the maximum constraint obtained during this study[27].

We observe that the photovoltaic production level is very high between 11.00 am and 1.00 pm, and that the flexibility volume is on the whole stable irrespective of the time of occurrence of the constraint. This is due to the fact that the maximum acceptable current at the feeder terminal is exceeded only very slightly, and therefore the flexibility volumes making it possible to resolve the constraint are very similar.

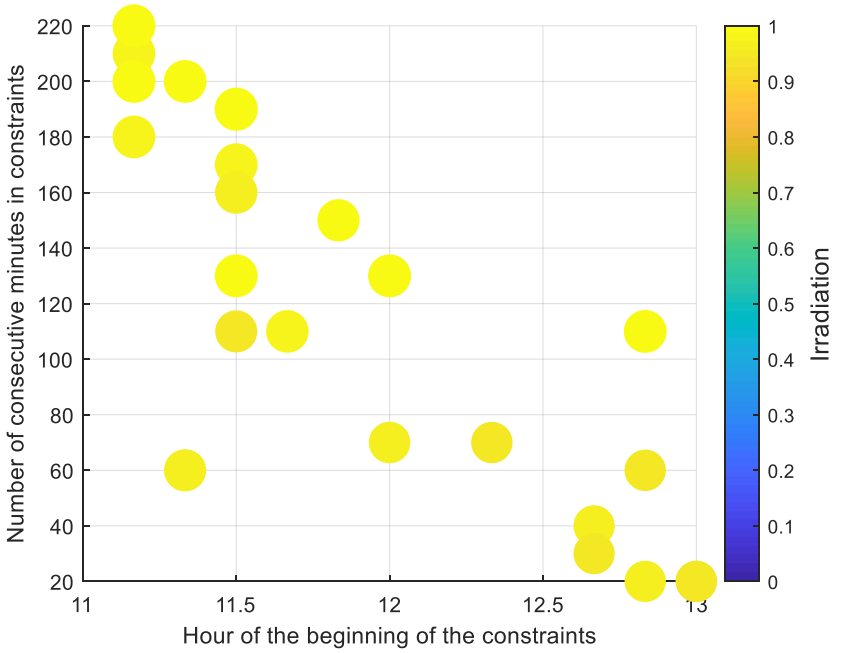

Figure 33 – Number of consecutive minutes potentially in current constraint at the feeder terminal, over two winters and inter-seasons, on the assumption of an HV N-1 configuration and according to the time of occurrence (size of the circles = relative significance of the constraint).

The graphs representing constrained months and days and their analyses have been placed in appendices.

Table 14 - Detail of constrained periods

Distribution of constraints	Months impacted	Days of the week impacted
	April – May	Every day of the week

Current constraint in the HV/MV transformer

[27] For example, if there is a voltage rise ranging between +2.8% and +2%, +2.8% is the largest circle.

Figure 34 **Erreur ! Source du renvoi introuvable.**below presents useful flexibility activation durations according to the constraint occurrence times. The graph includes:

- A third dimension (coloured) which represents the maximum insolation perceived by photovoltaic power production during the constraint.
- A fourth dimension (size of the circles) representing the maximum consumption level obtained throughout the constraint.

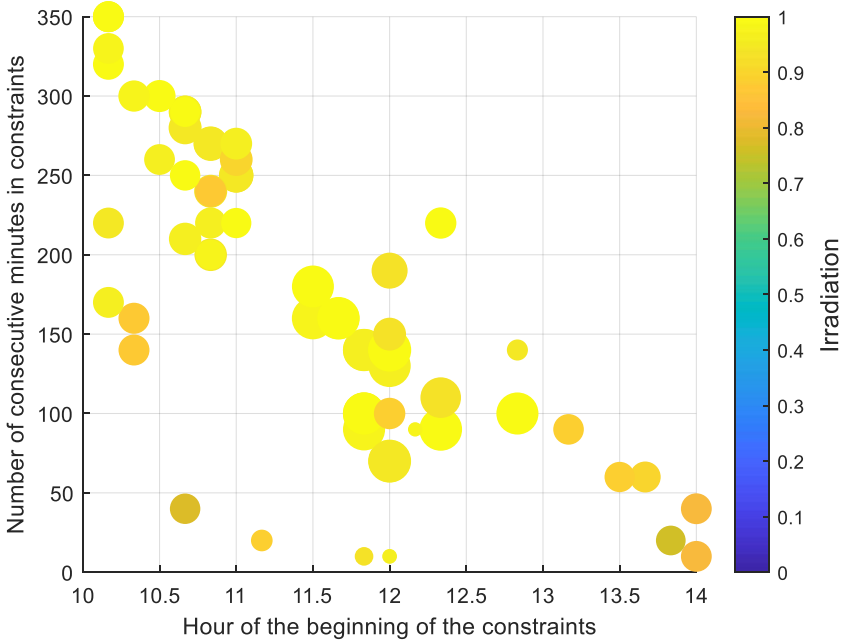

Figure 34 - Number of consecutive minutes potentially in current constraint at the source substation, over two winters and inter-seasons, on the assumption of an HV N-1 configuration and according to the time of occurrence (size of the circles = maximum consumption level seen during the constraint).

After simulations, we can note that all the potential current constraints at the source substation apparently occur between 10.00 am and 2.00 pm. The longest constraints apparently occur before 11.00 am, with low consumption levels and fairly high photovoltaic production levels. We can see another rather interesting effect, namely that the level of consumption during the constraints between 11.00 am and 1.00 pm is higher than for the longest constraints.

Erreur ! Source du renvoi introuvable. Figure 35 below shows the same results, with this time, for the 4th dimension, the magnitude of the constraint (or the magnitude of the flexibility capable of resolving the constraint). The larger the circle, the closer one is to the maximum constraint obtained during this study[28].

With this second graph we note that, on the whole, the flexibility volume is apparently larger when the duration of the constraint is longer and when production is high.

[28] For example, if there is a voltage rise ranging between +2.8% and +2%, +2.8% is the largest circle.

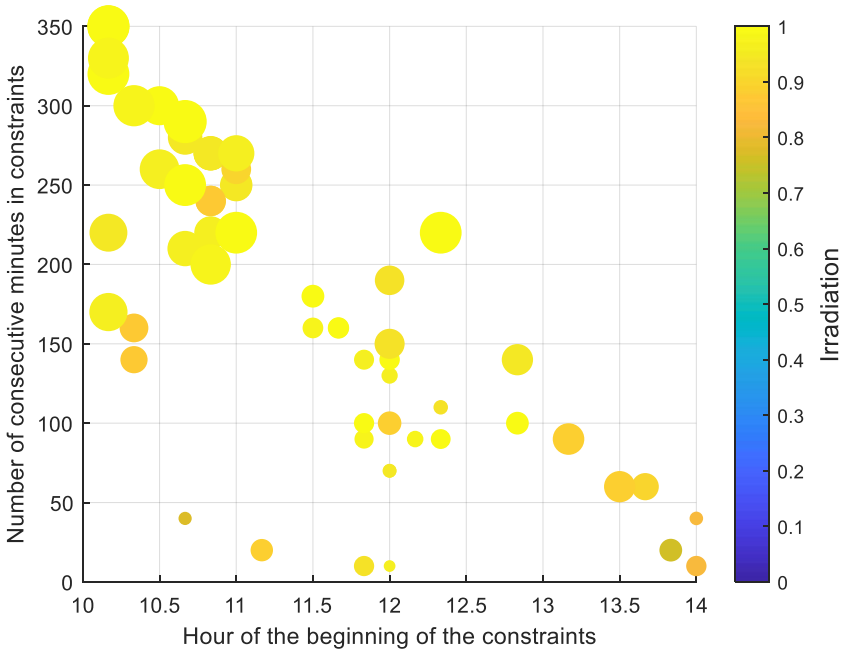

Figure 35 – Number of consecutive minutes potentially in current constraint at the source substation, over two winters and inter-seasons, on the assumption of an HV N-1 configuration and according to the time of occurrence (size of the circles = relative significance of the constraint)

The graphs representing constrained months and days and their analyses have been placed in appendices.

Table 15- Detail of constrained periods

Distribution of constraints	Months impacted	Days of the week impacted
	April - May	Every day of the week

Voltage rise constraint

Erreur ! Source du renvoi introuvable. Figure 36 below presents useful flexibility activation durations according to activation times. The graph includes:

- A third dimension (coloured) which represents the maximum insolation perceived by photovoltaic power production during the constraint.
- A fourth dimension (size of the circles) representing the maximum consumption level obtained throughout the constraint.

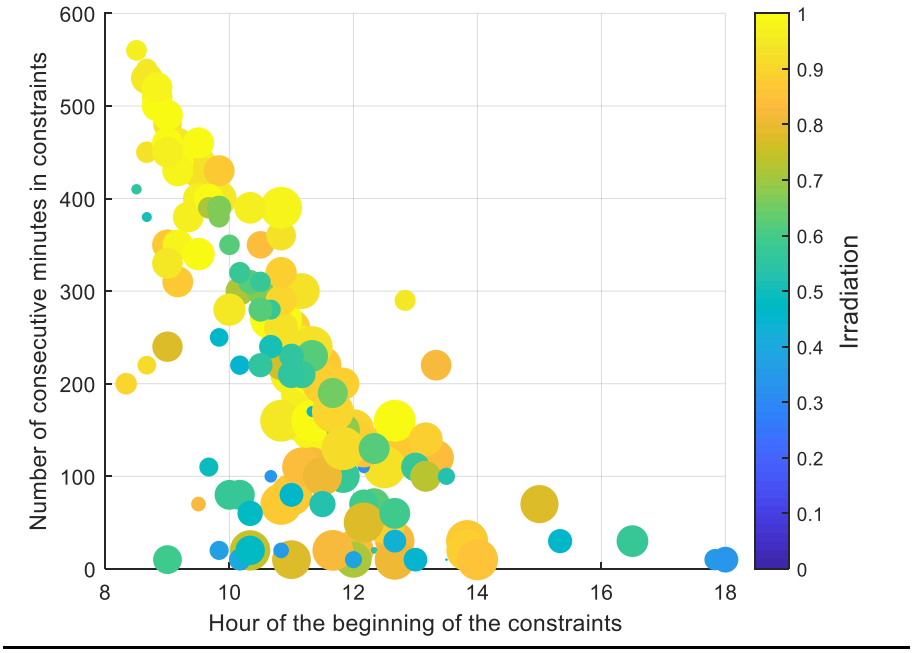

Figure 36 – Number of consecutive minutes potentially in voltage rise constraint, over two winters and inter-seasons, on the assumption of an HV N-1 configuration and according to the time of occurrence (size of the circles = maximum consumption level seen during the constraint).

After simulations, we can note that all of the potential constraints apparently occur between 8.00 am and 2.00 pm. The longest constraints apparently occur between 8.00 am and 11.00 am, i.e. with low consumption levels and photovoltaic power levels ranging between 40% and 60% of their maximum capacity. Between 10.00 am and 2.00 pm the level of consumption is higher, but the PV production level likewise.

Erreur ! Source du renvoi introuvable. Figure 37 below shows the same results, with this time, for the 4th dimension, the magnitude of the constraint (or the magnitude of the flexibility capable of resolving the constraint). The larger the circle, the closer one is to the maximum constraint obtained during this study[29].

With this second graph we note that the flexibility volume is apparently larger when the duration is greater and when production is high (>60%).

[29] For example, if there is a voltage rise ranging between +2.8% and +2%, +2.8% is the largest circle.

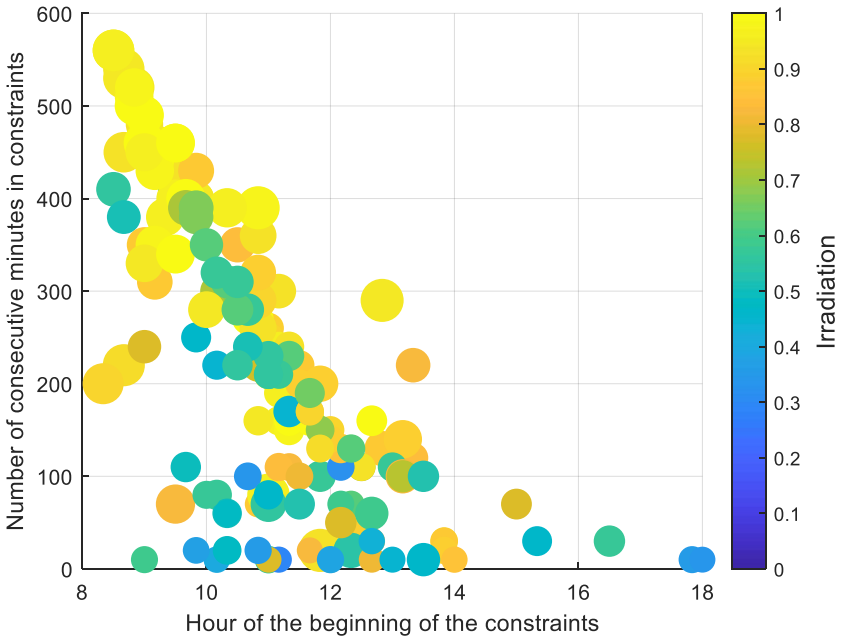

Figure 37 – Number of consecutive minutes potentially in voltage rise constraint, over two winters and inter-seasons, on the assumption of an HV N-1 configuration and according to the time of occurrence (size of the circles = relative significance of the constraint).

The graphs representing constrained months and days and their analyses have been placed in appendices.

Table 16 - Detail of constrained periods

	Months impacted	Days of the week impacted
Distribution of constraints	March - April – May - October - November	Every day of the week

Voltage drop constraint

Figure 38**Erreur ! Source du renvoi introuvable.** below presents useful flexibility activation durations according to activation times. The graph includes a third dimension (size of the circles) representing the maximum consumption level obtained throughout the constraint.

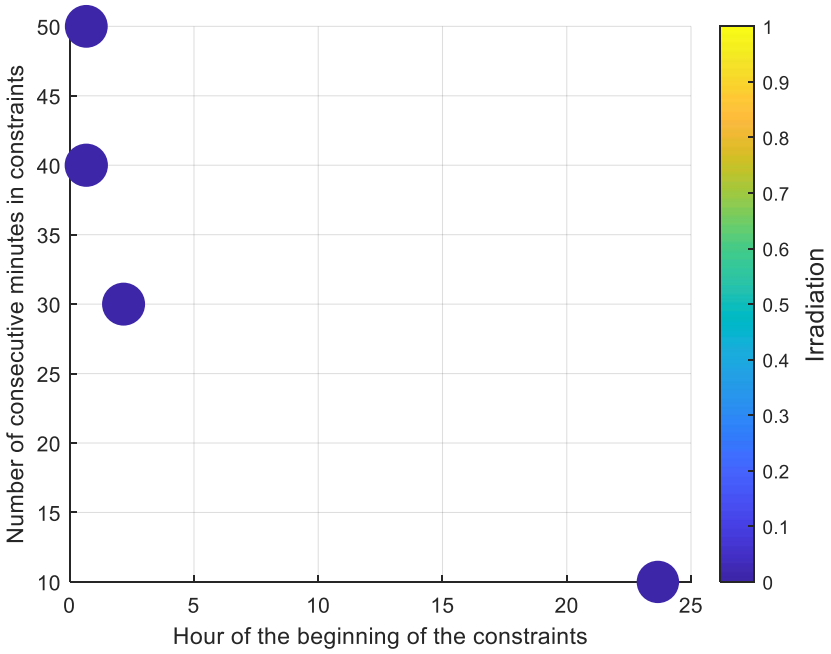

Figure 38 – Number of consecutive minutes potentially in undervoltage constraint, over two winters and inter-seasons, on the assumption of an HV N-1 configuration and according to the time of occurrence (size of the circles = maximum consumption level seen during the constraint).

After simulations, we can note that the four potential constraints apparently occur between 11.30 pm and 2.00 am. The longest constraint of 50 minutes apparently occurs very early in the morning.

Figure 39**Erreur ! Source du renvoi introuvable.** below shows the same results, with this time, for the 3rd dimension, the magnitude of the constraint (or the magnitude of the flexibility capable of resolving the constraint). The larger the circle, the closer one is to the maximum constraint obtained during this study[30].

With this second graph we note that whatever the constraint, the flexibility volume will be more or less equivalent.

[30] For example, if there is a voltage rise ranging between +2.8% and +2%, +2.8% is the largest circle.

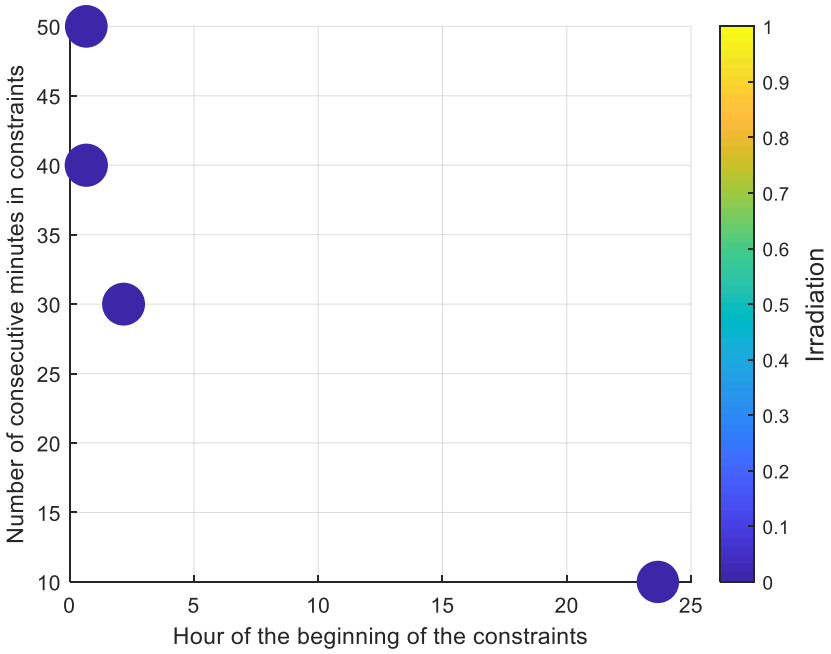

Figure 39 – Number of consecutive minutes potentially in undervoltage constraint, over two winters and inter-seasons, on the assumption of an HV N-1 configuration and according to the time of occurrence (size of the circles = relative significance of the constraint).

The graphs representing constrained months and days and their analyses have been placed in appendices.

Table 17 – Detail of constrained periods

Distribution of constraints	Months impacted	Days of the week impacted
	November – December	Monday – Wednesday - Sunday

2. Results of simulations corresponding to situation 20

As a reminder, simulation 20 corresponds to the following situation:

Table 18 – Summary table of situations simulated

Simulation 20	
Scenario	Green
PV locations	2
EV locations	1
Situation	N-1
Seasonality	Winter & inter-seasons

For information's sake, Figure 40**Erreur ! Source du renvoi introuvable.** below shows the location of the big producers on the constrained feeder.

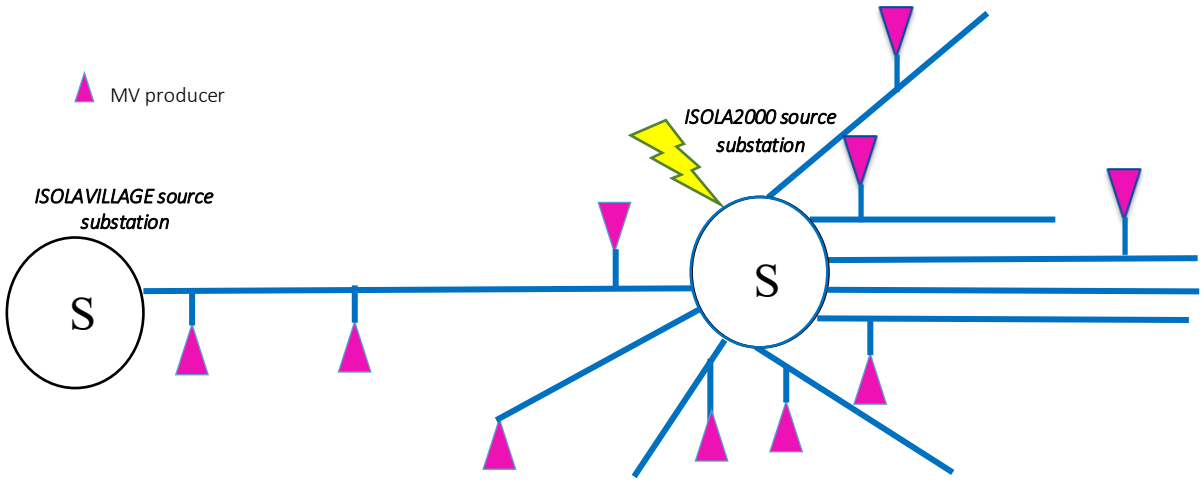

Figure 40 – Diagram of the constrained feeder with location of the big producers (>250 kVA)

Like for the previous case, we can see that 8 new producers have been placed randomly in this sample. However, their distribution on the grid is different, which will generate slightly different results.

3D graph with consumption (excluding EVs), PV production and hydropower production

The graph below shows the states under constraint or not depending on the levels of hydropower production, PV production and consumption (excluding EVs):

- according to the locations simulated;
- for the constrained backup feeder and the constrained transformer;
- in a recovery configuration in an HV N-1 situation for winters and inter-seasons;
- in projected conditions in 2035/2036.

The graph shows five types of constraints:

- Overcurrent in grid equipment in draw-off and injection (lines/cables).
- Overcurrent in the HV/MV transformer.
- Overcurrent at the feeder terminal.
- Voltage rise
- Voltage drop.

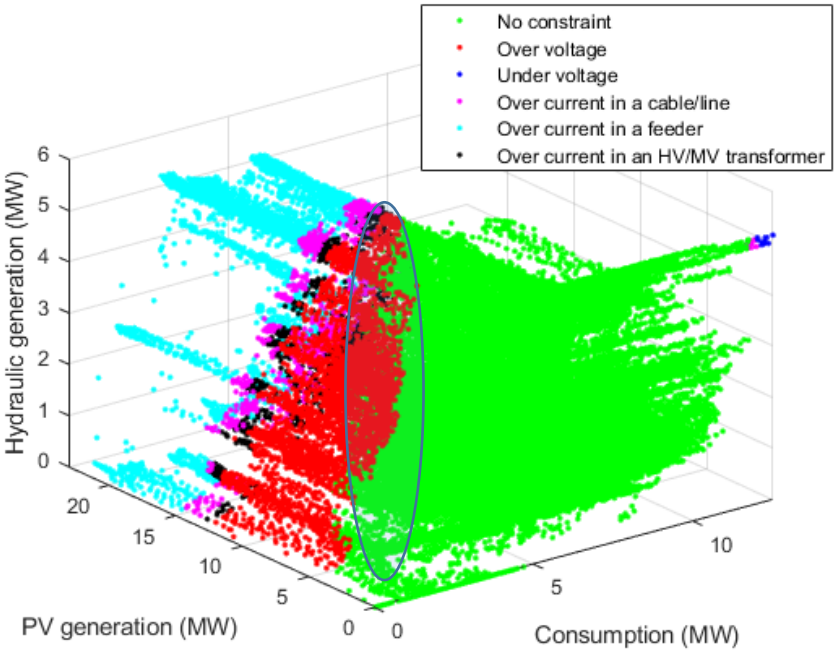

Figure 41 – 3D graph: Consumption (excluding EVs), PV Production and Hydropower Production for the constrained backup feeder at Isola in winter & inter-season, on the assumption of an N-1 configuration

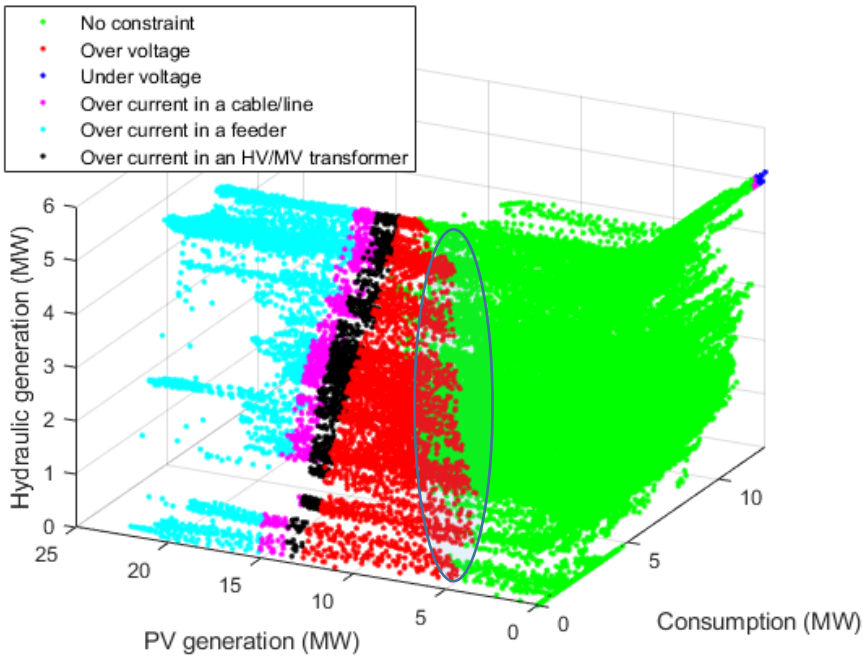

Figure 42 – Another view of the 3D graph under constraints: Consumption (excluding EVs), PV Production and Hydropower Production for the constrained backup feeder at Isola in winter & inter-season, on the assumption of an N-1 configuration

Like in the previous case, we can see clearly on this graph the separation between zones under current constraint and zones with no current constraints. On the other hand, it is not possible to distinguish very clearly between the voltage constraint zone and the zone with no constraint, the "encircled zone". This is notably due to the fact that other factors are

involved, in particular the consumption level of the electric vehicles, which, although sometimes very low, could result in a transition from an unconstrained state to a constrained state.

Regarding constraints related to the injection of production, these appear at ***consumption levels lower than or equal to approximately 9 MW***, i.e. about 73% of the feeder's maximum charge, and when the ***injection of the photovoltaic panels exceeds 3.3, i.e. about 14% of their installed capacity***.

Regarding constraints related to draw-off, these appear at ***high consumption levels exceeding 11.7 MW***, i.e. about 93% of the feeder's maximum charge, and when the ***injection of the photovoltaic panels is zero***.

Erreur ! Source du renvoi introuvable.Erreur ! Source du renvoi introuvable. Table 19 shows the maximum flexibility volumes for each constraint, **on the assumption of an HV N-1 configuration over the two complete years of summer 2035/2036**. The maximum constraint for voltage rise does not occur at the same time as the other production-related constraints (cf § 4.5.1) Note that certain flexibility volumes based on an increase in consumption have not been given because they would exceed the maximum capacity of the source substation, which would be meaningless. The difference in flexibility volume can be explained by the fact that production is injected at fixed and negative tanφ. Accordingly, when the injected production is reduced, the consumption of reactive power is reduced. There are therefore two conflicting effects, one positive regarding a reduction of the constraint (decline in production) and the other negative (decline in consumption of reactive power). In the case of consumption flexibility, since tanφ is positive with consumption, both effects go in the same direction.

Table 19 - Table of the useful flexibility volume resolving constraints and the ratio of useful flexibility to the consumption or PV production of the area

Type of flexibility	Type of constraint:					
	Current (injection)	Current at the feeder terminal (injection)	Current in the transformer (injection)	Voltage rise	Voltage drop	Current (draw-off)
Increase in consumption	-	-	-	11.9 MW 95%	--	
Reduction in consumption	-	-	-	-	-0.55 MW -4%	-0.8 MW -6%
Reduction in MV production	12.2 MW 53%	11 MW 48%	13.6 MW 59%	14.8 MW 64%	-	-

It should be remembered that these potential flexibility volumes (or potential constraints) are extreme and that at present Enedis would not have connected these producers under these conditions and would have found solutions to avoid these constraints.

Time slots of constraint occurrence

The overall results concerning the existence of constraints have been presented, and we will now present more detailed duration and period results for each type of constraint.

Current constraint in injection and draw-off

Erreur ! Source du renvoi introuvable. Figure 43 below presents useful flexibility activation durations according to activation times. The graph includes:

- A third dimension (coloured) which represents the maximum insolation perceived by photovoltaic power production during the constraint.
- A fourth dimension (size of the circles) representing the maximum consumption level obtained throughout the constraint.

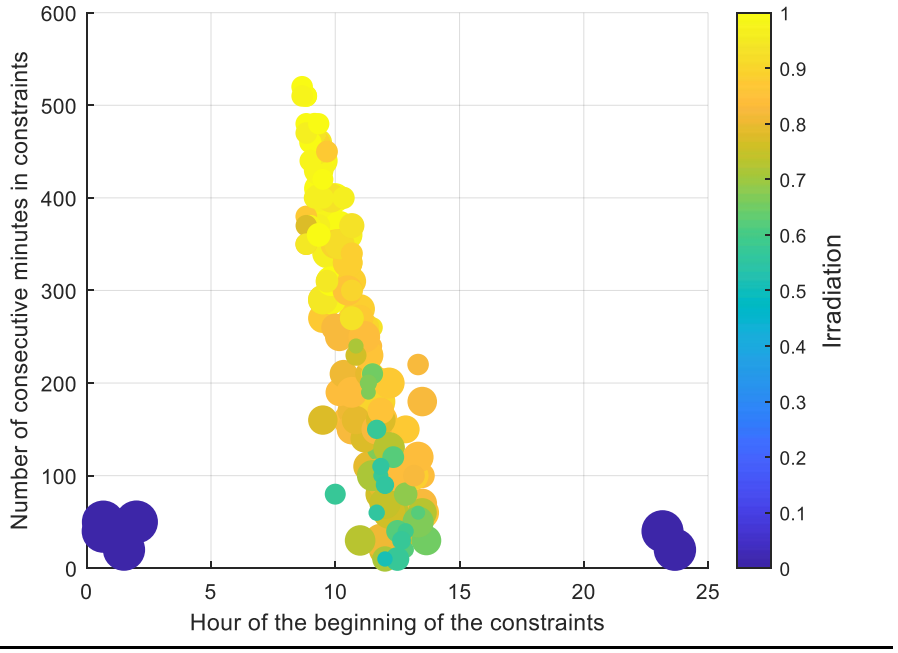

Figure 43 – Number of consecutive minutes potentially in current constraint, over two winters and inter-seasons, on the assumption of an HV N-1 configuration and according to the time of occurrence (size of the circles = maximum consumption level seen during the constraint).

After simulations, we can note that:

- all the potential constraints apparently occur between 8.30 am and 2.30 pm for injection constraints with low consumption and high photovoltaic power production.
- the draw-off constraints apparently occur between 11.00 pm and 2.00 am with a very high consumption level and a photovoltaic power production level of zero.
- It is worth noting that the longest potential constraints apparently occur between 8.30 am and 11.00 am.

Figure 44**Erreur ! Source du renvoi introuvable.** below shows the same results, with this time, for the 4th dimension, the magnitude of the constraint (or the magnitude of the flexibility capable of resolving the constraint). The larger the circle, the closer one is to the maximum constraint obtained during this study[31]. With this second graph we note that:

[31] For example, if there is a voltage rise ranging between +2.8% and +2%, +2.8% is the largest circle.

- For injection-related constraints, the longer the duration of the constraint, the greater the flexibility volume. This is notably due to the fact that photovoltaic power production is substantial.
- For draw-off-related constraints, the flexibility volume is slightly greater when the constraint occurs after midnight.

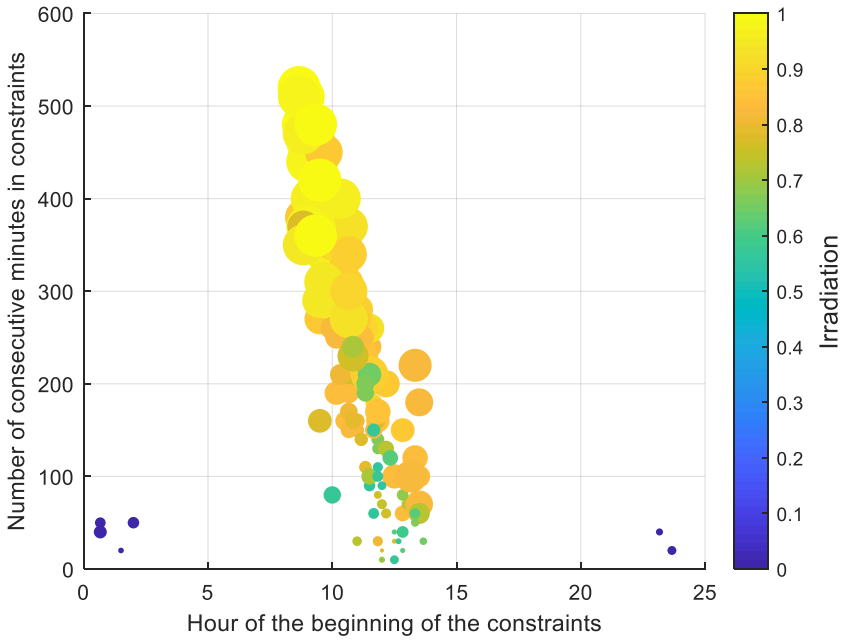

Figure 44 - Number of consecutive minutes potentially in current constraint, over two winters and inter-seasons, on the assumption of an HV N-1 configuration and according to the time of occurrence (size of the circles = relative significance of the constraint).

The graphs representing constrained months and days and their analyses have been placed in appendices.

Table 20 - Detail of constrained periods

Distribution of constraints	Months impacted	Days of the week impacted
Distribution of draw-off constraints	March - November - December	Every day of the week
Distribution of injection constraints	April - May - October	Every day of the week

Current constraint at the feeder terminal

Figure 45**Erreur ! Source du renvoi introuvable.** below presents useful flexibility activation durations according to activation times. The graph includes:

- A third dimension (coloured) which represents the maximum insolation perceived by photovoltaic power production during the constraint.
- A fourth dimension (size of the circles) representing the maximum consumption level obtained throughout the constraint.

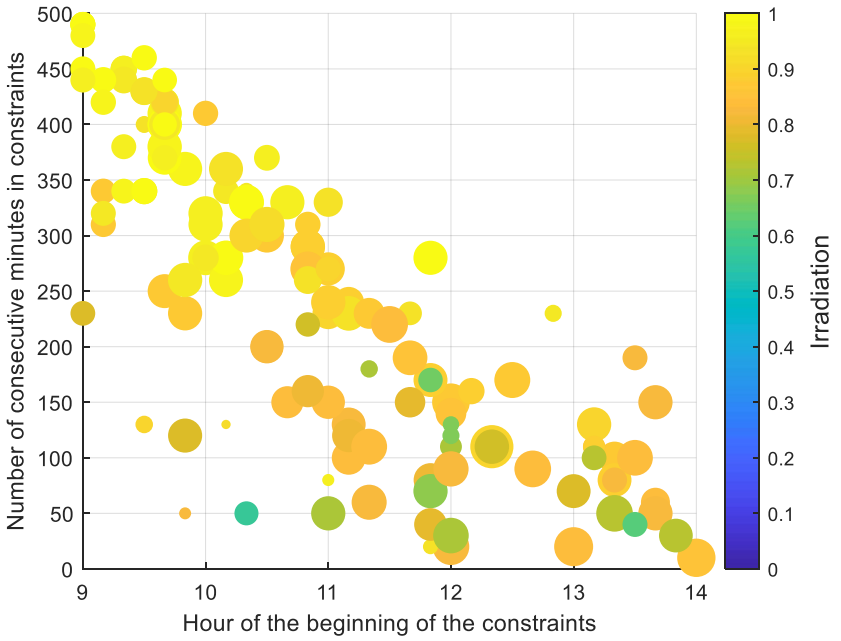

Figure 45 – Number of consecutive minutes potentially in current constraint at the feeder terminal, over two winters and inter-seasons, on the assumption of an HV N-1 configuration and according to the time of occurrence (size of the circles = maximum consumption level seen during the constraint).

After simulations, we can note that:

- all of the potential constraints apparently occur between 9 am and 2.00 pm with a higher level of consumption after 11.00 am.
- It is worth noting that the longest potential constraints apparently occur before midday.

Erreur ! Source du renvoi introuvable. Figure 46 below shows the same results, with this time, for the 4th dimension, the magnitude of the constraint (or the magnitude of the flexibility capable of resolving the constraint). The larger the circle, the closer one is to the maximum constraint obtained during this study[32].

With this second graph we note that there seems to be a strong correlation between the duration of the constraint, the severity of the constraint and photovoltaic power production.

[32] For example, if there is a voltage rise ranging between +2.8% and +2%, +2.8% is the largest circle.

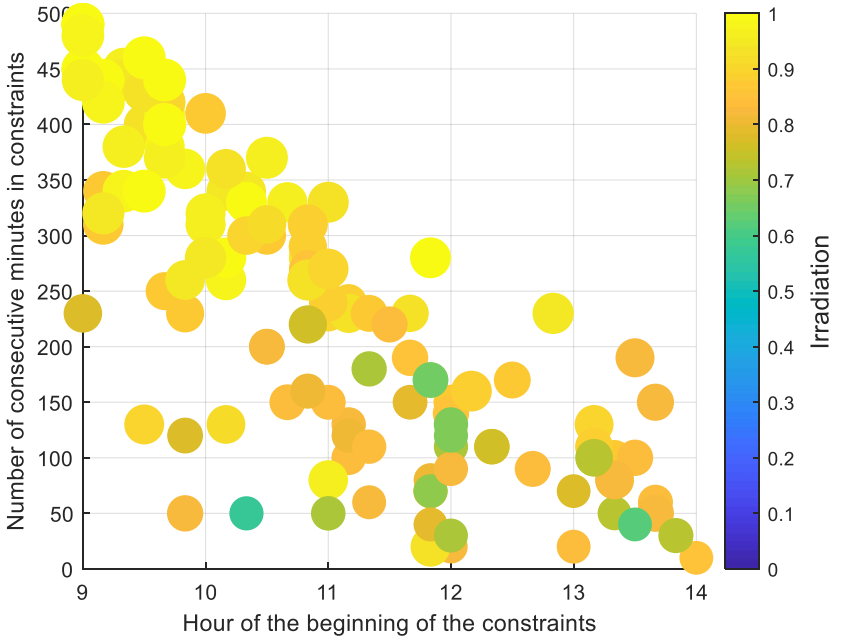

Figure 46 – Number of consecutive minutes potentially in current constraint at the feeder terminal, over two winters and inter-seasons, on the assumption of an HV N-1 configuration and according to the time of occurrence (size of the circles = relative significance of the constraint).

The graphs representing constrained months and days and their analyses have been placed in appendices.

Table 21 - Detail of constrained periods

	Months impacted	Days of the week impacted
Distribution of constraints	March - April – May - October	Every day of the week

Current constraint in the HV/MV transformer

Figure 47***Erreur ! Source du renvoi introuvable.*** below presents useful flexibility activation durations according to activation times. The graph includes:

- A third dimension (coloured) which represents the maximum insolation perceived by photovoltaic power production during the constraint.
- A fourth dimension (size of the circles) representing the maximum consumption level obtained throughout the constraint.

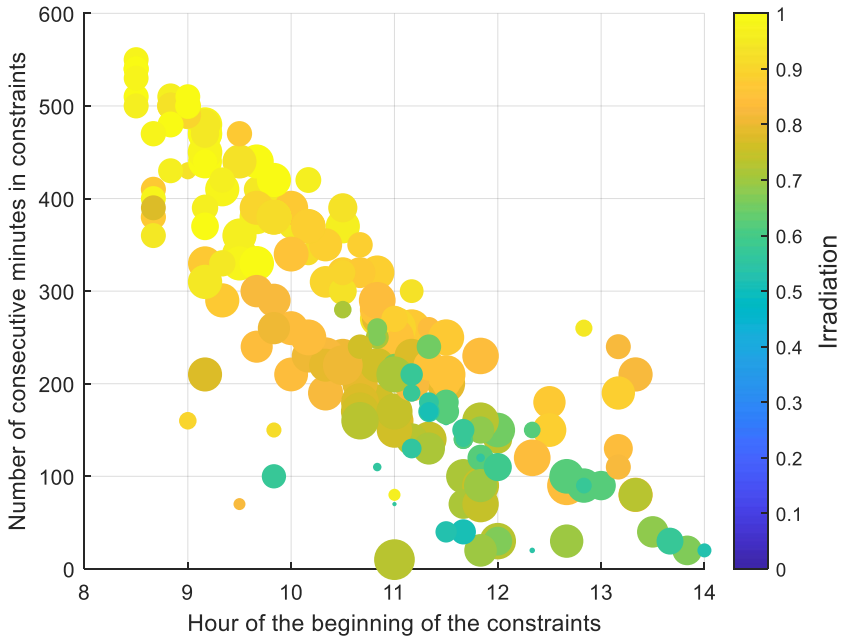

Figure 47 – Number of consecutive minutes potentially in current constraint at the source substation, over two winters and inter-seasons, on the assumption of an HV N-1 configuration and according to the time of occurrence (size of the circles = maximum consumption level seen during the constraint).

After simulations, we can note that all of the potential constraints apparently occur between 8.00 am and 2.00 pm. The longest constraints apparently occur before 11.00 am, i.e. with low consumption levels and fairly high photovoltaic production levels.

Erreur ! Source du renvoi introuvable. Figure 48 below shows the same results, with this time, for the 4th dimension, the magnitude of the constraint (or the magnitude of the flexibility capable of resolving the constraint). The larger the circle, the closer one is to the maximum constraint obtained during this study[33].

With this second graph we note that the flexibility volume is apparently larger when the duration is greater and when production is high.

[33] For example, if there is a voltage rise ranging between +2.8% and +2%, +2.8% is the largest circle.

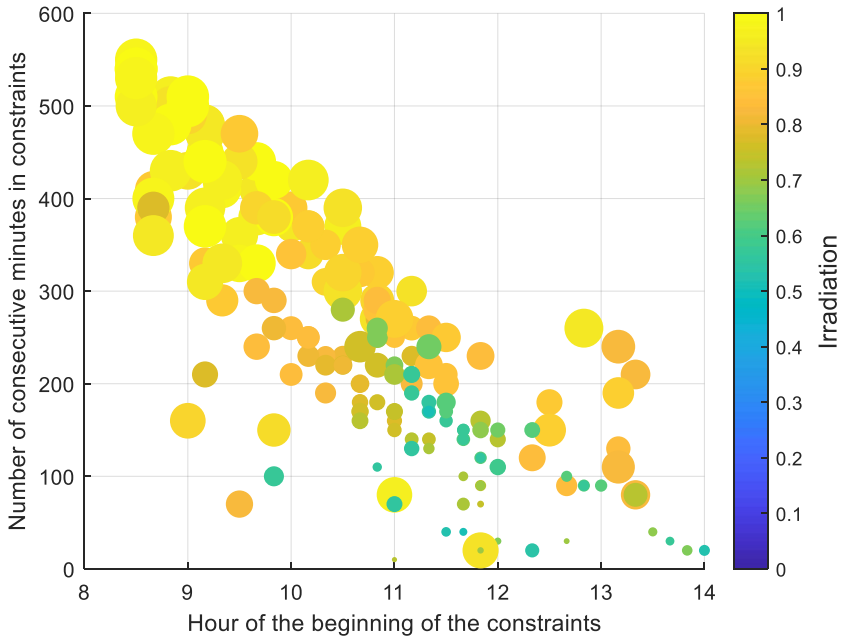

Figure 48 – Number of consecutive minutes potentially in current constraint at the source substation, over two winters and inter-seasons, on the assumption of an HV N-1 configuration and according to the time of occurrence (size of the circles = relative significance of the constraint).

The graphs representing constrained months and days and their analyses have been placed in appendices.

Table 22 - Detail of constrained periods

	Months impacted	Days of the week impacted
Distribution of constraints	March - April – May - October	Every day of the week

Voltage rise constraint

Erreur ! Source du renvoi introuvable. Figure 49 below presents useful flexibility activation durations according to activation times. The graph includes:

- A third dimension (coloured) which represents the maximum insolation perceived by photovoltaic power production during the constraint.
- A fourth dimension (size of the circles) representing the maximum consumption level obtained throughout the constraint.

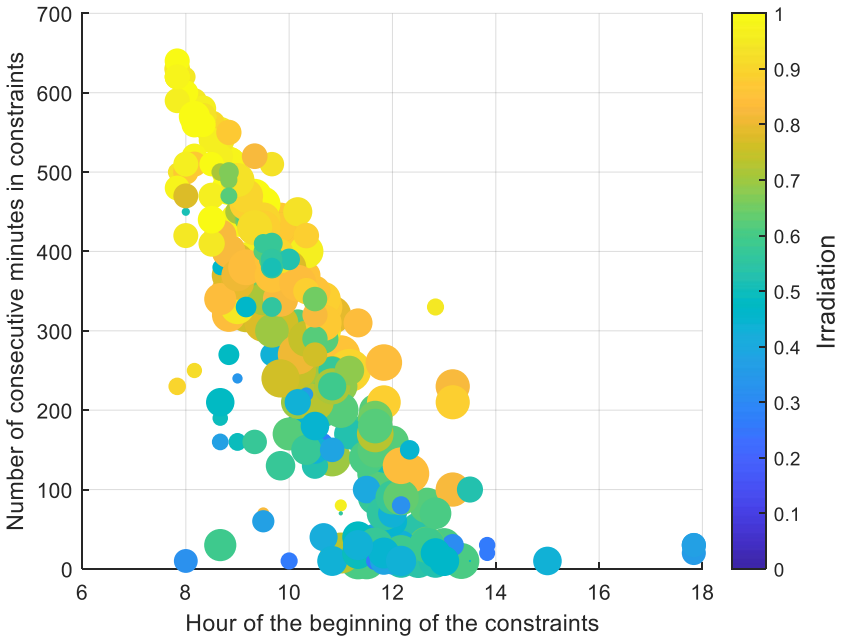

Figure 49 – Number of consecutive minutes potentially in voltage rise constraint, over two winters and inter-seasons, on the assumption of an HV N-1 configuration and according to the time of occurrence (size of the circles = maximum consumption level seen during the constraint).

After simulations, we can note that most of the potential constraints apparently occur between 8 am and 2.00 pm. The longest constraints apparently occur between 8 am and 10 am, i.e. with low or moderate consumption levels and photovoltaic power levels exceeding 60% of their maximum capacity. Between 10.00 am and 2.00 pm the level of consumption is higher, but the PV production level is also higher except for a few moments.

Erreur ! Source du renvoi introuvable. Figure 50 below shows the same results, with this time, for the 4th dimension, the magnitude of the constraint (or the magnitude of the flexibility capable of resolving the constraint). The larger the circle, the closer one is to the maximum constraint obtained during this study[34].

With this second graph we note that the flexibility volume is apparently larger when the duration is greater and when production is high (>60%).

[34] For example, if there is a voltage rise ranging between +2.8% and +2%, +2.8% is the largest circle.

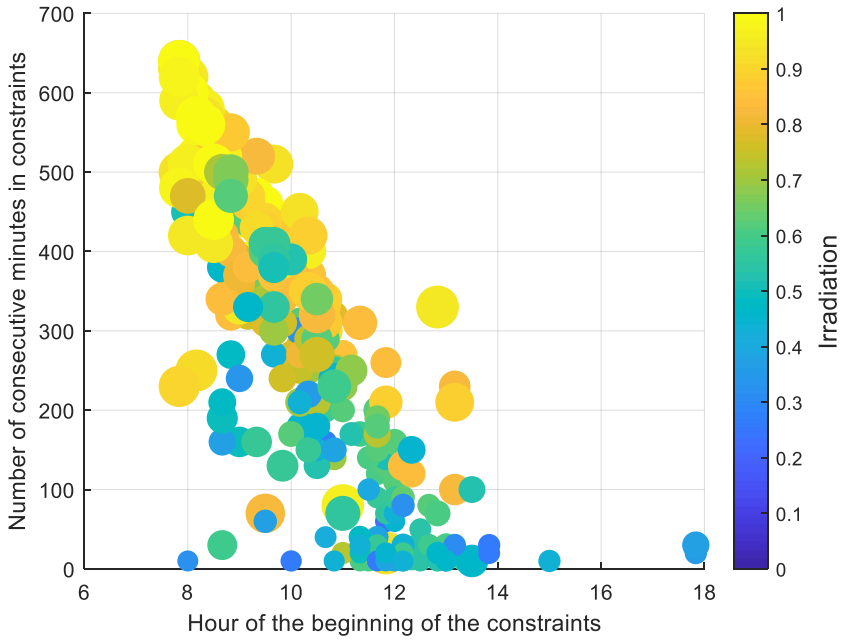

Figure 50 – Number of consecutive minutes potentially in voltage rise constraint, over two winters and inter-seasons, on the assumption of an HV N-1 configuration and according to the time of occurrence (size of the circles = relative significance of the constraint).

The graphs representing constrained months and days and their analyses have been placed in appendices.

Table 23 - Detail of constrained periods

Distribution of constraints	Months impacted	Days of the week impacted
	Every month	Every day of the week

Low-voltage constraint (voltage drop)

Figure 51**Erreur ! Source du renvoi introuvable.** below presents useful flexibility activation durations according to activation times.

The graph includes:

- A third dimension (size of the circles) representing the maximum consumption level obtained throughout the constraint.

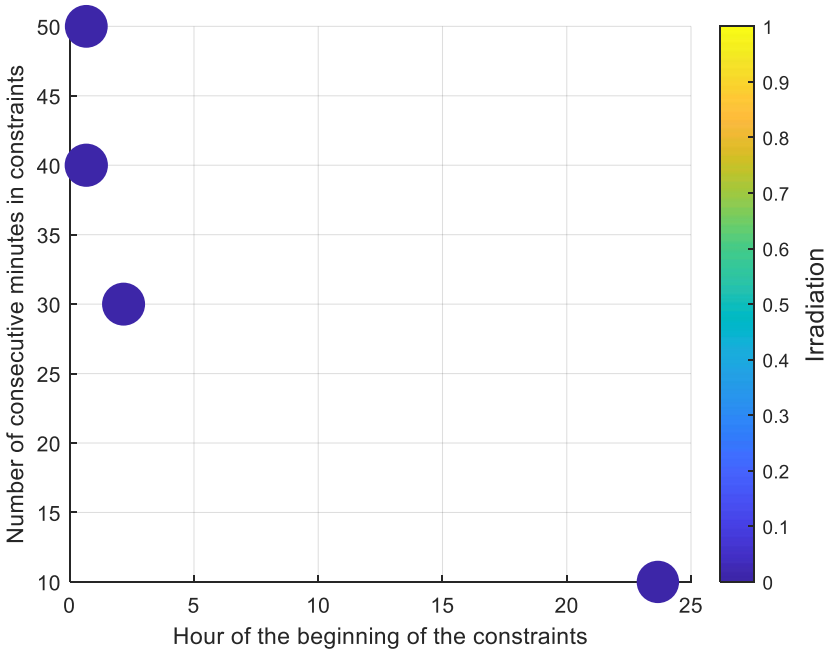

Figure 51 – Number of consecutive minutes potentially in low-voltage constraint, over two winters and inter-seasons, on the assumption of an HV N-1 configuration and according to the time of occurrence (size of the circles = maximum consumption level seen during the constraint).

We can note that most of the potential constraints apparently occur between 11.30 pm and 2.30 am. The longest constraint apparently occurs very early in the morning.

Erreur ! Source du renvoi introuvable. Figure 52 below shows the same results, with this time, for the 3rd dimension, the magnitude of the constraint (or the magnitude of the flexibility capable of resolving the constraint). The larger the circle, the closer one is to the maximum constraint obtained during this study[35].

With this second graph we note that, whatever the constraint, the flexibility volume will be more or less equivalent.

[35] For example, if there is a voltage rise ranging between +2.8% and +2%, +2.8% is the largest circle.

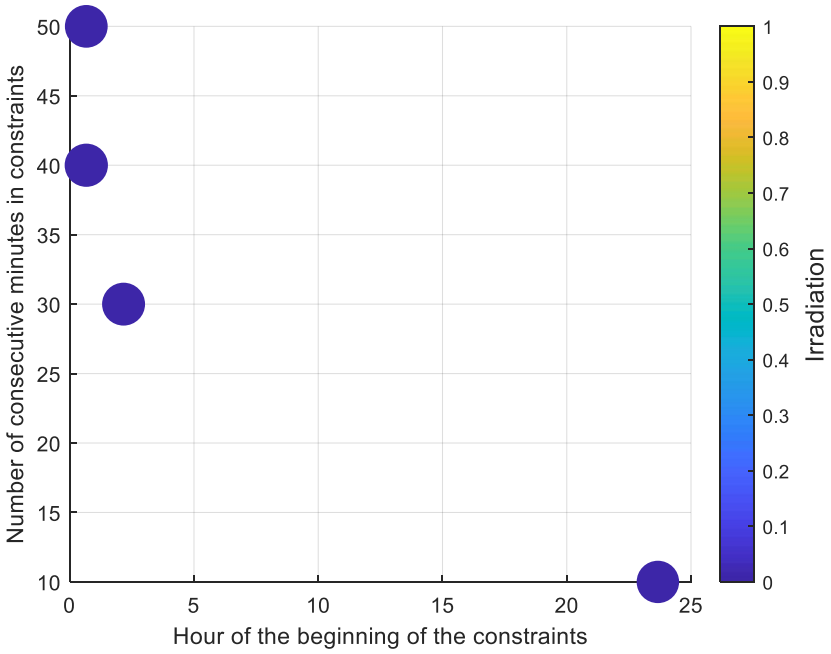

Figure 52 – Number of consecutive minutes potentially in undervoltage constraint, over two winters and inter-seasons, on the assumption of an HV N-1 configuration and according to the time of occurrence (size of the circles = relative significance of the constraint).

The graphs representing constrained months and days and their analyses have been placed in appendices.

Table 24 - Detail of constrained periods

Distribution of constraints	Months impacted	Days of the week impacted
	November – December	Monday - Tuesday - Sunday

3. Results of simulations corresponding to situation 21

As a reminder, simulation 21 corresponds to the following situation:

Table 25 – Summary table of situations simulated

Simulation 21	
Scenario	Green
PV locations	3
EV locations	1
Situation	N-1
Seasonality	Winter & inter-seasons

For information's sake, Figure 53**Erreur ! Source du renvoi introuvable.** below shows the location of the big producers on the constrained feeder.

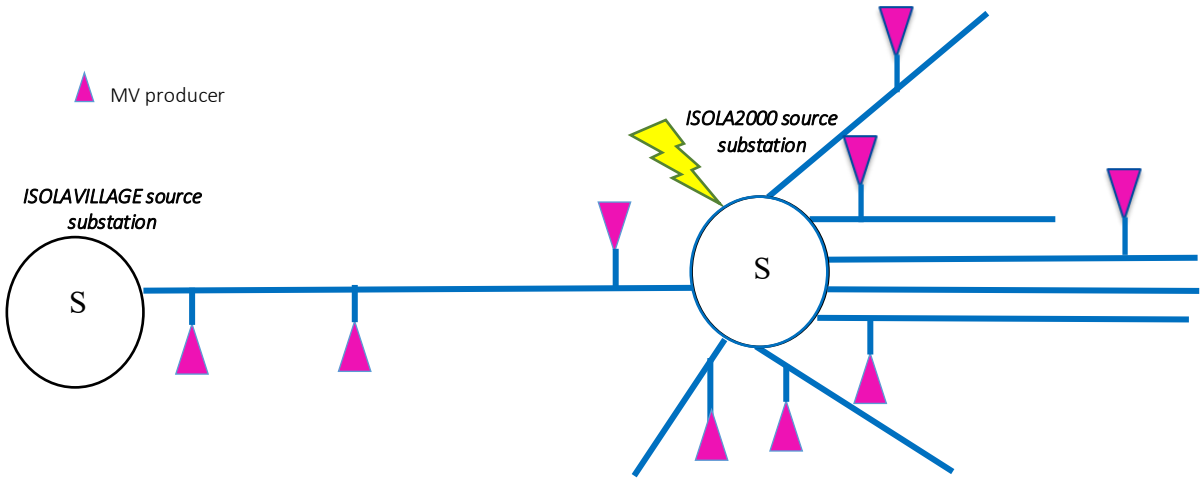

Figure 53 – Diagram of the constrained feeder with location of the big producers (>250 kVA)

For this new sample, 7 new producers were placed on the Isola2000 source substation, generating de facto fewer constraints than for the previous two placements which had 8 of them.

3D graph with consumption (excluding EVs), PV production and hydropower production

The graph below shows the states under constraint or not depending on the levels of hydropower production, PV production and consumption (excluding EVs):

- according to the locations simulated;
- for the constrained backup feeder and the constrained transformer;
- in a recovery configuration in an HV N-1 situation for winters and inter-seasons;
- in projected conditions in 2035/2036.

The graph shows five types of constraints:

- Current in grid equipment in draw-off and injection (lines/cables).
- Current in the HV/MV transformer.
- Current at the feeder terminal.
- Voltage rise.
- Voltage drop.

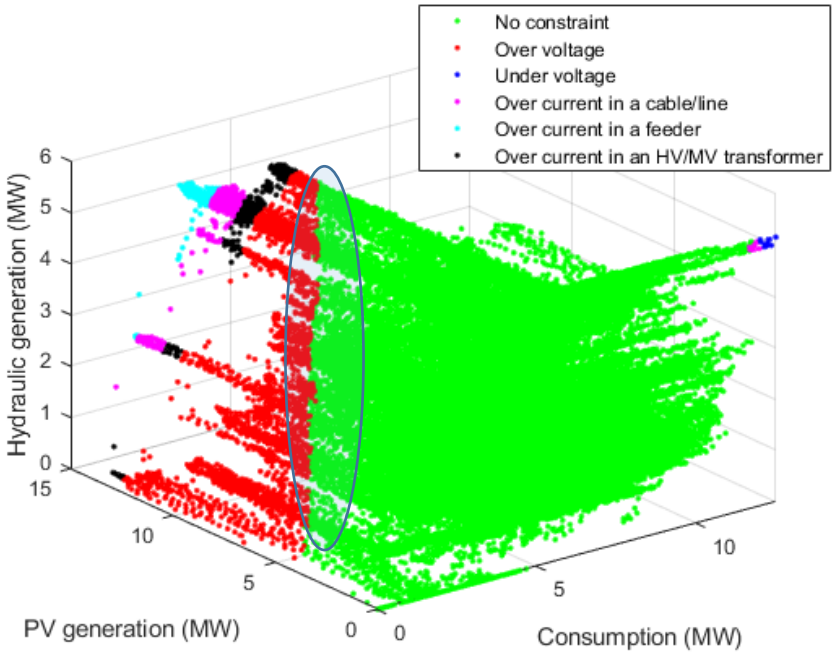

Figure 54 – 3D graph: Consumption (excluding EVs), PV Production and Hydropower Production for the constrained backup feeder at Isola in winter & inter-season, in an N-1 configuration

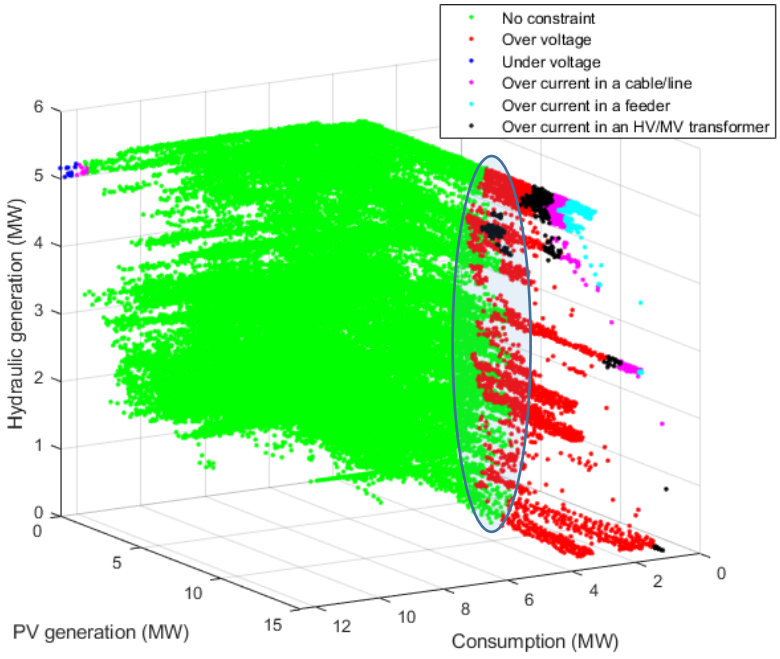

Figure 55 – Another view of the 3D graph under constraints: Consumption (excluding EVs), PV Production and Hydropower Production for the constrained backup feeder at Isola in winter & inter-season, in an N-1 configuration

Like in the previous cases, we can see on this graph the separation between zones under current constraint and zones with no current constraints. On the other hand, it is not possible to distinguish very clearly between the voltage constraint zone and the zone with no constraint, the "encircled zone". This is notably due to the fact that other factors are

involved, in particular the consumption level of the electric vehicles, which, although sometimes very low, could result in a transition from an unconstrained state to a constrained state.

Regarding constraints related to the injection of production, these appear at ***consumption levels lower than or equal to approximately 6 MW***, i.e. about 49% of the feeder's maximum charge, and when the ***injection of the photovoltaic panels exceeds 3.4 MW, i.e. about 23% of their installed capacity***.

Regarding constraints related to draw-off, these appear at ***high consumption levels exceeding 11.7 MW***, i.e. about 93% of the feeder's maximum charge, and when the ***injection of the photovoltaic panels is zero***.

Table 26 shows the maximum flexibility volumes for each constraint, **on the assumption of an HV N-1 configuration over the two complete years of summer 2035/2036**. The maximum constraint for voltage rise does not occur at the same time as the other production-related constraints (cf § 4.5.1).

The inversion of the consumption flexibility volume/production flexibility volume ratio is therefore potentially normal, and it could be explained by several reasons. One of those reasons would be the distribution of hydropower which is not the same at these two times: in one case the two producers produce, while in the other case only one of the two (cf APPEXNDIX B. § 1 - Impact of the location of flexibility). This difference could also be explained by the fact that production is injected at fixed and negative tanφ. Accordingly, when the injected production is reduced, the consumption of reactive power is reduced. There are therefore two conflicting effects, one positive regarding a reduction of the constraint (decline in production) and the other negative (decline in consumption of reactive power). In the case of consumption flexibility, since tanφ is positive with consumption, both effects go in the same direction.

Table 26 - Detail of useful flexibility volumes resolving the constraints and the ratio of useful flexibility to the consumption or PV production of the area

Type of flexibility	Flexibility volume for the type of constraint:					
	Current (injection)	Current at the feeder terminal (injection)	Current in the transformer (injection)	Voltage rise	Voltage drop	Current (draw-off)
Increase in consumption	3.02 MW 24%	1.76 MW 12%	4.55 MW 36%	6.3 MW 50%	-	-
Reduction in consumption	-	-	-	-	0.55 MW	0.8 MW
Reduction in MV production	2.84 MW 20%	1.65 MW 12%	3.95 MW 28%	7.75 MW 55%	-	-

Time slots of constraint occurrence

The overall results concerning the existence of constraints have been presented, and we will now present more detailed duration and period results for each type of constraint.

Current constraint in injection and draw-off

Erreur ! Source du renvoi introuvable. Figure 56 below presents useful flexibility activation durations according to activation times. The graph includes:

- A third dimension (coloured) which represents the maximum insolation perceived by photovoltaic power production during the constraint.
- A fourth dimension (size of the circles) representing the maximum consumption level obtained throughout the constraint.

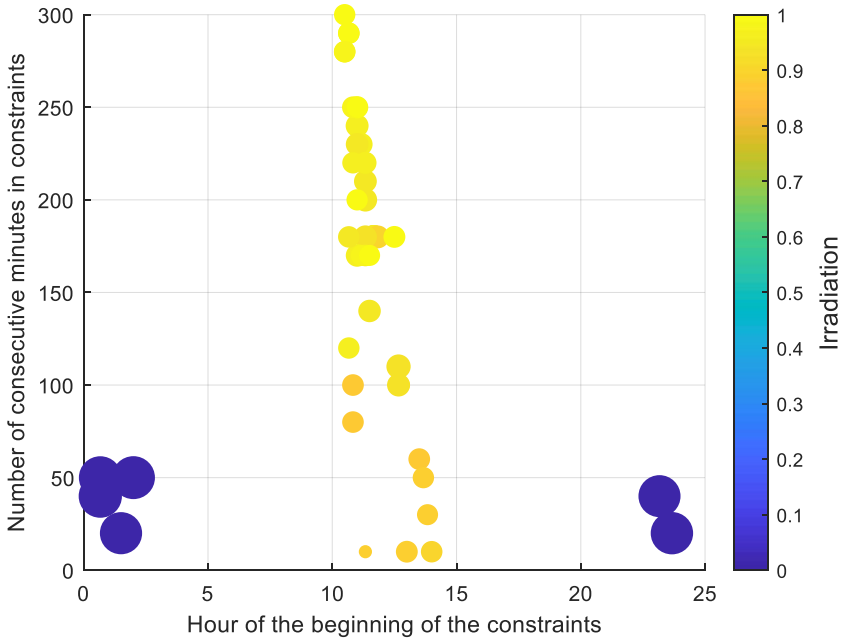

Figure 56 – Number of consecutive minutes potentially in current constraint, over two winters and inter-seasons, on the assumption of an HV N-1 configuration and according to the time of occurrence (size of the circles = maximum consumption level seen during the constraint).

After simulations, we can note that most of the potential constraints apparently occur between 10.00 am and 2.30 pm for injection constraints with low consumption and a high level of photovoltaic power (>70% of their maximum capacity) and for draw-off constraints between 11.00 pm and 2.30 in the morning with a very high consumption level and a photovoltaic power level of zero.

Erreur ! Source du renvoi introuvable. Figure 57 below shows the same results, with this time, for the 4th dimension, the magnitude of the constraint (or the magnitude of the flexibility capable of resolving the constraint). The larger the circle, the closer one is to the maximum constraint obtained during this study[36].

With this second graph we note that for injection-related constraints, the longer the duration of the constraint, the greater the flexibility volume related to the massive injection of photovoltaic power. For draw-off-related constraints, the flexibility volume is greatest when the constraint appears very early in the morning.

[36] For example, if there is a voltage rise ranging between +2.8% and +2%, +2.8% is the largest circle.

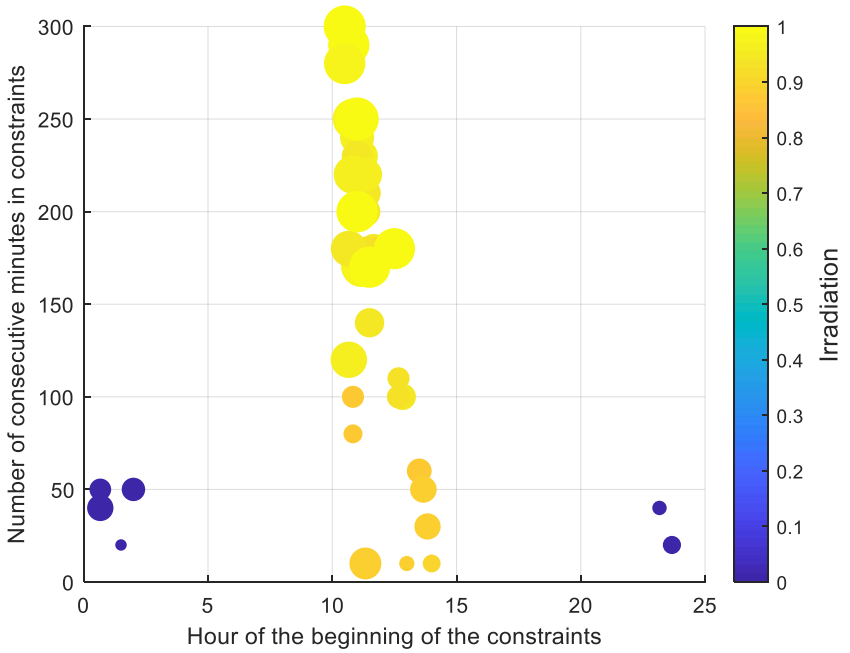

Figure 57 – Number of consecutive minutes potentially in current constraint, over two winters and inter-seasons, on the assumption of an HV N-1 configuration and according to the time of occurrence (size of the circles = relative significance of the constraint). The graphs representing constrained months and days and their analyses have been placed in appendices.

Table 27 - Detail of constrained periods

Distribution of constraints	Months impacted	Days of the week impacted
Distribution of draw-off constraints	November – December	Monday – Tuesday – Saturday - Sunday
Distribution of injection constraints	April – May	Every day of the week

Current constraint at the feeder terminal

Erreur ! Source du renvoi introuvable. Figure 58 below presents useful flexibility activation durations according to activation times. The graph includes:

- A third dimension (coloured) which represents the maximum insolation perceived by photovoltaic power production during the constraint.
- A fourth dimension (size of the circles) representing the maximum consumption level obtained throughout the constraint.

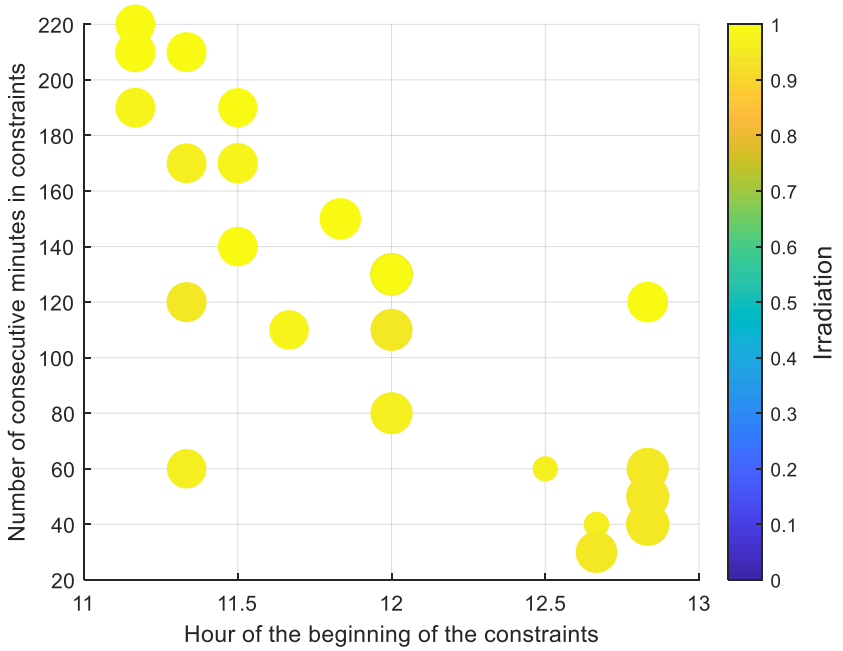

Figure 58 – Number of consecutive minutes potentially in current constraint at the feeder terminal, over two winters and inter-seasons, on the assumption of an HV N-1 configuration and according to the time of occurrence (size of the circles = maximum consumption level seen during the constraint).

After simulations, we can note that all of the potential constraints apparently occur between 11 am and 1.00 pm, with a very high photovoltaic production level (>90% of their maximum capacity). It is worth noting that the longest potential constraints apparently occur before midday.

Erreur ! Source du renvoi introuvable. Figure 59 below shows the same results, with this time, for the 4th dimension, the magnitude of the constraint (or the magnitude of the flexibility capable of resolving the constraint). The larger the circle, the closer one is to the maximum constraint obtained during this study[37].

With this second graph we note that the flexibility volume is roughly equivalent whatever the duration of the constraint.

[37] For example, if there is a voltage rise ranging between +2.8% and +2%, +2.8% is the largest circle.

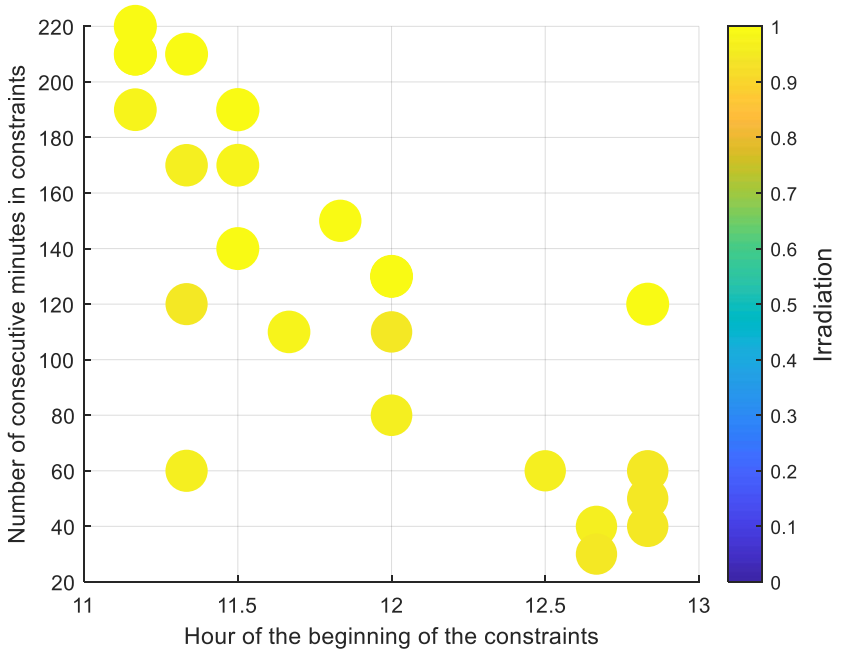

Figure 59 – Number of consecutive minutes potentially in current constraint at the feeder terminal, over two winters and inter-seasons, on the assumption of an HV N-1 configuration and according to the time of occurrence (size of the circles = relative significance of the constraint).

The graphs representing constrained months and days and their analyses have been placed in appendices.

Table 28 - Detail of constrained periods

Distribution of constraints	Months impacted	Days of the week impacted
	April - May	Every day of the week

Current constraint in the HV/MV transformer

Figure 60**Erreur ! Source du renvoi introuvable.** below presents useful flexibility activation durations according to activation times. The graph includes:

- A third dimension (coloured) which represents the maximum insolation perceived by photovoltaic power production during the constraint.
- A fourth dimension (size of the circles) representing the maximum consumption level obtained throughout the constraint.

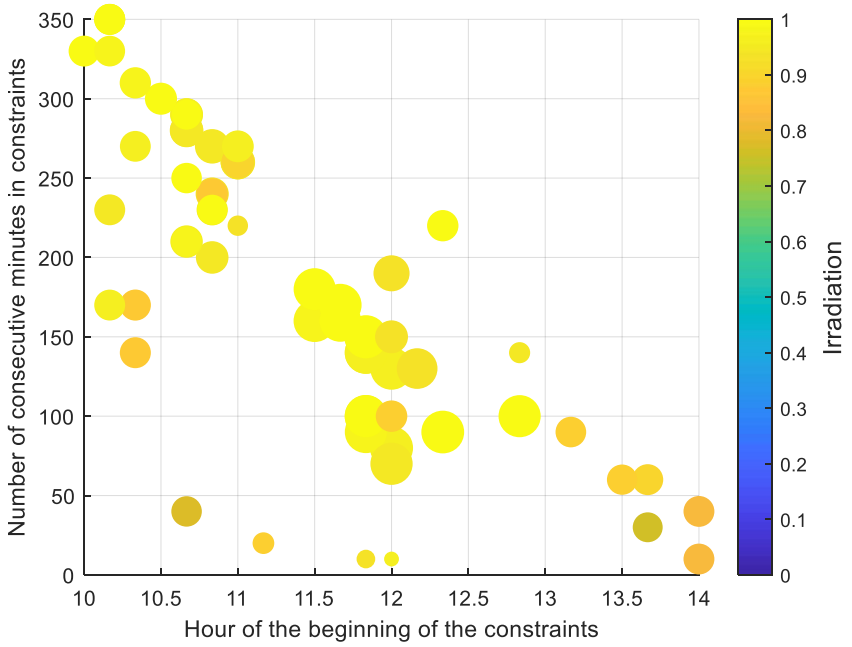

Figure 60 – Number of consecutive minutes potentially in current constraint at the source substation, over two winters and inter-seasons, on the assumption of an HV N-1 configuration and according to the time of occurrence (size of the circles = maximum consumption level seen during the constraint).

After simulations, we can note that most of the potential constraints apparently occur between 10.00 am and 2.00 pm. The longest constraints apparently occur before 11 am, i.e. with moderate consumption levels and very high photovoltaic production levels (>80% of their maximum capacity).

Erreur ! Source du renvoi introuvable. Figure 61 below shows the same results, with this time, for the 4th dimension, the magnitude of the constraint (or the magnitude of the flexibility capable of resolving the constraint). The larger the circle, the closer one is to the maximum constraint obtained during this study[38].

With this second graph we note on the whole that the flexibility volume is apparently larger when the duration is greater and when production is high (>90%).

[38] For example, if there is a voltage rise ranging between +2.8% and +2%, +2.8% is the largest circle.

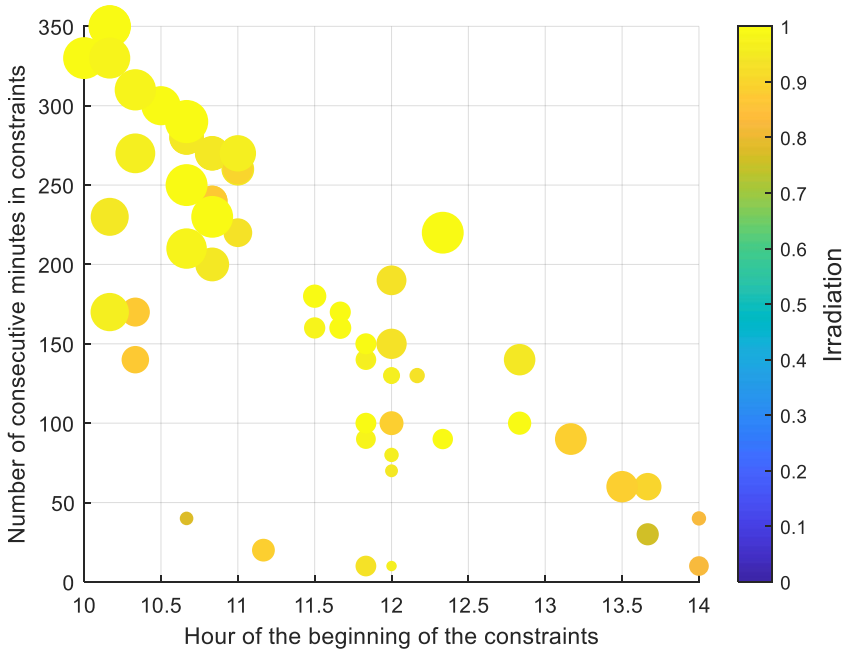

Figure 61 – Number of consecutive minutes potentially in current constraint at the source substation, over two winters and inter-seasons, on the assumption of an HV N-1 configuration and according to the time of occurrence (size of the circles = relative significance of the constraint).

The graphs representing constrained months and days and their analyses have been placed in appendices.

Table 29 - Summary table of constrained months and days: simulations for winter & inter-seasons

Distribution of constraints	Months impacted	Days of the week impacted
	April - May	Every day of the week

Voltage rise constraint

Erreur ! Source du renvoi introuvable. Figure 62 below presents useful flexibility activation durations according to activation times. The graph includes:

- A third dimension (coloured) which represents the maximum insolation perceived by photovoltaic power production during the constraint.
- A fourth dimension (size of the circles) representing the maximum consumption level obtained throughout the constraint.

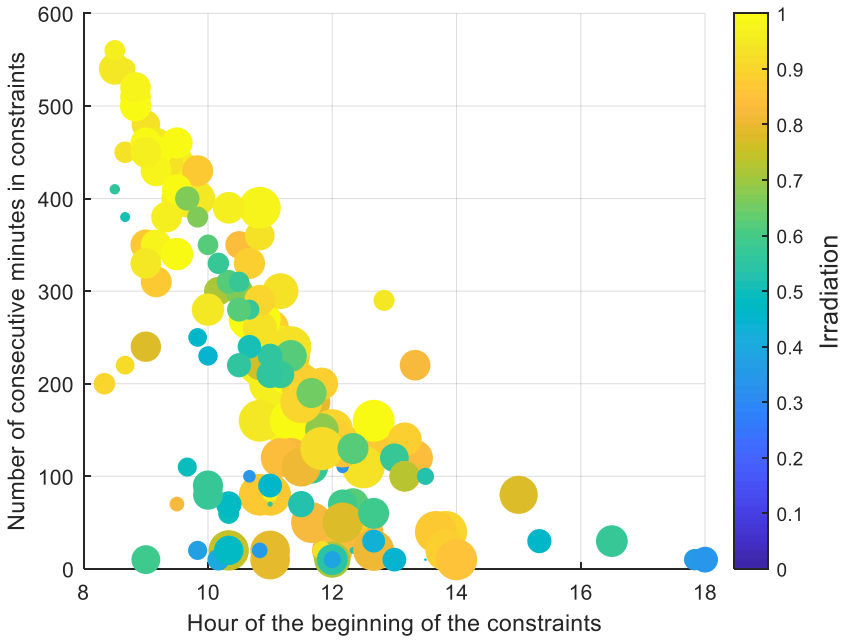

Figure 62 – Number of consecutive minutes potentially in voltage rise constraint, over two winters and inter-seasons, on the assumption of an HV N-1 configuration and according to the time of occurrence (size of the circles = maximum consumption level seen during the constraint).

After simulations, we can note that most of the potential constraints apparently occur between 8.00 am and 6.00 pm. The longest constraints apparently occur between 8 am and 10 am, i.e. with low or moderate consumption levels and photovoltaic power levels exceeding 70% of their maximum capacity. Between 10.00 am and 2.00 pm the level of consumption is high, but the PV production level is also high except for a few moments.

Erreur ! Source du renvoi introuvable. Figure 63 below shows the same results, with this time, for the 4th dimension, the magnitude of the constraint (or the magnitude of the flexibility capable of resolving the constraint). The larger the circle, the closer one is to the maximum constraint obtained during this study[39].

With this second graph we note that the flexibility volume is apparently larger when the duration is greater and when production is high (>60%).

[39] For example, if there is a voltage rise ranging between +2.8% and +2%, +2.8% is the largest circle.

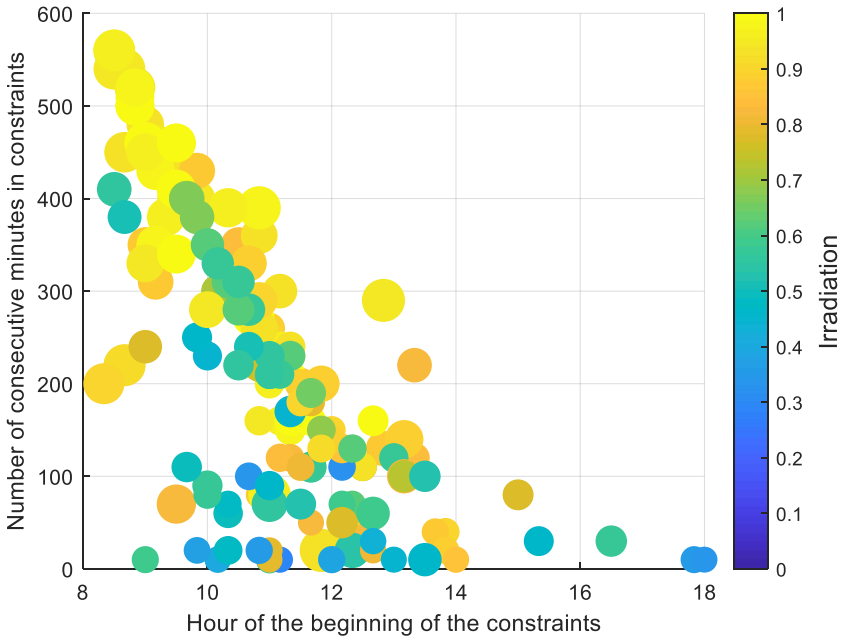

Figure 63 – Number of consecutive minutes potentially in current constraint at the source substation, over two winters and inter-seasons, on the assumption of an HV N-1 configuration and according to the time of occurrence (size of the circles = relative significance of the constraint).

The graphs representing constrained months and days and their analyses have been placed in appendices.

Table 30 - Summary table of constrained months and days: simulations for winter & inter-seasons

	Months impacted	Days of the week impacted
Distribution of constraints	March - April - May - October - November	Every day of the week

Voltage drop constraint

Erreur ! Source du renvoi introuvable. Figure 64 below presents useful flexibility activation durations according to activation times.

The graph includes:

- A third dimension (size of the circles) representing the maximum consumption level obtained throughout the constraint.

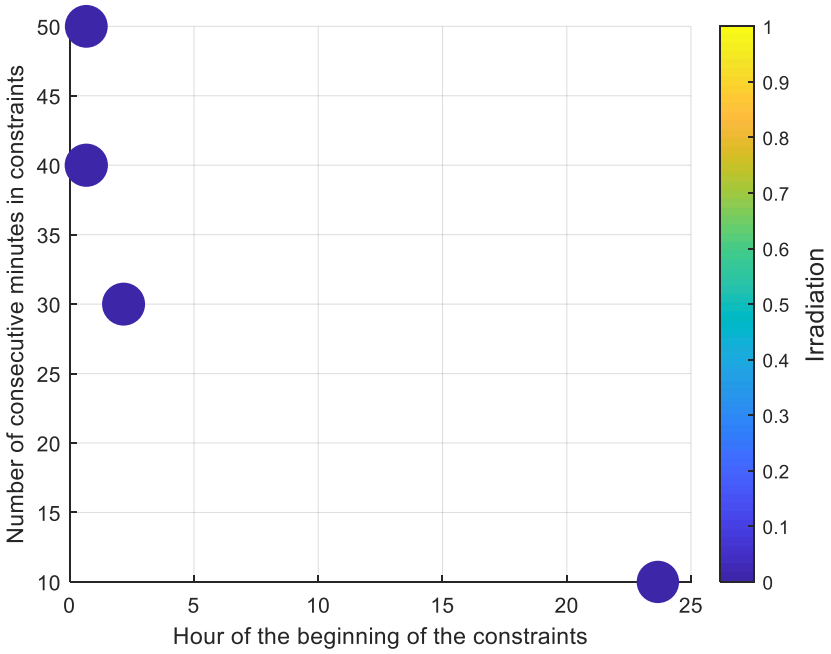

Figure 64 – Number of consecutive minutes potentially in current constraint at the source substation, over two winters and inter-seasons, on the assumption of an HV N-1 configuration and according to the time of occurrence (size of the circles = maximum consumption level seen during the constraint).

After simulations, we can note that most of the potential constraints apparently occur between 11.30 pm and 2.30 am.

Erreur ! Source du renvoi introuvable. Figure 65 below shows the same results, with this time, for the 3rd dimension, the magnitude of the constraint (or the magnitude of the flexibility capable of resolving the constraint). The larger the circle, the closer one is to the maximum constraint obtained during this study[40].

With this second graph we note that whatever the constraint, the flexibility volume would be practically identical.

[40] For example, if there is a voltage rise ranging between +2.8% and +2%, +2.8% is the largest circle.

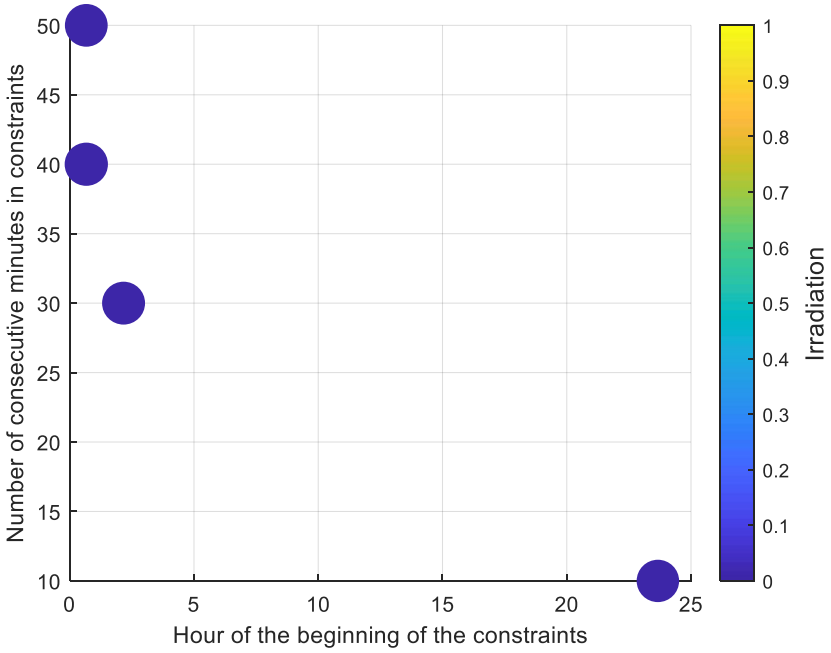

Figure 65 – Number of consecutive minutes potentially in current constraint at the source substation, over two winters and inter-seasons, on the assumption of an HV N-1 configuration and according to the time of occurrence (size of the circles = relative significance of the constraint).

The graphs representing constrained months and days and their analyses have been placed in appendices.

Table 31 - Detail of constrained periods

Distribution of constraints	Months impacted	Days of the week impacted
	November – December	Monday - Tuesday - Sunday

4. Results of simulations corresponding to situation 22

As a reminder, simulation 22 corresponds to the following situation:

Table 32: Summary table of situations simulated

Simulation 22	
PV location	1
EV location	1
Scenario	Green
Situation	N-1
Seasonality	Summer

The number and location of MV producers is the same as for the batteries of simulations No. 19.

Like for the previous section, the results are represented via three-dimensional graphs.

3D graph with consumption (excluding EVs), PV production and hydropower production

The graph below shows the states under constraint or not depending on the levels of hydropower production, PV production and consumption (excluding EVs):

- depending on the sample simulated;
- for the constrained backup feeder and the constrained transformer;
- in a recovery configuration in an HV N-1 situation for summers;
- in projected conditions in 2035/2036.

The graph shows four types of constraints:

- Overcurrent in grid equipment in draw-off and injection (lines/cables).
- Overcurrent in the HV/MV transformer.
- Overcurrent at the feeder terminal.
- Voltage rise

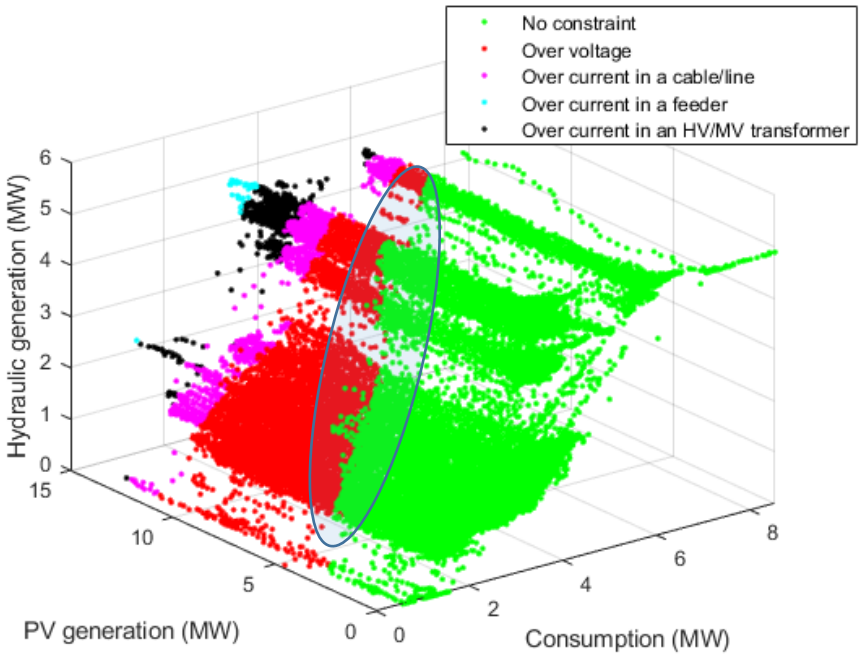

Figure 66 – 3D graph: Consumption (excluding EVs), PV Production and Hydropower Production for the constrained backup feeder at Isola in summer, in an N-1 configuration

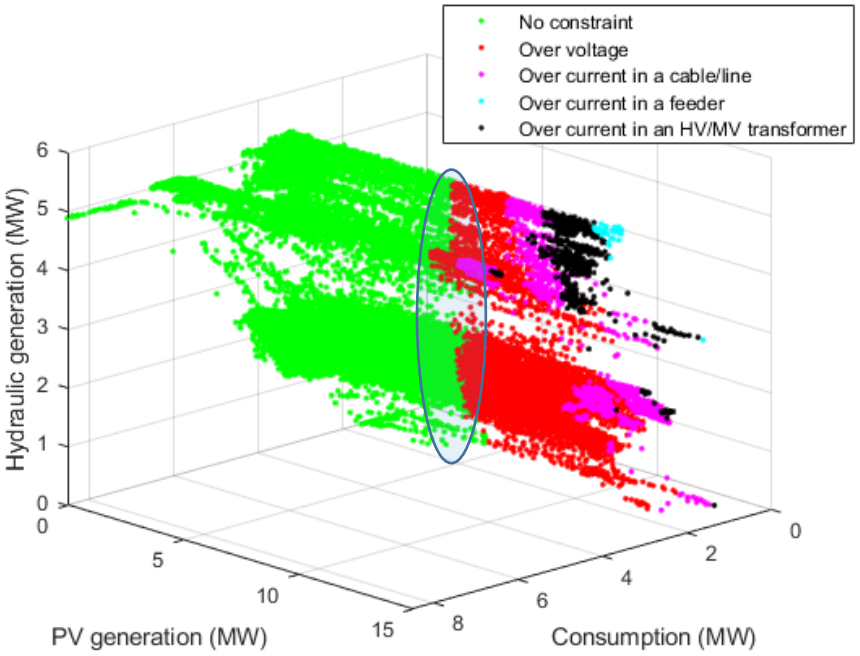

Figure 67- Another view of the 3D graph under constraints: Consumption (excluding EVs), PV Production and Hydropower Production for the constrained backup feeder at Isola in summer, in an N-1 configuration

Like in the previous cases, we can see on this graph the clear separation between zones under current constraint and zones with no current constraints. On the other hand, it is not possible to very easily distinguish a clear boundary between the voltage constraint zone and the zone with no constraint, the "encircled zone". This is notably due to the fact that other factors are involved, such as the consumption level of the electric vehicles, which, although sometimes very low, could result in a transition from an unconstrained state to a constrained state.

Regarding constraints related to the injection of production, these appear at ***consumption levels lower than or equal to 6 MW***, i.e. about 70% of the feeder's maximum charge, and when the ***injection of the photovoltaic panels exceeds 3.4 MW, i.e. about 24% of their installed capacity***.

Useful flexibility volume capable of resolving constraints

Table 33 shows the maximum flexibility volumes for each constraint, **on the assumption of an HV N-1 configuration over the two complete years of summer 2035/2036**. Note that the maximum constraint for voltage rise does not appear at the same time as the other production-related constraints (cf § 4.5.1).

The inversion of the consumption flexibility volume/production flexibility volume ratio is therefore potentially normal and it could be explained by several reasons. One of those reasons would be the distribution of hydropower which is not the same at these two times: in one case the two producers produce, while in the other case only one of the two (cf. APPENDIX C - § 1 Impact of the location of flexibility). This difference could also be explained by the fact that production is injected at fixed and negative tanφ. Accordingly, when the injected production is reduced, the consumption of reactive power is reduced. There are therefore two conflicting effects, one positive regarding a reduction of the constraint (decline in production) and the other negative (decline in consumption of reactive power).

In the case of consumption flexibility, since tanφ is positive with consumption, both effects go in the same direction.

Table 33: Useful flexibility volumes capable of resolving each constraint and the ratio of useful flexibility to the consumption or PV production of the area

Type of flexibility	Type of constraint			
	Current (injection)	Current at the feeder terminal (injection)	Current in the transformer (injection)	Voltage rise
Rise in consumption	5.4 MW 63%	1.15 MW 13%	3.9 MW 46%	7.05 MW 83%
Fall in MV production	4.9 MW 35%	1.1 MW 8%	3.4 MW 24%	8.5 MW 60%

Time slots of constraint occurrence

The overall results concerning the existence of constraints have been presented, and we will now present more detailed duration and period results by type of constraint.

Current constraint in injection

Figure 68 below presents useful flexibility activation durations according to activation times. The graph includes:

- A third dimension (coloured) which represents the maximum insolation perceived by photovoltaic power production during the constraint.
- A fourth dimension (size of the circles) representing the maximum consumption level obtained throughout the constraint.

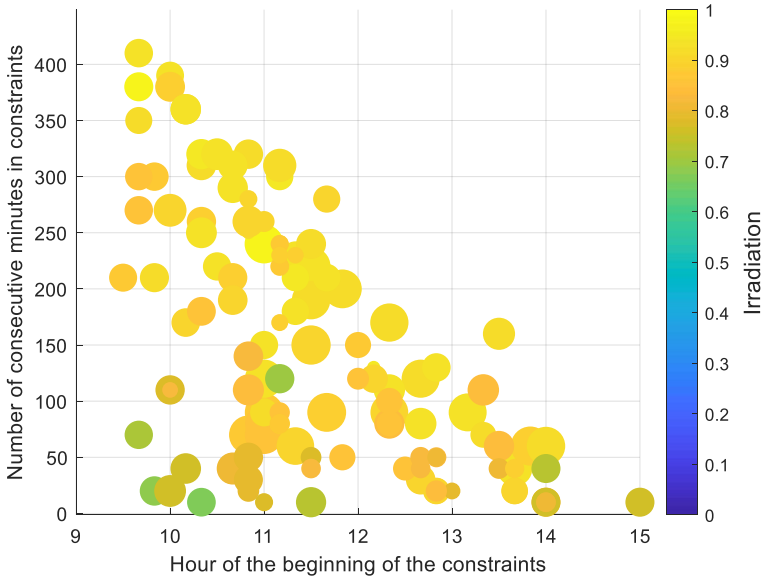

Figure 68 – Number of consecutive minutes potentially in current constraint, over two summers, on the assumption of an HV N-1 configuration and according to the time of occurrence (size of the circles = relative significance of the constraint).

After simulations, we can note that:

- All of the potential constraints apparently occur between 9.30 am and 3.00 pm with a high photovoltaic production level (>60% of their maximum capacity).
- It is worth noting that most of the constraints apparently occur before midday. This is due to the fact that the PV production profile rises to a maximum when the sun is at its zenith, and then comes back down.

Figure 69**Erreur ! Source du renvoi introuvable.** below shows the same results, with this time, for the 4th dimension, the magnitude of the constraint (or the magnitude of the flexibility capable of resolving the constraint). The larger the circle, the closer one is to the maximum constraint obtained during this study[41].

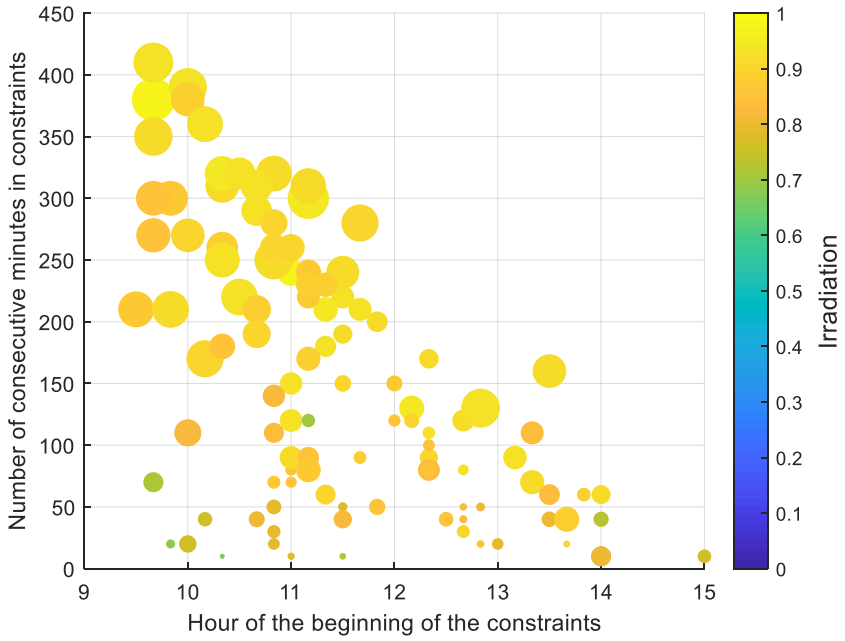

Figure 69 – Number of consecutive minutes potentially in voltage rise constraint, over two summers, on the assumption of an HV N-1 configuration and according to the time of occurrence (size of the circles = relative significance of the constraint).

With this second graph we note that the longer the duration of the constraint, the greater the flexibility volume. This is notably due to the fact that photovoltaic power production is substantial.

The graphs representing constrained months and days and their analyses have been placed in appendices. The following table summarizes the results obtained.

Table 34 - Detail of constrained periods

Distribution of constraints	Months impacted	Days of the week impacted
	June – July - August	Every day of the week

[41] For example, if there is a voltage rise ranging between +2.8% and +2%, +2.8% is the largest circle.

Current constraint at the feeder terminal

Figure 70**Erreur ! Source du renvoi introuvable.** below presents useful flexibility activation durations according to activation times. The graph includes:

- A third dimension (coloured) which represents the maximum insolation perceived by photovoltaic power production during the constraint.
- A fourth dimension (size of the circles) representing the maximum consumption level obtained throughout the constraint.

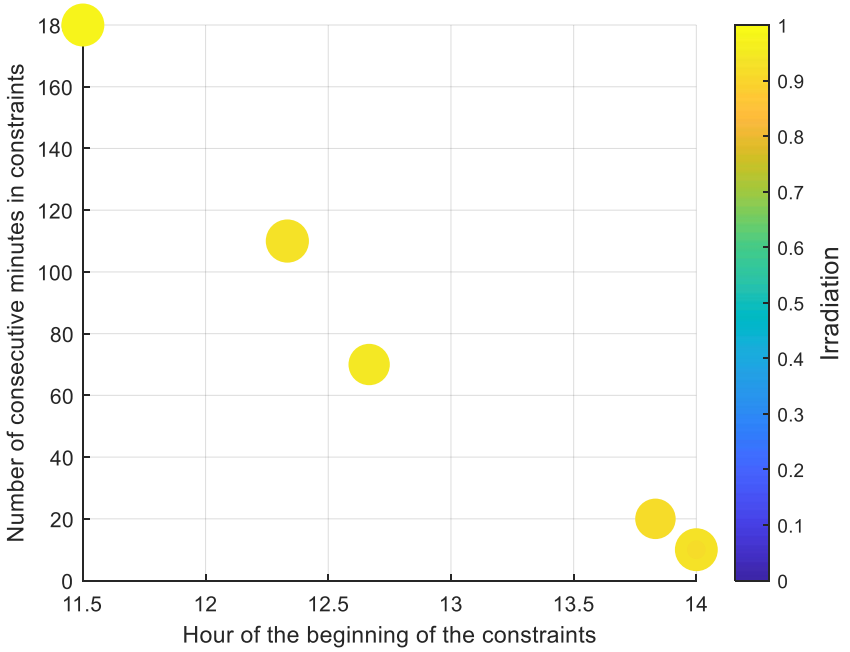

Figure 70 – Number of consecutive minutes potentially in current constraint at the source substation, over two summers, on the assumption of an HV N-1 configuration and according to the time of occurrence (size of the circles = maximum consumption level seen during the constraint).

After simulations, we can note that:

- All of the potential constraints apparently occur between 11.30 am and 2.00 pm with a high production level exceeding 90% of their maximum capacity.
- It is worth noting that the longest potential constraint apparently occurs before midday. This is due to the fact that the PV production profile rises to a maximum when the sun is at its zenith, and then comes back down.

Figure 71**Erreur ! Source du renvoi introuvable.** below shows the same results, with this time, for the 4th dimension, the magnitude of the constraint (or the magnitude of the

flexibility capable of resolving the constraint). The larger the circle, the closer one is to the maximum constraint obtained during this study[42].

With this second graph we note that, whatever the duration of the constraint, the useful flexibility volumes capable of resolving the constraint are apparently very similar.

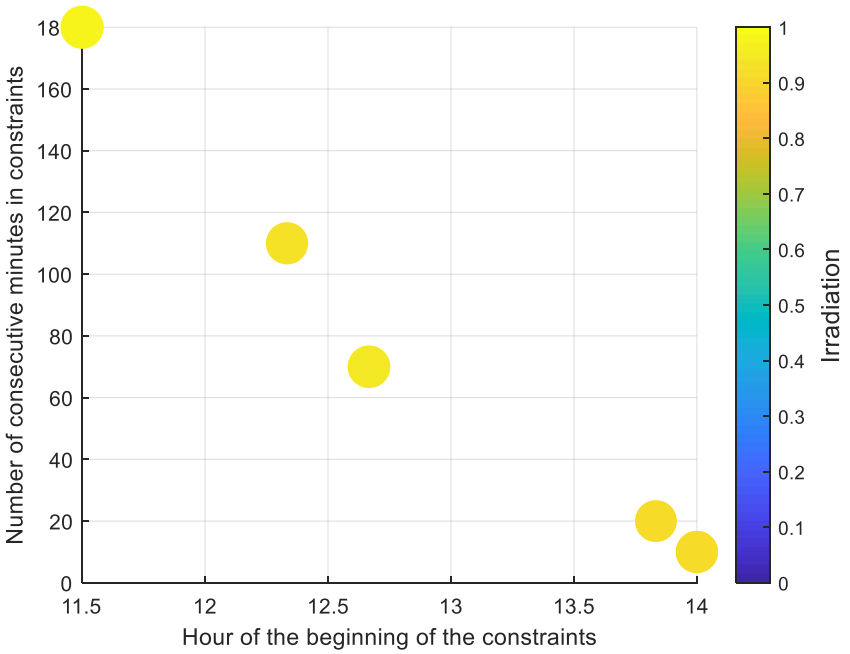

Figure 71 – Number of consecutive minutes potentially in current constraint at the feeder terminal, over two summers, on the assumption of an HV N-1 configuration and according to the time of occurrence (size of the circles = relative significance of the constraint).

The graphs representing constrained months and days and their analyses have been placed in appendices. The following table summarizes the results obtained.

Table 35 - Detail of constrained periods

Distribution of constraints	Months impacted	Days of the week impacted
	June - July - August	Every day of the week

Current constraint in the HV/MV transformer

Figure 72**Erreur ! Source du renvoi introuvable.** below presents useful flexibility activation durations according to activation times. The graph includes:

- A third dimension (coloured) which represents the maximum insolation perceived by photovoltaic power production during the constraint.

[42] For example, if there is a voltage rise ranging between +2.8% and +2%, +2.8% is the largest circle.

- A fourth dimension (size of the circles) representing the maximum consumption level obtained throughout the constraint.

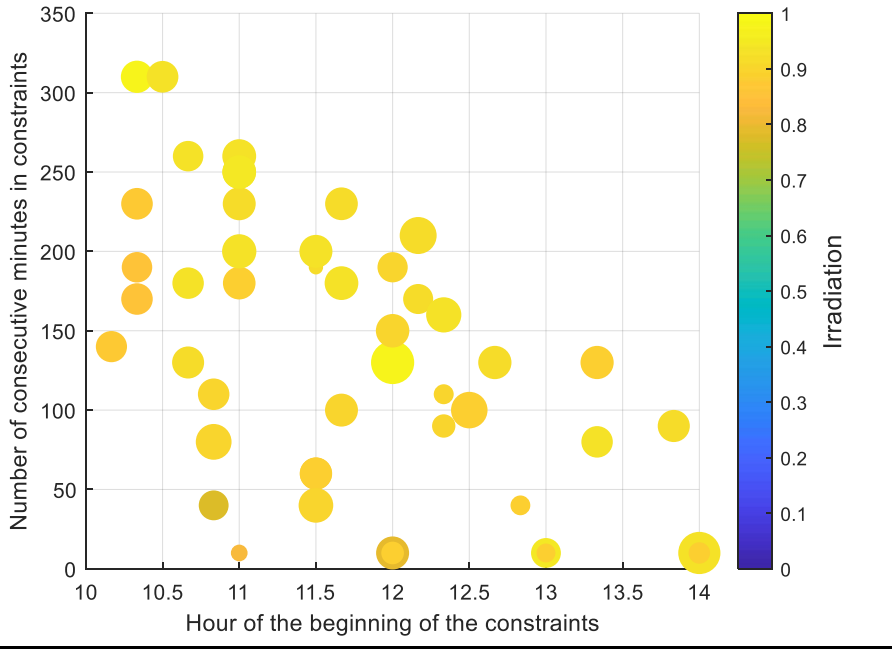

Figure 72 – Number of consecutive minutes potentially in current constraint at the source substation, over two summers, on the assumption of an HV N-1 configuration and according to the time of occurrence (size of the circles = maximum consumption level seen during the constraint).

After simulations, we can note that all of the potential constraints apparently occur between 10.00 am and 2.00 pm. The longest constraints apparently occur with very high photovoltaic power levels (>80% of their maximum capacity).

Erreur ! Source du renvoi introuvable. Figure 73 below shows the same results, with this time, for the 4th dimension, the magnitude of the constraint (or the magnitude of the flexibility capable of resolving the constraint). The larger the circle, the closer one is to the maximum constraint obtained during this study[43].

With this second graph we note that the smallest flexibility volumes apparently occur on constraints of duration less than 150 min., i.e. 2.5 hours. There seems therefore to be a strong correlation between the duration and magnitude of the constraint.

[43] For example, if there is a voltage rise ranging between +2.8% and +2%, +2.8% is the largest circle.

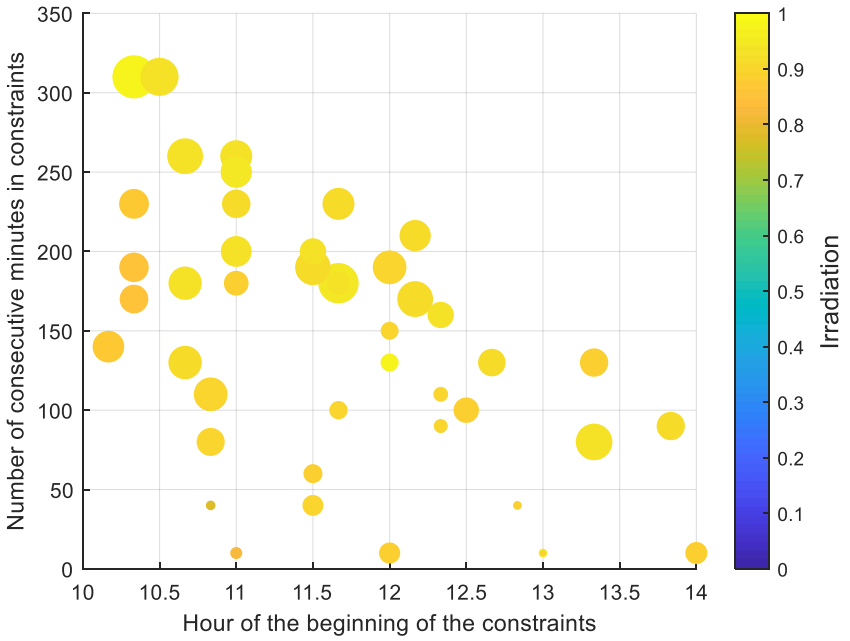

Figure 73 – Number of consecutive minutes potentially in current constraint at the source substation, over two summers, on the assumption of an HV N-1 configuration and according to the time of occurrence (size of the circles = relative significance of the constraint).

The graphs representing constrained months and days and their analyses have been placed in appendices. The following table summarizes the results obtained.

Table 36 - Detail of constrained periods

Distribution of constraints	Months impacted	Days of the week impacted
	June – July - August	Every day of the week

Voltage rise constraint

Erreur ! Source du renvoi introuvable. Figure 74 below presents useful flexibility activation durations according to activation times. The graph includes:

- A third dimension (coloured) which represents the maximum insolation perceived by photovoltaic power production during the constraint.
- A fourth dimension (size of the circles) representing the maximum consumption level obtained throughout the constraint.

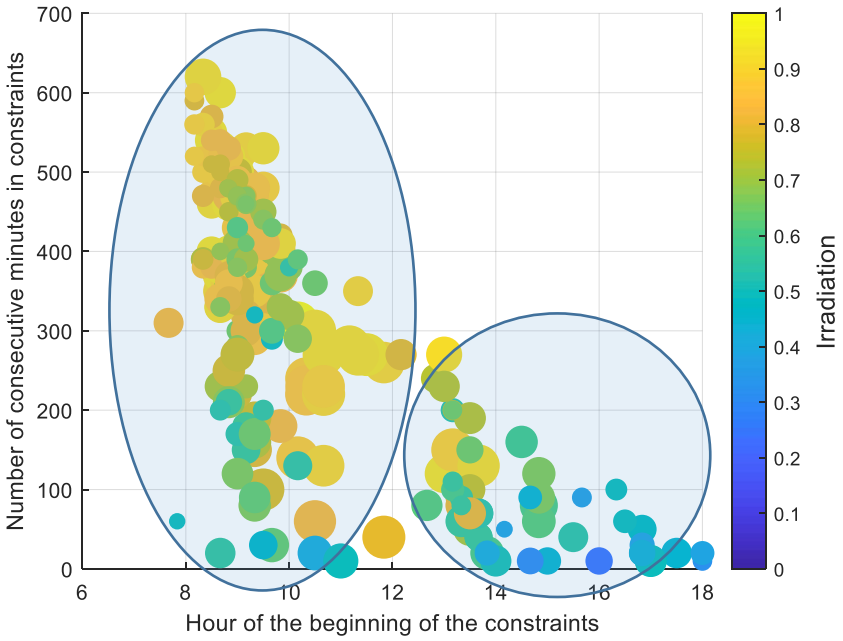

Figure 74 – Number of consecutive minutes potentially in current constraint at the source substation, over two summers, on the assumption of an HV N-1 configuration and according to the time of occurrence (size of the circles = maximum consumption level seen during the constraint).

After simulations, we can note that most of the potential constraints apparently occur over the entire solar day, with a major concentration between 8.00 am and 12.00, and then between 12.00 and 6.00 pm. The second concentration has lower PV levels (40% of maximum capacity), but consumption is lower, resulting in a (production, consumption) pair generating constraints.

Erreur ! Source du renvoi introuvable. Figure 75 below shows the same results, with this time, for the 4th dimension, the magnitude of the constraint (or the magnitude of the flexibility capable of resolving the constraint). The larger the circle, the closer one is to the maximum constraint obtained during this study[44].

With this second graph we note that the flexibility volume is apparently larger when the duration is longer and when production is high (>60% of maximum capacity). There is apparently again a correlation between the duration and the maximum constraint level. This is due to the fact that the PV production profile rises to a maximum when the sun is at its zenith, and then comes back down. If the constraint occurs early, therefore, it will last a long time and generate a greater flexibility volume, whereas if it occurs after production has peaked, the duration of the constraint will be less long and less constraining. This principle remains correct so long as consumption sustains no major variations.

[44] For example, if there is a voltage rise ranging between +2.8% and +2%, +2.8% is the largest circle.

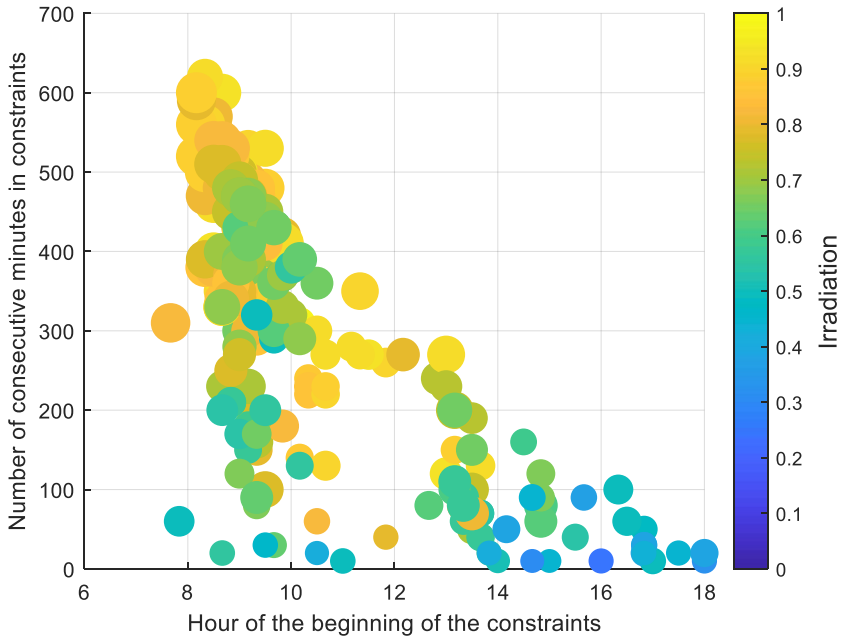

Figure 75 – Number of consecutive minutes potentially in current constraint at the feeder terminal, over two summers, on the assumption of an HV N-1 configuration and according to the time of occurrence (size of the circles = relative significance of the constraint).

The graphs representing constrained months and days and their analyses have been placed in appendices. The following table summarizes the results obtained.

Table 37 - Detail of constrained periods

Distribution of constraints	Months impacted	Days of the week impacted
	All the summer months	Every day of the week

5. Results of simulations corresponding to situation 23

As a reminder, simulation 23 corresponds to the following situation:

Table 38: Recap of situations simulated

Simulation 23	
Scenario	Green
PV location	2
EV location	1
Situation	N-1
Seasonality	Summer

The number and location of MV producers is the same as for the batteries of simulations No. 20.

Like for the previous section, the results will be represented via three-dimensional graphs.

3D graph with consumption (excluding EVs), PV production and hydropower production

The graph below shows the states under constraint or not depending on the levels of hydropower production, PV production and consumption (excluding EVs):

- according to the locations simulated;
- for the constrained backup feeder and the constrained transformer;
- in a recovery configuration in an HV N-1 situation for summers;
- in projected conditions in 2035/2036.

The graph shows four types of constraints:

- Overcurrent in grid equipment in draw-off and injection (lines/cables).
- Overcurrent in the HV/MV transformer.
- Overcurrent at the feeder terminal.
- Voltage rise.

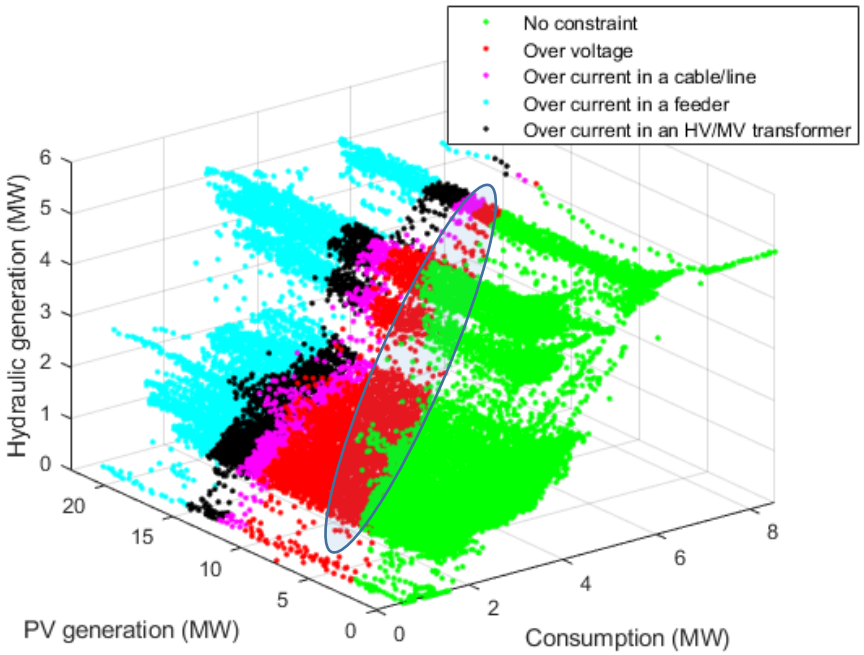

Figure 76 – 3D graph: Consumption (excluding EVs), PV Production and Hydropower Production for the constrained backup feeder at Isola in summer, in an N-1 configuration

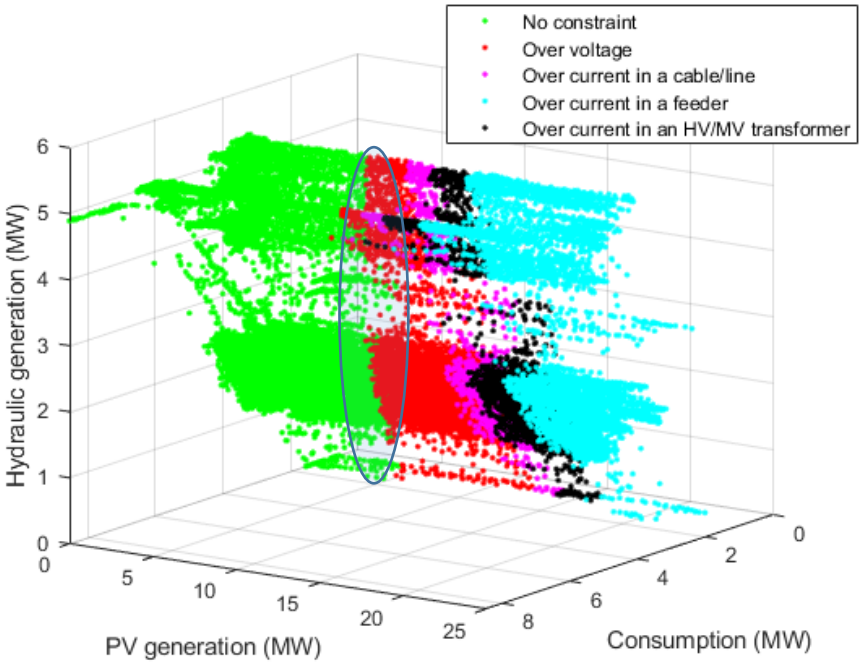

Figure 77 – Another view of the 3D graph under constraints: Consumption (excluding EVs), PV Production and Hydropower Production for the constrained backup feeder at Isola in summer, in an N-1 configuration

Like in the previous case, we can see clearly on this graph the separation between zones under current constraint and zones with no current constraints. On the other hand, it is not possible to very easily distinguish a clear boundary between the voltage constraint zone and the zone with no constraint, the "encircled zone". This is notably due to the fact that other factors are involved, such as the consumption level of the electric vehicles, which, although sometimes very low, could result in a transition from an unconstrained state to a constrained state.

Regarding constraints related to the injection of production, these appear at ***consumption levels lower than or equal to about 7.3 MW***, i.e. about 86% of the feeder's maximum charge, and when the ***injection of the photovoltaic panels exceeds 3.7 MW, i.e. about 16% of their installed capacity***.

Table 39**Erreur ! Source du renvoi introuvable.** shows the maximum flexibility volumes for each constraint, **on the assumption of an HV N-1 configuration over the two complete years of summer 2035/2036**. Note that certain flexibility volumes based on an increase in consumption have not been given because they would exceed the maximum capacity of the source substation, which would be meaningless.

The inversion of the consumption flexibility volume/production flexibility volume ratio is therefore potentially normal, and it could be explained by several reasons. One of those reasons would be the distribution of hydropower which is not the same at these two times: in one case the two producers produce, while in the other case only one of the two (cf. APPENDIX C - § 1 Impact of the location of flexibility). This difference could also be explained by the fact that production is injected at fixed and negative tanφ. Accordingly, when the injected production is reduced, the consumption of reactive power is reduced. There are therefore two conflicting effects, one positive regarding a reduction of the constraint (decline in production) and the other negative (decline in consumption of reactive power).

In the case of consumption flexibility, since tanφ is positive with consumption, both effects go in the same direction.

Table 39 - Useful flexibility volumes resolving the constraints and the ratio of useful flexibility to the consumption or PV production of the area

Type of flexibility	Flexibility volume for the type of constraint			
	Current (injection)	Current at the feeder terminal (injection)	Current in the transformer (injection)	Voltage rise
Rise in consumption	-	-	-	-
Fall in MV production	14.1 MW 60%	10.2 MW 44%	12.85 MW 56%	15.45 MW 67%

It should be remembered that these potential flexibility volumes (or potential constraints) are extreme and that at present Enedis would not have connected these producers under these conditions and would have found solutions to avoid these constraints.

Time slots of constraint occurrence

The overall results concerning the existence of constraints have been presented, and we will now present more detailed duration and period results for each type of constraint.

Current constraint in injection

Figure 78**Erreur ! Source du renvoi introuvable.** below presents useful flexibility activation durations according to activation times. The graph includes:

- A third dimension (coloured) which represents the maximum insolation perceived by photovoltaic power production during the constraint.
- A fourth dimension (size of the circles) representing the maximum consumption level obtained throughout the constraint.

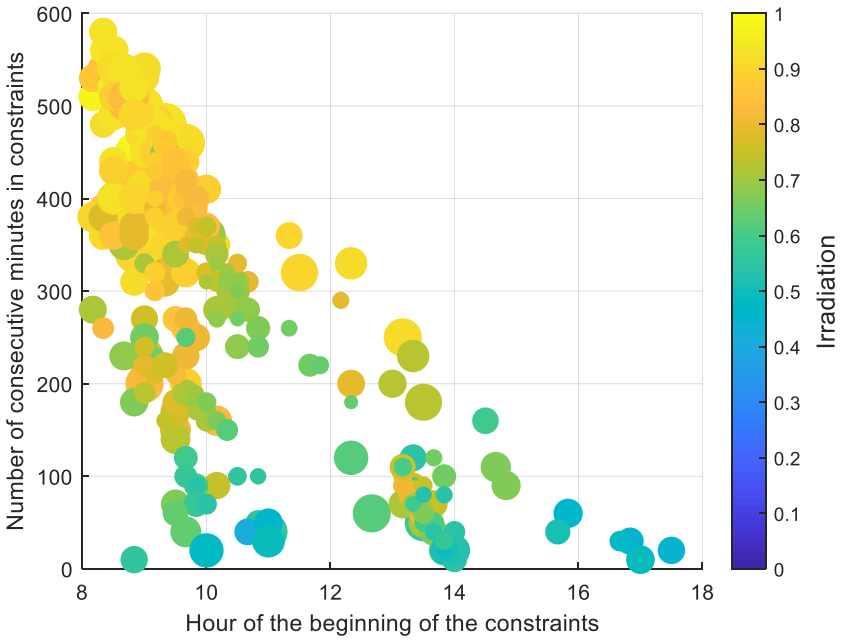

Figure 78 – Number of consecutive minutes potentially in current constraint, over two summers, on the assumption of an HV N-1 configuration and according to the time of occurrence (size of the circles = maximum consumption level seen during the constraint).

After simulations, we can note that:

- Two-thirds of the potential constraints apparently occur before midday with a high photovoltaic production level.
- It is worth noting that the longest potential constraints apparently occur between 8.30 am and 10.30 am and that the consumption level is apparently lower than in the afternoon.

Figure 79**Erreur ! Source du renvoi introuvable.** below shows the same results, with this time, for the 4th dimension, the magnitude of the constraint (or the magnitude of the flexibility capable of resolving the constraint). The larger the circle, the closer one is to the maximum constraint obtained during this study[45].

With this second graph we note that the longer the duration of the constraint, the greater the flexibility volume. This is notably due to the fact that photovoltaic power production is substantial (>60% of maximum capacity).

[45] For example, if there is a voltage rise ranging between +2.8% and +2%, +2.8% is the largest circle.

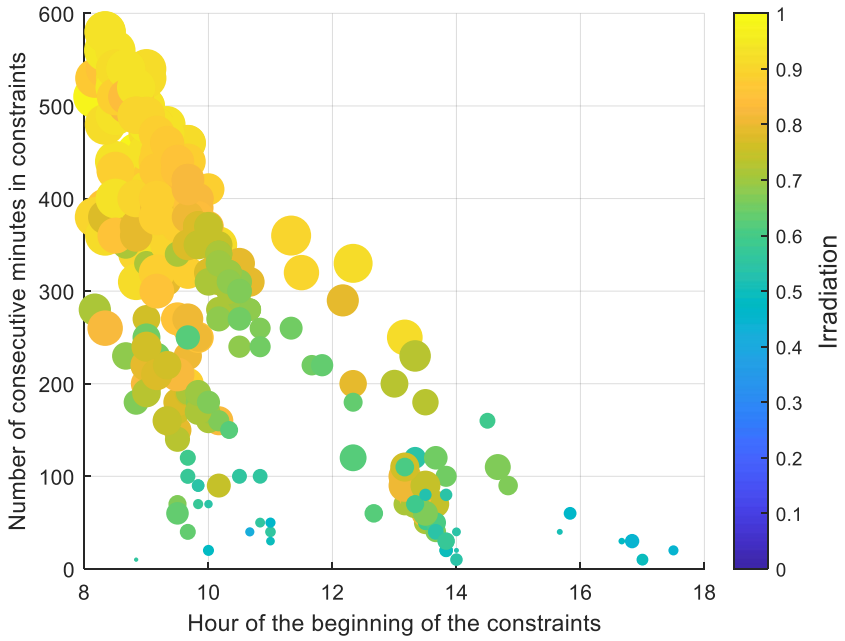

Figure 79 – Number of consecutive minutes potentially in current constraint, over two summers, on the assumption of an HV N-1 configuration and according to the time of occurrence (size of the circles = relative significance of the constraint).

The graphs representing constrained months and days and their analyses have been placed in appendices. The following table summarizes the results obtained.

Table 40 - Detail of constrained periods

Distribution of constraints	Months impacted	Days of the week impacted
	Every month	Every day of the week

Current constraint at the feeder terminal

Figure 80**Erreur ! Source du renvoi introuvable.** below presents useful flexibility activation durations according to activation times. The graph includes:

- A third dimension (coloured) which represents the maximum insolation perceived by photovoltaic power production during the constraint.
- A fourth dimension (size of the circles) representing the maximum consumption level obtained throughout the constraint.

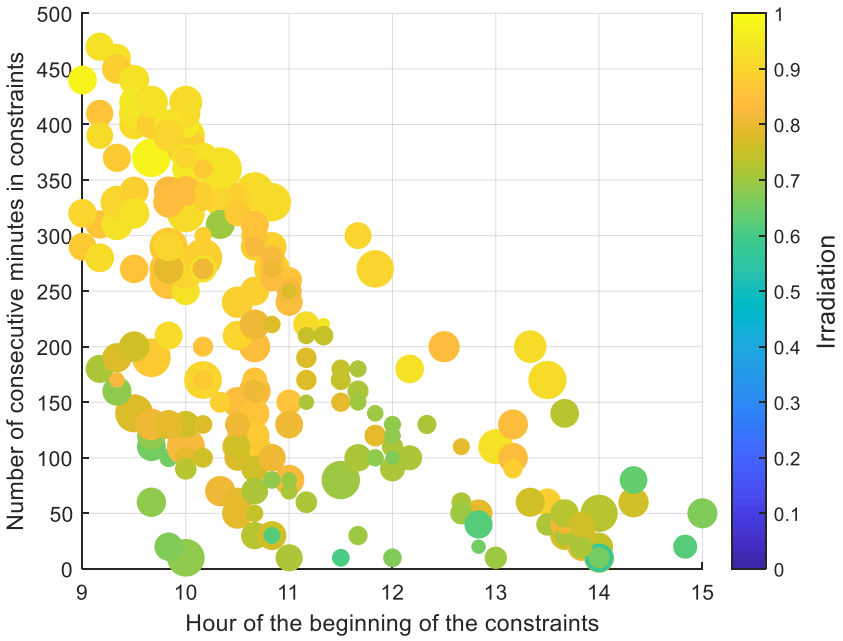

Figure 80 – Number of consecutive minutes potentially in current constraint at the source substation, over two summers, on the assumption of an HV N-1 configuration and according to the time of occurrence (size of the circles = maximum consumption level seen during the constraint).

After simulations, we can note that:

- All of the potential constraints apparently occur between 9.00 am and 3.00 pm with a higher level of consumption after 11.00 am.
- Two-thirds of the constraints apparently occur before 12.00 with a majority of the longest constraint durations and a high production level (>60% of maximum capacity).
- It is interesting to note that the longest potential constraints apparently also occur before midday.

Erreur ! Source du renvoi introuvable. Figure 81 below shows the same results, with this time, for the 4th dimension, the magnitude of the constraint (or the magnitude of the flexibility capable of resolving the constraint). The larger the circle, the closer one is to the maximum constraint obtained during this study[46].

With this second graph we note that the constraints which have a shorter duration apparently have a slightly lower flexibility requirement.

[46] For example, if there is a voltage rise ranging between +2.8% and +2%, +2.8% is the largest circle.

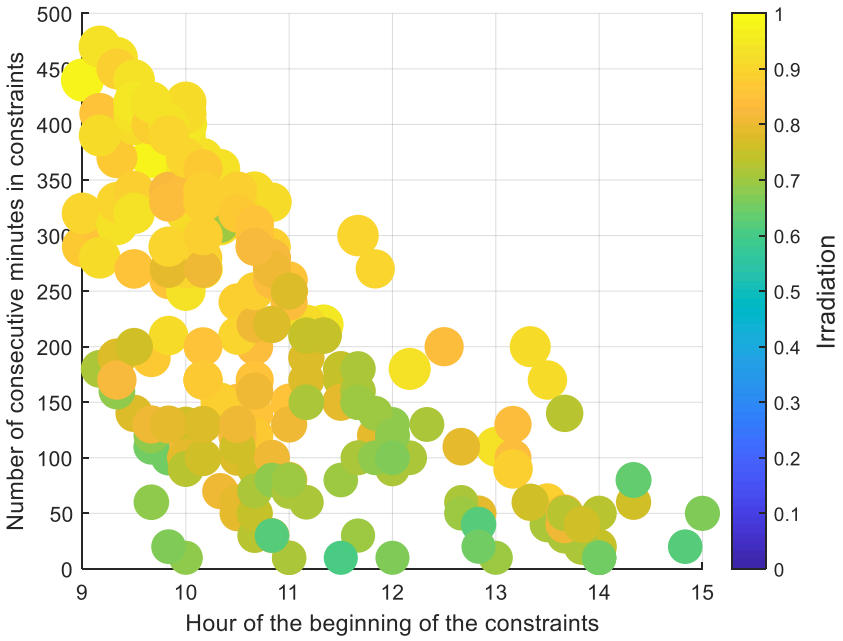

Figure 81 – Number of consecutive minutes potentially in current constraint at the feeder terminal, over two summers, on the assumption of an HV N-1 configuration and according to the time of occurrence (size of the circles = relative significance of the constraint).

The graphs representing constrained months and days and their analyses have been placed in appendices. The following table summarizes the results obtained.

Table 41 - Detail of constrained periods

Distribution of constraints	Months impacted	Days of the week impacted
	Every month	Every day of the week

Current constraint in the HV/MV transformer

Erreur ! Source du renvoi introuvable. Figure 82 below presents useful flexibility activation durations according to activation times. The graph includes:

- A third dimension (coloured) which represents the maximum insolation perceived by photovoltaic power production during the constraint.
- A fourth dimension (size of the circles) representing the maximum consumption level obtained throughout the constraint.

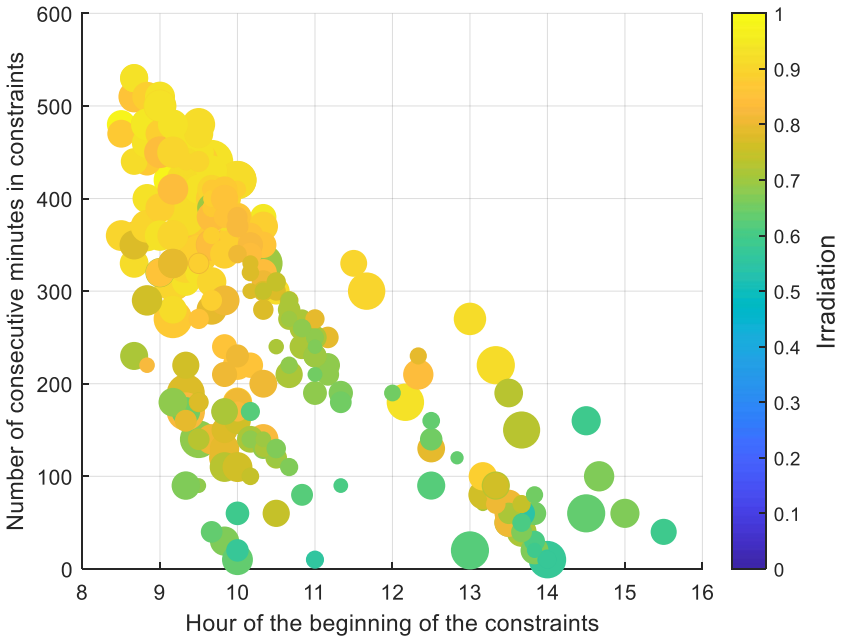

Figure 82 – Number of consecutive minutes potentially in current constraint at the source substation, over two summers, on the assumption of an HV N-1 configuration and according to the time of occurrence (size of the circles = maximum consumption level seen during the constraint).

After simulations, we can note that all the potential constraints apparently occur between 8.30 am and 3.30 pm. The longest constraints apparently occur before 11 am, i.e. with low consumption levels and fairly high photovoltaic production levels (>60% of their maximum capacity).

Figure 83**Erreur ! Source du renvoi introuvable.** below shows the same results, with this time, for the 4th dimension, the magnitude of the constraint (or the magnitude of the flexibility capable of resolving the constraint). The larger the circle, the closer one is to the maximum constraint obtained during this study[47].

[47] For example, if there is a voltage rise ranging between +2.8% and +2%, +2.8% is the largest circle.

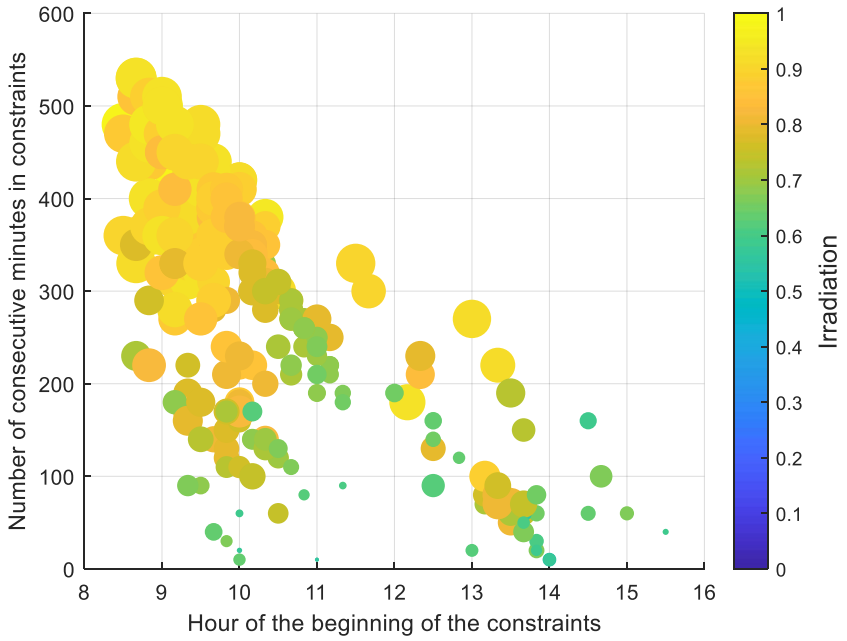

Figure 83 – Number of consecutive minutes potentially in current constraint at the feeder terminal, over two summers, on the assumption of an HV N-1 configuration and according to the time of occurrence (size of the circles = relative significance of the constraint).

With this second graph we note that the flexibility volume is apparently larger when the duration is longer and when production is high. The smallest flexibility volumes apparently occur with constraints of duration less than 100 min., i.e. 1h40min. There seems therefore to be a strong correlation between the duration and magnitude of the constraint.

The graphs representing constrained months and days and their analyses have been placed in appendices. The following table summarizes the results obtained.

Table 42 - Detail of constrained periods

Distribution of constraints	Months impacted	Days of the week impacted
	Every month	Every day of the week

Voltage rise constraint

Figure 84**Erreur ! Source du renvoi introuvable.** below presents useful flexibility activation durations according to activation times. The graph includes:

- A third dimension (coloured) which represents the maximum insolation perceived by photovoltaic power production during the constraint.
- A fourth dimension (size of the circles) representing the maximum consumption level obtained throughout the constraint.

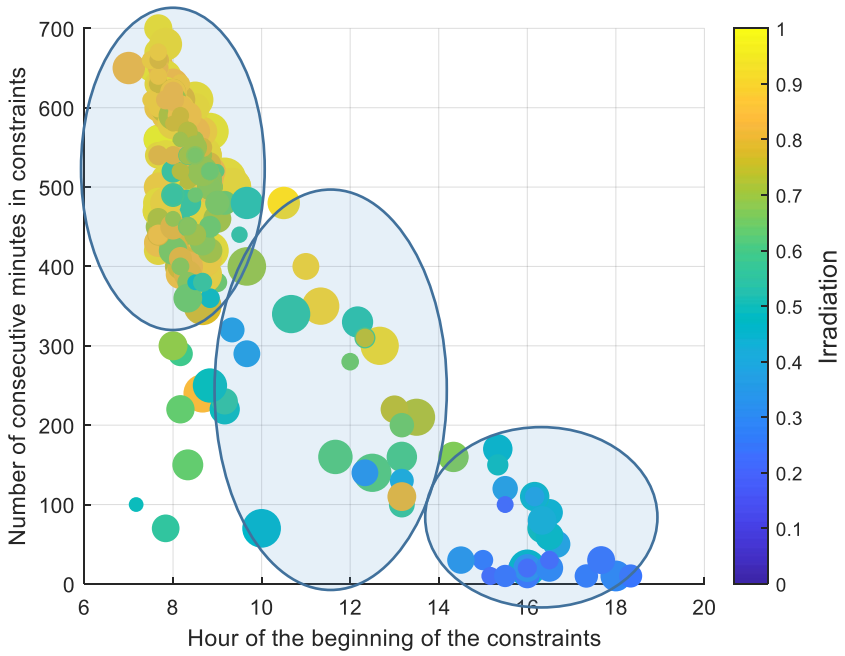

Figure 84 – Number of consecutive minutes potentially in current constraint at the source substation, over two summers, on the assumption of an HV N-1 configuration and according to the time of occurrence (size of the circles = maximum consumption level seen during the constraint).

After simulations, we can note that most of the potential constraints apparently occur between 7.30 am and 6.00 pm. The longest constraints apparently occur between 7.30 am and 10.00 am, with photovoltaic power levels exceeding 60% of their maximum capacity. Between 10.00 am and 2.00 pm, there is no clear trend. Between 2.00 pm and 6.00 pm the consumption level is lower, but the production level is also lower (>40% of maximum capacity).

Erreur ! Source du renvoi introuvable. Figure 85 below shows the same results, with this time, for the 4th dimension, the magnitude of the constraint (or the magnitude of the flexibility capable of resolving the constraint). The larger the circle, the closer one is to the maximum constraint obtained during this study[48].

With this second graph we note that the flexibility volume is apparently larger when the duration is greater and when production is high (>60% of maximum capacity). The flexibility volume will be smaller for constraints having a lower consumption and production level. There is apparently again a correlation between the duration and the maximum constraint level. This is due to the PV production profile, which rises to a maximum when the sun is at its zenith, and then comes back down. If the constraint occurs early, it will last a long time and generate a large flexibility volume, whereas if it occurs after production has peaked, the duration of the constraint will be less long and less constraining.

[48] For example, if there is a voltage rise ranging between +2.8% and +2%, +2.8% is the largest circle.

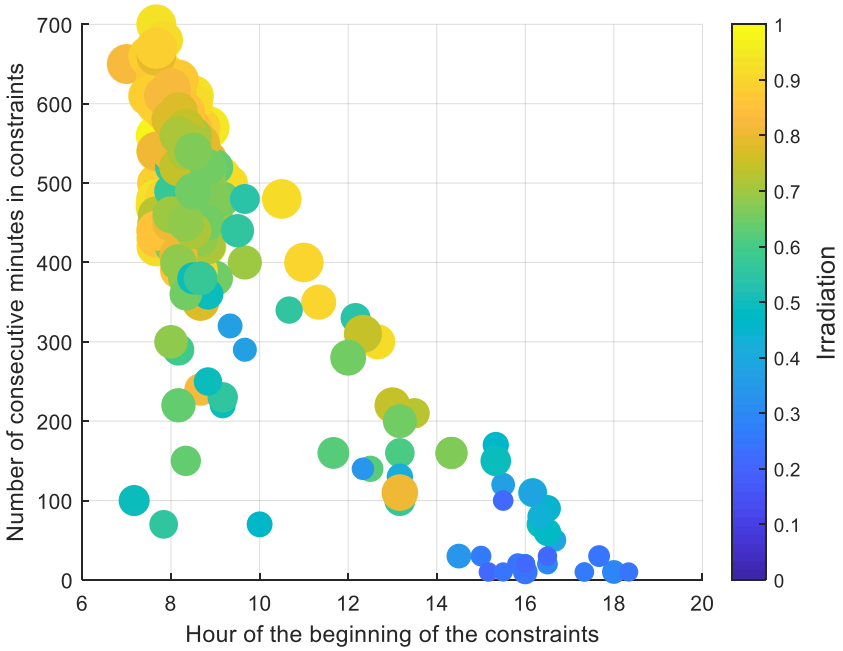

Figure 85 – Number of consecutive minutes potentially in current constraint at the feeder terminal, over two summers, on the assumption of an HV N-1 configuration and according to the time of occurrence (size of the circles = relative significance of the constraint).

The graphs representing constrained months and days and their analyses have been placed in appendices. The following table summarizes the results obtained.

Table 43 - Detail of constrained periods

Distribution of constraints	Months impacted	Days of the week impacted
	Every month	Every day of the week

6. Results of simulations corresponding to situation 24

As a reminder, simulation 24 corresponds to the following situation:

Table 44 - Recap of situations simulated

Simulation 24	
Scenario	Green
PV sample	3
EV sample	1
Situation	N-1
Seasonality	Summer

The number and location of MV producers is the same as for the batteries of simulations No. 21.

Like for the previous section, the results will be represented via three-dimensional graphs.

3D graph with consumption (excluding EVs), PV production and hydropower production

The graph below shows the states under constraint or not depending on the levels of hydropower production, PV production and consumption (excluding EVs):

- according to the locations simulated;
- for the constrained backup feeder and the constrained transformer;
- in a recovery configuration in an HV N-1 situation for summers;
- in projected conditions in 2035/2036.

The graph shows four types of constraints:

- Overcurrent in grid equipment in draw-off and injection (lines/cables).
- Overcurrent in the HV/MV transformer.
- Overcurrent at the feeder terminal.
- Voltage rise.

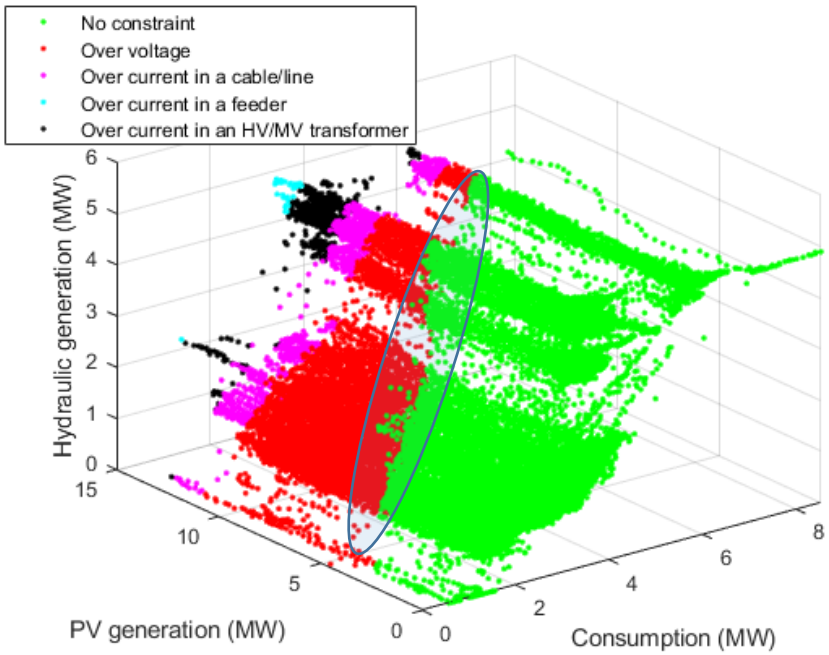

Figure 86 – 3D graph: Consumption (excluding EVs), PV Production and Hydropower Production for the constrained backup feeder at Isola in summer, in an N-1 configuration

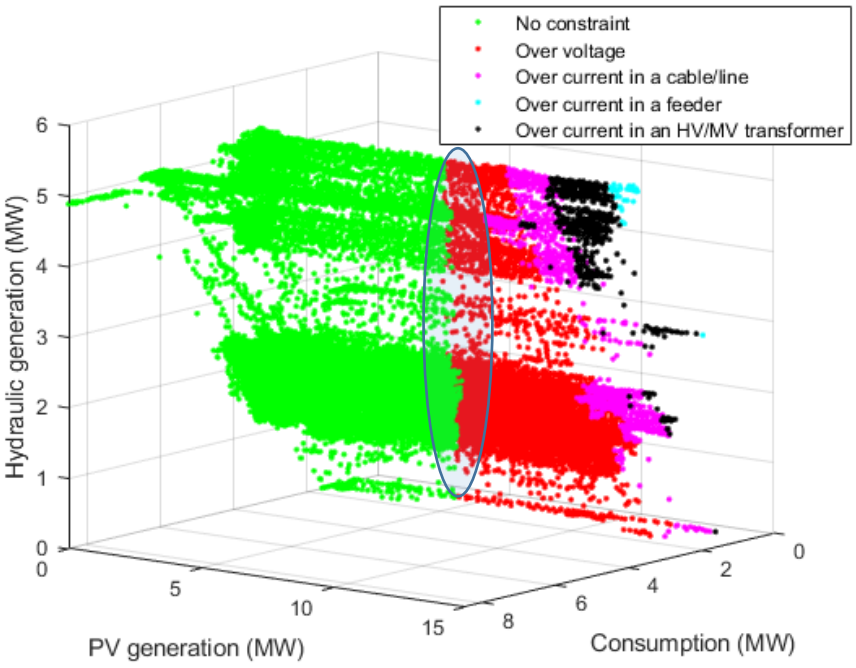

Figure 87 – Another view of the 3D graph under constraints: Consumption (excluding EVs), PV Production and Hydropower Production for the constrained backup feeder at Isola in summer, in an N-1 configuration

Like in the previous cases, we can see on this graph the separation between zones under current constraint and zones with no current constraints. On the other hand, it is not possible to very easily distinguish a clear boundary between the voltage constraint zone and the zone with no constraint. This is notably due to the fact that other factors are involved, in particular the consumption level of the electric vehicles, which, although sometimes very low, could result in a transition from an unconstrained state to a constrained state.

Regarding constraints related to the injection of production, these appear at ***consumption levels lower than or equal to 6 MW***, i.e. about 70% of the feeder's maximum charge, and when the ***injection of the photovoltaic panels exceeds 3.4 MW, i.e. about 24% of their installed capacity***.

Table 45 shows the maximum flexibility volumes for each constraint, **on the assumption of an HV N-1 configuration over the two complete years of summer 2035/2036**. We can note that the flexibility volume is always larger using a flexibility of the rise-in-consumption type, except in the case of the voltage rise constraint. Note that the maximum voltage rise constraint does not occur at the same time as the other constraints. This is due to the local hydropower production of the zone which, although the total for the sector is practically identical point by point, is distributed over several producers. The location of production therefore has a major impact on the voltage constraint. (cf § 4.5.1).

The inversion of the consumption flexibility volume/production flexibility volume ratio is therefore potentially normal and it could be explained by several reasons. One of those reasons would be the distribution of hydropower which is not the same at these two times: in one case the two producers produce, while in the other case only one of the two (cf. APPENDIX C - § 1 Impact of the location of flexibility). This difference could also be explained by the fact that production is injected at fixed and negative tanφ. Accordingly, when the injected production is reduced, the consumption of reactive power is reduced. There are therefore two conflicting effects, one positive regarding a reduction of the constraint (decline in production) and the other negative (decline in consumption of reactive power).

In the case of consumption flexibility, since tanφ is positive with consumption, both effects go in the same direction.

Table 45 – Useful flexibility volume resolving the constraints and the ratio of useful flexibility to the consumption or PV production of the area

Type of flexibility	Flexibility volume for the type of constraint			
	Current (injection)	Current at the feeder terminal (injection)	Current in the transformer (injection)	Voltage rise
Rise in consumption	5.45 MW 64%	1.25 MW 15%	3.95 MW 46%	7.1 MW 83%
Fall in MV production	4.95 MW 35%	1.15 MW 8%	3.45 MW 24%	8.4 MW 59%

Time slots of constraint occurrence

The overall results concerning the existence of constraints have been presented, and we will now present more detailed duration and period results for each type of constraint.

Current constraint in injection

Figure 88 below presents useful flexibility activation durations according to activation times. The graph includes:

- A third dimension (coloured) which represents the maximum insolation perceived by photovoltaic power production during the constraint.
- A fourth dimension (size of the circles) representing the maximum consumption level obtained throughout the constraint.

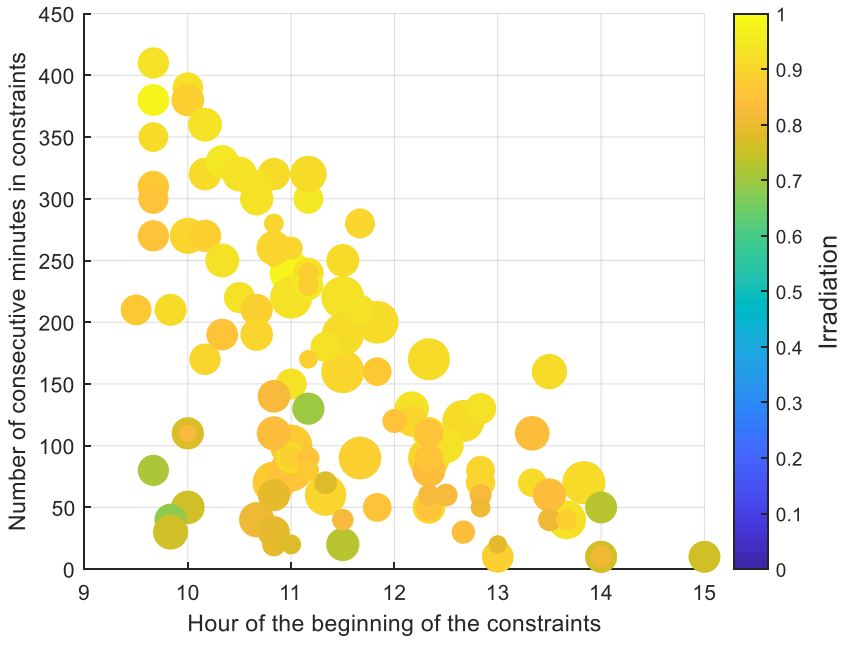

Figure 88 – Number of consecutive minutes potentially in current constraint, over two summers, on the assumption of an HV N-1 configuration and according to the time of occurrence (size of the circles = maximum consumption level seen during the constraint).

After simulations, we can note that most of the potential constraints apparently occur between 9.30 am and 3.00 pm, with a high photovoltaic power level (>70% of maximum capacity).

Erreur ! Source du renvoi introuvable. Figure 89 below shows the same results, with this time, for the 4th dimension, the magnitude of the constraint (or the magnitude of the flexibility capable of resolving the constraint). The larger the circle, the closer one is to the maximum constraint obtained during this study[49].

With this second graph we note that the longer the duration of the constraint, the greater the flexibility volume due to the massive injection of photovoltaic power (>80% of maximum capacity).

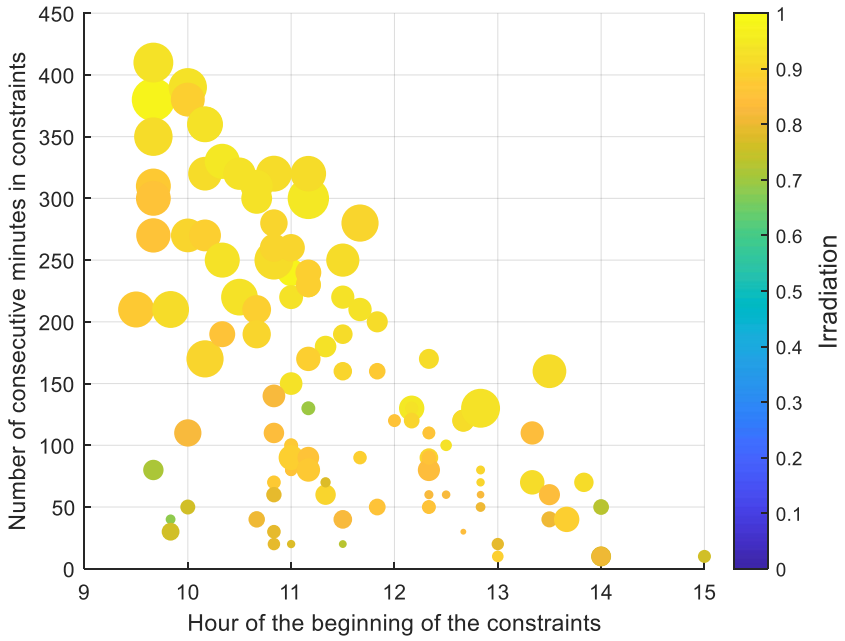

Figure 89 - Number of consecutive minutes potentially in current constraint, over two summers, on the assumption of an HV N-1 configuration and according to the time of occurrence (size of the circles = relative significance of the constraint).

The graphs representing constrained months and days and their analyses have been placed in appendices. The following table summarizes the results obtained.

Table 46 - Detail of constrained periods

Distribution of constraints	Months impacted	Days of the week impacted
	June - July - August	Every day of the week

[49] For example, if there is a voltage rise ranging between +2.8% and +2%, +2.8% is the largest circle.

Current constraint at the feeder terminal

Erreur ! Source du renvoi introuvable. Figure 90 below presents useful flexibility activation durations according to activation times. The graph includes:

- A third dimension (coloured) which represents the maximum insolation perceived by photovoltaic power production during the constraint.
- A fourth dimension (size of the circles) representing the maximum consumption level obtained throughout the constraint.

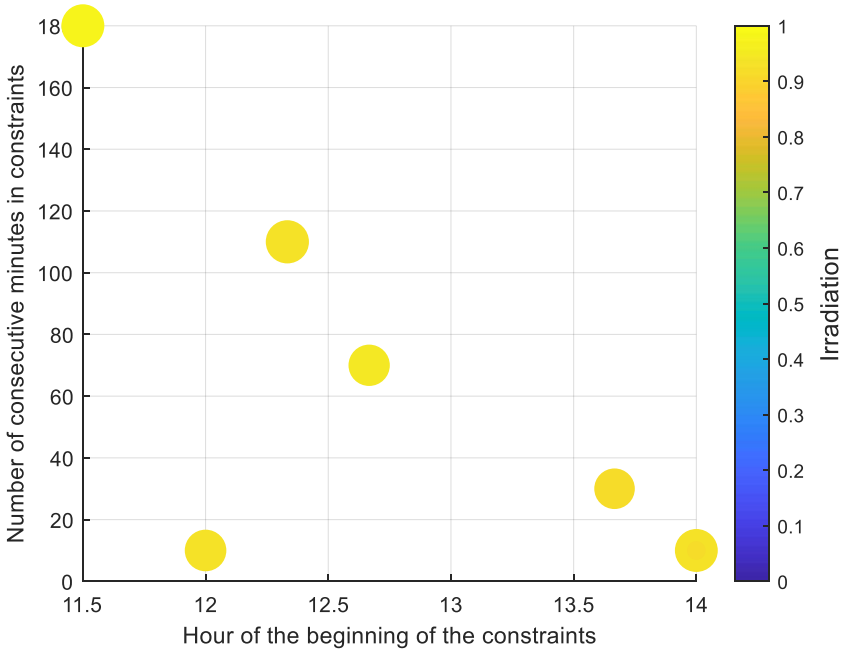

Figure 90 – Number of consecutive minutes potentially in current constraint at the source substation, over two summers, on the assumption of an HV N-1 configuration and according to the time of occurrence (size of the circles = maximum consumption level seen during the constraint).

After simulations, we can note that all of the potential constraints apparently occur between 11.30 am and 2.00 pm, with a stable higher consumption level and a fairly high production level (>90% of maximum capacity). It is worth noting that the longest potential constraints apparently occur before midday.

Erreur ! Source du renvoi introuvable. Figure 91 below shows the same results, with this time, for the 4th dimension, the magnitude of the constraint (or the magnitude of the flexibility capable of resolving the constraint). The larger the circle, the closer one is to the maximum constraint obtained during this study[50].

With this second graph we note that, whatever the duration of the constraint, the useful flexibility volumes capable of resolving the constraint are apparently very similar.

[50] For example, if there is a voltage rise ranging between +2.8% and +2%, +2.8% is the largest circle.

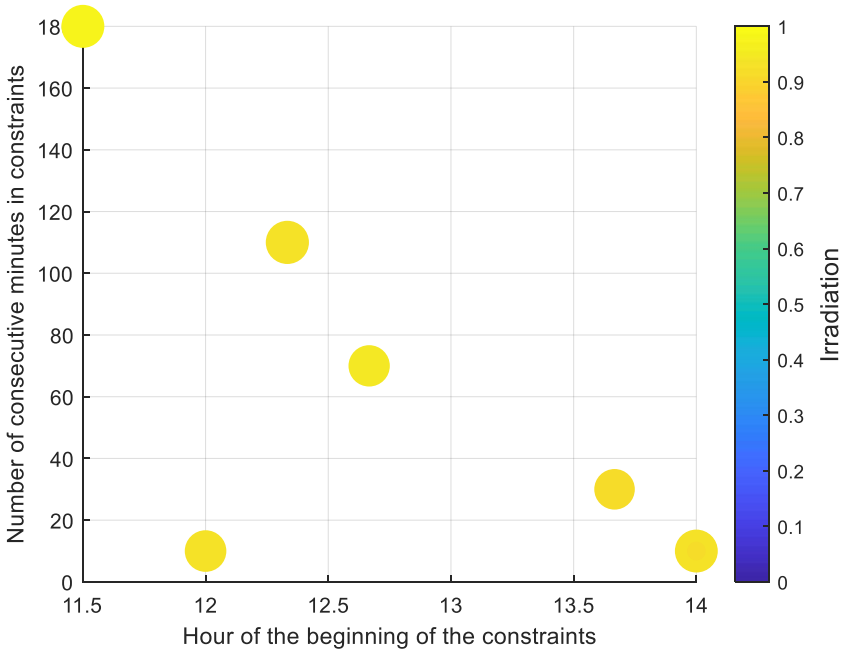

Figure 91 – Number of consecutive minutes potentially in current constraint at the feeder terminal, over two summers, on the assumption of an HV N-1 configuration and according to the time of occurrence (size of the circles = relative significance of the constraint).

The graphs representing constrained months and days and their analyses have been placed in appendices.

Table 47 - Detail of constrained periods

	Months impacted	Days of the week impacted
Distribution of constraints	June	Every day of the week except Thursday

Current constraint in the HV/MV transformer

Erreur ! Source du renvoi introuvable. Figure 92 below presents useful flexibility activation durations according to activation times. The graph includes:

- A third dimension (coloured) which represents the maximum insolation perceived by photovoltaic power production during the constraint.
- A fourth dimension (size of the circles) representing the maximum consumption level obtained throughout the constraint.

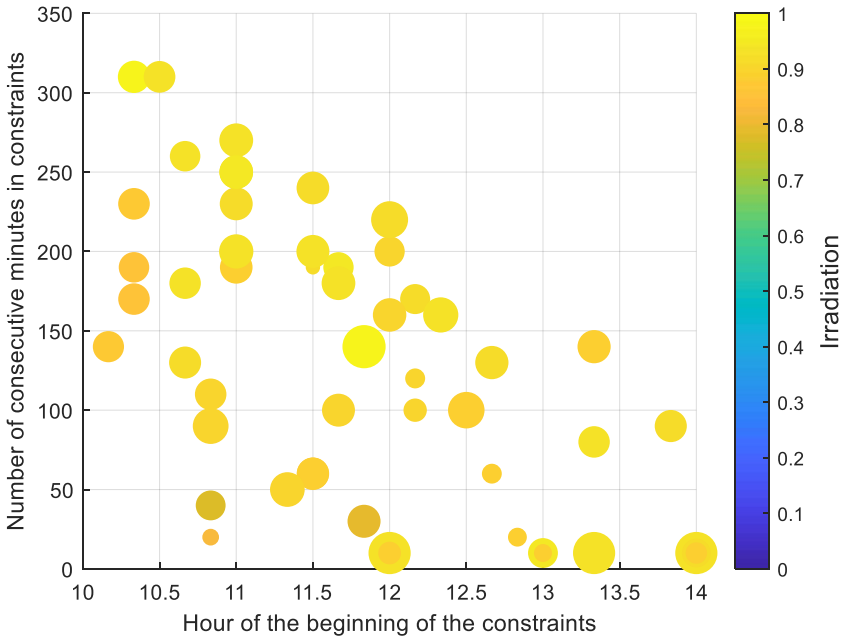

Figure 92 – Number of consecutive minutes potentially in current constraint at the source substation, over two summers, on the assumption of an HV N-1 configuration and according to the time of occurrence (size of the circles = maximum consumption level seen during the constraint).

After simulations, we can note that most of the potential constraints apparently occur between 10.00 am and 2.00 pm. The longest constraints apparently occur before 12.00 and with very high photovoltaic power levels (>80% of their maximum capacity). Certain constraints of very quick duration have high consumption levels with high production levels.

Erreur ! Source du renvoi introuvable. Figure 93 below shows the same results, with this time, for the 4th dimension, the magnitude of the constraint (or the magnitude of the flexibility capable of resolving the constraint). The larger the circle, the closer one is to the maximum constraint obtained during this study[51].

With this second graph we note that the smallest flexibility volumes apparently occur on constraints of duration less than 100 min., i.e. 1h40min. There seems therefore to be a strong correlation between the duration and magnitude of the constraint.

[51] For example, if there is a voltage rise ranging between +2.8% and +2%, +2.8% is the largest circle.

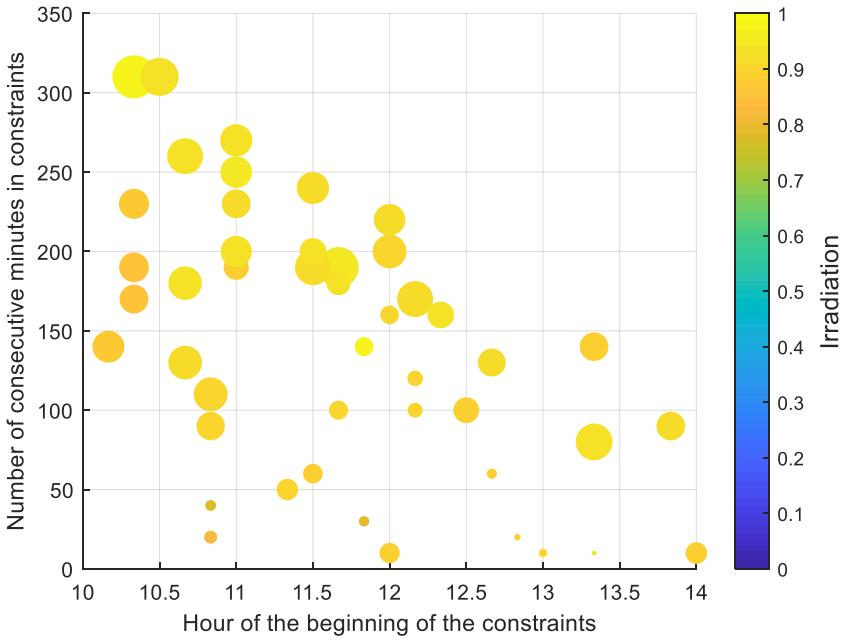

Figure 93 – Number of consecutive minutes potentially in current constraint at the feeder terminal, over two summers, on the assumption of an HV N-1 configuration and according to the time of occurrence (size of the circles = relative significance of the constraint).

The graphs representing constrained months and days and their analyses have been placed in appendices. The following table summarizes the results obtained.

Table 48 - Detail of constrained periods

Distribution of constraints	Months impacted	Days of the week impacted
	June – July - August	Every day of the week

Voltage rise constraint

Erreur ! Source du renvoi introuvable. Figure 94 below presents useful flexibility activation durations according to activation times. The graph includes:

- A third dimension (coloured) which represents the maximum insolation perceived by photovoltaic power production during the constraint.
- A fourth dimension (size of the circles) representing the maximum consumption level obtained throughout the constraint.

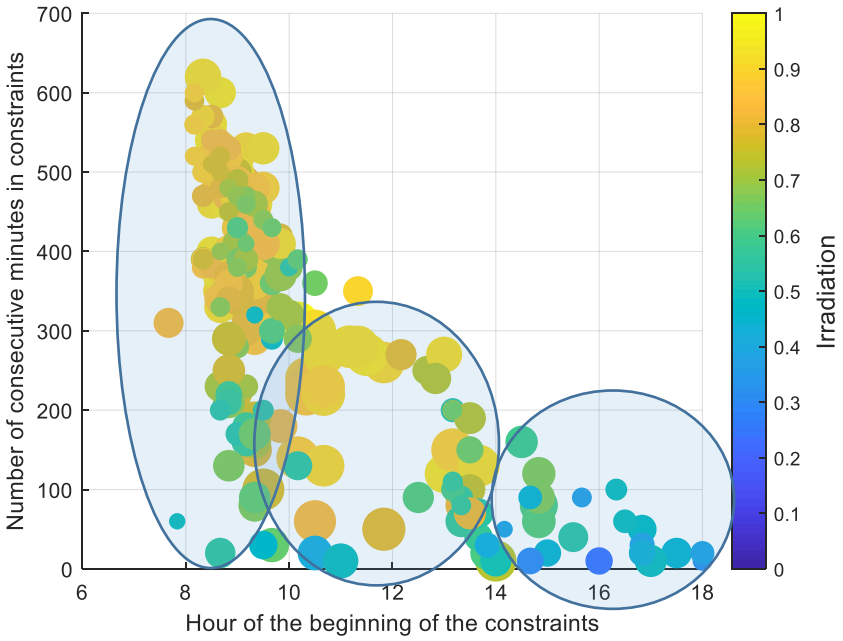

Figure 94 – Number of consecutive minutes potentially in current constraint at the source substation, over two summers, on the assumption of an HV N-1 configuration and according to the time of occurrence (size of the circles = maximum consumption level seen during the constraint).

After simulations, we can note that most of the potential constraints apparently occur between 8.00 am and 6.00 pm. The longest constraints apparently occur between 8 am and 10 am, i.e. with low or moderate consumption levels and photovoltaic power production levels exceeding 60% of their maximum capacity. Between 10.00 am and 2.00 pm the consumption level is high, and the production level remains high (>40% of maximum capacity). Between 2.00 pm and 6.00 pm the consumption level seems lower, and the production level is also lower (<40% of maximum capacity).

Erreur ! Source du renvoi introuvable. Figure 95 below shows the same results, with this time, for the 4th dimension, the magnitude of the constraint (or the magnitude of the flexibility capable of resolving the constraint). The larger the circle, the closer one is to the maximum constraint obtained during this study[52].

With this second graph we note that the flexibility volume is apparently larger when the duration is longer and when production is high (>50% of maximum capacity). There is apparently again a correlation between the duration and the maximum constraint level. This is due to the PV production profile, which rises to a maximum when the sun is at its zenith, and then comes back down. If the constraint occurs early, it will last a long time and generate a large flexibility volume, whereas if it occurs after production has peaked, the duration of the constraint will be less long and less constraining.

[52] For example, if there is a voltage rise ranging between +2.8% and +2%, +2.8% is the largest circle.

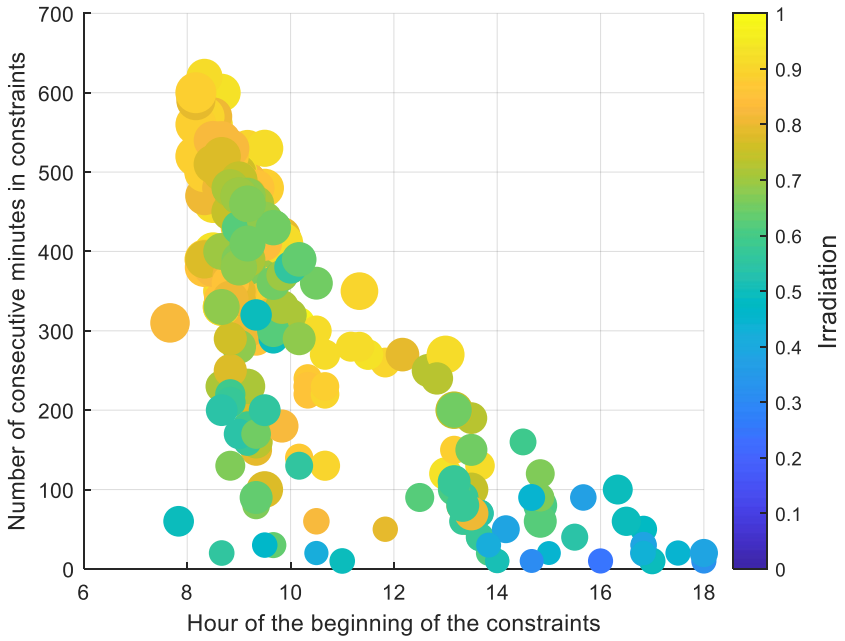

Figure 95 – Number of consecutive minutes potentially in current constraint at the source substation, over two summers, on the assumption of an HV N-1 configuration and according to the time of occurrence (size of the circles = relative significance of the constraint).

The graphs representing constrained months and days and their analyses have been placed in appendices. The following table summarizes the results obtained.

Table 49 - Detail of constrained periods

Distribution of constraints	Months impacted	Days of the week impacted
	Every month	Every day of the week

7. Conclusion of Appendix A

This study on the Isola zone shows that the potential constraints will be mostly related to the massive arrival of RES on the grid. These will appear at any time, depending on the type of constraint, and nearly every month in the periods could be concerned depending on the quantity of photovoltaic power production injected into the grid. Some draw-off constraints will persist in winter, related to the activity in the zone.

APPENDIX B: 2035 MV grid simulations: analysis of constraints spread per month and per day

1. CONSTRAINED TIME SLOTS IN THE CARROS ZONE

Only the results obtained concerning the winter & inter-season seasonality are presented in this section.

1.1. Results of simulations 18, Winter & Inter-season & sample 3

Figure 96 shows the distribution of voltage rise constraints per month. We can see that all the flexibility activations apparently occur in the months of March, April and May.

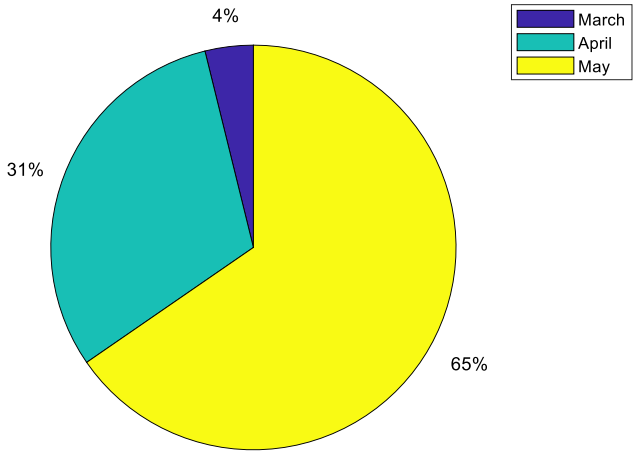

Figure 96 – Distribution of voltage rise constraints over the various months of the seasonality in question, on the assumption of an N-1 configuration

Figure 97 shows the distribution of voltage rise constraints over the various days of the week.

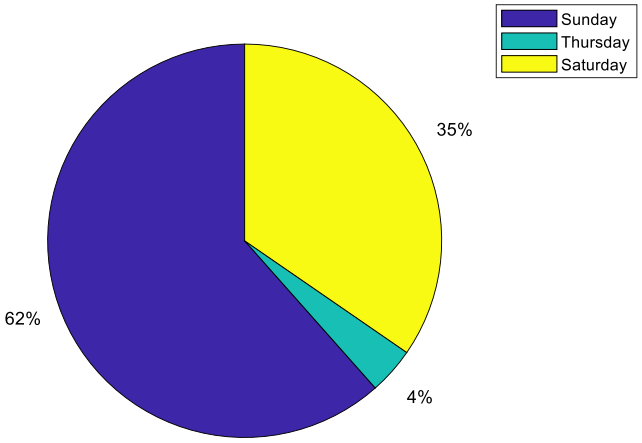

Figure 97 – Distribution of voltage rise constraints over the various days of the week for the seasonality in question, on the assumption of an N-1 configuration

The two main days of the week for which there are apparently potential flexibility needs are Sundays and Saturdays. One possible interpretation, although it cannot be verified, would be to say that these days are non-working days for a large proportion of the population and, as this source substation has a mainly industrial customer base, the decline in the factories' activity would not be offset by households' consumption compared with high production.

2. CONSTRAINED TIME SLOTS IN THE ISOLA ZONE

2.1. Results of simulations 19, Winter & Inter-season & sample 1

Only the results obtained concerning the winter & inter-season seasonality are presented in this section.

Current constraint

Figure 98 shows the distribution of current constraints per month (injection and draw-off combined). We can see that all the flexibility activations apparently occur in the first part of winter for the draw-off constraints and in spring for injection constraints.

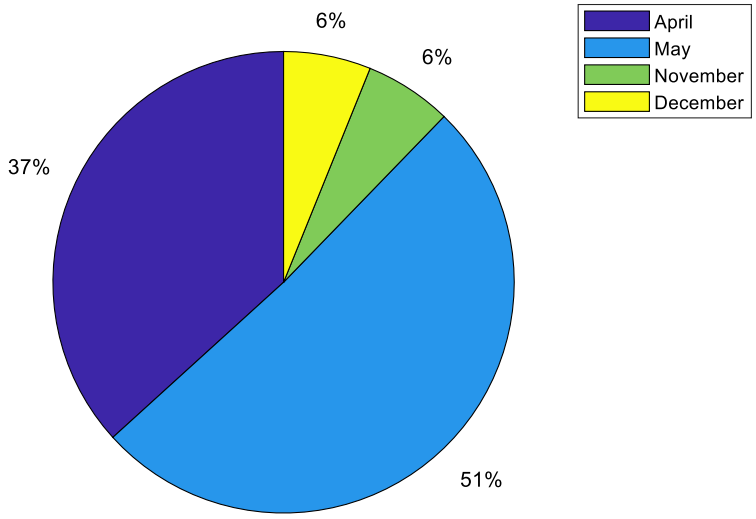

Figure 98 – Distribution of current constraints in the lines/cables over the various months of the seasonality in question, on the assumption of an N-1 configuration for the current constraint

Figure 99 shows the distribution of current constraints in the lines and cables over the various days of the week for the two winters & inter-seasons in question.

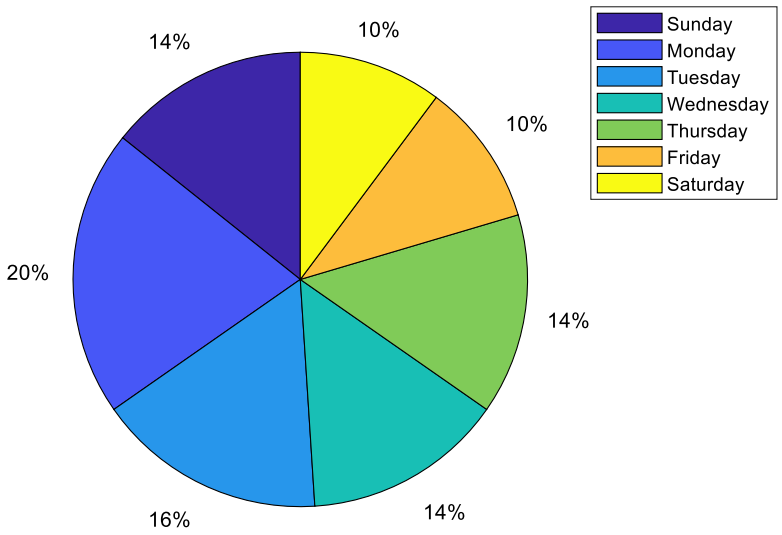

Figure 99 – Distribution of current constraints in the lines/cables over the various days of the week for the seasonality in question, on the assumption of an N-1 configuration

We can see that the constraints could occur on every day of the week. The proportions range from 10% on Saturdays and Fridays, up to 20% on Tuesdays.

Current constraint at the feeder terminal

Figure 100 shows the distribution of current constraints at the feeder terminal per month. We can see that all the flexibility activations apparently occur in the spring. One possible explanation would be that this is a period without the summer crowds of visitors and the Isola source substation mostly comprises recreational consumption. Accordingly, consumption there is relatively low in this period, whereas PV is injected extensively.

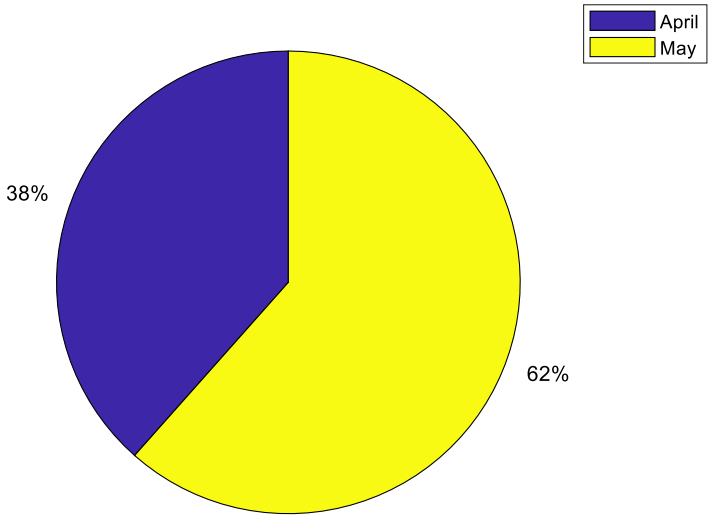

Figure 100 – Distribution of current constraints at the feeder terminal over the various months of the seasonality in question, on the assumption of an N-1 configuration

Figure 101 shows the distribution of current constraints at the feeder terminal over the various days of the week for the two winters & inter-seasons in question.

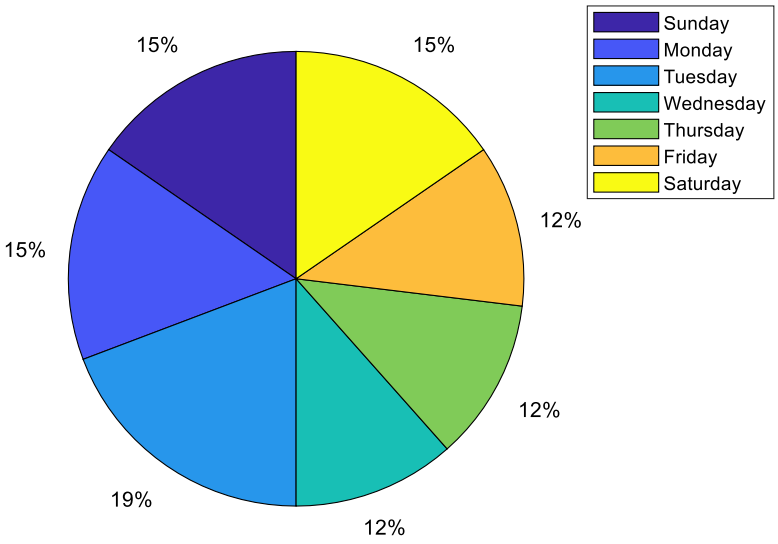

Figure 101 – Distribution of current constraints at the feeder terminal over the various days of the week for the seasonality in question, on the assumption of an N-1 configuration

Like for the case of current constraints in a cable or line, we can see that there is no day which stands out more than another.

Current constraint in the HV/MV transformer

Figure 102 shows the distribution of current constraints at the level of the HV/MV transformer. We can see that all the flexibility activations apparently occur in the spring. One possible explanation would be that this is a period without the summer crowds of visitors and the Isola source substation mostly comprises recreational consumption. Accordingly, consumption there is relatively low in this period, whereas PV is injected extensively, causing an imbalance which is responsible for the constraint.

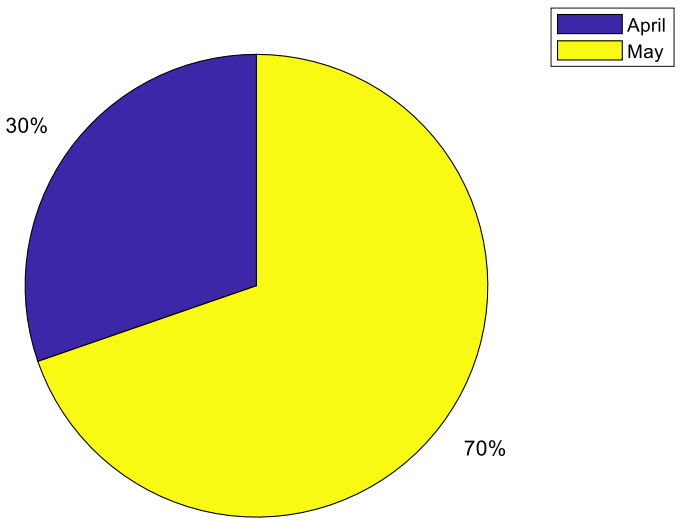

Figure 102 – Distribution of current constraints at the HV/MV transformer over the various months of the seasonality in question, on the assumption of an N-1 configuration

Figure 103 shows the distribution of current constraints in the HV/MV transformer over the various days of the week for the two winters & inter-seasons in question.

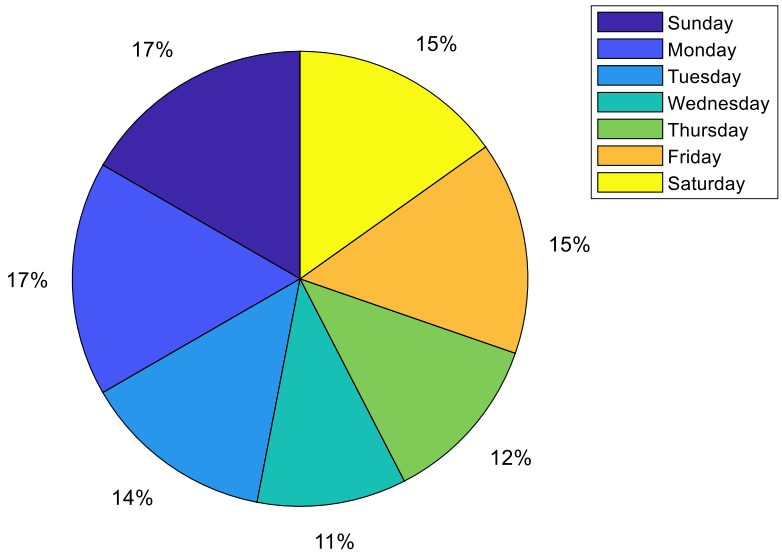

Figure 103 – Distribution of current constraints in the HV/MV transformer over the various days of the week for the seasonality in question, on the assumption of an N-1 configuration

Like for the case of current constraints in a cable or line, we can see that there is no day which stands out more than another.

Voltage rise constraint

Figure 104 shows the distribution of voltage rise constraints. We can see that the flexibility activations apparently occur mostly in the spring and autumn. One possible explanation could be that there is an asynchronism between the high consumption levels and high production levels, thereby causing voltage rise constraints. From December to March, consumption offsets the overproduction sufficiently to prevent any constraint on the grid.

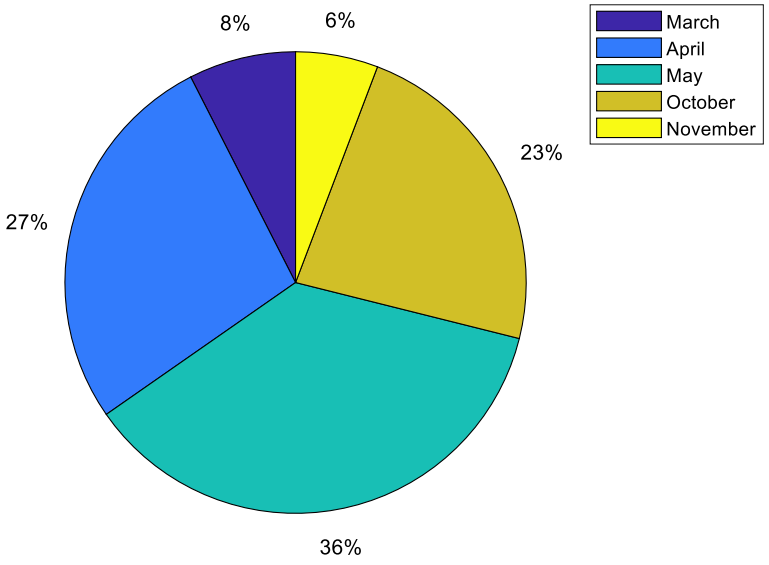

Figure 104 – Distribution of voltage rise constraints over the various months of the seasonality in question, on the assumption of an N-1 configuration

Figure 105 shows the distribution of voltage rise constraints over the various days of the week for the two winters & inter-seasons in question.

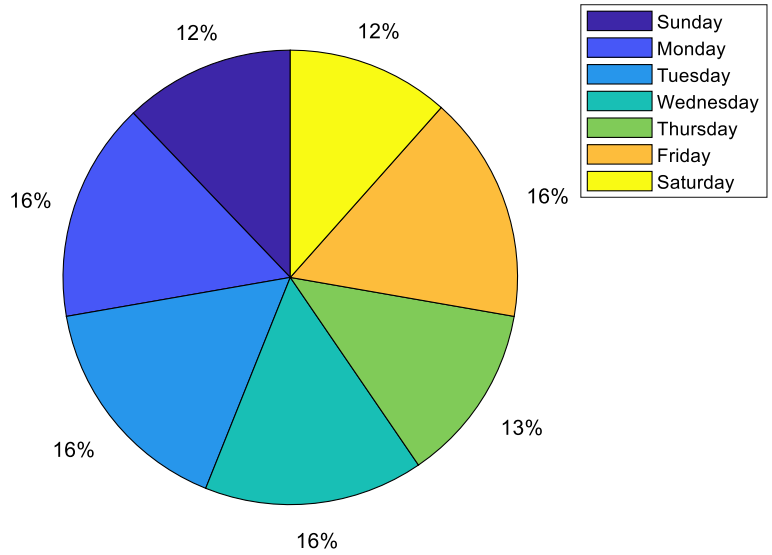

Figure 105 – Distribution of high-voltage constraints over the various days of the week for the seasonality in question, on the assumption of an N-1 configuration

Like for the case of voltage rise constraints, we can see that there is no day which stands out more than another.

Voltage drop constraint

Figure 106 shows the distribution of voltage drop constraints per month. We can see that all the flexibility activations apparently occur at the start of winter, i.e. in November and December.

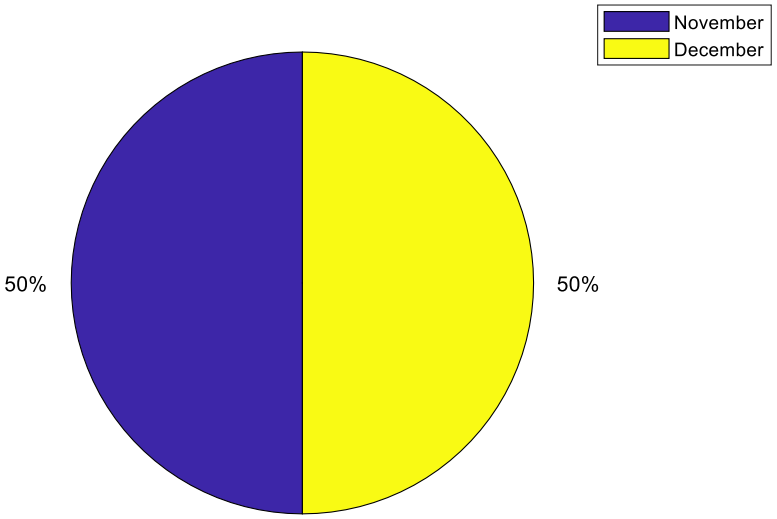

Figure 106 – Distribution of voltage drop constraints over the various months of the seasonality in question, on the assumption of an N-1 configuration

Figure 107 shows the distribution of voltage drop constraints over the various days of the week for the two winters & inter-seasons in question.

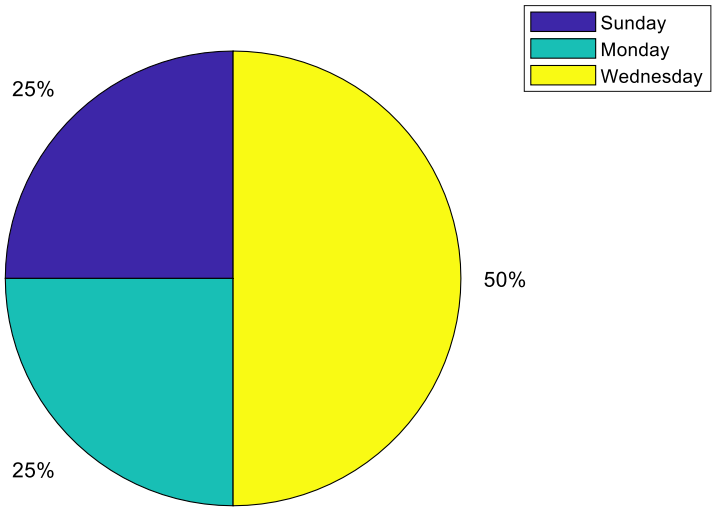

Figure 107 – Distribution of low-voltage constraints over the various days of the week for the seasonality in question, on the assumption of an N-1 configuration

The constraints occur mainly on Sundays, Mondays and Wednesdays. As yet no reliable explanation has been found for this observation.

2.2. Results of simulation 20: Winter & Inter-season & sample 2

Only the results obtained concerning the winter & inter-season seasonality are presented in this section.

Current constraint

Figure 108 shows the distribution of current constraints in injection and draw-off per month. We can see that all the flexibility activations apparently occur at the start and end of winter, and in the spring and autumn. The period potentially in constraint is greater than for the previous sample, which is mainly due to the massive addition of PV production (larger than for sample 1, cf Figure 27 **Erreur ! Source du renvoi introuvable.**).

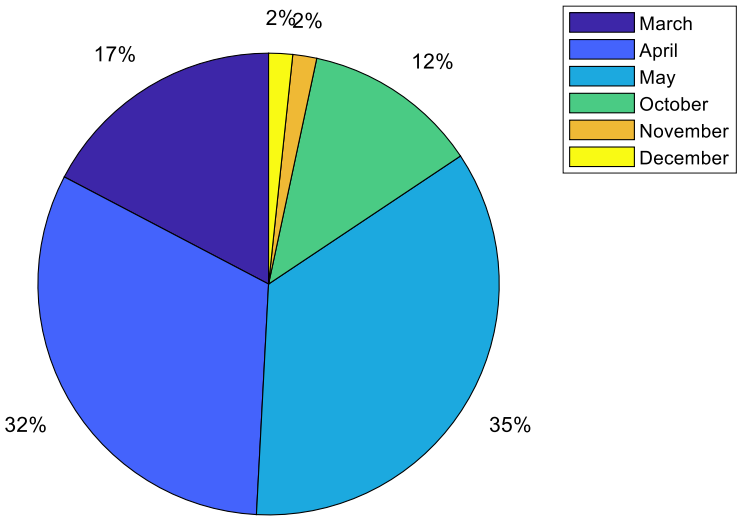

Figure 108 – Distribution of current constraints in the lines/cables over the various months of the seasonality in question on the assumption of an N-1 configuration

Figure 109 shows the distribution of grid constraints over the various days of the week for the two winters & inter-seasons in question.

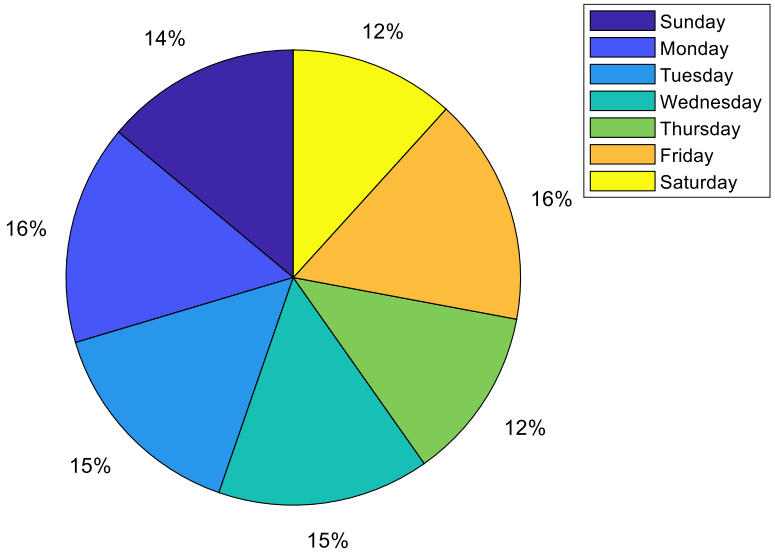

Figure 109 – Distribution of current constraints in lines/cables over the various days of the week for the seasonality in question, on the assumption of an N-1 configuration

For these simulations, the PV production level then is sufficiently high to be able to potentially generate constraints on each day of the seasonality in question.

Note that with regard to constraints in draw-off (and not in injection), these constraints apparently occur on Monday, Tuesday, Wednesday and Sunday, which corresponds to the source-substation consumption peaks.

Current constraint at the feeder terminal

Figure 110 shows the distribution of current constraints at the feeder terminal over the various months in question from October to May. We can see that the flexibility activations apparently occur mostly in the spring and autumn. One possible explanation could be that consumption there is low, whereas PV production is significant. Accordingly, since production has a greater seasonal variation than consumption, the ratio of production to consumption increases in the spring and autumn, thus causing potential constraints.

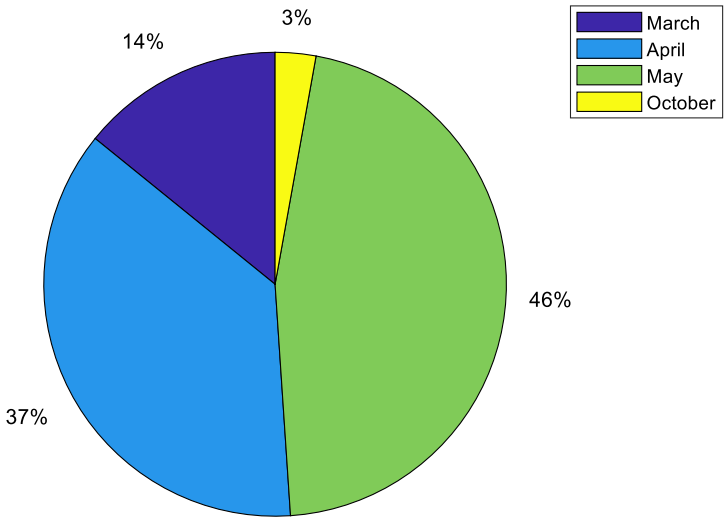

Figure 110 – Distribution of current constraints at the feeder terminal over the various months of the seasonality in question, on the assumption of an N-1 configuration

Figure 111 shows the distribution of current constraints at the feeder terminal over the various days of the week for the two winters & inter-seasons in question.

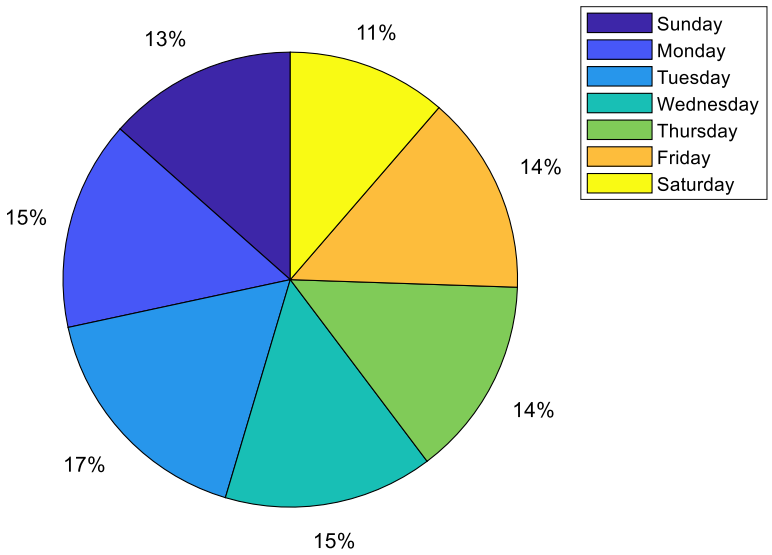

Figure 111 – Distribution of current constraints at the feeder terminal over the various days of the week for the seasonality in question, on the assumption of an N-1 configuration

For these simulations, the PV production level there is sufficiently high to be able to potentially generate constraints on each day of the seasonality in question.

Current constraint in the HV/MV transformer

Figure 112 shows the distribution of grid constraints over the various months from October to May. We can see that all the constraints apparently occur in the spring. One possible explanation could be that consumption there is low, whereas PV production is significant. Accordingly, since production has a greater seasonal variation than consumption, the ratio of production to consumption increases in the spring and autumn, thus causing potential constraints.

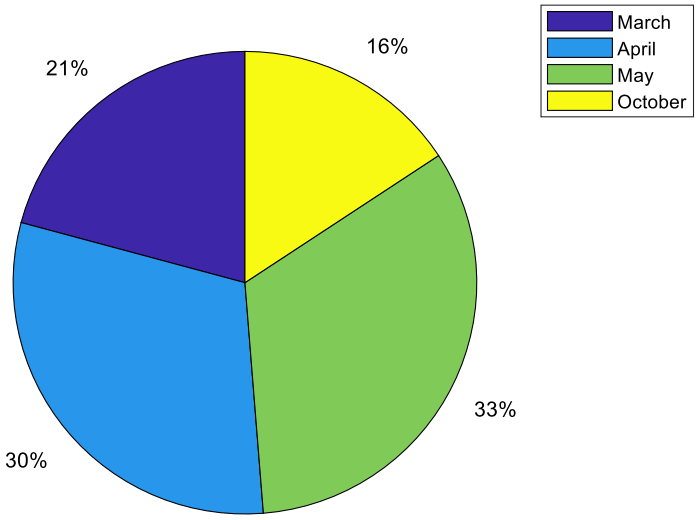

Figure 112 – Distribution of constraints at the HV/MV transformer over the various months of the seasonality in question, on the assumption of an N-1 configuration

Figure 113 shows the distribution of grid constraints over the various days of the week for the two winters & inter-seasons in question.

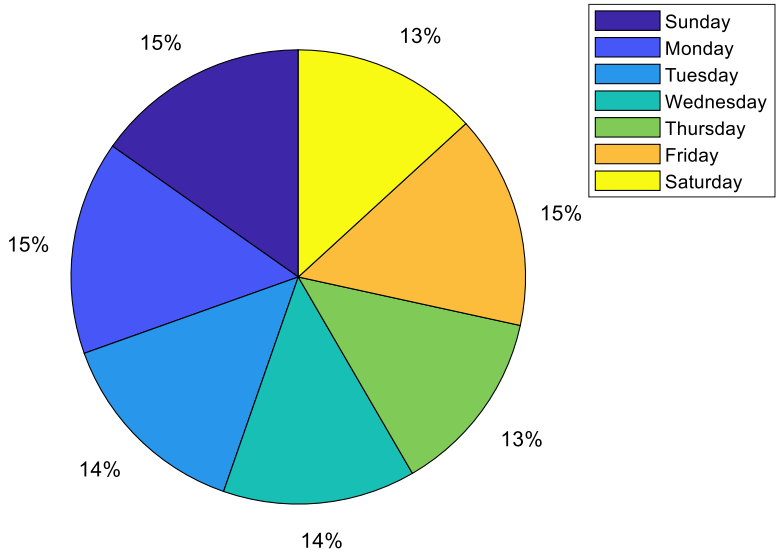

Figure 113 – Distribution of constraints at the HV/MV transformer over the various days of the week, on the assumption of an N-1 configuration

Voltage rise constraint

Figure 114 shows the distribution of grid constraints over the various months from October to May. We can see that all the flexibility activations apparently occur throughout the whole period, although in January and December there are few constraints due to higher consumption and slightly lower PV production than in the other months.

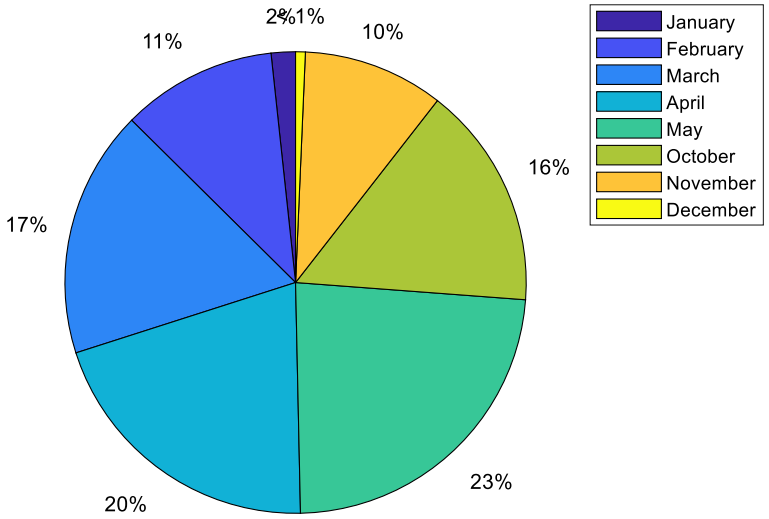

Figure 114 – Distribution of voltage rise constraints over the various months of the seasonality in question, on the assumption of an N-1 configuration

Figure 115 shows the distribution of voltage rise constraints over the various days of the week for the two winters & inter-seasons in question.

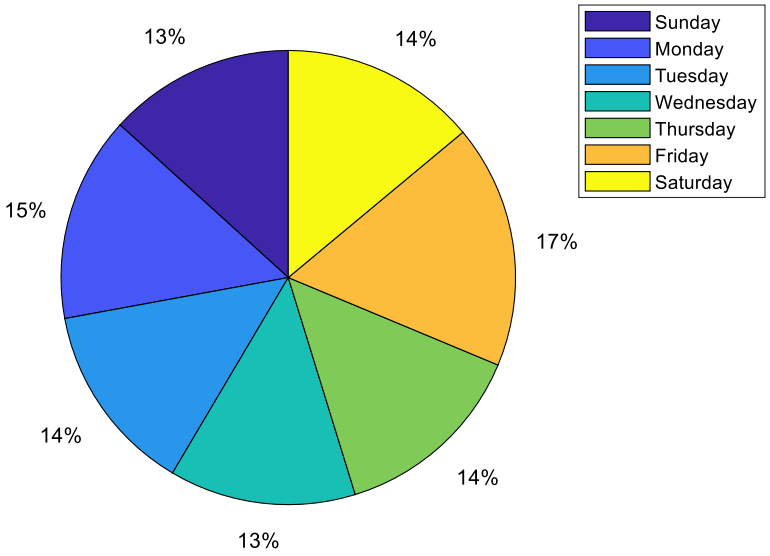

Figure 115 – Distribution of voltage rise constraints over the various days of the week for the seasonality in question, on the assumption of an N-1 configuration

As before, we can see that the constraints could occur on every day of the week. This ranges from 13% of cases on Sundays to 17% on Fridays.

Voltage drop constraint

Figure 116 shows the distribution of grid constraints over the various months from October to May. We can see that all the flexibility activations apparently occur during the first part of winter.

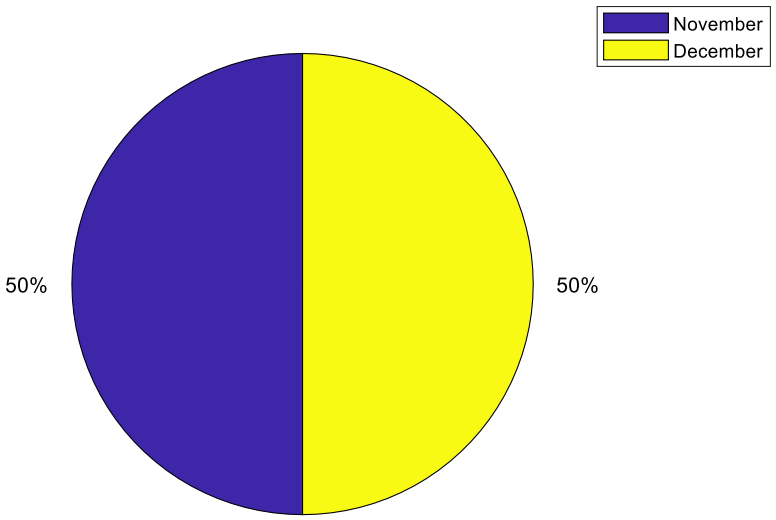

Figure 116 – Distribution of voltage drop constraints over the various months of the seasonality in question, on the assumption of an N-1 configuration

Figure 117 shows the distribution of low-voltage constraints over the various days of the week for the two winters & inter-seasons in question.

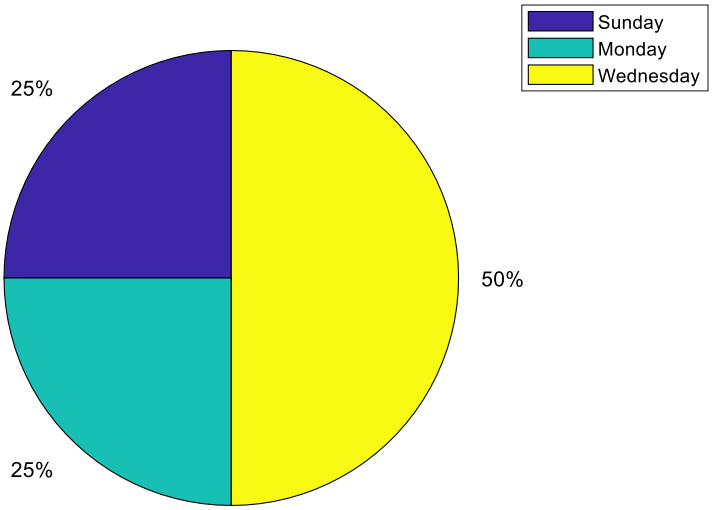

Figure 117 – Distribution of low-voltage constraints over the various days of the week for the seasonality in question, on the assumption of an N-1 configuration

The three main days of the week for which there are apparently potential flexibility needs are Sundays, Mondays and Saturdays. As yet no reliable explanation has been found for this observation.

2.3. Results of simulation 21: Winter & Inter-season & sample 3

Only the results obtained concerning the winter & inter-season seasonality are presented in this section.

Current constraint

Figure 118 shows the distribution of current constraints over the various months in question from October to May. We can see that all the flexibility activations apparently occur in the first part of winter for the draw-off constraints and in spring for injection constraints.

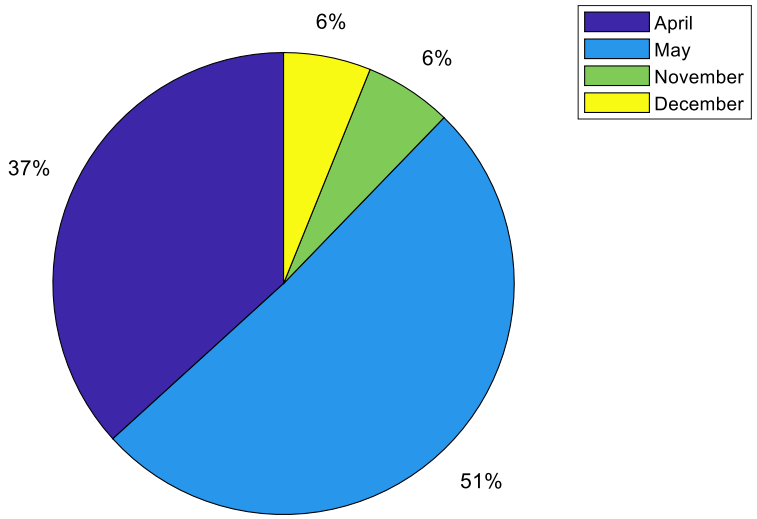

Figure 118 – Distribution of current constraints in the lines/cables over the various months of the seasonality in question, on the assumption of an N-1 configuration for the current constraint

Figure 119 shows the distribution of grid constraints over the various days of the week for the two winters & inter-seasons in question.

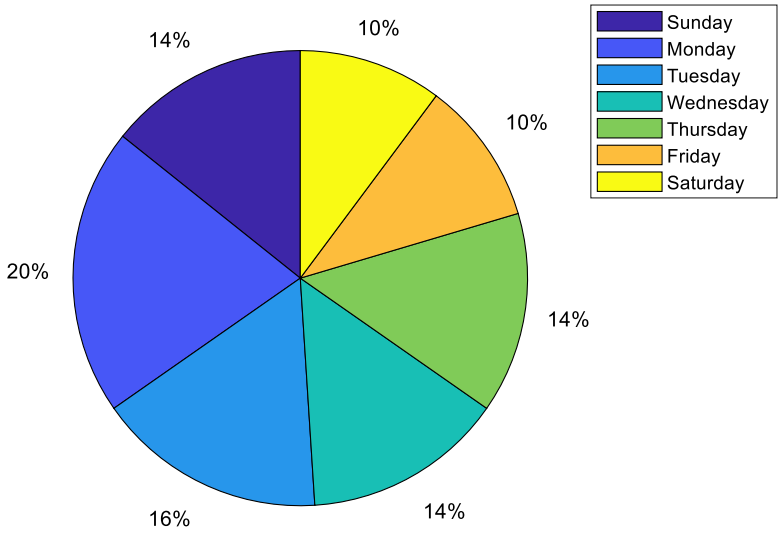

Figure 119 – Distribution of current constraints in the lines/cables over the various days of the week for the seasonality in question, on the assumption of an N-1 configuration

We can see that the constraints could occur on every day of the week. This ranges from 10% of cases on Saturdays and Fridays to 20% of cases on Tuesdays.

Current constraint at the feeder terminal

Figure 120 shows the distribution of current constraints at the feeder terminal over the various months in question from October to May. We can see that all the flexibility activations apparently occur in the spring. One possible explanation would be that this is a period without the summer crowds of visitors and the Isola source substation mostly comprises recreational consumption. Accordingly, consumption there is relatively low in this period, whereas PV is injected extensively.

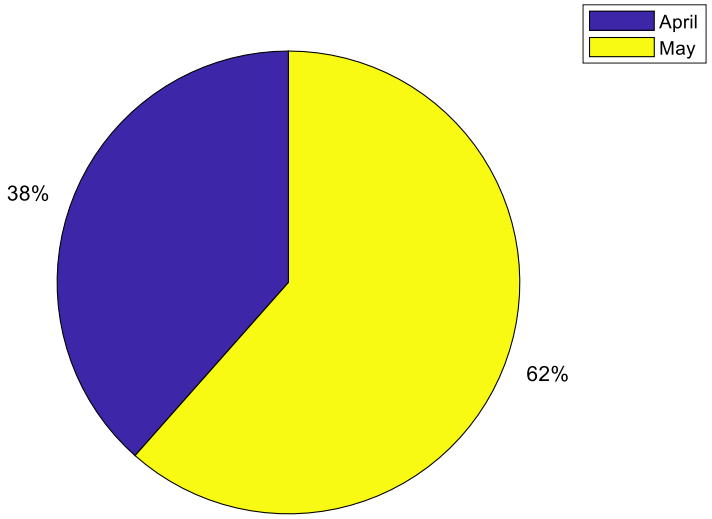

Figure 120 – Distribution of current constraints at the feeder terminal over the various months of the seasonality in question, on the assumption of an N-1 configuration

Figure 121 shows the distribution of current constraints at the feeder terminal over the various days of the week for the two winters & inter-seasons in question.

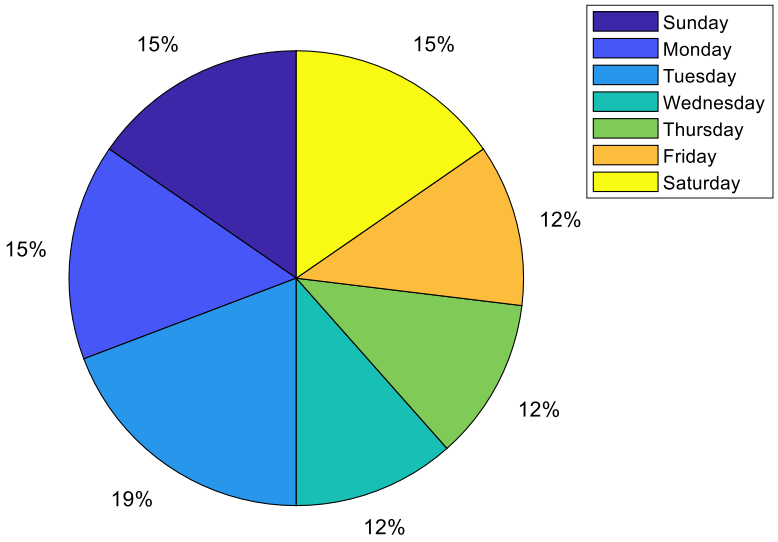

Figure 121 – Distribution of current constraints at the feeder terminal over the various days of the week for the seasonality in question, on the assumption of an N-1 configuration

Like for the case of current constraints in a cable or line, we can see that there is no day which stands out more than another.

Current constraint in the HV/MV transformer

Figure 122 shows the distribution of current constraints at the HV/MV transformer over the various months in question from October to May. We can see that all the flexibility activations apparently occur in the spring. One possible explanation would be that this is a period without the summer crowds of visitors and the Isola source substation mostly comprises recreational consumption. Accordingly, consumption there is relatively low in this period, whereas PV is injected extensively.

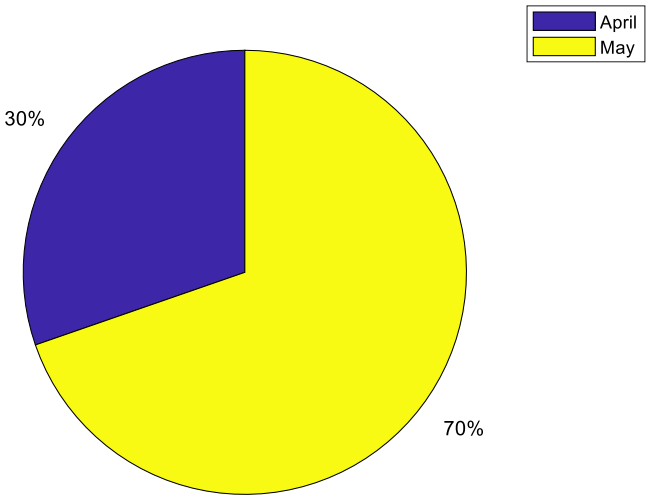

Figure 122 – Distribution of constraints at the HV/MV transformer over the various months of the seasonality in question, on the assumption of an N-1 configuration

Figure 123 shows the distribution of current constraints at the HV/MV transformer over the various days of the week for the two winters & inter-seasons in question.

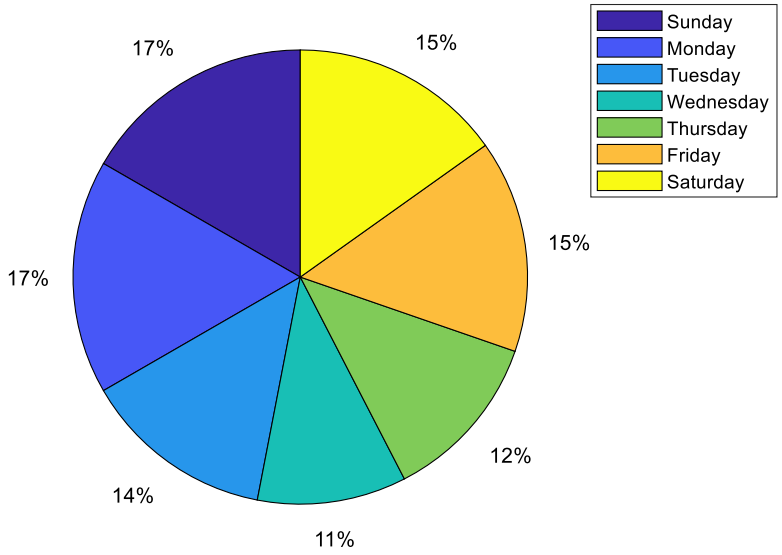

Figure 123 – Distribution of current constraints in the HV/MV transformer over the various days of the week for the seasonality in question, on the assumption of an N-1 configuration

Like for the case of current constraints in a cable or line, we can see that there is no day which stands out more than another.

Voltage rise constraint

Figure 124 shows the distribution of voltage rise constraints per month of the seasonality in question. We can see that all the flexibility activations apparently occur mostly in the spring and autumn. One possible explanation could be that there is an asynchronism between the high consumption levels and high production levels, thereby causing voltage rise constraints. From December to March, consumption offsets the overproduction sufficiently to prevent this type of constraint on the grid.

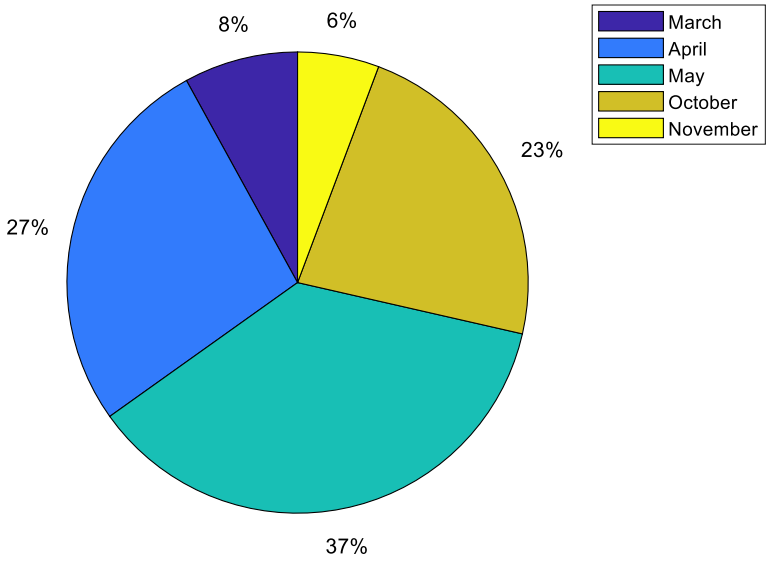

Figure 124 – Distribution of voltage rise constraints over the various months of the seasonality in question, on the assumption of an N-1 configuration

Figure 125 shows the distribution of voltage rise constraints over the various days of the week for the two winters & inter-seasons in question.

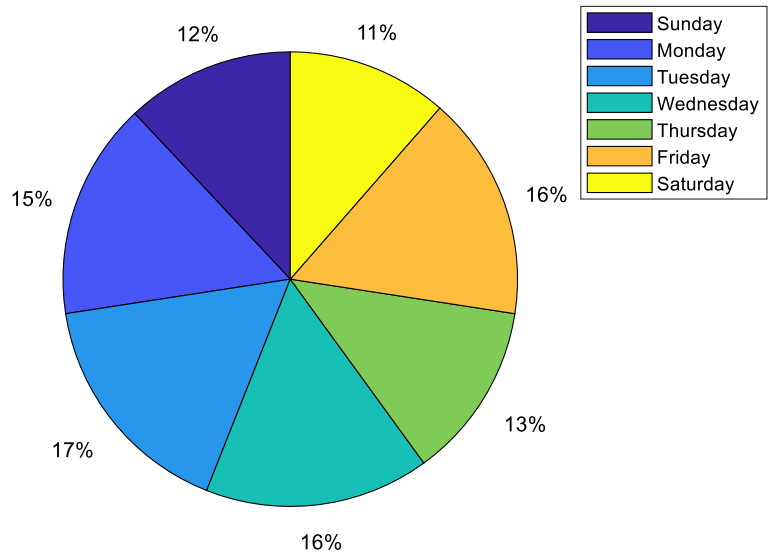

Figure 125 – Distribution of voltage rise constraints over the various days of the week for the seasonality in question, on the assumption of an N-1 configuration

We can see that there is no day which stands out more than another.

Voltage drop constraint

Figure 126 shows the distribution of voltage drop constraints per month. We can see that all the flexibility activations apparently occur at the start of winter, i.e. in November and December.

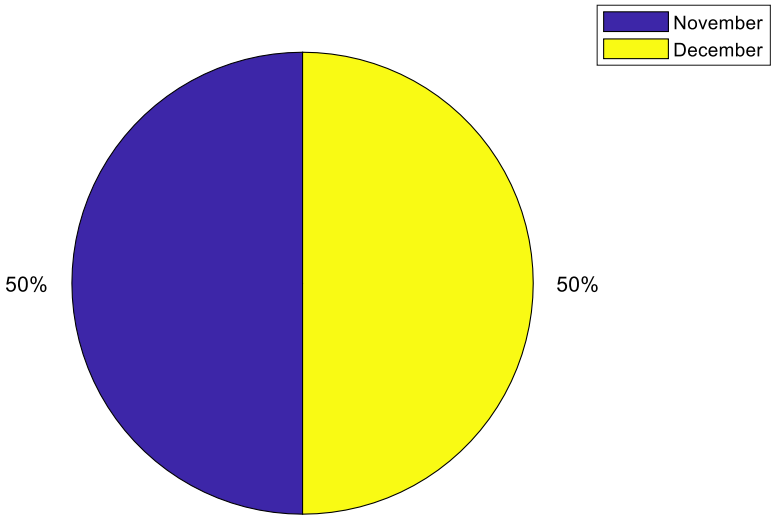

Figure 126 – Distribution of low-voltage constraints over the various months of the seasonality in question, on the assumption of an N-1 configuration

Figure 127 shows the distribution of grid constraints over the various days of the week for the two summers in question.

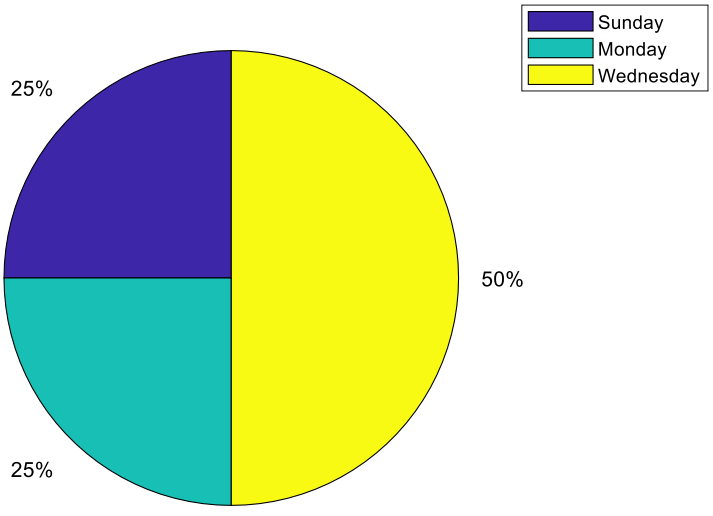

Figure 127 – Distribution of low-voltage constraints over the various days of the week for the seasonality in question, on the assumption of an N-1 configuration

The constraints occur mainly on Sundays, Mondays and Wednesdays. As yet no reliable explanation has been found for this phenomenon.

2.4. Results of simulation 22 Summer & sample 1

Only the results obtained concerning the summer seasonality are presented in this section.

Current constraint

Figure 128 shows the distribution of current constraints in injection per month. We can see that all the flexibility activations apparently occur in the middle of the summer season. This is mainly due to the high PV production at that time of year, coupled with relatively low consumption.

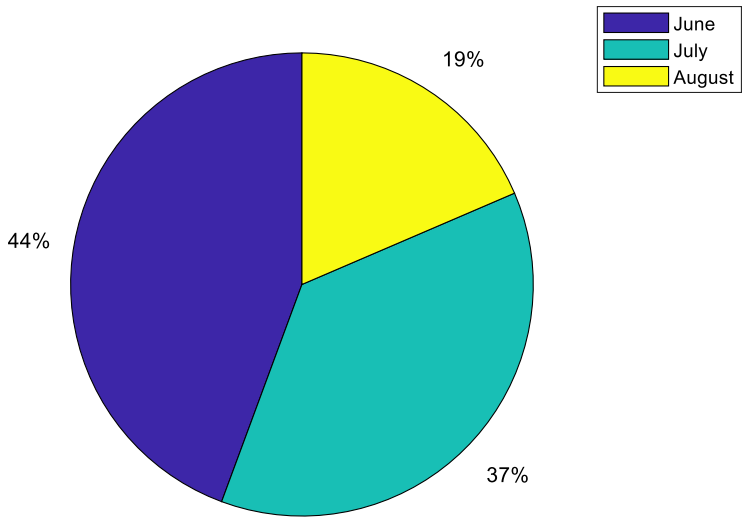

Figure 128 – Distribution of current constraints in the lines/cables over the various months of the seasonality in question, on the assumption of an N-1 configuration for the current constraint

Figure 129 shows the distribution of grid constraints over the various days of the week for the two summers in question.

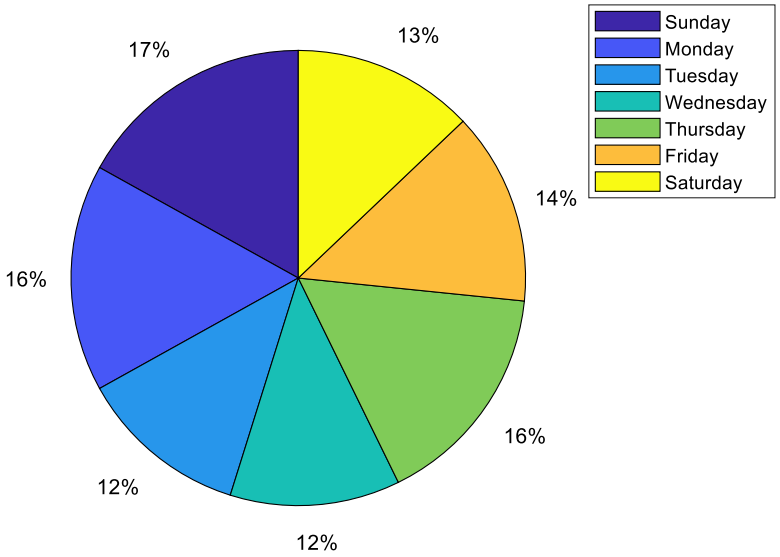

Figure 129 – Distribution of current constraints in the lines/cables over the various days of the week for the seasonality in question, on the assumption of an N-1 configuration

We can see that there is no day which stands out more than another.

Current constraint at the feeder terminal

Figure 130 shows the distribution of current constraints at the feeder terminal over the various months of the two summers in question. We can see that all the flexibility activations apparently occur in June. This can be explained by the fact that the production/consumption imbalance is largest in June in this zone.

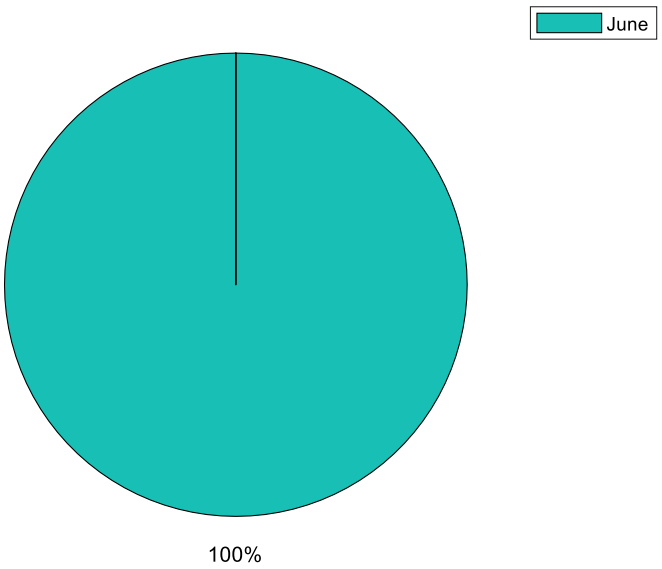

Figure 130 – Distribution of current constraints at the feeder terminal over the various months of the seasonality in question, on the assumption of an N-1 configuration

Figure 131 shows the distribution of grid constraints over the various days of the week for the two winters & inter-seasons in question.

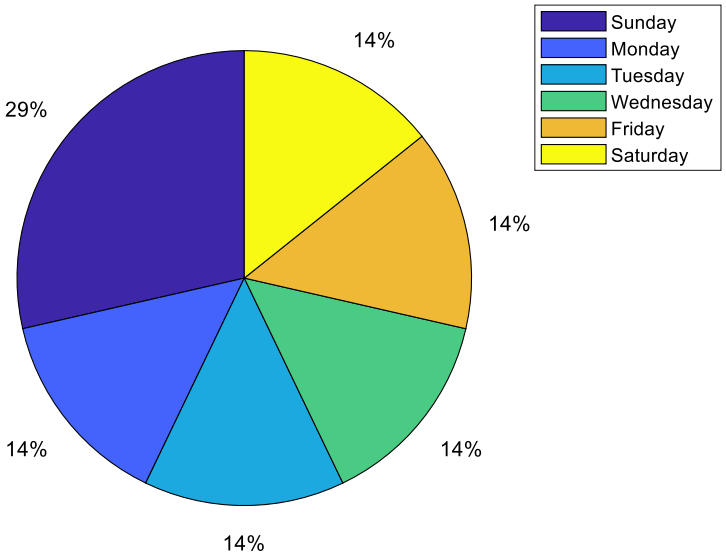

Figure 131 – Distribution of current constraints at the feeder terminal over the various days of the week for the seasonality in question, on the assumption of an N-1 configuration

We can see that the constraints could occur on every day of the week. This ranges from 14% of cases from Tuesday to Friday, up to 29% of cases on Mondays.

Current constraint in the HV/MV transformer

Figure 132 shows the distribution of current constraints at the level of the HV/MV transformer per month. We can see that all the flexibility activations apparently occur during the summer months. One possible explanation would be that the Isola source substation mostly comprises recreational consumption in winter. Accordingly, consumption there is relatively low in this period, whereas PV is injected massively.

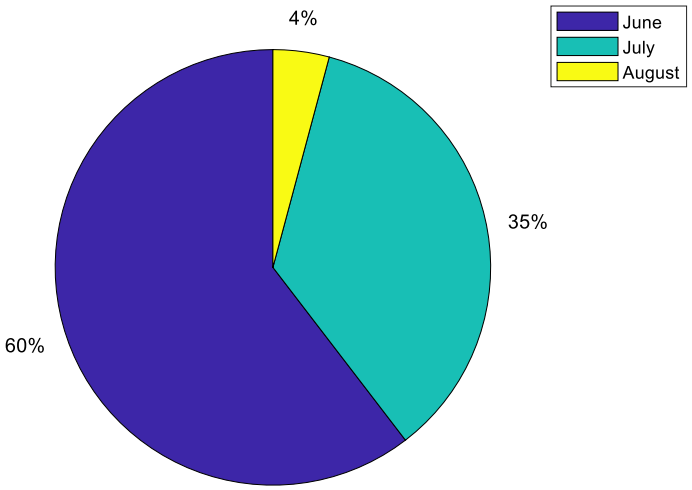

Figure 132 – Distribution of constraints at the HV/MV transformer over the various months of the seasonality in question, on the assumption of an N-1 configuration

Figure 133 shows the distribution of current constraints at the HV/MV transformer over the various days of the week for the two winters & inter-seasons in question.

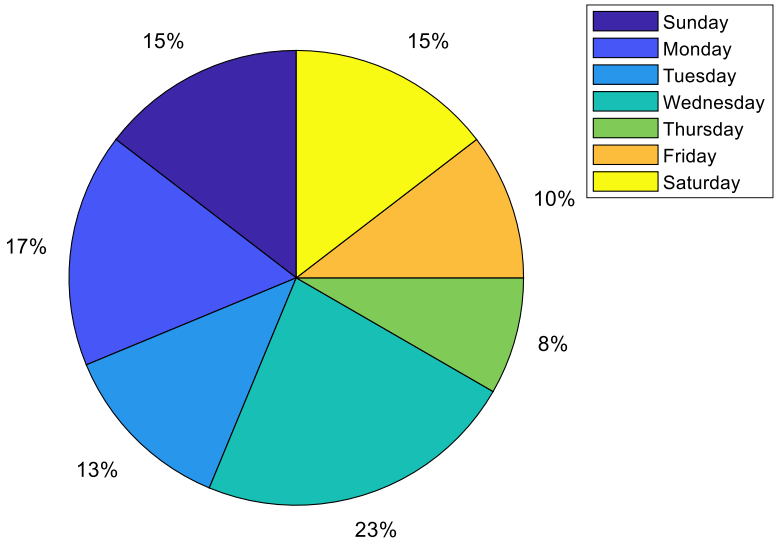

Figure 133 – Distribution of current constraints in the HV/MV transformer over the various days of the week for the seasonality in question, on the assumption of an N-1 configuration

We can see that the constraints could occur on every day of the week. This ranges from 8% of cases on Thursdays to 23% of cases on Wednesdays.

Voltage rise constraint

Figure 134 shows the distribution of voltage rise constraints per month. We can see that all the flexibility activations apparently occur throughout the summer season. One possible explanation would be that the Isola source substation mostly comprises recreational consumption in winter. Accordingly, consumption there is relatively low in this period, whereas PV is injected massively.

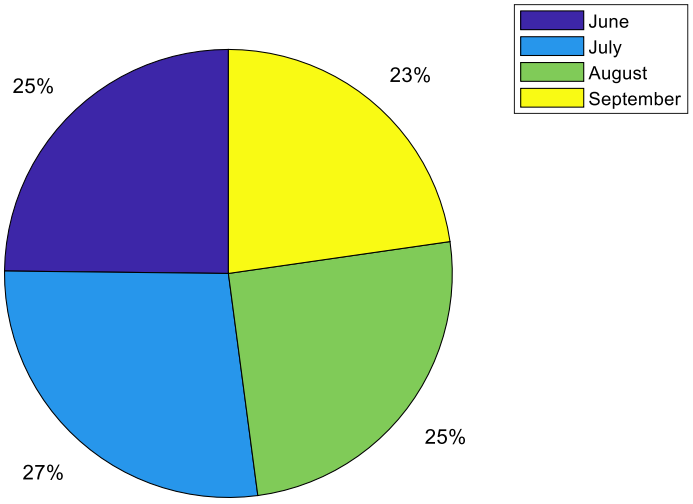

Figure 134 – Distribution of voltage rise constraints over the various months of the seasonality in question, on the assumption of an N-1 configuration

Figure 135 shows the distribution of voltage rise constraints over the various days of the week for the two summers in question.

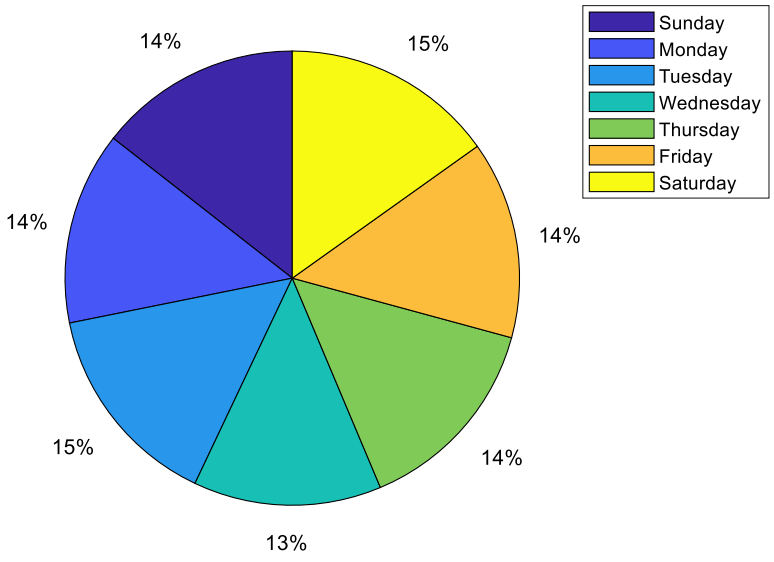

Figure 135 – Distribution of voltage rise constraints over the various days of the week for the seasonality in question, on the assumption of an N-1 configuration

Like for the other constraints, we can see that there is no day which stands out more than another.

2.5. Results of simulation 23 Summer & sample 2

Only the results obtained concerning the summer seasonality are presented in this section.

Current constraint in injection

Figure 136 shows the distribution of current constraints in injection over the various months of the two summers in question. We can see that all the flexibility activations apparently occur throughout the summer season. This is mainly due to the massive addition of PV production, which is higher than in the case of sample 1, coupled with the relatively low consumption of the source substation in this period.

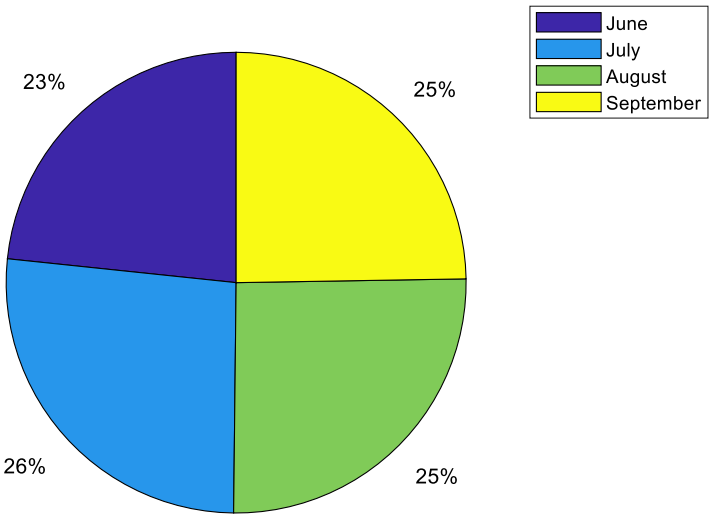

Figure 136 – Distribution of current constraints in the lines/cables over the various months of the seasonality in question, on the assumption of an N-1 configuration for the current constraint

Figure 137 shows the distribution of current constraints in the lines/cables over the various days of the week for the two summers in question.

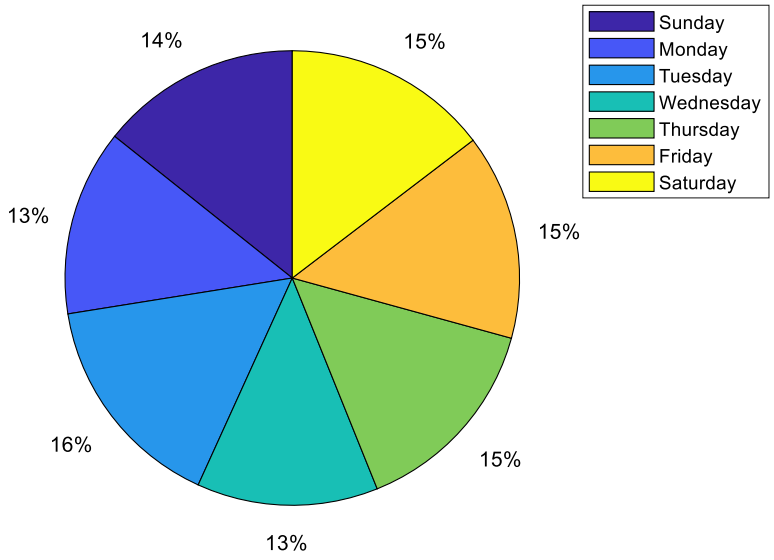

Figure 137 – Distribution of current constraints in lines/cables over the various days of the week for the seasonality in question, on the assumption of an N-1 configuration

We can see that there is no day which stands out more than another.

Current constraint at the feeder terminal

Figure 138 shows the distribution of grid constraints over the various months of the two summers in question. We can see that all the flexibility activations apparently occur throughout the summer season. This is mainly due to the massive addition of PV production, which is higher than in the case of sample 1 (cf Figure 27) and low consumption.

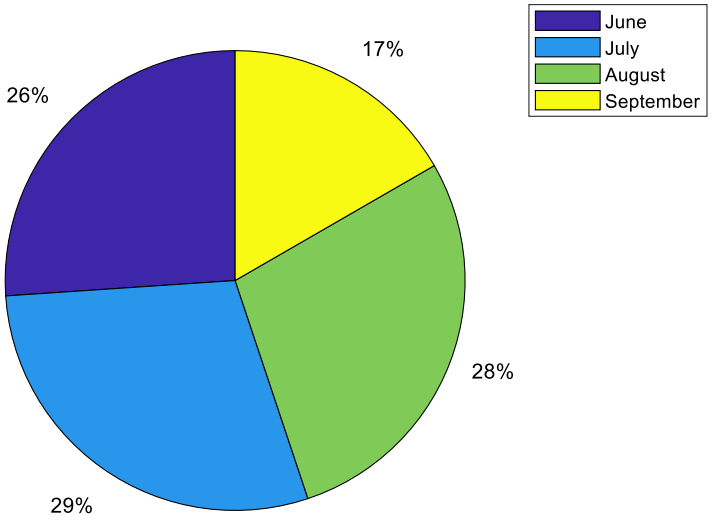

Figure 138 – Distribution of current constraints at the feeder terminal over the various months of the seasonality in question, on the assumption of an N-1 configuration

Figure 139 shows the distribution of current constraints at the feeder terminal over the various days of the week for the two summers in question.

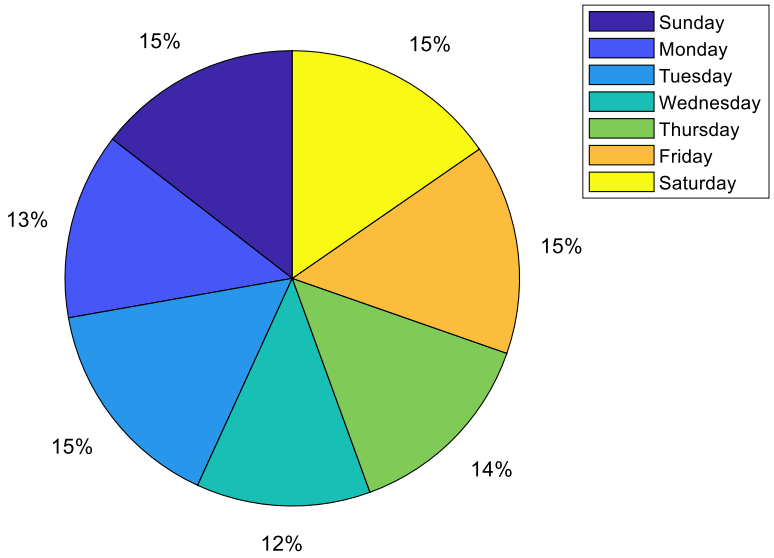

Figure 139 – Distribution of current constraints at the feeder terminal over the various days of the week for the seasonality in question, on the assumption of an N-1 configuration

We can see that there is no day which stands out more than another.

Current constraint in the HV/MV transformer

Figure 140 shows the distribution of current constraints at the HV/MV transformer over the various months of the two summers in question. We can see that all the flexibility activations apparently occur throughout the summer season. One possible explanation would be that this is a period without the summer crowds of visitors and the Isola source substation mostly comprises recreational consumption. Accordingly, consumption there is relatively low in this period, whereas PV is injected massively.

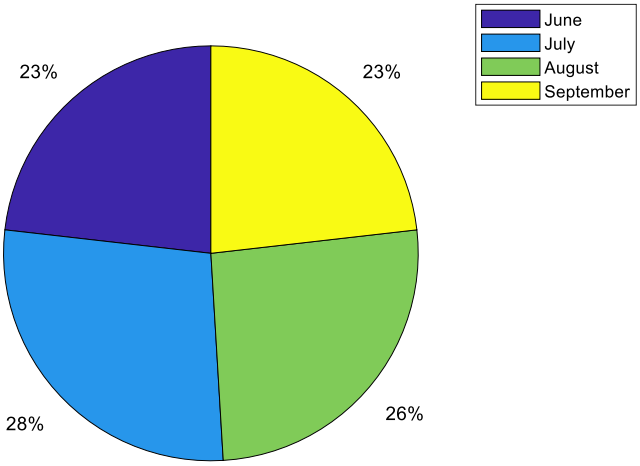

Figure 140 – Distribution of constraints at the HV/MV transformer over the various months of the seasonality in question, on the assumption of an N-1 configuration

Figure 141 shows the distribution of constraints at the HV/MV transformer over the various days of the week for the two summers in question.

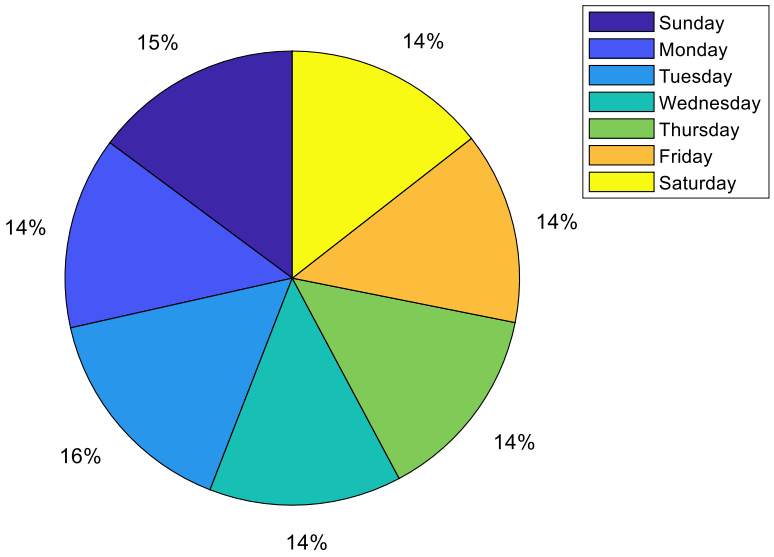

Figure 141 – Distribution of constraints at the HV/MV transformer over the various months of the seasonality in question, on the assumption of an N-1 configuration

We can see that there is no day which stands out more than another.

Voltage rise constraint

Figure 141 shows the distribution of voltage rise constraints. We can see that all the flexibility activations apparently occur throughout the summer season. One possible explanation would be that this is a period without the summer crowds of visitors and the Isola source substation mostly comprises recreational consumption. Accordingly, consumption there is relatively low in this period, whereas PV is injected massively.

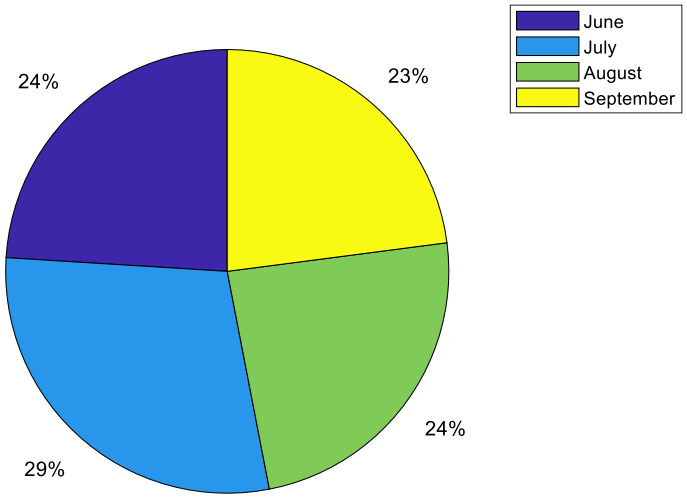

Figure 142 – Distribution of voltage rise constraints over the various months of the seasonality in question, on the assumption of an N-1 configuration

Figure 143 shows the distribution of voltage rise constraints over the various days of the week for the two winters & inter-seasons in question.

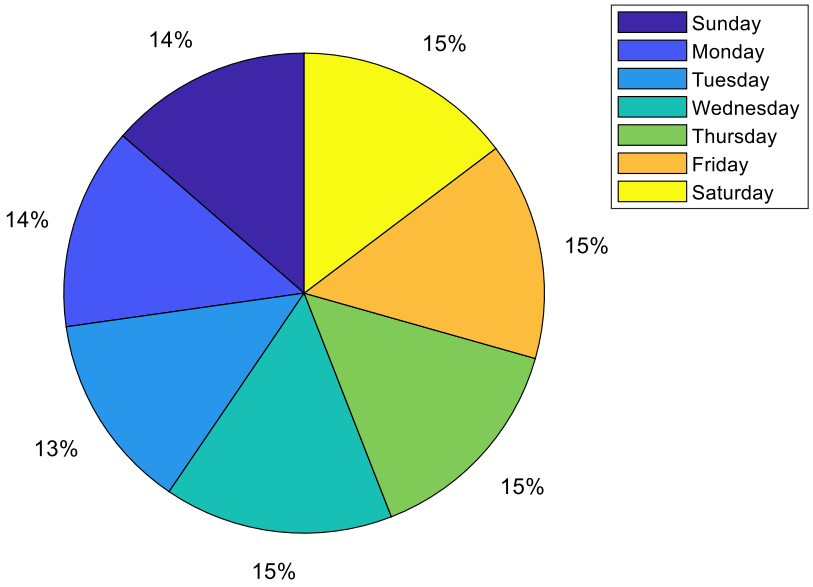

Figure 143 – Distribution of voltage rise constraints over the various days of the week for the seasonality in question, on the assumption of an N-1 configuration

Like for the other constraints, we can see that there is no day which stands out more than another.

2.6. Results of simulation 24: Summer & sample 3

Only the results obtained concerning the summer seasonality are presented in this section.

Current constraint

Figure 144 shows the distribution of current constraints in injection over the various months of the two summers in question from October to May. We can see that all the flexibility activations apparently occur during the summer months. This is mainly due to the massive addition of PV production and the relatively low consumption.

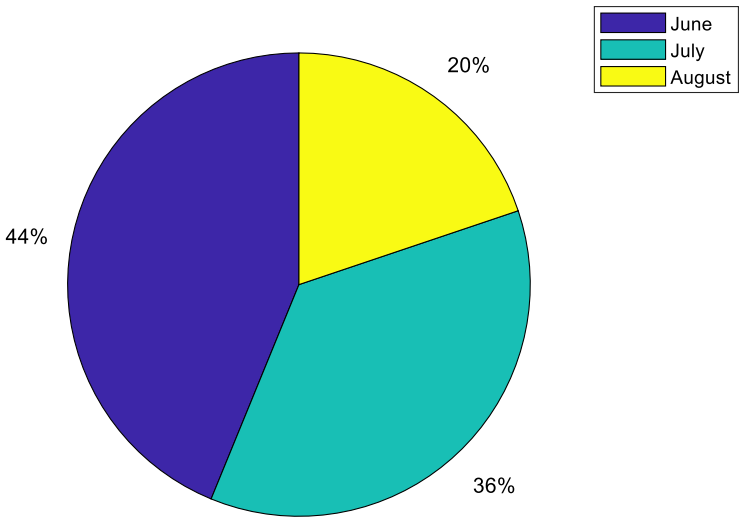

Figure 144 – Distribution of current constraints in the lines/cables over the various months of the seasonality in question, on the assumption of an N-1 configuration for the current constraint

Figure 145 shows the distribution of current constraints in the lines/cables over the various days of the week for the two winters & inter-seasons in question.

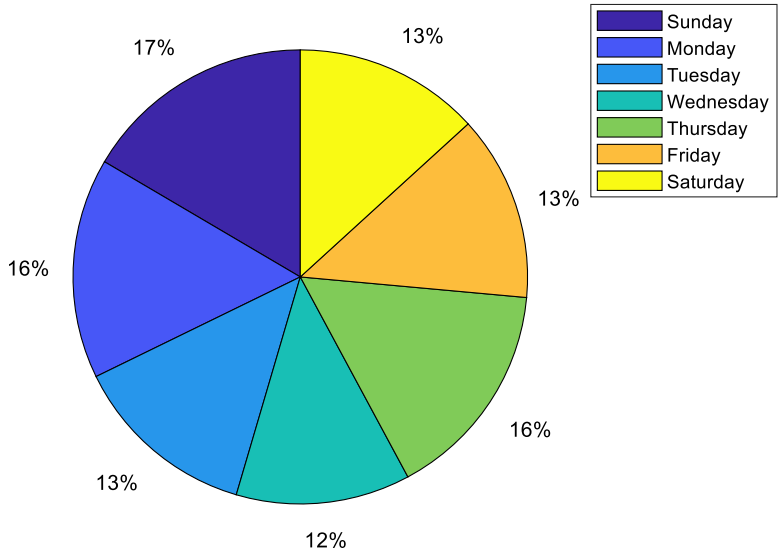

Figure 145 – Distribution of current constraints in the lines/cables over the various days of the week for the seasonality in question, on the assumption of an N-1 configuration

We can see that there is no day which stands out more than another.

Current constraint at the feeder terminal

Figure 146 shows the distribution of current constraints at the feeder terminal over the various months of the two summers in question. We can see that all the flexibility activations apparently occur in June. This can be explained by the fact that the production/consumption imbalance is largest in June in this zone.

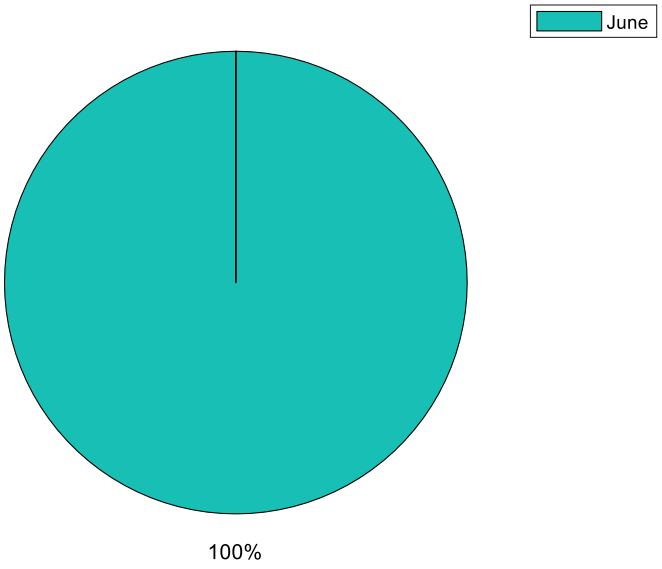

Figure 146 – Distribution of current constraints at the feeder terminal over the various months of the seasonality in question, on the assumption of an N-1 configuration

Figure 147 shows the distribution of current constraints at the feeder terminal over the various days of the week for the two summers in question.

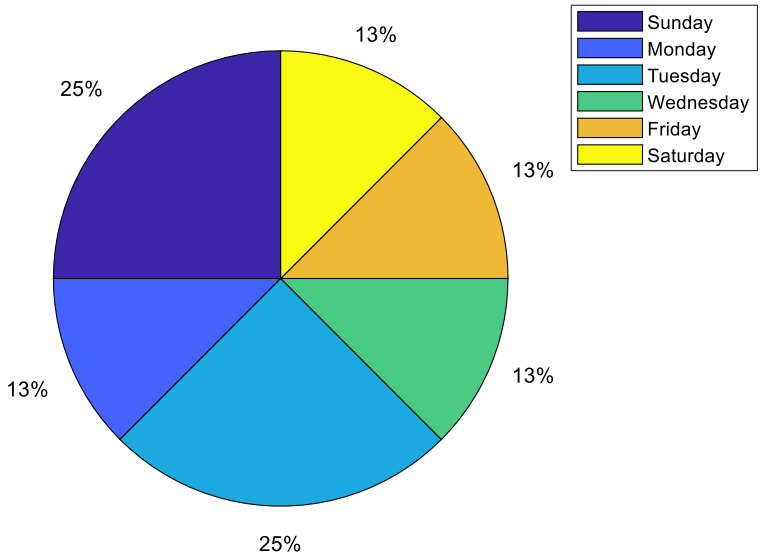

Figure 147 – Distribution of current constraints at the feeder terminal over the various days of the week for the seasonality in question, on the assumption of an N-1 configuration

We can see that the constraints could occur on every day of the week except Thursday. This ranges from 13% of cases on Tuesdays, Wednesdays, Fridays, Saturdays and Sundays, up to 25% of cases on Mondays and Thursdays.

Current constraint in the HV/MV transformer

Figure 148 shows the distribution of current constraints at the level of the HV/MV transformer per month. We can see that all the flexibility activations apparently occur during the summer months. One possible explanation would be that this is a period without the

summer crowds of visitors and the Isola source substation mostly comprises recreational consumption. Accordingly, consumption there is relatively low in this period, whereas PV is injected massively.

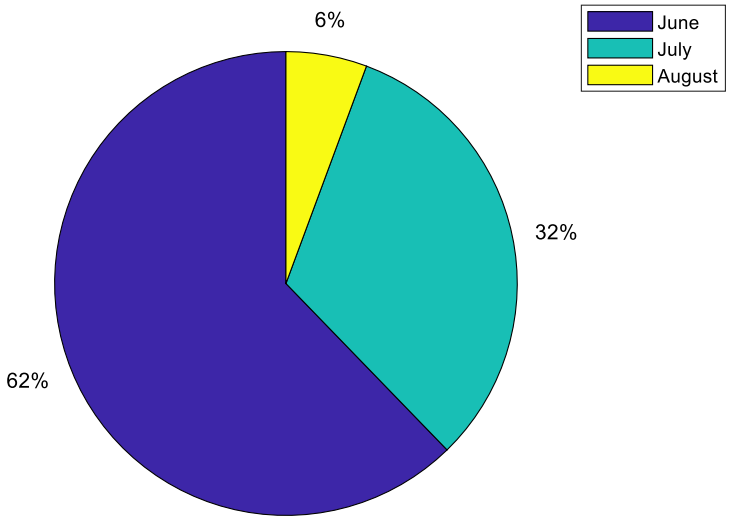

Figure 148 – Distribution of constraints at the HV/MV transformer over the various months of the seasonality in question, on the assumption of an N-1 configuration

Figure 149 shows the distribution of grid constraints over the various days of the week for the two winters & inter-seasons in question.

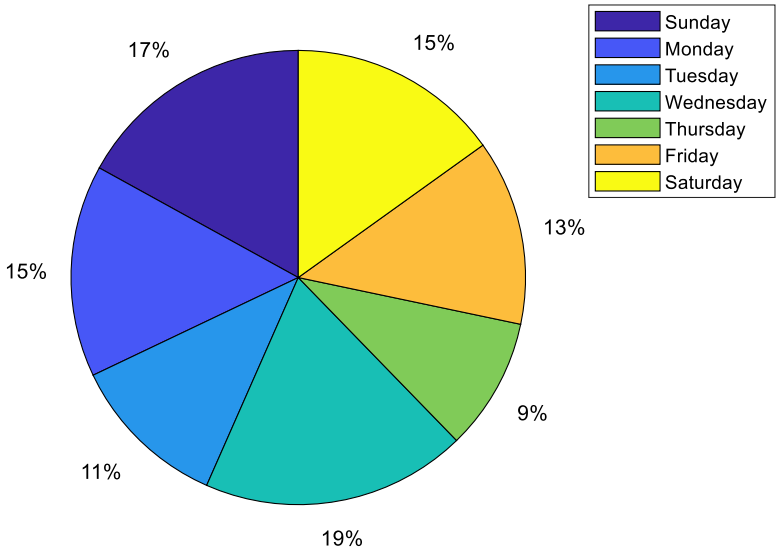

Figure 149 – Distribution of current constraints at the feeder terminal over the various days of the week for the seasonality in question, on the assumption of an N-1 configuration

We can see that the constraints could occur on every day of the week. This ranges from 9% of cases on Thursdays to 19% of cases on Wednesdays.

Voltage rise constraint

Figure 150 shows the distribution of voltage rise constraints per month. We can see that all the flexibility activations apparently occur throughout the summer season. One possible explanation would be that this is a period without the summer crowds of visitors and the Isola source substation mostly comprises recreational consumption. Accordingly, consumption there is relatively low in this period, whereas PV is injected massively.

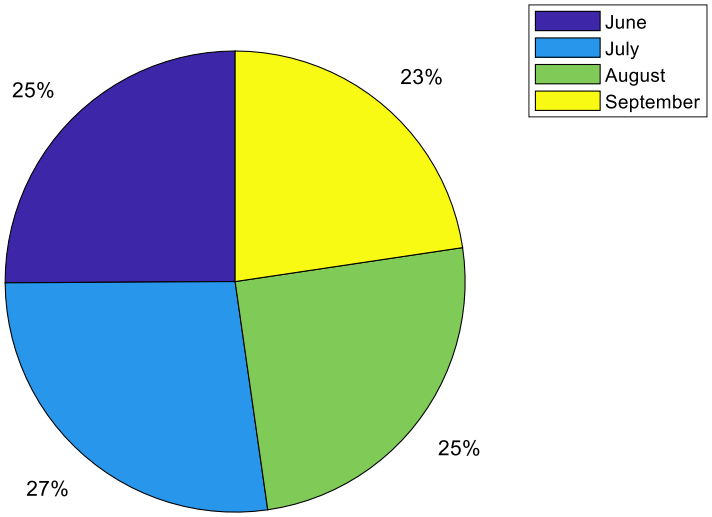

Figure 150 – Distribution of voltage rise constraints over the various months of the seasonality in question, on the assumption of an N-1 configuration

Figure 151 shows the distribution of voltage rise constraints over the various days of the week for the two summers in question.

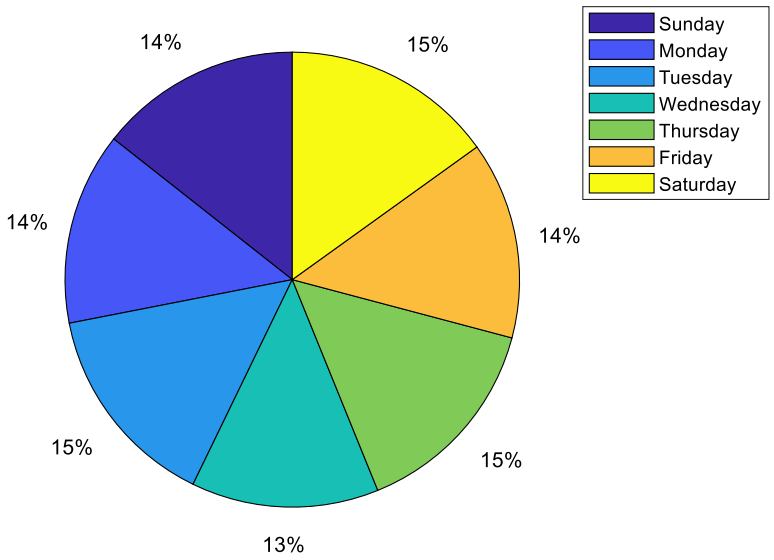

Figure 151 – Distribution of voltage rise constraints over the various days of the week for the seasonality in question, on the assumption of an N-1 configuration

We can see that there is no day which stands out more than another.

APPENDIX C: Impact of the location of the flexibility on volume, example of Guillaumes, Carros and Isola primary substation

1. IMPACT OF THE LOCATION OF THE FLEXIBILITY ON VOLUME

This section describes additional analyses performed on the Nice Smart Valley project zones regarding U and I constraints, in order to identify a framework for flexibility. This framework will make it possible to show the impact of the location of flexibility on useful volumes.

In all the results of this document, the source substation N-1 system is fixed irrespective of the zone's consumption level. The N-1 system input mode is not examined.

Note: The results presented below follow on from the initial results proposed in deliverable d9.1. The very great majority of the calculation assumptions have been kept, and we invite readers to refer to Appendix 1 to the deliverable, if necessary.

1.1. Methodology for estimation of flexibility volumes

1.1.1. I constraint: Homothetic useful flexibility volume

To define the flexibility framework to remove an I or S constraint, the constraint(s) will be removed by reducing the downstream load, via a positioning respectively:

- as close as possible to the constraint when the maximum flexibility volume is wanted;
- as far as possible from the start of the constraint when the minimum volume is wanted.

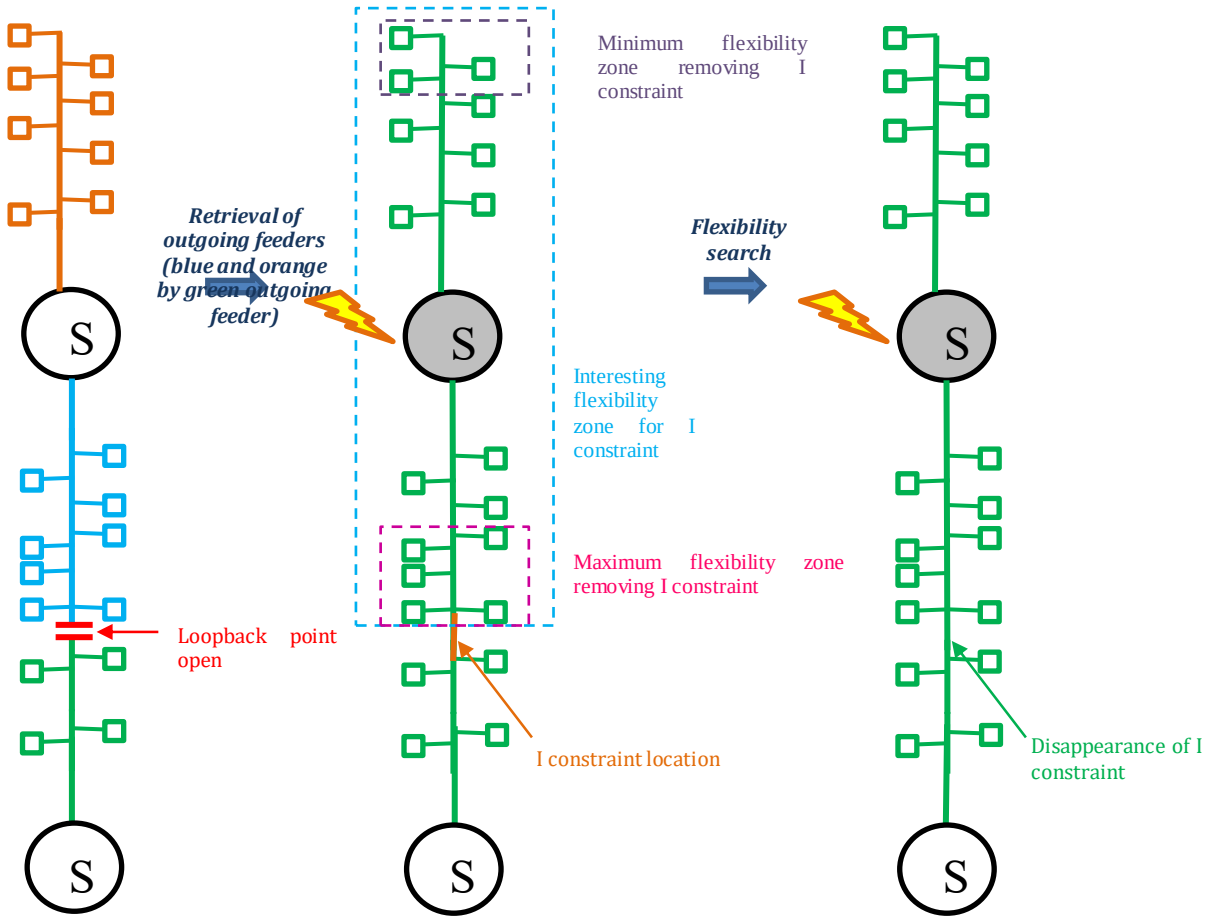

Figure 152 – Principle of I constraint resolution with flexibility framework

1.1.2. U constraint: Homothetic useful flexibility volume

For a grid U constraint, the constraint(s) will be removed by reducing loads whose geographic location is on the whole feeder in an HV N-1 system. This is because, unlike the I constraint, the loads on an outgoing feeder all have an influence on the U constraint (to a greater or lesser extent depending on their position relative to the constrained zone).

Remember, too, that the I constraint has already been eliminated. When the flexible load is in the zone selected to resolve the I constraint and the U constraint, the total flexibility volumes will be obtained by taking the sum of the volumes for the I constraint and U constraint.

Figure 153 shows the resolution principle applied to U constraints for each constrained outgoing feeder.

From a calculation viewpoint, if a limit coefficient γ is applied to the loads of the sub-zone in question, the flexibility volume capable of removing the U constraint (after removing the I constraint) is described by the following formula:

$$P_{flex}^{U}(\alpha) = \alpha P_{\max}^{zoneU}(1-\gamma)\cdot[1-(1-\beta)x]$$

Where:

- P_{flex}^{U} is the useful flexibility volume to eliminate the U constraint after eliminating the I constraint.
- $P_{\max}^{zoneU}$ is the maximum power consumed by the loads located in the selected sub-zone.
- *x* represents the proportion of consumption located in the flexibility search zone to remove the I constraint and U constraint where applicable ($xP_{\max}^{zoneU} = P_{\max}^{départ} \cap P_{\max}^{aval}$ with x=0 if there were no I constraint or if the flexibility search zones are different).
- *α* represents the load level studied on the normalized monotone, applied to all the loads in the zone.
- *β* is the limit coefficient applied to loads downstream of any I constraint resolved previously.
- γ is the limit coefficient applied to loads in the selected sub-zone to remove the constraint.

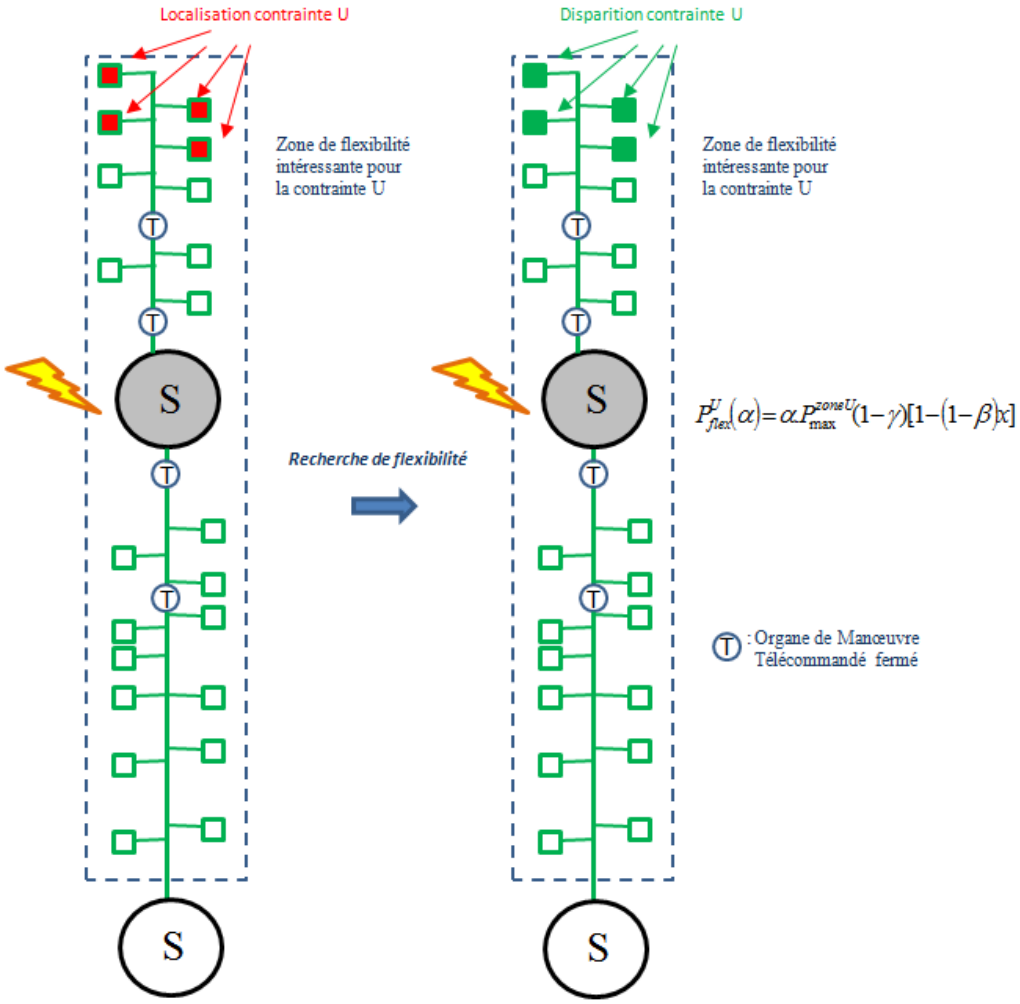

Figure 153 – Principle of U constraint resolution

These simulations can be used to define the useful flexibility volumes making it possible to remove constraints. In the case of a U and I multi-constraint, the flexibility volumes will be given to resolve the constraints separately (if the U constraint persists after elimination of the I constraint).

We will now assess the impact of the location of flexibility on the U constraint.

1.1.3. Evaluation of the impact of flexibility

This section aims to shed light on the impact of the location of flexibilities on the U or I constraint. The calculations described in the remainder of this section will not be systematic and will be run on the same single load level $\alpha = \alpha_{max}$.

We will now examine two fundamentally different approaches for estimating the flexibility volumes capable of removing these constraints depending on the size of the selected zone. The first concerns the search for extreme flexibility volumes on the complete outgoing feeder, in order to limit the flexibility volumes according to the maximum optimization and "deoptimization" of the location of flexibility. The second concerns the search for flexibility volumes by sub-zones.

In these two sections, the useful flexibility volumes are assessed according to the same principle as explained in the previous section.

We will now describe in detail the method that can be used to assess the extreme flexibility volumes.

1.1.3.1. Assessment of extreme flexibilities (maximum and minimum)

In *Nice Smart Valley*, the extreme flexibility volumes correspond to the minimum and maximum volumes which can remove the constraint. To define them, we must first hierarchically rank the utility of load flexibility. **In *Nice Smart Valley*, the criterion for hierarchic ranking of the utility of loads to solve the U constraint is the voltage drop at the level of the load connection points.**

Figure 154 shows the algorithm for assessment of extreme flexibility volumes described below. A voltage profile is first simulated on the outgoing feeder under an U or I constraint, then a sort is performed according to the voltage drop. Then, the load with the steepest voltage drop is lowered until another load has a larger voltage drop (searches for the minimum useful flexibility volume). If this case occurs, this new load is lowered until it is replaced by another. If the load reaches zero power, the algorithm then lowers the load with the highest voltage drop according to the voltage profile. The criterion for stopping this algorithm is the disappearance of the U or I constraint.

The volume thus obtained is the minimum flexibility volume for which the removed loads are ideally distributed to eliminate the constraint. The same reasoning applies to determine the maximum flexibility volume capable of removing the constraint this time by sorting the loads by increasing order of voltage drops (from the smallest to the largest). **The**

volume thus obtained corresponds to the flexibility most poorly distributed to resolve the U constraint (ΔU<8%) or I constraint (Imap≤100%).

NB: The Imap is the maximum current capacity of a cable.

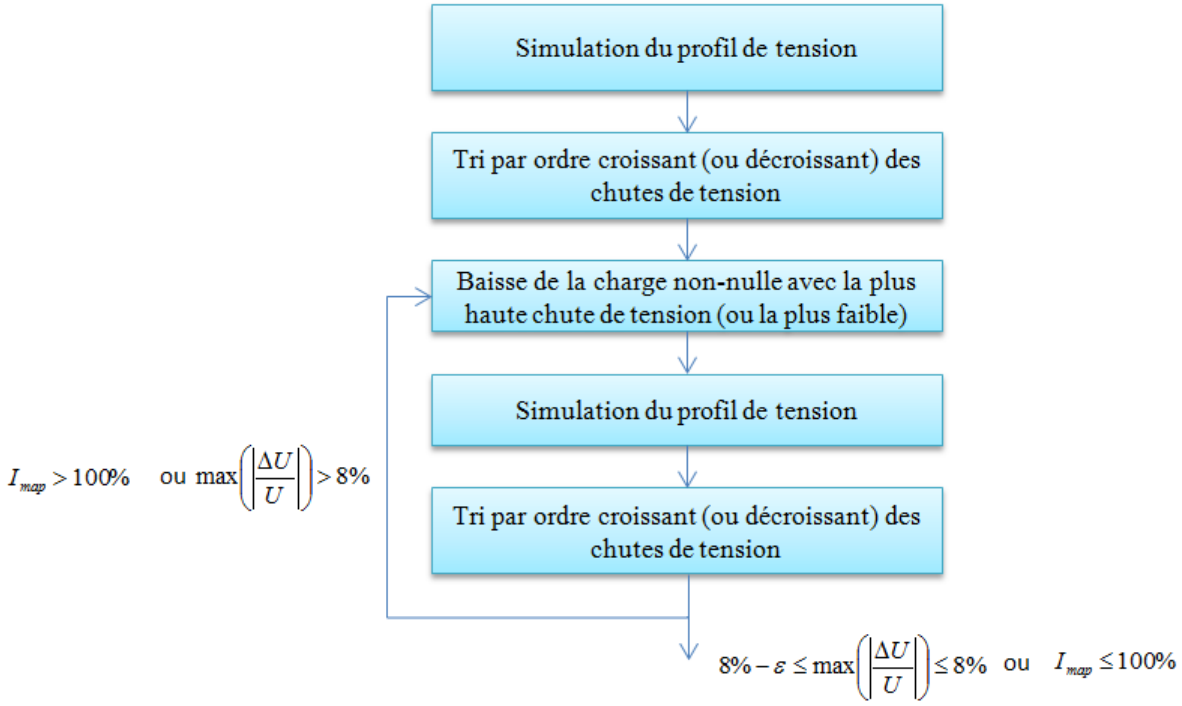

Figure 154 - Algorithm for assessment of extreme flexibility volumes capable of removing an I/S or U constraint

This method thus makes it possible to obtain a useful flexibility volume framework on the outgoing feeder which can remove the U or I constraint.

1.1.3.2. Determination of flexible sub-zones

To avoid numerous time-consuming simulations and obtain a benchmark, we should now no longer think in terms of individual loads but a group of loads. The idea is to estimate, for various sub-zone sizes (from the most localized up to the whole outgoing feeder area), the useful flexibility volume to remove the U constraint.

In *Nice Smart Valley*, we have chosen, like in the previous section, to define sub-zones ranked according to the voltage drop at the load connection point.

The method differs from Figure 155 on two specific points:

- **The voltage profile calculation is run only a single time before any reduction in the load**. The sub-zones are therefore fixed as of the first voltage profile calculation[53].
- **All the loads included in the sub-zone vary homothetically** until the constraint is eliminated, if possible (there is no longer any treatment/optimization load by load).

Figure 155 shows the method of selection of sub-zones to be tested. These sub-zones are defined via the sort by voltage drops proposed in the previous section, and are enlarged as it becomes authorized to take on greater loads. In other words, **the load(s) with large voltage drops will always appear in the sub-zones** (sub-zone 1 is included in sub-zone 2, etc.). Sub-zone 1 is the smallest load packet allowing the U constraint to be removed by applying homothetic load shedding.

Within the framework of *Nice Smart Valley*, the choice made concerned flexibility sub-zones comprising MV/LV substations and MV loads, with 1 MW incrementing from one zone to another).

[53] This is useful to limit not only the calculations, but also to limit the creation of geometrically non-adjacent sub-zones.

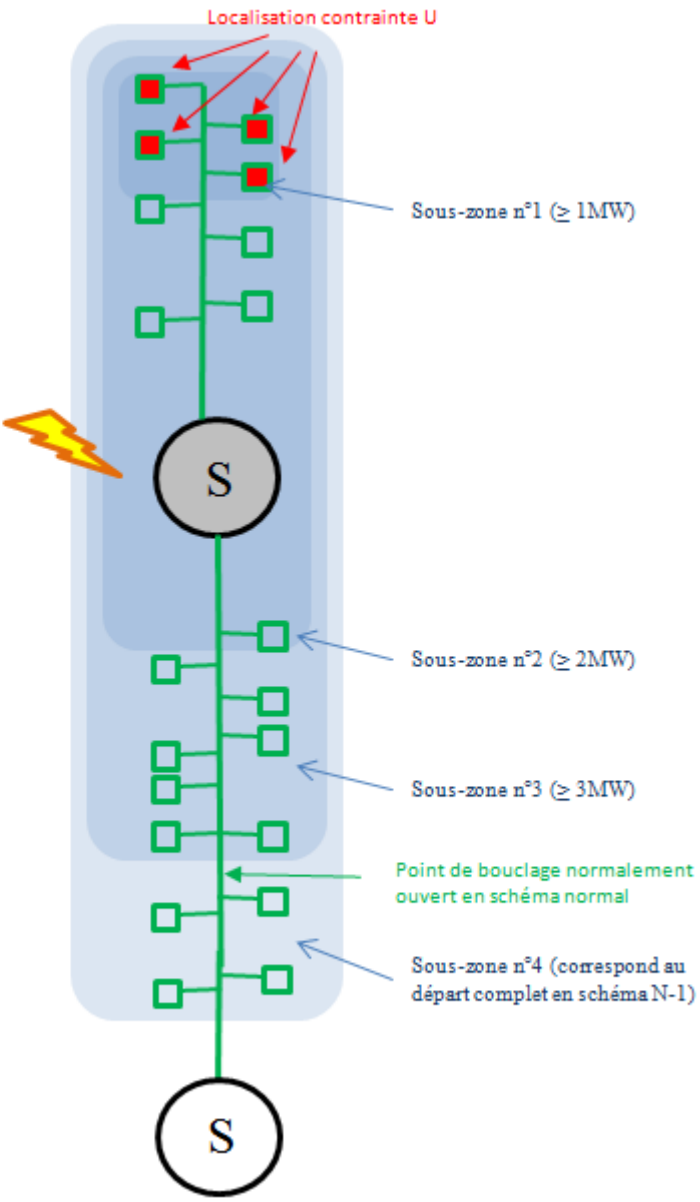

Figure 155 - Illustration of the definition of potentially flexible sub-zones to resolve the U constraint

Figure 156 shows the algorithm for assessment of flexibility volumes by sub-zone.

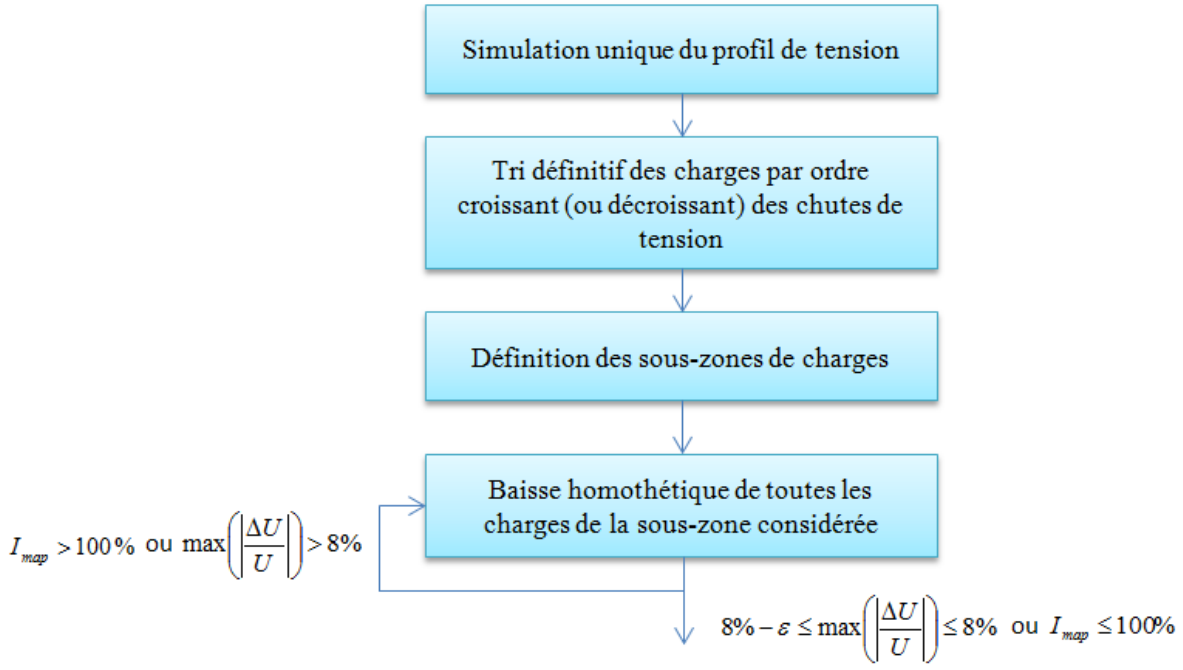

Figure 156 - Algorithm for assessment of flexibility volumes by sub-zone

The simulations with various flexible sub-zones will make it possible to assess the impact of the location of flexibility on useful volumes. Within the *Nice Smart Valley* framework, it has been chosen to assess the useful flexibility volumes relative to the zones having an impact on the constraint.

The situation without production has been dealt with, and we will now examine the situation with producers in the zone in an N-1 system.

1.2. Methodology to allow for producers

In this section, we describe the allowance for producers in our simulations. This method is intended to be more general than that described in deliverable D9.1, because the producers are considered individually and not in a synchronous manner over the entire seasonality of the study, as shown in Figure 157.

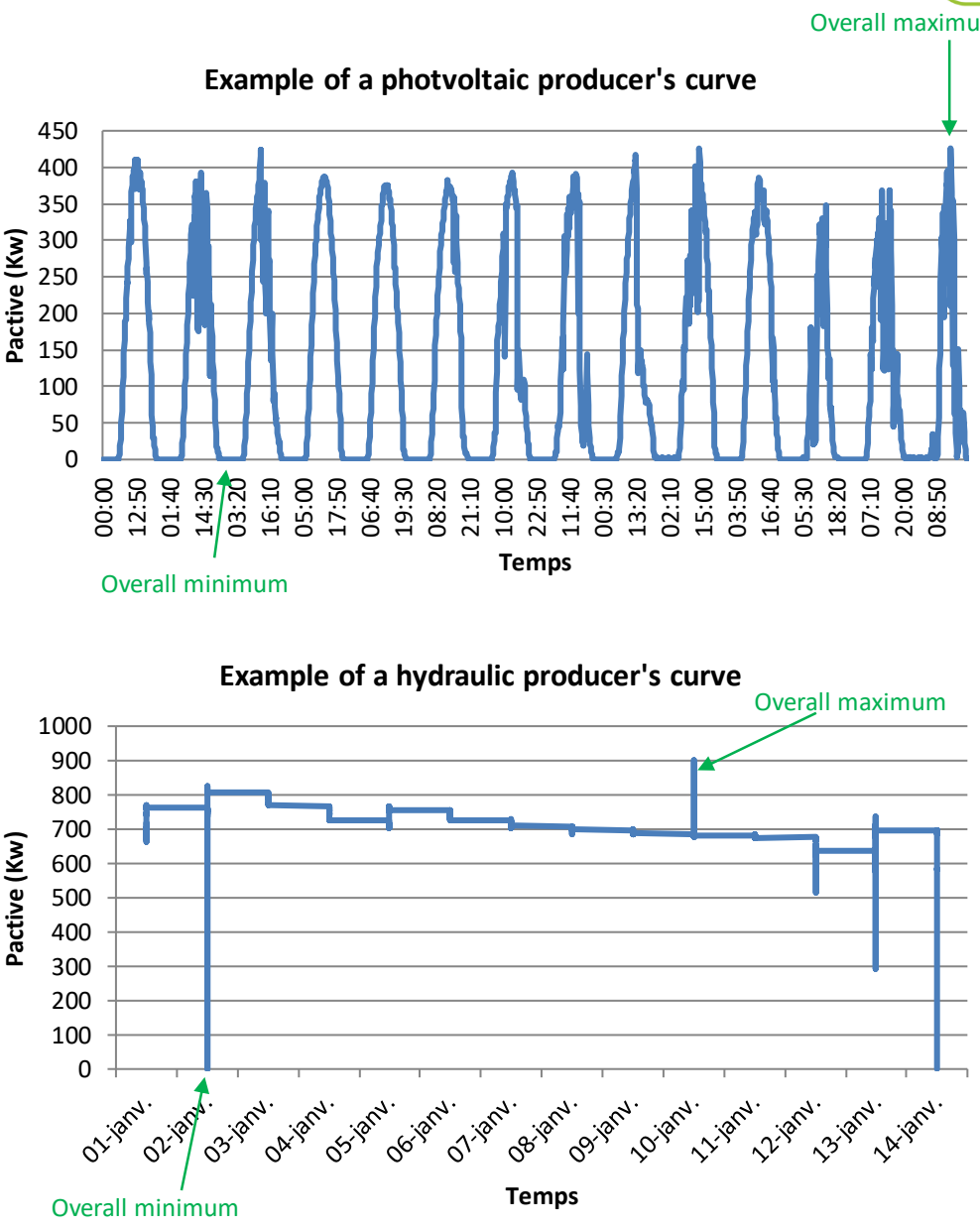

Figure 157 – Assessment of the two production levels by seasonality

When the production levels have been assessed, the useful flexibility levels should be assessed taking into account the injection by each of the producers. The aim then is to **simulate the minimum and maximum production levels of each of the producers (no probabilistic approach is implemented)**.

These simulations, notably those at maximum production and zero production, will make it possible to define a framework for the flexibility volume, according to a given load level (cf APPENDIX C - § 1.1).

2. IMPACT OF THE LOCATION OF FLEXIBILITY ON THE GUILLAUMES ZONE

2.1. Results of the simulations on the Guillaumes source substation

As a reminder, the simulations which are described in this section are based on **the assumption that the N-1 system is fixed for all the simulations**. They therefore do not take into account the probability that the two events could occur at the same time (cf. deliverable D.9.1).

Note: the following results are shown with the power consumption at the primary substation level and not over the portion of the grid where the flexibility would be useful to alleviate the constraint.

2.1.1. PUGET outgoing feeder "at zero production"

2.1.1.1. Voltage profile at zero production

Figure 158 below shows the voltage profile of the PUGET outgoing feeder at α_{max}. This illustrates the numerous constraints due to the very great length of the outgoing feeder (50 km). Moreover, beyond 18 km the substations exceed 8% of voltage drops (limit threshold on MV).

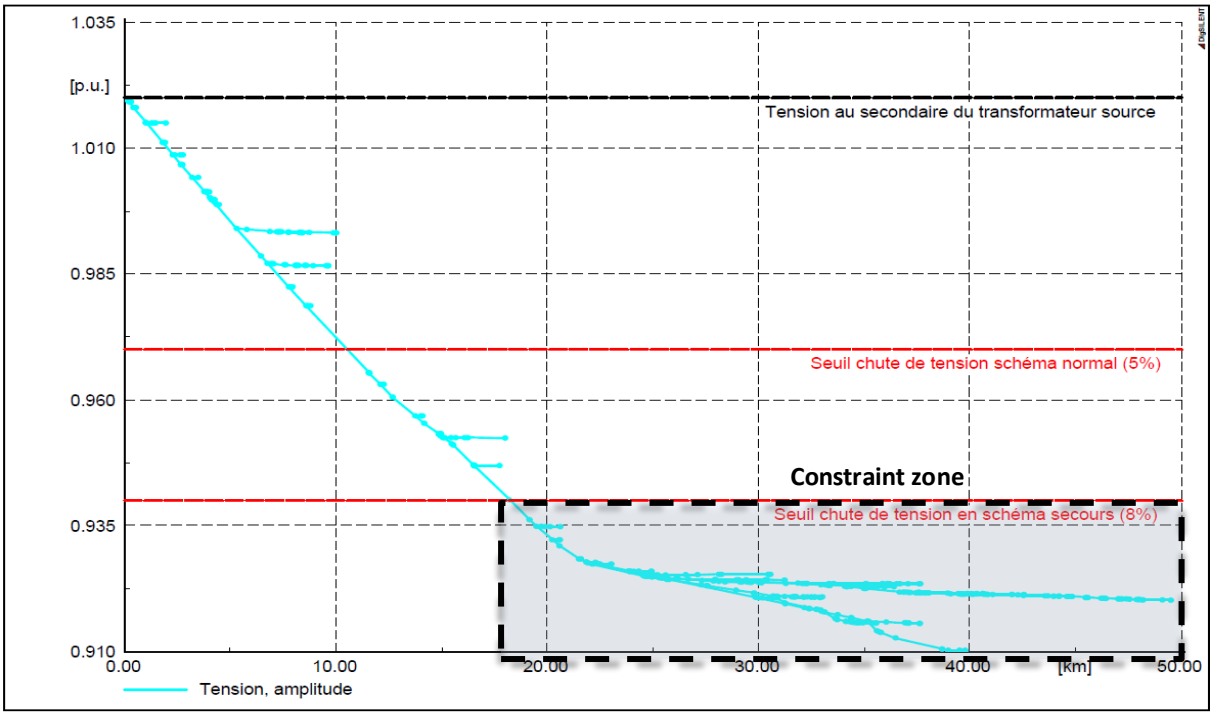

Figure 158 - Voltage profile of the PUGET outgoing feeder "at zero production"

2.1.1.2. I constraint

Figure 159 below shows the results of the simulations run in an N-1 system for various load levels of the winter & shoulder period[54]. In particular, it can be seen that at α_{max}, the maximum useful flexibility volume is 0.67 MW, while the minimum useful flexibility volume is 0.64 MW (if all the producers are not producing). The 25 kW difference at α_{max} shows that in this specific case the location of flexibility (on the PUGET auxiliary outgoing feeder) has only very little impact on the useful flexibility volume.

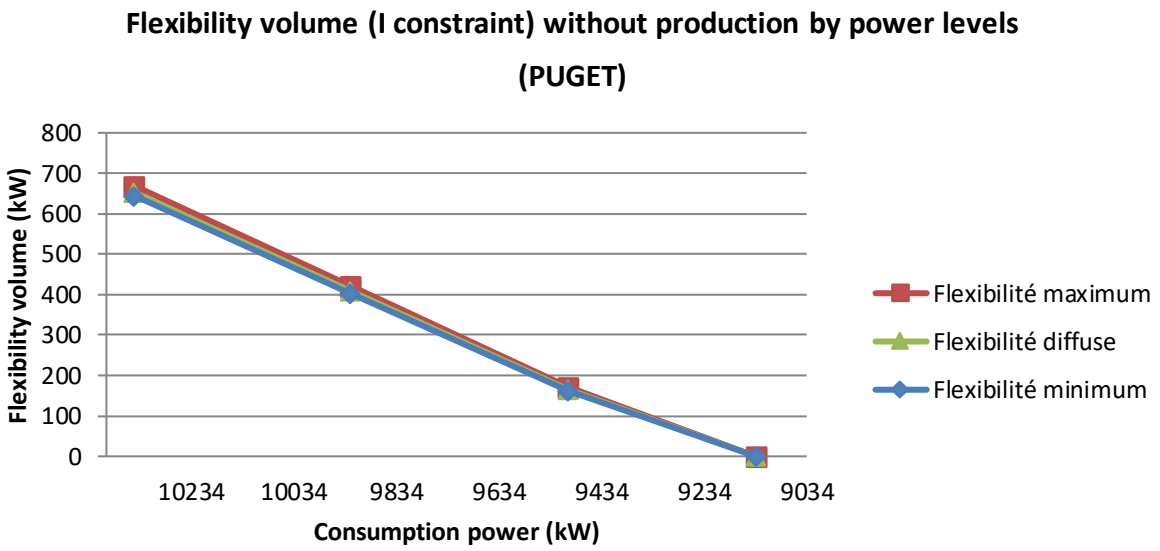

Figure 159 – Useful flexibility volume removing the I constraint (PUGET outgoing feeder) according to power levels

2.1.1.3. U constraint

We will now assess the impact of the location of flexibility on the U constraint for the PUGET outgoing feeder. The following flexibility volumes are given allowing for the elimination of the I constraint.

[54] Considered here as the winter period & the shoulder period between 1 January and 31 May and from 1 October to 31 December.

U constraint: By levels

Figure 160 below shows the results of the simulations run in an N-1 system for various load levels of the winter & shoulder period, for treatment of the U constraint. Excluding production, the maximum useful flexibility volume is 2.32 MW and the minimum flexibility 0.787 MW. The difference is 1.5 MW at α_{max}, which shows that in this specific case the location of flexibility (on the PUGET auxiliary outgoing feeder) is of capital importance for the useful flexibility volume.

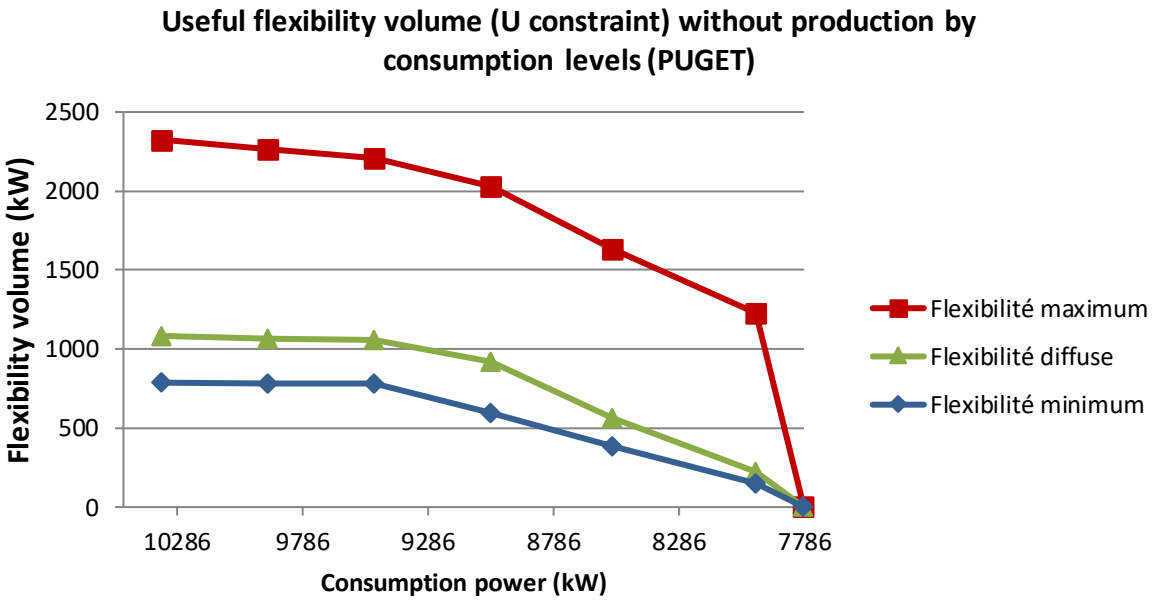

Figure 160 – Useful flexibility volume removing the U constraint (PUGET outgoing feeder) according to power levels

The sum of the flexibility volumes of the I and U constraints cannot be taken in this specific case, because the flexibility scope of the U and I constraints is not the same.

U constraint: By location of flexibility at αmax

Figure 161 below shows the results of the simulations run in an N-1 system for various load levels of the winter & shoulder period, for treatment of the U constraint by sub-zones. The results show that when the flexibility is located between zones 1 and 5, the flexibility volume is on the whole stable (irrespective of the location). Zones 6 and 7 being vast, the impact of flexibility becomes very significant (difference of 1.5 MW). So, the more flexibility is applied over a broad zone, the more there will be a need for flexibility.

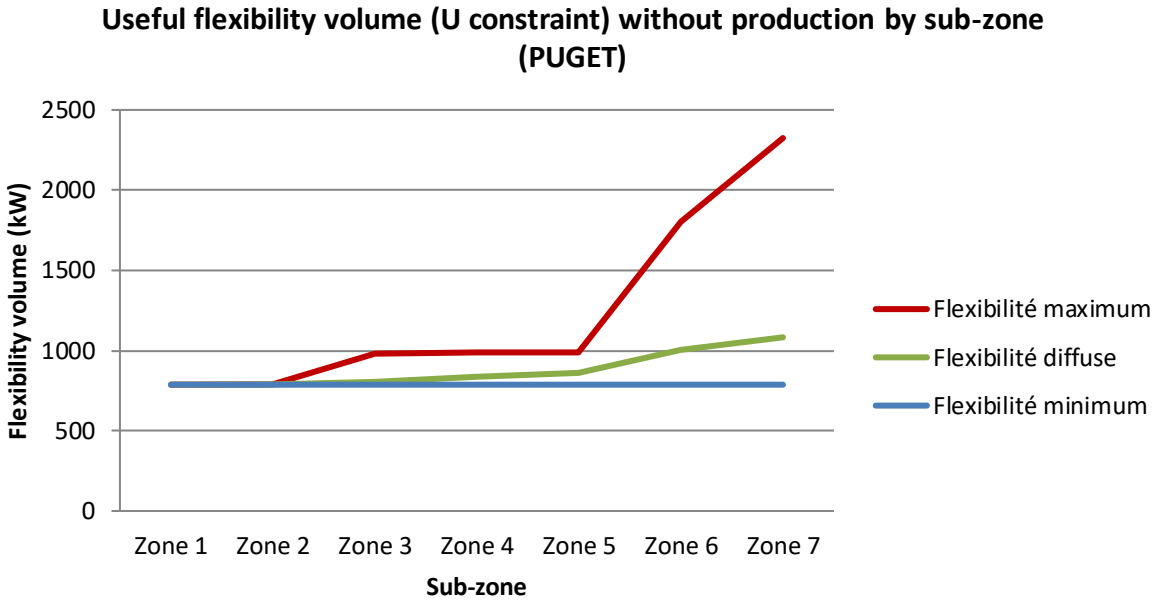

Figure 161 - Useful flexibility volume at Guillaumes (PUGET outgoing feeder) according to the power levels of the sub-zone under U constraint

2.1.2. PUGET outgoing feeder "at non-null production"

As explained in section 1.2, the following simulation results were obtained by placing the producers at their maximum and minimum production levels measured over the past two years.

2.1.2.1. Voltage profile at maximum production

Figure 162 below shows the voltage profile of the PUGET outgoing feeder at α_{max} allowing for the local production levels. This illustrates the fact that the load reduction due to the injection of production leads to the appearance of high voltage constraints in the case of N-1.

On a "mixed" outgoing feeder, i.e. comprising production and consumption, a high voltage constraint is a voltage rise exceeding Un+4%. The following voltage profile therefore highlights a failure to comply with the voltage map above a grid length of 21 km.[55]

[55] In the event of an incident, the Enedis regional control centre (ACR) will not keep connected a producer who caused a voltage rise which required a need for flexibility.

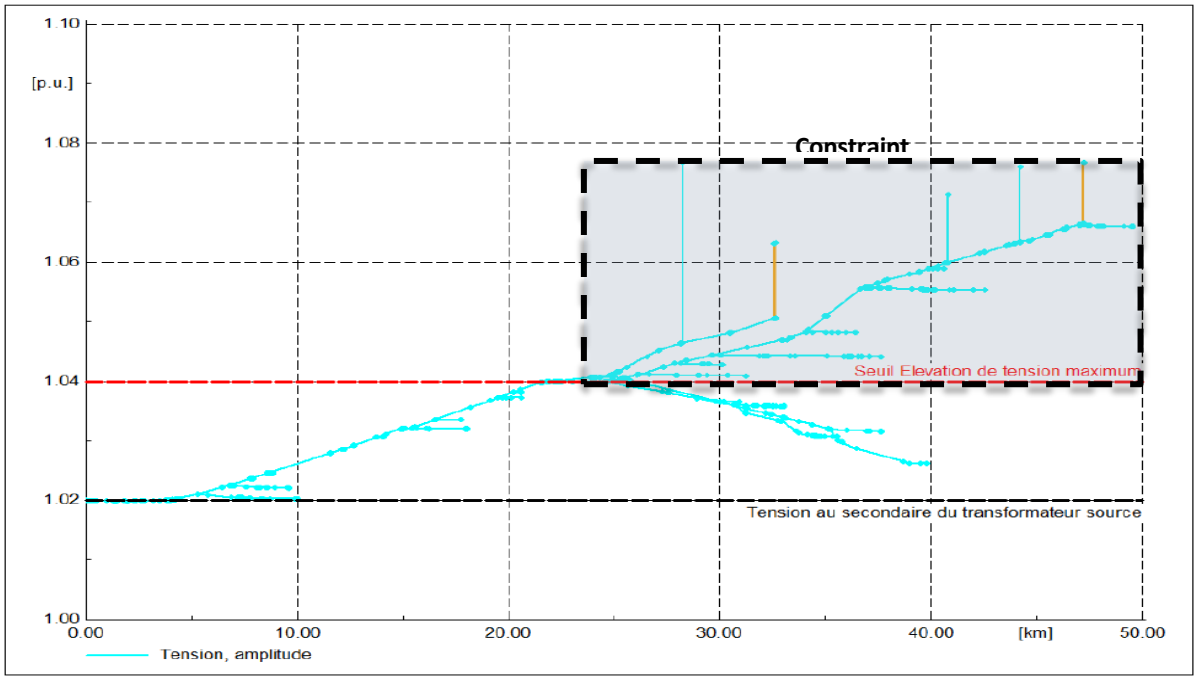

Figure 162 - Voltage profile of the PUGET outgoing feeder "at maximum production"

2.1.2.2. I constraint

On this specific outgoing feeder, the situation at minimum production is identical to the situation at zero production given that the minimum production of all the producers is zero.

Moreover, at maximum production, there is no longer any I constraint at α_{max}.

2.1.2.3. U constraint

Figure 163 below shows the results of the simulations run in an N-1 system for various load levels of the winter & shoulder period.

The maximum useful flexibility volume corresponds to the maximum volume at zero production, because the minimum seasonal production level of each producer is zero.

The minimum useful flexibility volume ranges from 0.72 MW to 1.99 MW. Since consumption is low on this outgoing feeder, maintaining the producers would result in a voltage rise. This is reflected by the fact that the greater the injection, the greater will be the flexibility volume. Note that, contrary to what may have been shown previously, there is no α_{lim} in this specific case given that the more the zone's consumption is reduced, the more there is a high voltage constraint.

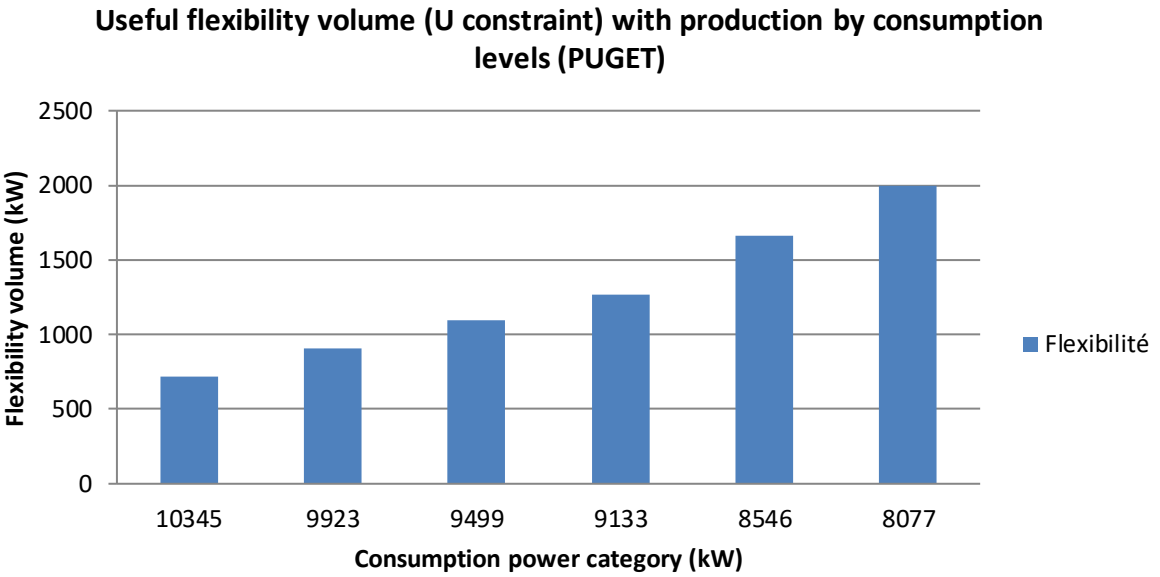

Figure 163 – Useful flexibility volume removing the U constraint (PUGET outgoing feeder) according to power levels with maximum seasonal production

2.1.3. SSAUV outgoing feeder "at zero production"

2.1.3.1. Voltage profile at zero production

Figure 164 below shows the voltage profile of the SAINT-SAUVEUR outgoing feeder. This illustrates the numerous constraints due to the very great length of the outgoing feeder (> 30 km). Moreover, beyond 12 km the substations exceed 8% of voltage drops (limit threshold on MV).

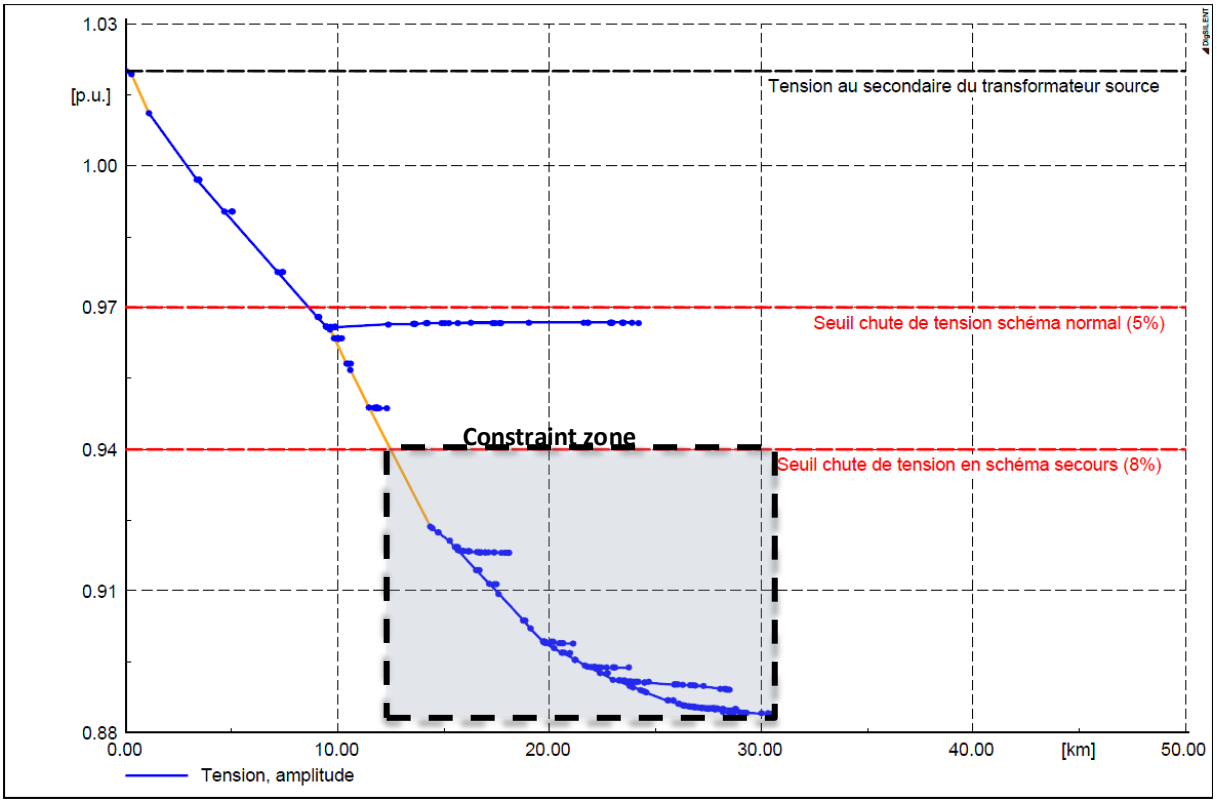

Figure 164 – Voltage profile of the SAINT SAUVEUR outgoing feeder "at zero production"

2.1.3.2. I constraint

Figure 165 below shows the results of the simulations run in an N-1 system for various load levels of the winter & shoulder period. The maximum useful flexibility volume is 0.685 MW and the minimum flexibility 0.474 MW if all the producers are not producing. The relatively large difference (0.211 MW, or 42% relative deviation) between the diffuse and maximum flexibility curves is due to the load distribution on the outgoing feeder. In this specific case the location of flexibility (on the SSAUV auxiliary outgoing feeder) has a major impact on the useful flexibility volume.

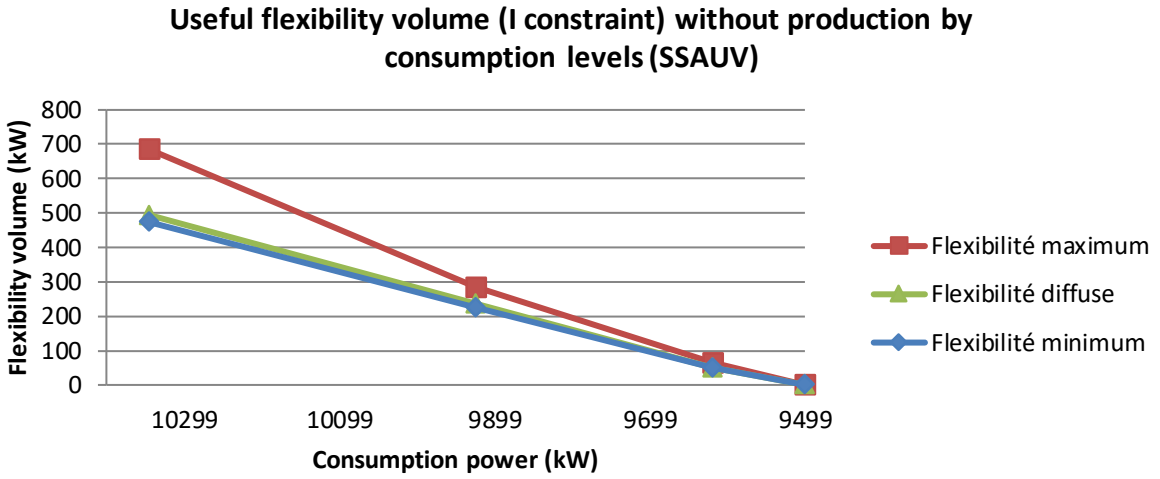

Figure 165 – Useful flexibility volume removing the I constraint (SSAUV outgoing feeder) according to power levels

2.1.3.3. U constraint

We will now assess the impact of the location of flexibility on the U constraint for the SSAUV outgoing feeder. The following flexibility volumes are given allowing for the elimination of the I constraint.

U constraint: Conventional

Figure 166 below shows the results of the simulations run in an N-1 system for various load levels of the winter & shoulder period, for treatment of the U constraint. The maximum useful flexibility volume is 2.56 MW and the minimum flexibility 1.58 MW if all the producers are not producing. The difference is 0.98 MW at α_{max}, which shows that in this specific case the location of flexibility (on the SSAUV auxiliary outgoing feeder) has a major impact on the useful flexibility volume.

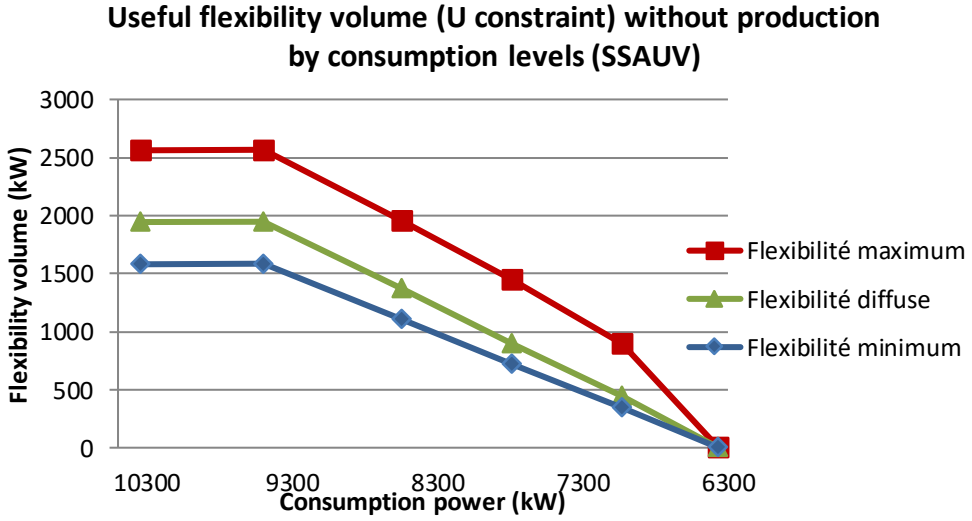

Figure 166 – Useful flexibility volume removing the U constraint (SSAUV outgoing feeder) according to power levels

Figure 167 below shows the results for the total useful flexibility volumes[56] making it possible to remove the I and U constraints. These curves show that the greater the consumption, the greater will be the constraint and the larger the useful flexibility volume. Excluding production, the maximum useful flexibility volume is 3.25 MW and the minimum flexibility 2.05 MW. The difference is 1.20 MW at α_{max}, which shows that in this specific case the location of flexibility (on the SSAUV auxiliary outgoing feeder) is of capital importance for the useful flexibility volume.

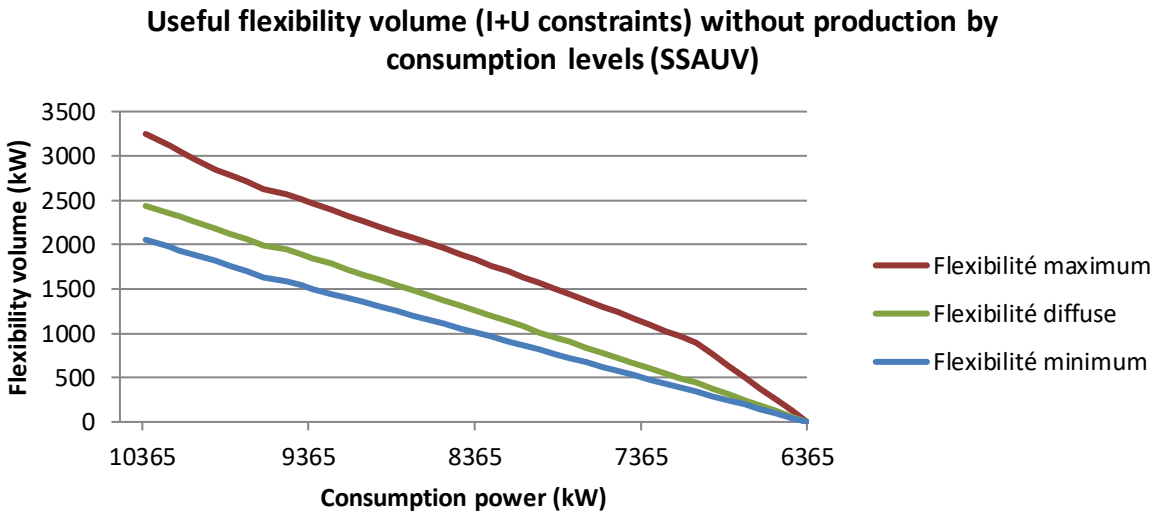

Figure 167 – Useful flexibility volume removing the I and U constraints (SSAUV outgoing feeder) according to the power levels of the zone

U constraint: By location of flexibility at αmax

Figure 168 below shows the results of the simulations run in an N-1 system for various load levels of the winter & shoulder period, for treatment of the U constraint by sub-zones. The curves show that when the flexibility is located between zones 2 and 3, the flexibility volume is on the whole stable (irrespective of the location). As of zone 4, since the zone is vast, the impact of flexibility becomes very significant (difference between 0.04 MW and 0.98 MW). So, the more flexibility is applied over a broad zone, the more there will be a need for flexibility. Note that the proposed flexibility volume in zone 1 would not be sufficient to remove the U constraint.

[56] The sum of the flexibility volumes can be taken in this specific case, because the flexibility scope of the U and I constraints is the same, or else it would not work.

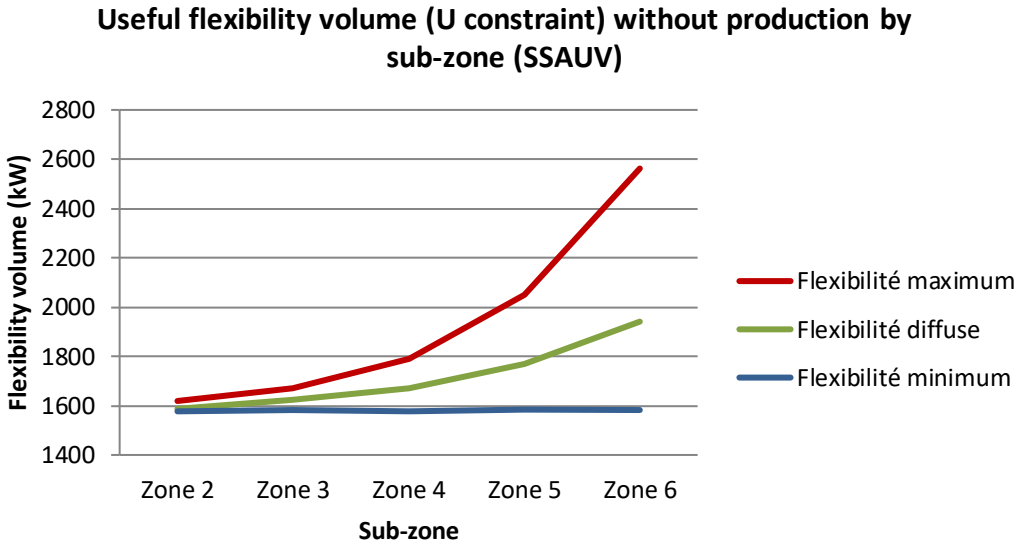

Figure 168 - Useful flexibility volume at Guillaumes (SSAUV outgoing feeder) according to the power levels of the sub-zone under U constraint

2.1.4. SSAUV outgoing feeder "at non-null production"

As explained in section 1.2, the following simulation results were obtained by placing the producers at their maximum and minimum production levels measured over the past two years.

2.1.4.1. Voltage profile at maximum production

Figure 169 below shows the voltage profile of the SSAUV outgoing feeder with producer. This illustrates the fact that the load reduction due to the injection of production does not reduce the constrained zone. Placing production on the outgoing feeder does not necessarily help to remove the constraint.

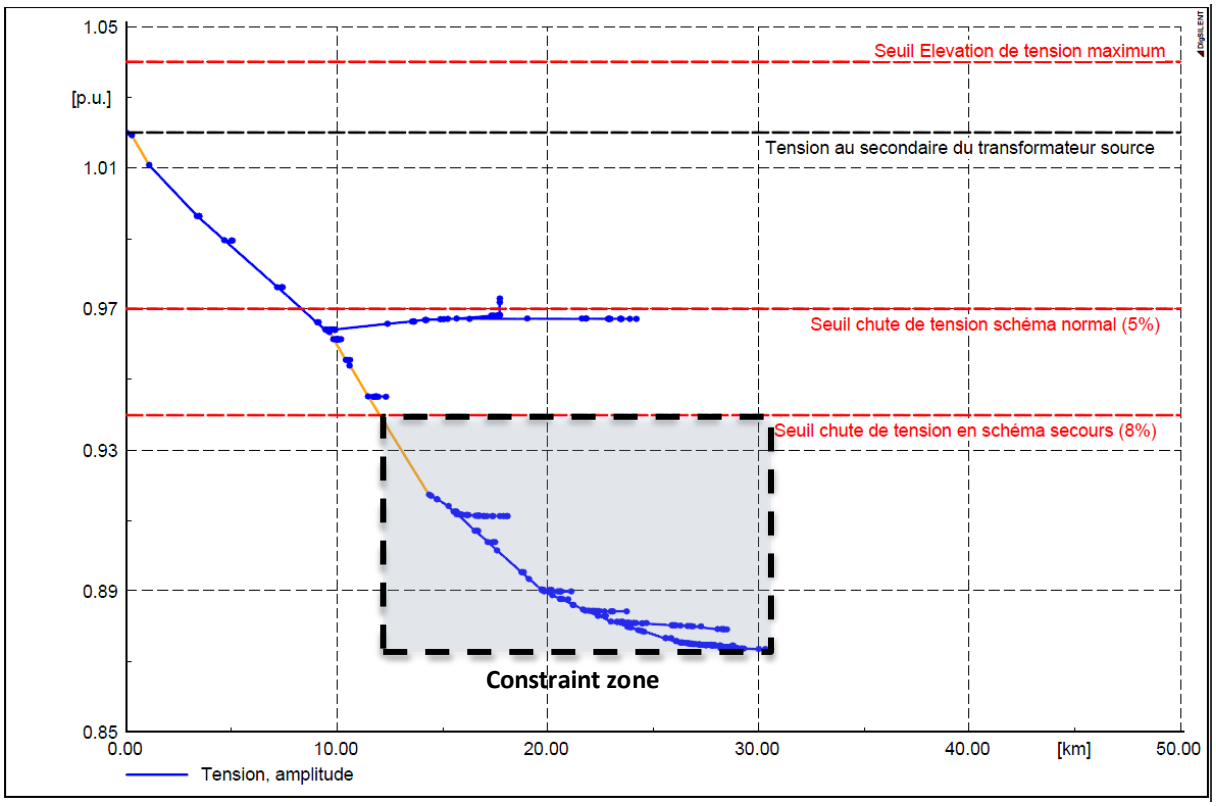

Figure 169 – Voltage profile of the SAINT SAUVEUR outgoing feeder "at non-null production"

2.1.4.2. I constraint

Allowance for the producers, whatever the situation (maximum or minimum injection) removes all the I constraints on this outgoing feeder.

2.1.4.3. U constraint

We will now assess the impact of the producers on the flexibility volume on the U constraint for the SSAUV outgoing feeder. As a reminder, the following flexibility volumes are given after removing the I constraint and watching the producers over the entire season.

Figure 170 below shows the results of the simulations run in an N-1 system for various load levels of the winter & shoulder period, for treatment of the U constraint with allowance for the producers. The maximum useful flexibility volume is 2.16 MW and the minimum flexibility volume is 2.03 MW if all the producers are producing at the seasonal minimum or maximum. The relatively small difference of 0.13 MW at α_{max} (after resolution of the I constraint) can be explained by the fact that overall production is stable.

This chart also shows that the injection of production into the grid results in a reduction of 0.53 MW in the flexibility volume compared with a case without production.

For simulations close to α_{lim}, a major plateau is observed due to the elimination of the I constraint leading to mitigation of the U constraint.

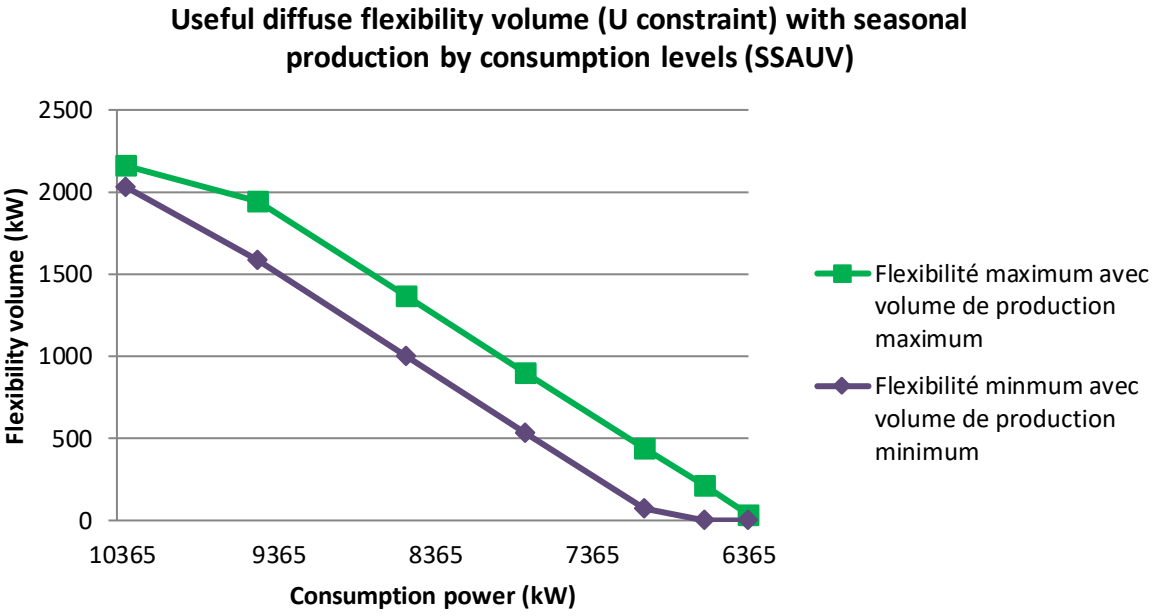

Figure 170 - Useful flexibility volume for the U constraint (SAINT-SAUVEUR outgoing feeder) according to power levels with seasonal production.

3. IMPACT OF THE LOCATION OF FLEXIBILITY ON THE IZOLA ZONE

3.1. Results of the simulations on the ISOLA source substation

As a reminder, the simulations which are described in this section are based on **the assumption that the N-1 system is fixed for all the simulations**. They therefore do not take into account the probability that the two events could occur at the same time (cf. deliverable D.9.1).

3.1.1. ISOLA VILLAGE outgoing feeder "at zero production"

3.1.1.1. Voltage profile at zero production

Figure 171 below shows the voltage profile of the ISOLA VILLAGE outgoing feeder at α_{max}. This shows that there are no constraints relating to voltage drops.

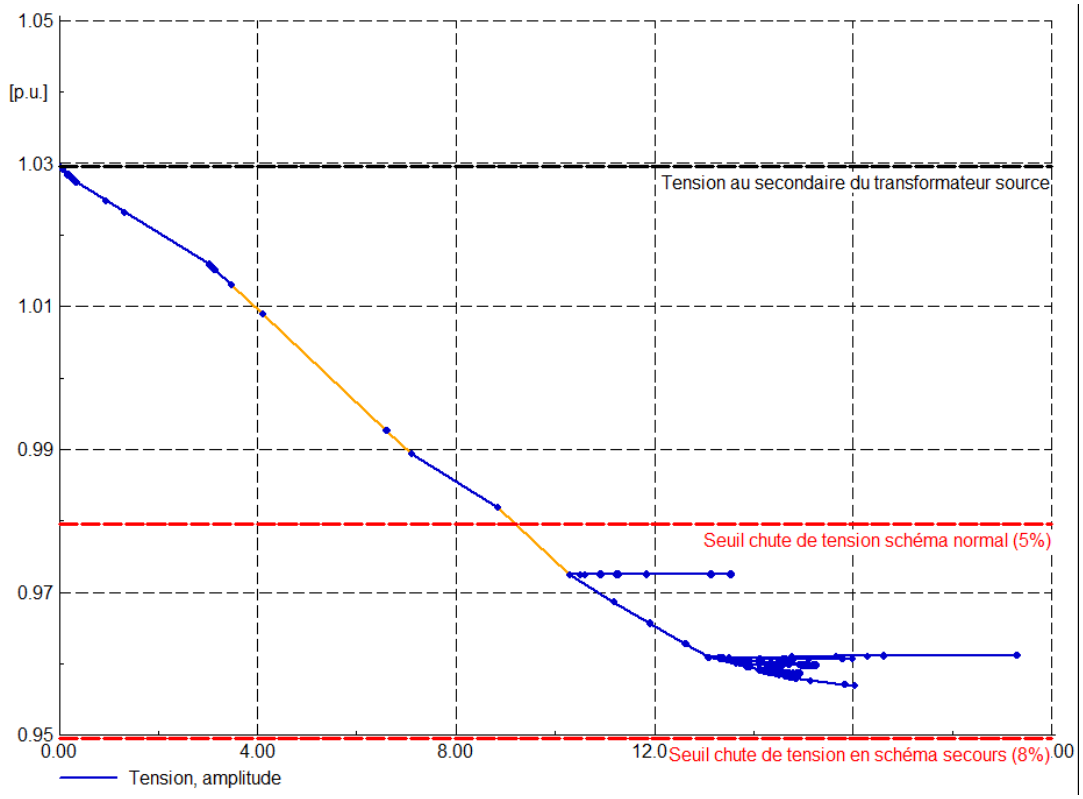

Figure 171 – Voltage profile of the SAINT SAUVEUR outgoing feeder "at zero production"

3.1.1.2. S & I constraint

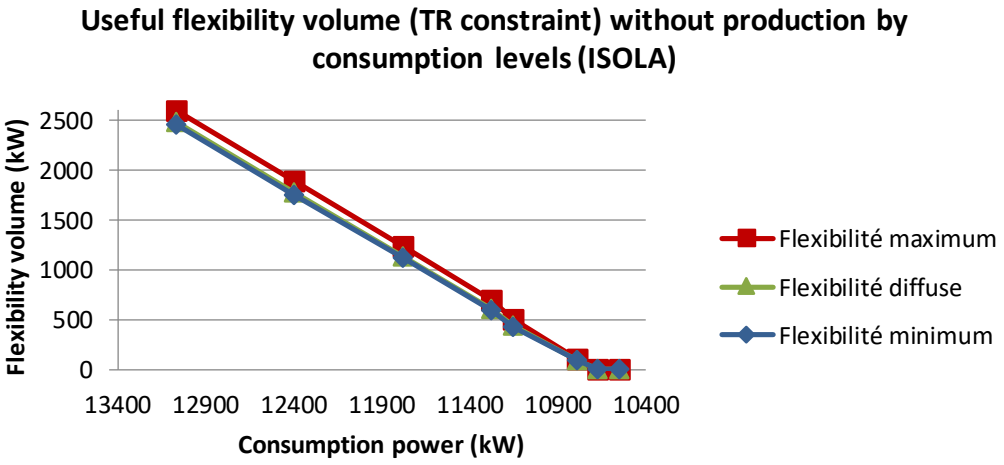

Figure 172 below shows the results of the simulations run in an N-1 system for various load levels of the winter & shoulder period. Since the TR constraint is preponderant over the I constraint, the following curve therefore shows the useful maximum, minimum and diffuse flexibility volumes to remove the two constraints. The difference is 0.144 MW at α_{max}, which

shows that in this specific case the location of flexibility does not have a major impact on the useful flexibility volume.

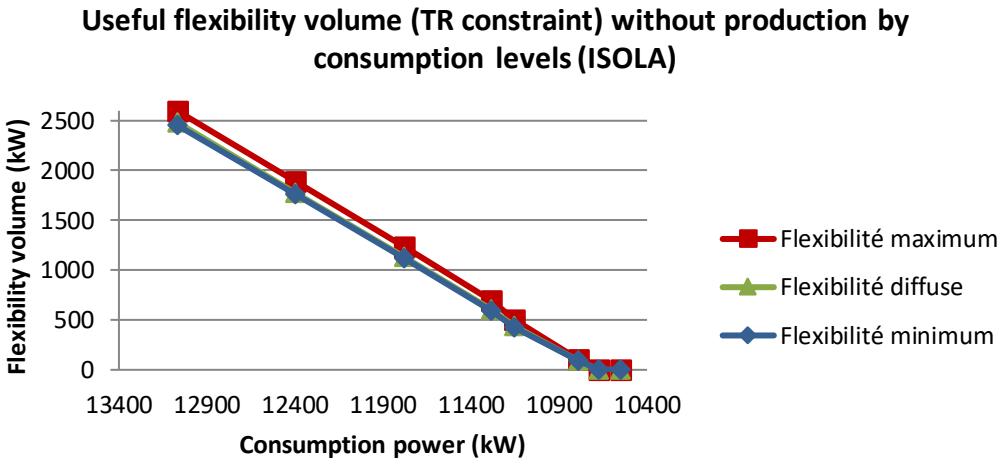

Figure 172 – Useful flexibility volume removing the TR constraint (ISOLA VILLAGE) according to power levels

3.1.1.3. U constraint

As shown by the voltage profile of the ISOLA VILLAGE outgoing feeder in section 3.1.1.1, no node on the grid exceeds 8% of voltage drops.

ISOLA VILLAGE outgoing feeder "at non-null production"

3.1.1.4. Production volume

As explained in section 1.2, the producers were watched at their maximum and minimum over the entire period examined (i.e. the two full years 2015/2016).

3.1.1.5. I constraint

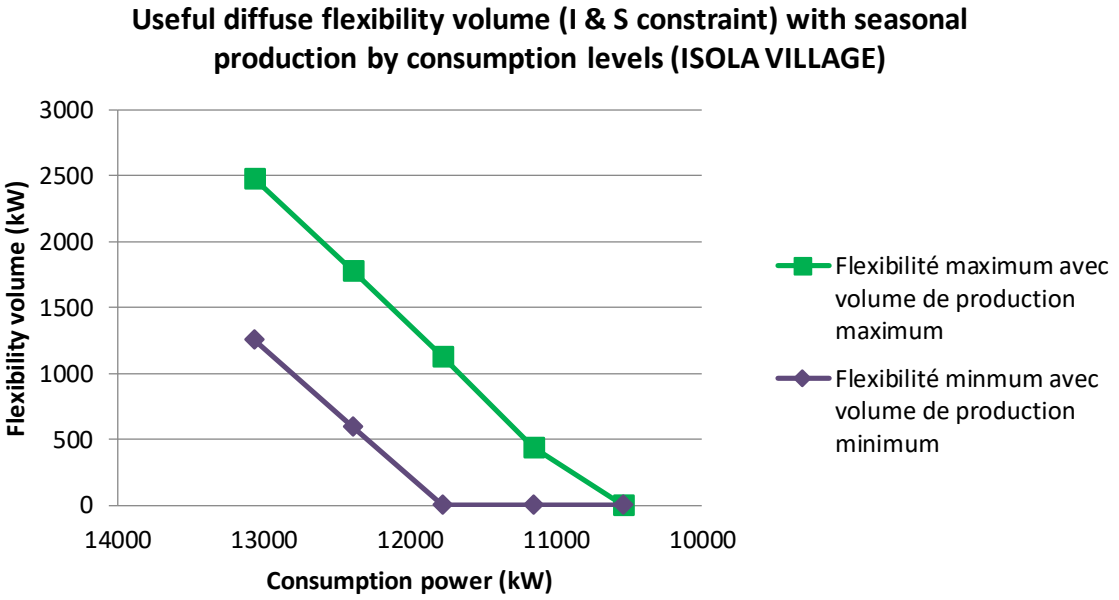

Figure 173 below shows the results of the simulations run in an N-1 system for various load levels of the winter & shoulder period. The maximum useful flexibility volume is 2.48 MW at minimum production (i.e. zero production) and the minimum flexibility is 1.26 MW at maximum production if all the producers are producing. So the production level has a major impact on the useful flexibility volume for the transformer constraint. Production cannot resolve the I constraint, because the production is located upstream of it and therefore has only a very small impact (cf. § 2.2 of Appendix 1 of deliverable D9.1).

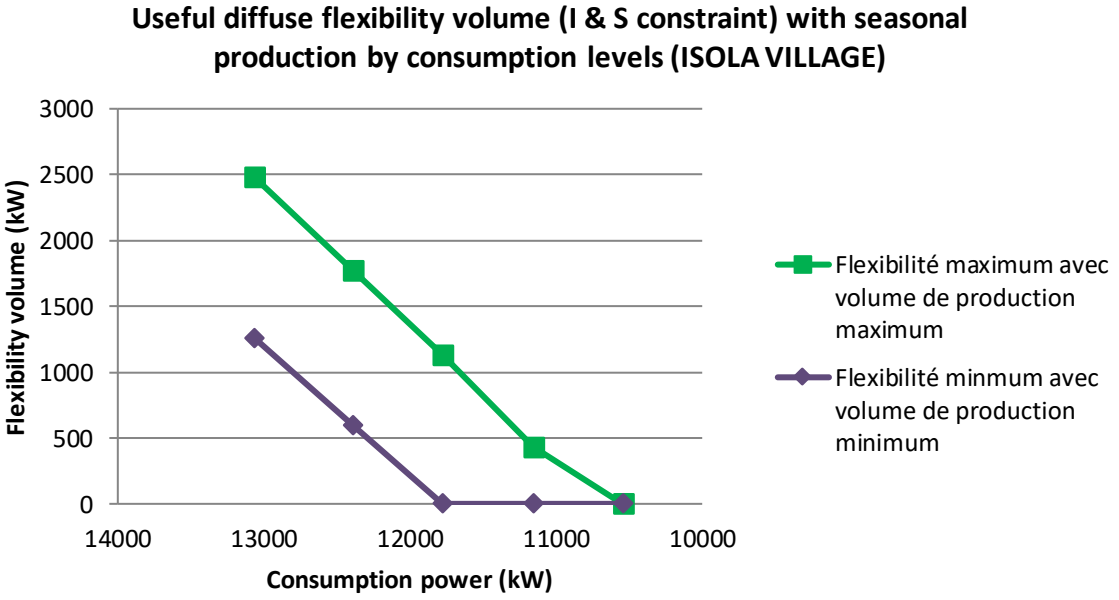

Figure 173 - Useful flexibility volume for the S & I constraint (ISOLA VILLAGE) according to power levels with seasonal production

4. IMPACT OF THE LOCATION OF THE FLEXIBILITY ON THE BROC-CARROS

4.1. Results of the simulations on the BROC-CARROS source substation

As a reminder, the simulations which are described in this section are based on **the assumption that the N-1 system is fixed for all the simulations**. They therefore do not take into account the probability that the two events could occur at the same time (cf. deliverable D.9.1).

4.1.1. CARROS outgoing feeder unit "at zero production"

4.1.1.1. Voltage profile at zero production

Figure 174 below shows the voltage profile of the CARROS outgoing feeder at α_{max}. This shows that there is no U constraint on the outgoing feeder in an N-1 system.

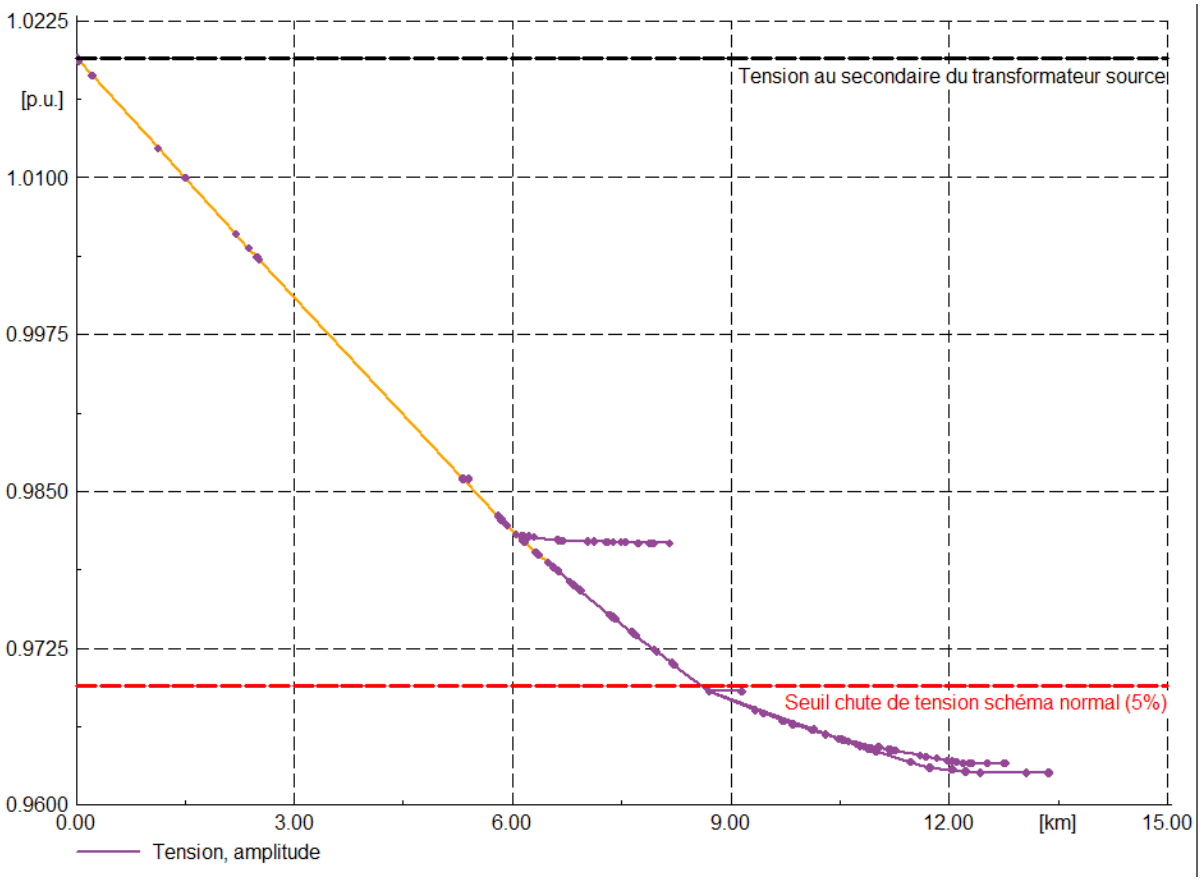

Figure 174 - Voltage profile of the CARROS outgoing feeder "at zero production"

4.1.1.2. I constraint

Figure 175 below shows the results of the simulations run in an N-1 system for various load levels of the winter & shoulder period. The maximum useful flexibility volume is 482 MW and the minimum flexibility 440 MW if all the producers are not producing. The relatively small difference (42 kW) between the maximum and minimum flexibility curves shows that the location of flexibility does not have a major impact on the volume to be activated (at fixed production).

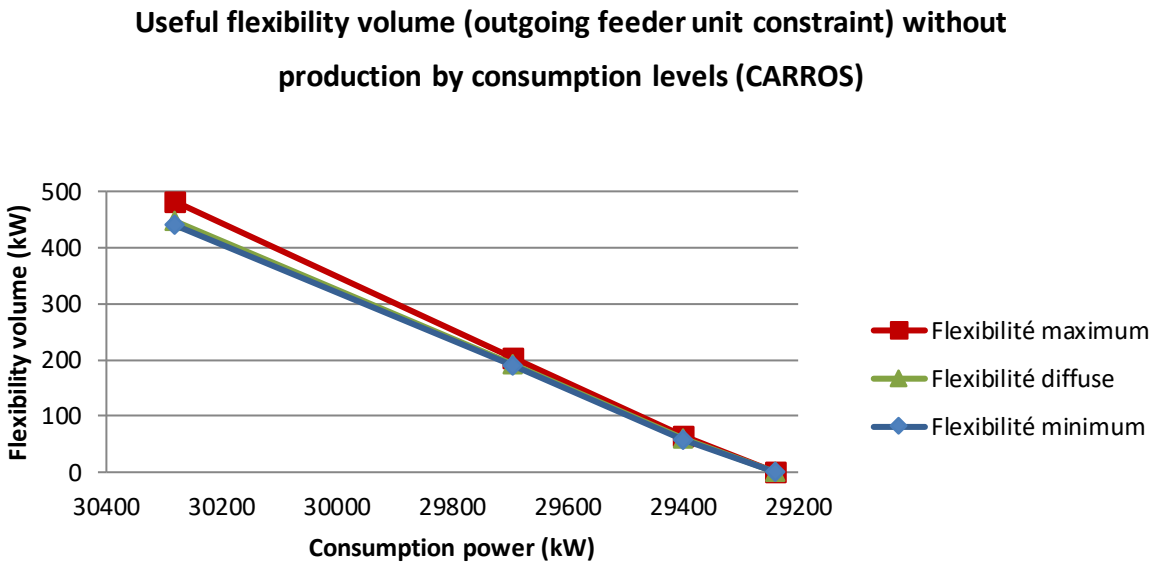

Figure 175 - Useful flexibility volume removing the outgoing feeder unit constraint (CARROS) according to power levels

4.1.1.3. U constraint

As shown by the voltage profile of the CARROS outgoing feeder in section 4.1.1.1, no node on the grid exceeds 8% of voltage drops.

4.1.2. CARROS outgoing feeder unit "at non-null production"

4.1.2.1. Production volume

As explained in section 1.2, the producers were fixed at their maximum and minimum over the entire period examined (i.e. the years 2015 and 2016).

4.1.2.2. I constraint

Allowance for the producers at their maximum injection would result in removal of the I constraints on this outgoing feeder. Since the minimum production of each of the producers in the zone was zero throughout the study period, the useful flexibility volume therefore remains identical to that without a producer.

5. Conclusion of Appendix C

As a reminder, the presented results lead in no way to a potential estimation of the occurrence of calls on flexibility.

The analysis of these results in the *Nice Smart Valley* zones enables us to illustrate several points.

First, the location of flexibility does not always have the same impact, depending on the grid examined. On the Isola and Carros grids, the location of flexibility does not have a major impact on the useful flexibility volume making it possible to remove the I constraint. At Guillaumes, on the other hand, the grids are longer due to the retrieval system (N-1 configuration). The load there is less condensed in a geographic area, which leads to a relatively large difference of useful flexibility volume for the I constraint. For I constraint, the impact of location comes from losses.

Next, as regards the U constraint, the results of these analyses highlighted the fact that the location of flexibility has a major impact on our three zones. We have been able to show that, at Guillaumes, the useful flexibility volume can vary by a factor of three depending on its location.

Finally, production on the spot can also potentially help to remove constraints. The above results (D.9.5 § 1) have shown, in particular, that at Carros and Isola, this can limit the useful consumption flexibility volumes as soon as the production is properly located. At Guillaumes, the production levels are such that they themselves generate flexibility volumes at high consumption (or at low production).